

**DEVELOPMENT AND EVALUATION OF A REACTIVE  
HYBRID TRANSPORT MODEL (RUMT3D)**

Dissertation  
zur Erlangung des Doktorgrades  
der Mathematisch-Naturwissenschaftlichen Fakultäten  
der Georg-August-Universität zu Göttingen

vorgelegt von

Sabine Maria Spießl (Spiessl)

aus Oberviechtach

Göttingen 2004

D 7

Referent: Prof. Dr. Martin Sauter

Korreferent: Dr. Rudolf Liedl, Eberhard-Karls-Universität Tübingen

Tag der mündlichen Prüfung: 9. Juni 2004

*Those who explore an unknown world are travelers without a map; the map is the result of the exploration. The position of their destination is not known to them, and the direct path that leads to it is not yet made.*

*Hideki Yukawa, Japanese physicist, cited in Robert Crease and Charles Mann, The Second Creation (1986)*

## **Abstract**

Areas that have undergone mining usually have numerous environmental problems such as groundwater contamination, which is often acidic and rich in dissolved metals and possibly radionuclides. A reactive hybrid transport model (RUMT3D, 3-Dimensional Reactive Underground Mine Transport Model) was developed to allow the quantification of dissolved contaminants and precipitated solid phases in flooded underground mines with time. This hybrid model specifically takes into account the two distinct different transport regimes within an underground mine: (i) rapid transport in the network of the highly conductive shafts, drifts, ventilation raises, roadways, conduits, pipes or in the conduit system and (ii) the low velocity regime in the considerably less permeable ore material (continuum). Since the representative elementary volume is macroscopically invalid for discrete conduit networks, reactive transport models that are only based upon continuum approaches (i.e., single, double and multiple models) cannot be used for the simulation of reactive transport in underground mines. RUMT3D basically consists of a standard transport model (MT3DMS), a conduit transport model and a standard geochemical model (PHREEQC-2).

As RUMT3D is coupled to PHREEQC-2, it can manage a wide range of chemically reactive processes including aqueous complexation, mineral dissolution/precipitation, ion-exchange and redox reactions in the ore material or continuum. Reactions might be assumed to occur as equilibrium reactions and or kinetically controlled. RUMT3D is applicable to mines of varying complexity and difficulty in structure and components as a robust numerical algorithm was additionally implemented to solve transport in the conduit system accurate and computationally efficient. Apart from underground mines, RUMT3D can be applied to all domains where a discrete conduit system is embedded, i.e., to discrete fractured and karstic systems as well as aquifer intersecting boreholes. Such domains with embedded discrete conduit systems are generally referred to as hybrid systems in this thesis.

Three different benchmark problems, a quasi-analytical solution and two numerical codes were selected as well as plausibility tests were conducted to evaluate and demonstrate that RUMT3D can be useful in solving hypothetical and real-world problems. The first problem verifies the coupling of the two transport models for the continuum and for the conduit system within RUMT3D by testing the proper implementation of the new-implemented transport solver for advection in the conduit system. A benchmark problem with a conduit system was chosen for which a quasi-analytical solution was already available. The other two problems (i.e., the AMD and the Königstein problem) verify the reactive transport in the continuum. The AMD problem simulates the principal processes

of the Acid Mine Drainage (AMD) phenomenon while the Königstein problem simulates transport of acidic water, sulphate, dissolved metals including dissolved uranium in an aquifer downgradient from a mine site. On the basis of the AMD problem, the consistency, stability and accuracy of the reactive simulation results were investigated with respect to the characteristics of a simple mine system (or generally a hybrid system) by means of plausibility tests.

For the first benchmark problem, good agreements of results between RUMT3D and the semi-analytical solution could be obtained even with the usage of much larger transport time step sizes and pipe discretisation compared to the standard finite difference method. Also, for the other two benchmark problems, satisfactory results of RUMT3D could be achieved by comparison of these to the respective numerical code. Plausibility of the reactive transport results using RUMT3D for a hybrid system could also be shown by the use of four different scenarios. These scenarios were first examined for the continuum system to better identify peculiar phenomena resulting from the incorporation of the conduit transport model.

The good agreements of the results of RUMT3D with the different types of solution and numerical codes as well as the plausibility tests indicate an appropriate coupling of the three different models within RUMT3D (i.e., of MT3DMS with the conduit transport model and with the PHREEQC-2 model) as well as that RUMT3D is a reliable reactive transport simulation tool for continuum and hybrid systems. Further, the simulation results suggest that for the simulation of contaminant transport in a hybrid system, consideration of rapid transport pathways are imperative. A conduit system determines significantly the hydraulics in a hybrid system and is therefore responsible for rapid changes in water chemistry.

**Keywords:**

Coupled discrete-groundwater system, coupled discrete-continuum system, conduit-matrix system, discrete system, continuum-conduit transport model, numerical model, discrete conduit transport model, pipe network formulation, numerical modelling, numerical simulation, reactive transport modelling.

## Zusammenfassung

In Gebieten, in denen Bergbauaktivitäten stattgefunden haben, werden häufig zahlreiche negative Auswirkungen auf die Umwelt, wie das Vorkommen von sauren Sickerwässern und erhöhte Gehalte an gelösten Schwermetallen sowie möglicherweise an Radionuklide beobachtet. In der vorliegenden Arbeit wurde ein reaktives Hybrid-Stofftransportmodell (RUMT3D, 3-Dimensional Reactive Underground Mine Transport Model) entwickelt, welches die zeitliche Quantifizierung von gelösten Schadstoffen und ausgefallenen Mineralphasen in gefluteten untertägigen Bergwerken erlaubt. Dieses Hybrid-Modell berücksichtigt speziell die sehr unterschiedlichen Transportregionen innerhalb eines Bergwerkes: (i) beschleunigter Transport in dem hochdurchlässigen Netzwerk der Schächte und Strecken oder in Röhrensystemen und (ii) verlangsamer Transport im vergleichsweise wenig durchlässiger erzführender geklüfteter Gesteinsmatrix. Reaktive Transportmodelle, die auf reinen Kontinuumansätzen (Einfach-, Doppel- und Mehrkontinuumsmodelle) basieren, können für die Modellierung des reaktiven Stofftransportes im untertägigen Bergwerken nicht eingesetzt werden, da das repräsentative Elementar-Volumen-Konzept im Regionmaßstab nicht für das diskrete Röhrennetz als Grundlage für die Formulierung des Transports verwendet werden kann. RUMT3D besteht aus einem Standard Transportmodell (MT3DMS), einem Röhrentransportmodell und einem Standard geochemischen Modell (PHREEQC-2).

Aufgrund der Kopplung von RUMT3D zu PHREEQC-2 kann es eine Vielzahl von Problemstellungen, die die Nachbildung von chemisch-reaktiven Prozessen, wie z. B., Komplexbildung, Lösung und Ausfällung von Mineralen, Ionenaustausch und Redoxreaktionen in der Gesteinsmatrix, handhaben. Sowohl Gleichgewichts- als auch kinetisch kontrollierte Reaktionen können simuliert werden. RUMT3D ist auf Bergbaugebiete unterschiedlicher Komplexität in Struktur und Anzahl von Komponenten anwendbar, da ein numerisch robuster Algorithmus zur effizienten Lösung des Transportes in den diskreten Röhren zusätzlich implementiert wurde. Außerdem kann RUMT3D für alle Domänen mit einem eingebetteten Röhrensystem, wie z.B., diskrete geklüftete Gebiete, diskrete Karstgebiete oder Aquifere mit Bohrlöchern, eingesetzt werden. Diese Domäne mit eingebetteten Röhrensystemen werden in dieser Arbeit allgemein als Hybridsystem bezeichnet.

RUMT3D wurde auf der Grundlage von drei unterschiedlichen Benchmark-Problemen, einer Quasi-analytischen Lösung und zwei numerischen Programm-codes sowie Plausibilitätsanalysen evaluiert. Das erste Problem verifiziert die Kopplung der zwei Transportmodelle für das Kontinuum und für das Röhrensystem innerhalb RUMT3D durch Überprüfung der Implementierung des neu integrierten Transportlösers für Advektion im Röhrensystem. Es wurde ein Benchmark-Problem mit einem Röhrensystem gewählt, für das eine Quasi-analytische Lösung bereits zur Verfügung stand. Die anderen zwei Probleme (das AMD und das Königstein Problem) verifizieren den reaktiven Transport in dem Kontinuum. Das AMD Problem simuliert die prinzipiellen Prozesse des Acid Mine Drainage Phänomens während das Königstein Problem den Transport von saurem Wasser, Sulfat und gelösten Metallen einschließlich gelöstem Uran in einem Grundwasserleiter stromabwärts von einem Bergwerksgebiet simuliert.

Auf der Basis des AMD Problems wurde die Konsistenz, Stabilität und die Genauigkeit der reaktiven Ergebnisse bezüglich der Charakteristiken eines einfachen Bergwerksystems (oder allgemein eines Hybridsystems) durch Plausibilitätsanalysen untersucht.

Für das erste Benchmark-Problem konnte eine gute Übereinstimmung der Ergebnisse von RUMT3D mit der Quasi-analytische Lösung erzielt werden. Diese Übereinstimmung war unter der Verwendung von wesentlich grösseren Transportzeitschritten und Röhrendiskretisierung im Vergleich zu der standard Finite Differenz Methode zu beobachten. Auch für die zwei anderen Benchmark-Probleme konnten zufriedenstellende Ergebnisse mit RUMT3D im Vergleich zu den jeweiligen numerischen Programmcodes erzielt werden. Plausibilität der reaktiven Ergebnisse von RUMT3D für ein Hybridsystem konnte durch vier unterschiedliche Szenarien gezeigt werden. Diese Szenarien wurden zuerst für das Kontinuumsystem analysiert, um ungewöhnliche Phänomene besser zu identifizieren, die sich eventuell durch die Inkorporation des Röhrentransportmodells ergeben haben könnten.

Die gute Übereinstimmung der Ergebnisse von RUMT3D mit den unterschiedlichen Lösungen und numerischen Programmcodes sowie der Plausibilitätsanalysen weisen auf eine angemessene Kopplung der drei unterschiedlichen Modelle (d.h., MT3DMS mit dem Röhrentransportmodell und PHREEQC-2) innerhalb RUMT3D hin. Somit ist RUMT3D ein verlässliches reaktives Simulationswerkzeug für Kontinuums- und Hystemsysteeme. Darüber hinaus zeigen die Ergebnisse, dass zur Simulation des Schadstofftransports in Hybridsystemen die Berücksichtigung von schnellen Transportwegen unerlässlich ist. Ein Röhrensystem bestimmt erheblich die hydraulischen Verhältnisse in einem Hybridsystem und ist deshalb für die schnellen Änderungen im hydrogeochemischen Milieu verantwortlich.

Schlagwörter:

Gekoppeltes diskretes Grundwasser System, gekoppeltes diskretes Kontinuum System, Röhren-Matrix System, diskretes System, Kontinuum-Röhrentransport Modell, numerisches Modell, diskretes Röhrentransportmodell, Röhrennetzformulierung, numerische Modellierung, numerische Simulation, reaktive Transportmodellierung.

*Success is a measure of interrelationship with people and organisations.*

## **Acknowledgements**

First of all, I am very much indebted to Prof. Dr. Martin Sauter, my PhD supervisor, who applied for funding at the European Commission and at the German Research Foundation (Deutsche Forschungsgemeinschaft, DFG, see preface); accepted me as a PhD candidate after having had troublesome experience with a researcher; gave me all the understanding, encouragement and patience in regards to my “big” problems and my objections as well as the most possible freedom within the framework of two projects (see preface) to try things out. Also, he supported me attending a couple of conferences and short courses where I had the opportunity meeting researchers around the world, in particular Professor Chunmiao Zheng, University of Alabama, USA.

Next, I am very grateful to Professor Chunmiao Zheng who invited and took me in for about 10-month in his working group at the University of Alabama. Through his input, I was able to implement the robust numerical algorithm for solving transport in the conduit system as well as to establish the important collaboration with Dr. Henning Prommer, Delft University of Technology, The Netherlands.

Likewise I feel very obliged to Dr. Henning Prommer who agreed to collaborate as well as to put in the effort to come over from Australia to the University of Alabama for 2 weeks. Moreover, he encouraged and helped me simulating reactive transport problems (in particular the Königstein problem) although having had very little background. Further, he was so kind to always provide immediate and helpful technical (and moral) support.

Furthermore, I would like to express my special thanks to Dr. Tobias Licha, Georg-August-University of Göttingen (Goettingen) who participated promptly my work by providing very valuable feedback, helpful comments and interesting discussions in respect with the geochemical aspects of my reactive transport simulations.

I would also like to thank Gaisheng Liu, University of Alabama who assisted me preparing the numerical algorithm for solving transport in the conduit system more efficiently.

Appreciation is also expressed to Dr. Stefan Birk and Dr. Sebastian Bauer, Eberhard-Karls-University of Tübingen (Tuebingen), Germany who helped me out when I run in trouble applying the hybrid flow model CAVE properly.

I also greatly appreciate the assistance from Dr. Ulrich Mayer, University of British Columbia, Canada and Jeff Bain, University of Waterloo, Canada in providing the data for the most challenging benchmark problem in this thesis work (i.e., the Königstein problem) and valuable suggestions to achieve comparable results.

I also want to thank members of the PIRAMID project (Passive In-situ Remediation of Acidic Mine/Industrial Drainage) for having had open ears for this research at the workshop meetings. I am very grateful having had the opportunity

meeting those with whom I may collaborate in future research projects.

Thanks also go to the European Commission which funded the PIRAMID project and the German Research Foundation (DFG) which funded the other project about simulating reactive transport in underground mines (see preface).

Jeff Bain; Janek Greskowiak, Leibniz-Institute of Freshwater Ecology and Inland Fisheries, Berlin, Germany; Dr. Tobias Licha; Dr. Rudolf Liedl, Eberhard-Karls-University of Tübingen; Gaisheng Liu; Chinnathambi Esakki Perumal, University of Alabama; Dr. Henning Prommer; Prof. Dr. Martin Sauter and Dr. Harald Zänker, Research Centre (Forschungszentrum) Rossendorf, Germany deserve special thanks for taking the time to review parts of this manuscript critically.

Further special thanks go to my friends who shared my happiness, frustrations and sorrows as well as to my parents who gave me moral support regarding what and where I wanted to pursue my higher education.

I could extend this list a lot more but will stop here to give the reader the opportunity to read about my research. I apologise for not having mentioned everyone with name who has helped me in this successful research endeavour. Thanks a lot.

## **Dedication**

This thesis is dedicated to Dr. Glenn S. Warner, University of Connecticut, USA who was my former supervisor of an internship and diploma thesis required by the Polytechnical Institute (Fachhochschule) Regensburg where I studied Applied Mathematics. Further, he was my supervisor of a subsequent Master of Science programme in the field of Natural Resources at the University of Connecticut. Dr. Glenn S. Warner was the one who stimulated my interest in the field of Soil Science/Water Resources and who encouraged me to pursue a scientific career.

*The known is finite, the unknown infinite; intellectually we stand on an islet in the midst of an illimitable ocean of inexplicability. Our business in every generation is to reclaim a little more land*

....

*Thomas Henry Huxley on the reception of On the Origin of the Species (1887)*

## Table of Contents

<b>1 INTRODUCTION</b>	<b>1</b>
1.1 MOTIVATION	1
1.2 OTHER POTENTIAL APPLICATION AREAS OF REACTIVE HYBRID TRANSPORT MODELS	2
1.3 OBJECTIVES AND SCOPE	4
1.4 ORGANISATION OF THE THESIS	5
<b>2 CONCEPTUAL FRAMEWORK AND SOLUTION APPROACHES</b>	<b>6</b>
2.1 INTRODUCTION	6
2.2 TRANSPORT MODELLING	7
2.2.1 <i>Types of Groundwater Systems</i>	8
2.2.2 <i>Transport Processes</i>	9
2.2.3 <i>REV Approach</i>	9
2.2.4 <i>Principle of Continuity</i>	10
2.3 TRANSPORT MODELS	10
2.3.1 <i>Coupled Conduit-Continuum Systems</i>	10
2.3.2 <i>Hybrid Systems</i>	12
2.4 REACTIVE TRANSPORT MODELLING	13
2.4.1 <i>Definition of Reactive Transport</i>	13
2.4.2 <i>Equilibrium Vs. Kinetic Formulation in Reactive Transport Models</i>	14
2.4.3 <i>Coupling Techniques</i>	17
2.4.4 <i>Numerical Techniques and Computational Time</i>	19
2.5 REACTIVE TRANSPORT MODELS	21
2.5.1 <i>Continuum Systems</i>	21
2.5.2 <i>Hybrid Systems</i>	30
2.6 SUMMARY AND IMPLICATIONS	33
<b>3 THEORETICAL DEVELOPMENTS</b>	<b>35</b>
3.1 HYBRID FLOW MODELLING APPROACH: CAVE	35
3.2 HYBRID TRANSPORT MODELLING APPROACH: UMT3D	40
3.2.1 <i>Transport Solvers for the Conduit System</i>	43
3.2.2 <i>Time Criterion for the Transport Solvers for the Conduit System</i>	43
3.2.3 <i>Mass Balance in the Conduit System</i>	44
3.3 REACTIVE HYBRID TRANSPORT MODELLING APPROACH: RUMT3D	44
<b>4 EVALUATION OF REACTIVE TRANSPORT MODELS</b>	<b>46</b>
4.1 TERM DEFINITIONS AND DISCUSSIONS	47
4.1.1 <i>Evaluation, Verification and Validation</i>	47
4.1.2 <i>Illustration and Plausibility</i>	48
4.1.3 <i>Benchmark Problems</i>	48
4.2 GENERAL DESCRIPTION OF METHODS OF EVALUATION AND EXAMPLES	48
4.2.1 <i>Verification</i>	49
4.2.2 <i>Illustration</i>	50

4.2.3	<i>Validation</i>	50
4.2.4	<i>“Benchmarking” Models</i>	51
4.3	SUMMARY AND IMPLICATIONS	51
<b>5</b>	<b>VERIFICATION OF UMT3D BY PERFORMANCE COMPARISON OF THE TRANSPORT SOLVERS FOR THE CONDUIT SYSTEM</b>	<b>53</b>
5.1	INTRODUCTION	53
5.2	DESCRIPTION OF THE CONDUIT SYSTEM	53
5.3	PERFORMANCE OF UMT3D	54
5.4	SUMMARY	56
<b>6</b>	<b>VERIFICATION OF THE REACTIVE PACKAGE WITHIN RUMT3D AND PLAUSIBILITY TESTS</b>	<b>57</b>
6.1	ACID MINE DRAINAGE (AMD)	57
6.1.1	<i>Description of the Benchmark Problem</i>	58
6.1.2	<i>Geochemical Processes during Transport</i>	60
6.1.3	<i>Setup of the Benchmark Problem and Model Comparison</i>	61
6.1.4	<i>Description of the Hybrid System</i>	73
6.1.5	<i>Setup of the Hybrid System</i>	73
6.1.6	<i>Flow Field of the Hybrid System</i>	74
6.1.7	<i>Plausibility Tests</i>	76
6.1.8	<i>Plausibility of the Reactive Transport Results in the Pure Continuum System</i>	78
6.1.9	<i>Plausibility of the Reactive Transport Results in a Hybrid System</i>	89
6.1.10	<i>Summary</i>	98
6.2	EFFECT OF ACIDIC PROCESS WATER UPON AN AQUIFER FROM A URANIUM MINE SITE	99
6.2.1	<i>Description of the Benchmark Problem</i>	100
6.2.2	<i>Model Parameters</i>	102
6.2.3	<i>Problem Setup</i>	105
6.2.4	<i>Simulation Results and Geochemical Processes during Transport (Calcite Scenario)</i>	108
6.2.5	<i>Accuracy of the Simulation Results</i>	123
6.2.6	<i>Summary</i>	126
<b>7</b>	<b>RECOMMENDATIONS</b>	<b>127</b>
7.1	KINETICALLY CONTROLLED INTRA-AQUEOUS REACTIONS	127
7.2	GEOCHEMICAL REACTIONS IN THE CONDUIT SYSTEM	128
7.3	HETEROGENEOUS SURFACE REACTIONS	128
7.4	RATE LIMITING DISSOLUTION-PRECIPIATION REACTIONS	130
7.5	NUMERICAL OPTIMISATION	131
7.6	COLLOIDS	133
7.7	SUMMARY	135
<b>8</b>	<b>CONCLUSIONS</b>	<b>136</b>

## List of Tables

Table 1: Main characteristics of reactive transport models.	23
Table 2: Initial chemical composition of the recharge, tailing and aquifer solution of the McNab model.	59
Table 3: Chemical reaction equations of the considered mineral phases in the McNab model, along with their thermodynamic constants (pK, mainly taken from the WATEQ database).	60
Table 4: Characteristics of the investigated cases for the introduced conduit system in the McNab problem.	73
Table 5: Description of the scenarios for the plausibility tests.	77
Table 6: Initial chemical composition of the recharge solution for scenario 4 and of the aquifer solution for scenarios 3.	77
Table 7: Dissolved and precipitated amounts and fractions of the different mineral phases of scenarios 1-4 for a continuum system after 20 years.	81
Table 8: Dissolved and precipitated amounts and fractions of the different mineral phases of scenarios 1-4 for a hybrid system with a conduit system consisting of 2 nodes, using an exchange coefficient of $6 \times 10^{-6} \text{ m}^2 \text{ s}^{-1}$ after 20 years.	92
Table 9: Dissolved and precipitated amounts and locations of the different mineral phases of scenarios 1-4 for a hybrid system with a conduit system consisting of 2 nodes, using an exchange coefficient of $1 \times 10^{-7} \text{ m}^2 \text{ s}^{-1}$ after 20 years.	95
Table 10: Dissolved and precipitated amounts and locations of the different mineral phases of scenarios 1-4 for a hybrid system with a conduit system consisting of 70 nodes, using an exchange coefficient of $5 \times 10^{-8} \text{ m}^2 \text{ s}^{-1}$ after 20 years.	97
Table 11: Reactive transport sensitivity studies as given by Bain et al. (2001).	102
Table 12: Hydrogeological parameters of the 4 <sup>th</sup> aquifer ( <i>Short Section</i> , WASY, 1995, Bain et al. 2001).	102
Table 13: Source and background water composition (Bain et al. 2001).	103
Table 14: Initial aquifer mineralogy for the calcite scenario.	104
Table 15: Chemical reaction equations of the considered mineral phases for the <i>Short Section</i> , calcite scenario (Bain et al. 2001).	105

## List of Figures

Fig. 1: Schematic of groundwater systems with embedded conduit systems.	8
Fig. 2: Model components of CAVE, UMT3D and RUMT3D.	36
Fig. 3: Illustration of porous material cell-conduit exchange.	42
Fig. 4: Evaluation instruments for models.	46
Fig. 5: Configuration of the 3 way pipe network system of the test problem.	54
Fig. 6: Comparison of the simulation results using the FD method with pipe discretisations of 1 and 0.1 m.	55
Fig. 7: Comparison of the simulation results using the EMCNOT and the FD method.	56
Fig. 8: 1D McNab model for simulation of simple acid mine drainage phenomena (McNab 2001).	58
Fig. 9: Simplified dissolution/precipitation processes of the aqueous and solid phases in the aquifer in the McNab model.	61
Fig. 10: Comparison of simulated tracer profiles of the McNab problem with the RUMT3D and PHREEQC-2 models using different spatial discretisations of 10, 2 and 1 m per cell after 1 year. The recharge, tailing and aquifer solution had initial concentrations of 0.01, 0.005, 0.001 mol L <sup>-1</sup> , respectively.	62
Fig. 11: Comparison of simulated calcium (a, c, e, g) and pH (b, d, f, h) profiles after 0, 1, 2 and 5 years, respectively, for the McNab problem using different discretisations of 10, 2 and 1 m per cell. Results are compared to the PHREEQC-2 model.	66
Fig. 12: Comparison of simulated calcium profiles with the PHREEQC and RUMT3D models after 1 year, for the McNab problem using discretisation of 10 m per cell. Two different reaction time step (ts) sizes were used for the RUMT3D model per year (100 and 1000).	68
Fig. 13: Comparison of simulated pH, sulphate, Fe(II) and goethite profiles after 20 years, for the McNab problem using 10, 100 and 200 reaction time steps (ts) per year in RUMT3D. Results are compared to the PHREEQC-2 model.	70
Fig. 14: Simulated sulphate, Al(III) and goethite profiles after 10 and 20 years, for the McNab problem using the PHREEQC-2 and RUMT3D models.	72
Fig. 15: Simulated pyrite profiles after 20 years, for the McNab problem with the PHREEQC-2 and RUMT3D models, using initial calcite concentrations of 1 and 10 mol L <sup>-1</sup> in the aquifer.	72
Fig. 16: Comparison of simulated tracer profiles for a hybrid system consisting of a single conduit after 1 year using 50 and 750 subsections within the single conduit.	74
Fig. 17: Effect of the conduit system in the McNab problem upon head distribution along the tailing and aquifer.	75
Fig. 18: Effect of the conduit systems in the McNab problem upon flow rates in the continuum.	76
Fig. 19: Simulated pH profiles of scenarios 1-4 for a continuum system after 20 years.	79

Fig. 20: Simulated temporal pH profiles of scenario 1 for a continuum system.	79
Fig. 21: Simulated temporal pH profiles of scenario 4 for a continuum system.	80
Fig. 22: Simulated kaolinite profiles of scenarios 1, 2 and 3 for a continuum system after 20 years.	82
Fig. 23: Simulated goethite profiles of scenarios 1-4 for a continuum system after 20 years.	83
Fig. 24: Simulated gypsum profiles of scenarios 1-4 for a continuum system after 20 years.	83
Fig. 25: Simulated pyrite profiles of scenarios 1-4 for a continuum system after 20 years.	84
Fig. 26: Simulated Fe(II) profiles of scenarios 1-4 for a continuum system after 20 years.	85
Fig. 27: Simulated sulphate profiles of scenarios 1-4 for a continuum system after 20 years.	85
Fig. 28: Simulated pe profiles of scenarios 1-4 along the column for a continuum system after 20 years.	86
Fig. 29: Simulated Fe(II) profiles of scenario 1 for a continuum system after 20 years, using initial calcite concentrations of 1 and 10 mol L <sup>-1</sup> in the aquifer.	87
Fig. 30: Simulated pH profiles of scenarios 1-3 for a continuum system after 20 years, using an initial calcite concentration of 10 mol L <sup>-1</sup> in the aquifer.	88
Fig. 31: Simulated pe profiles of scenarios 1-3 for a continuum system after 20 years, using an initial calcite concentration of 10 mol L <sup>-1</sup> in the aquifer.	88
Fig. 32: Simulated pH profiles of scenarios 1-4 for a hybrid system consisting of 1 conduit with 2 nodes, using an exchange coefficient of 6 x10 <sup>-6</sup> m <sup>2</sup> s <sup>-1</sup> after 20 years.	90
Fig. 33: Simulated Fe(II) profiles of scenarios 1-4 for a hybrid system consisting of 1 conduit with 2 nodes, using an exchange coefficient of 6 x10 <sup>-6</sup> m <sup>2</sup> s <sup>-1</sup> after 20 years.	90
Fig. 34: Simulated pH profiles of scenario 1 for a hybrid system consisting of 1 conduit with 2 nodes, using an exchange coefficient of 6 x10 <sup>-6</sup> m <sup>2</sup> s <sup>-1</sup> .	91
Fig. 35: Simulated pH profiles of scenarios 1-4 for a hybrid system consisting of 1 conduit with 2 nodes, using an exchange coefficient of 1 x10 <sup>-7</sup> m <sup>2</sup> s <sup>-1</sup> after 20 years.	94
Fig. 36: Simulated pH profiles of scenario 1 after 20 years for a hybrid system consisting of 70 conduits (70con) using 4 different exchange coefficients (ex) versus only a continuum system.	96
Fig. 37: Geographical and hydrogeological setting of the Königstein mine as provided by Bain et al. (2001).	100
Fig. 38: Conceptual model for the <i>Short Section</i> , calcite scenario.	104
Fig. 39: Comparison of simulated chloride concentrations for the conservative scenario with the RUMT3D model using different spatial discretisations (2.5, 5 and 10 m per cell). The conservative and the calcite scenario of the MIN3P model are also shown.	106
Fig. 40: Comparison of simulated chloride concentrations for the conservative and	

calcite scenario with the RUMT3D model using different spatial discretisations (2.5, 5 and 10 m per cell) and dispersivities (disp) of 2.5 and 5 m. The calcite scenario of the MIN3P model is also depicted.	107
Fig. 41: Simulated concentrations of siderite, uraninite and ra-barite at the 1000 m observation point using RUMT3D (calcite scenario).	109
Fig. 42: pH buffering stages for the calcite scenario as simulated at the 1000 m observation point.	109
Fig. 43: Simulated concentrations of calcite, gibbsite, ferrihydrite and gypsum at the 1000 m observation point using RUMT3D (calcite scenario).	110
Fig. 44: Transport and attenuation of sulphate and metals in the calcite, gibbsite and ferrihydrite stages.	111
Fig. 45: Simulated Fe(III) concentrations at the 1000 m observation point for both, the MIN3P and RUMT3D models (conservative case and calcite scenario).	112
Fig. 46: Simulated Fe(II) concentrations at the 1000 m observation point for both, the MIN3P and RUMT3D models (conservative case and calcite scenario).	113
Fig. 47: Simulated U(VI) concentrations at the 1000 m observation point for both, the MIN3P and RUMT3D models (conservative case and calcite scenario).	113
Fig. 48: Simulated U(IV) concentrations at the 1000 m observation point for both, the MIN3P and RUMT3D models (conservative case and calcite scenario).	114
Fig. 49: Simulated pe at the 1000 m observation point for both, the MIN3P and RUMT3D models (conservative case and calcite scenario).	114
Fig. 50: Simulated calcium concentrations at the 1000 m observation point for both, the MIN3P and RUMT3D models (conservative case and calcite scenario).	115
Fig. 51: Simulated sulphate at the 1000 m observation point for both, the MIN3P and RUMT3D models (conservative case and calcite scenario).	116
Fig. 52: Simulated carbonate concentrations at the 1000 m observation point for both, the MIN3P and RUMT3D models (conservative case and calcite scenario).	116
Fig. 53: Simulated otavite, Cr(OH) <sub>3</sub> and smithsonite concentrations at the 1000 m observation point for both, the MIN3P and RUMT3D models (conservative case and calcite scenario).	117
Fig. 54: Simulated Cd(II) concentrations at the 1000 m observation point for both, the MIN3P and RUMT3D models (conservative case and calcite scenario).	118
Fig. 55: Simulated Cr(III) concentrations at the 1000 m observation point for both, the MIN3P and RUMT3D models (conservative case and calcite scenario).	118
Fig. 56: Simulated Zn(II) concentrations at the 1000 m observation point for both, the MIN3P and RUMT3D models (conservative case and calcite scenario).	119
Fig. 57: Simulated aluminium concentrations at the 1000 m observation point for both, the MIN3P and RUMT3D models (conservative case and calcite scenario).	120
Fig. 58: Simulated SiO <sub>2</sub> concentrations at the 1000 m observation point for both, the MIN3P and RUMT3D models (conservative case and calcite scenario).	120
Fig. 59: Simulated silicon concentrations at the 1000 m observation point for both, the MIN3P and RUMT3D models (conservative case and calcite scenario).	121

Fig. 60: Simulated potassium concentrations at the 1000 m observation point for both, the MIN3P and RUMT3D models (conservative case and calcite scenario).	121
Fig. 61: Simulated barium concentrations at the 1000 m observation point for both, the MIN3P and RUMT3D models (conservative case and calcite scenario).	122
Fig. 62: Simulated radium concentrations at the 1000 m observation point for both, the MIN3P and RUMT3D models (conservative case and calcite scenario).	123
Fig. 63: Comparison of simulated U(VI) concentrations of the calcite scenario with the RUMT3D and MIN3P models. 5 m and 2.5 m represent a spatial discretisation of 5 m and 2.5 m per cell, 7300ts refers to a reaction time step size of 5 days and disp denotes dispersivity.	124
Fig. 64: Comparison of simulated U(VI) concentrations of the calcite scenario with the RUMT3D and MIN3P models. A spatial discretisation of 5 and 10 m per cell and a reaction time step size of 5 and 36.5 m are used in the RUMT3D model, respectively.	125
Fig. 65: Simulated chloride concentrations at the 1000 m observation point for both, the MIN3P and RUMT3D models (conservative case and calcite scenario).	145
Fig. 66: Simulated fluoride concentrations at the 1000 m observation point for both, the MIN3P and RUMT3D models (conservative case and calcite scenario).	146
Fig. 67: Simulated phosphorus concentrations at the 1000 m observation point for both, the MIN3P and RUMT3D models (conservative case and calcite scenario).	146
Fig. 68: Simulated lead concentrations at the 1000 m observation point for both, the MIN3P and RUMT3D models (conservative case and calcite scenario).	147
Fig. 69: Simulated magnesium concentrations at the 1000 m observation point for both, the MIN3P and RUMT3D models (conservative case and calcite scenario).	147
Fig. 70: Simulated nickel concentrations at the 1000 m observation point for both, the MIN3P and RUMT3D models (conservative case and calcite scenario).	148
Fig. 71: Simulated sodium concentrations at the 1000 m observation point for both, the MIN3P and RUMT3D models (conservative case and calcite scenario).	148

*The sciences do not try to explain, they hardly even try to interpret, they mainly make models. By a model is meant a mathematical construct which, with the addition of certain verbal interpretations, describes observed phenomena.*

*John von Neumann, physicist*

## **Preface**

This PhD thesis is the result of two projects, started at Friedrich-Schiller-University of Jena, Germany and completed at the Georg-August-University of Göttingen, Germany under the supervisor of Prof. Dr. Martin Sauter.

Main financial support came from the European Commission (EU) within the context of the consortium PIRAMID (Passive In-situ Remediation of Acidic Mine/Industrial Drainage) led by Prof. Paul Younger at the University of Newcastle upon Tyne, UK. PIRAMID was funded within the Fifth Framework Research and Technical Development (RTD) Programme of the EU (Key Action 1: Sustainable Management and Quality of Water), Contract Number EVK1-CT-1999-000021. Research institutions from five EU member states (France, Germany, Spain, Sweden and the UK) and one accession state (Slovenia) contributed to the PIRAMID project. Within this project, I was responsible for the development and evaluation of a reactive hybrid transport model (RUMT3D) that would be able to address concentration loads of contaminants from flooded underground mine workings to passive in-situ remediation systems such as wetlands. Contributions from the other research institutions can be found at <http://www.piramid.org>.

Funding was continued by the German Research Foundation (Deutsche Forschungsgemeinschaft, DFG, Sa 15-1) within the context of a project in collaboration with the Department of Physical Chemistry at the Friedrich-Schiller-University of Jena (Dr. Jürgen Sonneberg and Prof. Dr. Wolfram Vogelberger). Two main objectives of this project were also to simulate discharge of contaminants from flooded underground mine workings, applicable to, e.g., the former WISMUT uranium mining area of Ronneburg (East Germany) and to eventually predict the kinetically-controlled uranium release in underground mines.

Further funding came from Professor Chunmiao Zheng, University of Alabama, U.S.A. He sponsored my 10-month stay (10. August 2001 - 31. May 2002) in his working group at the University of Alabama. He paid not only several months of salary but also an AGU conference trip to Washington DC and the 2 weeks stay of Dr. Henning Prommer at the University of Alabama. Dr. Henning Prommer, Delft University of Technology, The Netherlands collaborated to this thesis or rather to the above two projects by merging his with my model developments. Further, he supported me evaluating the model (see also acknowledgements).

Initial contribution to this thesis was made by Dr. Hari S. Viswanathan. He established a coupled MT3DMS model version that was capable to simulate instantaneous mixing in shafts, shifts, ventilation raises, adits or conduit systems within underground mines. He was funded by the state Thuringia (Thüringen) of

Germany and through the German Exchange Service Organisation DAAD (Deutscher Akademischer Austausch Dienst).

Further initial contribution to this thesis came from Dr. Sebastian Bauer, Dr. Steffen Birk, Dr. Torsten Clemens, Dr. Dirk Hückinghaus, Dr. Rudolf Liedl, Prof. Dr. Georg Teutsch, Eberhard-Karls-University of Tübingen and Prof. Dr. Martin Sauter who designed the hybrid flow model CAVE. CAVE is necessary to compute the flow field for RUMT3D.

*One learns to hope that nature possesses an order that one may aspire to comprehend.*

*Chen Ning Yang, Chinese-American Nobel Prize winner for his work in developing symmetry theory in quantum fields, Elementary Particles (1961)*

## Chapter

### 1 Introduction

#### 1.1 Motivation

Groundwater contamination by acidic drainage from mines and also from mine wastes is one of the main environmental problems faced by many countries (Nordstrom & Alpers 1998; Mayer 1999). Additionally, at sites of uranium mining, exposure of receptors to radioactivity might result from the migration of radionuclides within the subsurface. In many cases the oxidation of naturally abundant pyrite has shown to be the key process that causes the acidic geochemical environment (Singer & Stumm 1970; Wisotzky 1996; Wunderly et al. 1996). Germany, for instance, is facing such problems. Statistically, the German Democratic Republic (GDR) was the third largest producer of uranium (Kinze 2002) until 1989 worldwide behind the United States and Canada (Merkel et al. 1995). Most of the mines in the GDR got closed after the unification of Germany due to environmental concern. Since then the remediation company WISMUT, which was the former uranium mining company established by the Russian in the GDR, has had to deal with remediation of their former production sites. A remediation technique used in abandoned underground mines is flooding, which re-establishes the reducing conditions in order to prevent further pyrite oxidation and its associated effects such as acid production and high concentrations of dissolved iron and sulphate (Singer & Stumm 1970). Predictions of the potential generation and release of polluted drainage from mines support rehabilitation and remediation as well as prevention of damage to the environment, e.g., during and also after flooding of old mine workings (Bain et al. 2001).

Underground mines are typically composed of networks of highly conductive 'pipes' or 'conduits', representing shafts, drifts, ventilation raises, or roadways (Younger 2002) within an otherwise considerably less permeable ore material (country rock, goaf, porous matrix, background aquifer or continuum). These highly conductive conduits are often sparsely-distributed and also likely possess no characteristic size limits in the porous matrix. As result of such a discrete conduit system, mines are characterised by two distinct flow (and transport) regimes: (i) rapid, perhaps turbulent flow in discrete conduits and, (ii) flow at comparably small velocities within the surrounding continuum flow system. Consequently, it can be expected that existing geochemical constituents will very probably be more spread out in mines than in systems without conduits. Since

the characteristic properties of the conduits cannot be formulated with uniform continuous variables, the representative elementary volume is macroscopically invalid for the discrete conduit networks. Therefore, reactive transport models that are only based upon continuum approaches (i.e., single, double and multiple continuum models) cannot be employed for the simulation of reactive transport in mines (see also Chapter 2.3.2). Also, because the quantification of contaminant flux from the solid mineral phase into the mobile water phase as well as chemical reactions are controlled by the actual surface area between rock matrix and mobile conduit water, continuum models cannot handle such problems. Simulation of transport in such domains might best be accomplished by so-called "hybrid" models, which combine aspects of discrete and continuum models (Berkowitz 2002). Such a hybrid model allows basically process-orientated simulations of the reactive transport within underground mines while obtaining results in a reasonable time. Further, with such a model, the controlling (physical as well as chemical) parameters in mines may more readily be identified. In literature, however, there are only very few reactive hybrid transport models available that have considered main geochemical reactions in domains such as underground mines (compare Chapter 2.5.2).

## **1.2 Other Potential Application Areas of Reactive Hybrid Transport Models**

Reactive hybrid transport models could also be used as predictive and or explorative tools for the decision making over whether passive in-situ remediation techniques are suitable for the remediation of polluted discharge from underground mines, or for the assessment of the scope for natural attenuation to yield waters of acceptable quality. Prerequisites for such type of assessments are to quantify the likely ranges of contaminant concentrations (spatial and temporal). This in turn implies a robust understanding of the processes of contaminant movement and retardation. A passive treatment system such as a specific type of wetland can be considered as a suitable technique for remediation only if the maximum concentration ranges of the discharged contaminants stay within tolerable limits. Apart from maximum concentration ranges, it is important for the designer of the wetland to know which types of contaminants and concentration variations can possibly be expected in the discharge water under given conditions. A wetland is an alternative remediation method for cleaning contaminated water. In contrast to traditional methods of treatment, wetlands require little maintenance and make use of the power of nature. Traditional methods for cleaning contaminated water involve water handling and chemical treatment.

For a few years now, several nations have been planning on disposing or already disposed their radioactive wastes in

- mines like ancient salt mines (Wilhelm et al. 2002),
- low-permeability formations (Steeffel & Lichtner 1998b),
- evaporite (e.g, halite) formations (Berkowitz 2002),
- crystalline rock (Gylling et al. 1999) where fractured media is predominant.

Also, karstic or fractured systems can prevail networks of highly conductive and sparsely-distributed conduits or discrete conduit networks (compare Chapter 2.2.1). For the safe operation of nuclear waste repositories, which may take tens to hundreds of thousands of years, the physical and chemical properties of the mines or fractured host rocks should remain ideally constant (Steeffel & Lichtner 1998b). It is advisable in terms of time, cost and potential environmental disasters to use reactive transport models (in some cases hybrid models might be better) as predictive and study tools. As a matter of fact, it is unrealistic to perform experiments over hundreds of years. Also, such experiments could become expensive and may require release of contaminants into mines or fractures to investigate their threat to the environment and humans. Through parameter variations, critical reaction-induced modifications of the physical and chemical properties of the near-field host or ore rock (which could change behaviour of the system) could possibly be identified through the use of reactive hybrid transport models. In general, variability of the dissolution and precipitation rates (i.e., solubilities) depend upon various factors, such as:

- the chemical composition of the rock matrix and the aqueous solution,
- the rock-solution interface area,
- the thickness of the diffusional layer adjacent to the interface,
- the occurrence of surface coatings,
- the temperature and the flow conditions (Berkowitz 2002).

Wilhelm et al. (2002) indicated that in ancient salt mines, formation waters of different origin may penetrate the repository, which may then mobilise radionuclides. Evaporite (e.g., halite) formations in areas of waste repositories could trigger land subsidence through dissolution processes, which in turn has an effect on the long-term viability of the repositories. Apart from that, because evaporite formations exhibit relatively high solubilities and reactivities, they have a critical influence on the evolution of the groundwater system as well as of the groundwater quality (Berkowitz 2002). In Nordic countries, safe operation of nuclear waste deposits may not be performed anymore when dissolved oxygen from melting ice penetrates to certain depths. The concern is that the dissolved oxygen would oxidise the rock matrix and trigger the release of heavy metals such as uranium. According to Suksi et al. (2002), examples concerning uranium mobilisation related to the late stage of the glacial cycle were reported by Blomqvist et al. (2000) which were studied in scope of a European-funded Palmottu natural analogue project. Also, Rasilainen et al. (2003) investigated the uranium release triggered through glacial melt water pulses in rock matrix adjacent to water-carrying fractures.

Reactive hybrid transport models can possibly be further employed to assess vulnerability of discrete karstic system and the physico-chemical effects surrounding the immediate area of injection boreholes in complex hydrogeological environments. Especially in fractured or karstic systems, interactions between the mass transport mechanisms and the changing properties of the media through the dissolution and precipitation processes need additionally be accounted for.

### 1.3 Objectives and Scope

One of the main objectives of this thesis is to develop or build a basis for a 3-D reactive hybrid transport model (RUMT3D, 3-Dimensional Reactive Underground Mine Transport Model), which is capable of handling transport in the porous matrix (continuum) and discrete conduit network and the main geochemical reaction processes (i.e., redox, complexation, and dissolution/precipitation) including the capability to consider kinetic rate expressions in the continuum. Mass exchange between the continuum and conduit system is controlled by local parameters such as hydraulic conductivity of the matrix and geometrical factors, hydraulic heads and concentration. RUMT3D may also be referred to as 3-Dimensional Reactive Underground Mass Transport Model or it may also be thought of an expansion of the 3-Dimensional Mass Transport model, MT3D developed by Zheng & Wang (1999). MT3D or rather MT3DMS, a standardised transport model for multi-species in saturated porous media, is one of the three models that is coupled in RUMT3D. The other two models that are coupled in RUMT3D are the geochemical model PHREEQC-2 developed by Parkhurst & Appelo (1999) and a conduit transport model similar to the one developed by Birk (2001) or Liedl et al. (2003).

The second objective of this thesis work is to implement a robust numerical algorithm to solve transport in the conduit system more efficiently and with less numerical dispersion than the standard finite difference method so that RUMT3D can be applied in solving reactive problems with complex conduit systems and large numbers of reactive components.

The third objective of this work is to evaluate and demonstrate that RUMT3D can be useful in solving hypothetical and real-world problems. This is accomplished by solving three different types of benchmark problems. In one case study, the newly implemented more robust transport solver is applied for a conduit system as compared to a semi-analytical solution and the standard finite difference method. Coupling of the two transport models (i.e., MT3DMS and the conduit transport model) in RUMT3D was thereby verified. The other two problems evaluate the coupling of the reactive module, i.e., PHREEQC-2 to the transport models within RUMT3D. One problem simulates the principle processes of the Acid Mine Drainage (AMD) phenomena (McNab 2001) while the other one simulates transport of acidic water, sulphate, dissolved metals including dissolved uranium in an aquifer downgradient from a mine site (Bain et al. 2001). The latter problem uses real-world data from a former uranium mine site located in Saxony, Germany. Performance of RUMT3D was verified against two models (PHREEQC-2 and MIN3P). McNab (2001) used PHREEQC-2 to simulate the AMD problem using its 1D transport capacity while Bain et al. (2001) used MIN3P. MIN3D is a general-purpose multicomponent reactive transport model developed by Mayer (1999). Because of its lower complexity, the AMD problem was in addition taken as basis for investigating the reactive simulation results of RUMT3D in a simple mine system towards consistency, accuracy and stability by means of plausibility tests. The influence of the conduit discretisation and of the magnitude of the conduit-matrix exchange is thereby also studied.

---

## 1.4 Organisation of the Thesis

This thesis reports both the development and evaluation of the process-based numerical tool RUMT3D supporting the quantification of reactive transport in flooded underground mines of saturated hybrid systems in general. Accordingly, the first major part of this thesis is devoted to (i) the introduction of processes, concepts and solution approaches involved in modelling (reactive) transport (Chapter 2) and (ii) the development of RUMT3D by outlining its underlying theory including implementation of a robust numerical transport solver for the conduit system (Chapter 3). The second major part of this thesis defines evaluation of models (Chapter 4.1), presents evaluation procedures in general (Chapter 4.2) and those of RUMT3D (Chapters 5 and 6). Specifically, Chapter 5 deals with the verification of the two transport models (for the continuum and for the conduit system) within RUMT3D and Chapter 6 focuses on the verification of the reactive transport module within RUMT3D and on plausibility tests. The next chapter (7) suggests further developments and applications of RUMT3D to make the model applicable to a wide range of existing problems of varying complexity. The last chapter (8) concludes this thesis.

*Scientific theory is just one of the ways in which human beings have sought to make sense of their world by constructing schema, models, metaphors and myths. Scientific theory is a particular kind of myth that answers to our practical purposes with regard to nature.*

*Mary Hesse, professor, Cambridge University, The New York Times (Oct. 22, 1989)*

## Chapter

### 2 Conceptual Framework and Solution Approaches

To contribute towards a better understanding of the selected conceptual framework and solution approaches for the reactive hybrid transport model RUMT3D developed in this thesis, this chapter discusses those of several (reactive) (hybrid) transport models to date. It is divided into six sections. The first section outlines necessity of fundamental (reactive) transport models as well as various factors that have controlled the types and sophistication of (reactive) transport models. The second section is devoted to presenting concept for modelling conservative transport while the fourth one is assigned to introducing concept and solution approaches for modelling reactive transport. The third and the fifth sections provide overview of different types of transport and reactive transport models, respectively, which are available in literature to simulate (reactive) transport in systems with and without conduits. In the fifth section, examples of different types of reactive transport models are also given. The sixth section summarises this chapter as well as raises some implications for the development and usage of reactive (hybrid) transport models.

#### 2.1 Introduction

Clinton W. Hall, the director of the National Risk Management Research Laboratory, Subsurface Protection and Remediation Division, USA and Yeh & Cheng (1999) stated in a foreword and the abstract of an EPA report describing a three-dimensional model of density-dependent subsurface flow and thermal multispecies-multicomponent HYDROGEOCHEMical Transport (3DHYDROGEOCHEM): “*Subsurface fate and transport models provide (1) a tool of application, with which one is able to deal with a variety of real-world problems, (2) a tool of education, with which one can study how a factor would affect the whole system, and (3) a substructure, which one could modify to handle specific problems.*” In other words, Clinton W. Hall and Yeh & Cheng (1999) supported the necessity to develop fundamental reactive transport models as predictive and study tools, which can be used in industry as well as in academia. Such fundamental models can also be modified for the inclusion of certain effects observed in the laboratory or field. Therefore, reactive transport models could be useful tools for, e.g.,

- interpreting phenomena such as weathering, diagenesis, ore deposition, etc. in geochemistry,

- predicting displacement of oil by chemical flooding in reservoir engineering,
- forecasting fate of pollutants in soil, groundwater and deep rock formations in contaminant hydrology and hydrogeology,
- quantifying fluxes along flow paths that control element cycling in biogeochemistry (Cvetkovic 1997).

In particular, increase in the contamination of groundwater resources has led to the development of numerous (reactive) transport models in recent years. Typical factors that have controlled types and sophistication of such models are:

- type of (groundwater) system,
- type and or level of contamination,
- reaction type (equilibrium versus kinetic),
- available computational power,
- degree of process understanding,
- possible conceptualisation of the coupled flow, transport and geochemical mechanisms,
- availability of existing model modules, including flow models,
- available coupling as well as numerical techniques,
- financial and time constraints (limitations),
- objectives or purposes of studies (e.g., model to support remediation of former mining areas or model to assess lifetime performance of waste repository),
- necessity of comparing performance of models having different concepts and techniques,
- production of a more reliable description of the system behaviour, especially when no analytical solutions are available,
- accuracy or reliability of predictions (Pfingsten & Carnahan 1995).

From the aforementioned factors, it is quite understandable that developing one universal reactive transport model that can solve all the (reactive) transport problems is highly improbable. In general, the more comprehensive a model is, the more input parameters are required. Moreover, a comprehensive model tends to have many degrees of freedom. Where too few input parameters are known, the model results may be incorrect. In many cases, the different types of questions to be answered towards the investigation of a practical problem may be better answered by means of a specially designed model with comparably small computational requirements and therefore little time.

## 2.2 Transport Modelling

As this section introduces concept for modelling conservative transport in different types of (groundwater) systems, it provides brief overviews of the

- different types of systems existing in the environment,

- important processes involved in simulating transport,
- conceptualisation of the transport processes into a model (REV approach),
- principle of continuity.

### 2.2.1 Types of Groundwater Systems

The most idealised groundwater system consists of one solid phase distributed uniformly throughout the water-saturated soil body, i.e., of one homogeneous solid phase and of the water phase. In most existing groundwater systems, however, many solid phases co-exist which are in nearly all cases non-uniformly distributed throughout the water-saturated soil body. Therefore, existing groundwater systems are very often heterogeneous systems. Additionally, different chemicals may be dissolved in the water phase due to various reasons such as injection and or dissolution of solid phases (see Chapter 6). Along with the water and solid phases, other phases may be present in groundwater systems, namely the gaseous phase and phases that are liquid phases but are immiscible with the other phases. These immiscible phases are referred to as non-aqueous liquid phases, i.e., NAPLs.

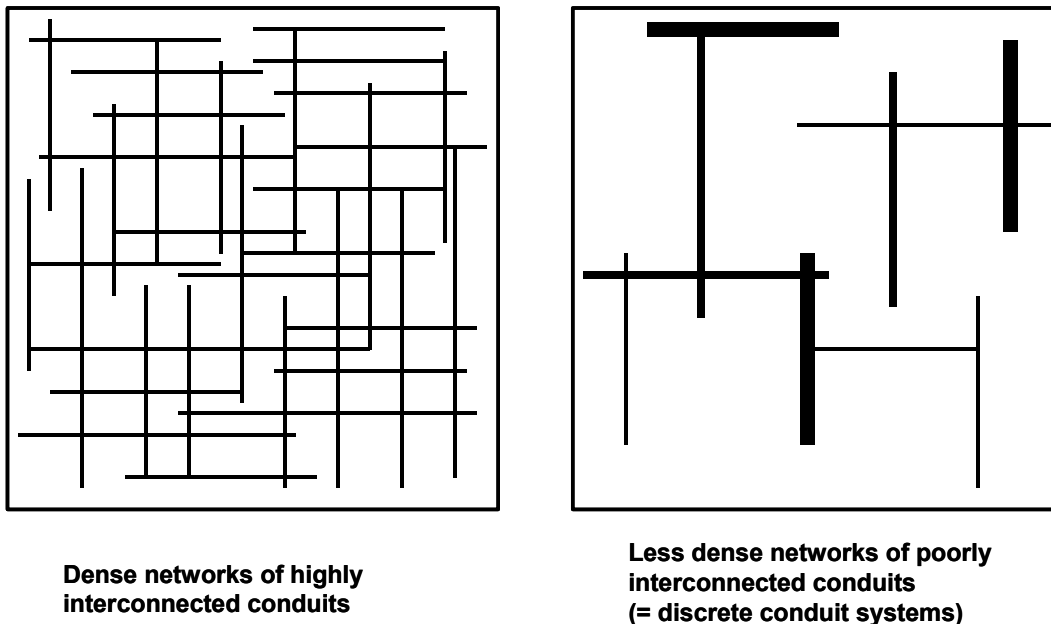


Fig. 1: Schematic of groundwater systems with embedded conduit systems.

Further, there are groundwater systems, either naturally formed or man-made, that enclose networks of fractures, roadways, shafts or general conduits. These networks can be dense/less dense with highly/poorly interconnected conduits (Fig. 1). Both types of networks (dense and less dense) with (highly and poorly interconnected) conduits can be found in fractured/karstic systems while sparse single distributed or discrete conduits are predominant in underground mines and

also aquifers intersected by boreholes. Also, the discrete conduits do not likely possess any characteristic size limits (compare Chapter 1.1). In this work, systems with dense networks of highly interconnected conduits are referred to as coupled conduit-continuum systems and the systems with the poorly interconnected networks are referred to as coupled discrete-continuum or hybrid systems.

### 2.2.2 Transport Processes

Advection, dispersion and molecular diffusion are the main processes that control the contaminant transport in groundwater systems. The bulk displacement of (dissolved) species with the flowing groundwater causes advective transport in the aqueous phase. The hydraulic gradient is thereby the driving force for this transport mechanism (Mayer 1999). Dispersion is caused by mechanical dispersion, a result of deviations of the actual velocity on a microscale from the average groundwater velocity (Zheng 1990) or more generally as a result of heterogeneity in the flow field (Fabritz 1995). Thus, dispersion in porous media causes spreading of contaminants over a greater region than would be predicted solely from the groundwater velocity vectors (Zheng 1990). Molecular diffusion is technically a chemical process in which the concentration gradients cause the transport of dissolved species (Mayer 1999). In common modelling practice, diffusion and dispersion are combined into a lumped term, into a so-called hydrodynamic dispersion term. Diffusion process becomes more important at low groundwater velocities. For many practical transport problems in groundwater, the advection term dominates. Advection-dominated problems are also referred to as sharp front problems (Zheng 1990).

### 2.2.3 REV Approach

Like groundwater flow models, (reactive) transport models are also a conceptualisation of a natural system (Mayer 1999). The concept can be explained as the replacement of a discrete physical system consisting of mineral particles and pore spaces partially filled with water by a continuum in which physico-chemical variables vary continuously in space (Lichtner 1996). This conceptualisation is based on the Representative Elementary Volume (REV) approach introduced by Bear (1972). The REV approach expresses the physical-chemical parameters such as concentrations or generally the discrete characteristics of a natural system as average (mean) values or variables on a scale, known as the REV-scale, though they are actually microscopic parameters. This approach also permits any number of continua to occupy the same physical space at the same time (Bear 1972; Lichtner 1996) and allows the coexistence of any number of species within each phase (Bear 1972; Mayer 1999). Simply, the physical characteristics of a natural system, which can microscopically be very heterogeneous, are averaged over a special volume. As such, the mean variables can be described by functions which are continuous at the macroscale in space and time (Bear 1972; Lichtner 1995; Lichtner 1996; Mayer 1999). The REV-concept is the basis for the continuum approach. Once

system variables can be expressed in the form of continuous functions, the physical transport of a constituent (component or species) can be mathematically expressed by Partial Differential Equations (PDE). These equations include the important physical transport processes such as advection and sources/sink terms in the model domain.

#### **2.2.4 Principle of Continuity**

The principle of continuity states that no mass can be lost. REV also obeys this principle i.e., all (dissolved) species in each REV that are transported follows this principle of continuity.

### **2.3 Transport Models**

As long as a (groundwater) system possesses any homogenisation scale, at least in mathematical terms, a REV can be defined, and the concepts of continuum models can be used. In literature, numerous single, double and multiple interacting continua models can be found (see Chapter 2.3.1). Obviously, the more phases and processes as well as heterogeneities need to be considered for a simulation, the more comprehensive a model needs to be at the end. Transport in a system consisting just of the water and solid phases can be simulated with a transport model that is developed for saturated porous media such as MT3D (Zheng 1990). But when the gaseous phase takes up a significant portion of the groundwater system, a transport model for unsaturated porous media should be used in order to obtain more appropriate results. Depending upon the existence of heterogeneity structures in model domains, various deterministic and stochastic formulations of equations can be used in transport models. Heterogeneity structures can significantly spatially vary velocity fields. Such velocity fields may be better quantified with stochastic models such as Monte Carlo, by means of perturbation, and random walk analyses than with the deterministic models which only condition heterogeneity structures in model domains (Berkowitz 2002). The following two subsections discuss model approaches to simulate transport in coupled conduit-continuum and hybrid systems.

#### **2.3.1 Coupled Conduit-Continuum Systems**

Homogenisation scales can also be found in groundwater systems with embedded dense networks of highly interconnected conduits or fractures (Berkowitz 2002). Therefore, for such coupled conduit-continuum systems, the REV approach can be used and concepts of continuum models can be applied. Similar to hybrid systems, two different aspects are combined in coupled conduit-continuum, namely the velocities in conduits are often relatively high compared to the ones in the continuum matrix. Thus, the combination of conductive conduits and considerably less permeable continuum results in two possible very distinct flow and transport regimes, i.e., one in the conduits and one in the continuum (compare Chapter 1.1). However, depending upon the magnitude of

exchange between conduits and porous matrix, migration rates along possible highly conductive conduits can also significantly be reduced (Ghogomu & Therrien 2000 for fractured systems). Generally, it can be stated that in systems with embedded conduits, the hydrodynamic dispersion arises mainly from advective and diffusive exchange between faster flow in the conduit and slower flow (or possibly even immobile water) in the rock matrix (Xu & Pruess 2001). Factors such as the relative time scales for global flow and transport in coupled conduit-continuum systems and degree of interaction between the conduit and matrix system to establish a local equilibrium determine the type of (single, double or multiple) continuum models that is to be used (Berkowitz 2002). The basic idea behind all these approaches is to explicitly resolve domains with different advective velocities through appropriate spatial discretisation (gridding) to account for their “hydrodynamic dispersion” (Xu & Pruess 2001).

*Single continuum model approach.* This is the simplest, maybe also the first and foremost convenient approximation of modelling the contaminant transport in groundwater systems with dense networks of highly interconnected conduits. It uses the concept of a single or an effective continuum - equivalent porous medium - model (ECM). The individual conduits are treated, as would they be individual pores in the porous media with different hydraulic conductivities. In each REV, the ECM assumes that the conduits and matrix have the same state variables such as concentrations (Pruess et al. 1990; Xu & Pruess 2001; Berkowitz 2002).

*Double continuum model approach.* For groundwater systems with dense networks of highly interconnected conduits for which the ECM is not valid, it is maybe more appropriate to use the concept of a double porosity or double continua, in which the conduits and matrix are treated as two separate interacting continua. In this methodology, a network of interconnected conduits is embedded in a matrix block of low permeability in each REV. The double-porosity approach considers only global flow and transport through the conduit network, which describes the effective porous continuum (Xu & Pruess 2001). The porous host rock behaves thereby as a storage/release reservoir for solutes. For such flow and transport conditions, various phenomenological “mobile-immobile” models have been developed (Berkowitz 2002). To let the two continua interact, an exchange function is introduced. Fluid is thereby exchanged between the matrix continuum and conduits locally, through so-called “interporosity flow”, which is controlled by the difference in, such as the hydraulic heads between the two continua (Xu & Pruess 2001). When in addition to the conduit network, as the matrix has to take an active part in transporting solutes, the concept of a dual- or double-permeability approach can be used. In this approach, the interaction between conduits and adjacent “host rock” strongly control the flow and transport through the entire system (Berkowitz 2002).

*Multiple continuum model approach.* If the embedded conduit networks have different properties or scales themselves (which may be the case for fractures which were generated by more than one process), but are still dense and the conduits within these networks are highly interconnected, a more accurate representation of the “dispersive processes” in the coupled conduit-continuum system may be achieved with the method of “multiple or overlapping interacting

continua” (Berkowitz 2002). In this approach, the matrix rock is partitioned into several interacting continua that are defined based on the distance from the nearest conduit (Xu & Pruess 2001). Also, to describe more accurately transient interporosity flow and transport by resolving driving gradients such as of concentration at the conduit-matrix interface, the method of multiple interacting continua (MINC) can be utilised. Resolution of gradients near the conduit-matrix interface can be achieved by appropriate subgridding the matrix blocks. The TOUGH family models, for instance, use the MINC concept (Pruess 1983; Pruess & Narasimhan 1985). According to Xu & Pruess (2001), the MINC method is similar to the “shrinking core” model (Davis & Ritchie 1986; Wunderly et al. 1996). Comparable multiple interacting continua conceptualisations have been used in studies to describe the interplay between fast advective transport in rootholes, wormholes, and cracks, with slow flow and diffusive transport in the soil matrix (Gwo et al. 1996; Xu & Pruess 2001). Apparently, multiple interacting continua approaches require larger computational requirements than other types of continuum models due to the further detailed discretisation of a rock matrix. It is to be noted that multi-continuum model approaches find only validity for heterogeneous media in which regions of higher permeability form spatially extensive correlated structures (Xu & Pruess 2001).

### 2.3.2 Hybrid Systems

As already discussed in Chapter 1.1, in coupled discrete-continuum or hybrid systems with non-homogenisation scale, the REV approach is not valid for the discrete conduit system. Therefore, hybrid models, which combine aspects of discrete, and continuum models were suggested to simulate (reactive) transport in such domains. As such, the discrete part of a hybrid model could explicitly account for effects of individual conduits on fluid flow and solute transport (Ghohomu & Therrien 2000), which continuum models could not account for. This is in particular necessary for old mines that are often geometrically complex. The simplest hybrid model considers flow and transport processes within a single conduit (Berkowitz 2002).

Similarity between simulating flow and transport in underground mines shows that eventually a hybrid approach is necessary to deal with uncertainties and complexity of mine structures. Several methods for estimating the duration of the first flush are briefly described here. The first flush refers essentially to the process of initial displacement of the volume of the mined system through recharged water after completion of rebound or the time that it took for the mine to completely flood following the cessation of pumping ( $=dr(T)$ ). Prediction of  $dr$  is necessary to intercept polluted mine waters before causing damage to the surface environment.  $dr$  could theoretically be predicted from mine survey records because it is a function of the void volume of the flooded mined system and the rate of recharge if

- direct measurement of ‘goaf’ areas (collapsed roof strata) in mines were more practical,
- the estimation techniques for that purpose were more reliable and or

- the volume of unmined strata around the mine voids which have been dewatered by mine drainage were more precisely known.

However, since, as outlined above, measurement techniques do not or cannot provide precise numbers about the mine void volume, two other types of approximations can be utilised which were in particular acknowledged useful by Younger (2002), namely, the semi-distributed lumped-parameter and the physically-based, distributed models. Semi-distributed lumped-parameter models, also known as 'pond models' or 'box models', are often sufficiently simple that they can be implemented within a spreadsheet environment. This is possible by reducing the complexity of both mined void volumes and recharge processes through 'lumping together' large volumes of extensively-interconnected mine voids as single hydrological units ("ponds"). In general, pond-based rebound models are best applied to relatively large-scale mine systems, such as hundreds to thousands of square kilometre underlying areas (Younger 2002). Physically-based, distributed models regard mines as systems of conduits (representing mine roadway networks / stopes, in which flow may well be turbulent) routed through heterogeneous, variably-saturated porous media (representing the enclosing rockmass, both intact strata and rocks which have fractured in response to mining of voids nearby). However, unlike the 'pond' models, these demand numerical methods to find solutions. The mined voids can be mathematically expressed in many ways. One option is to use the Navier-Stokes theory to represent the mine system as a multiple-fracture system. This option is probably the most appropriate when the "conduits" are irregular, planar fractures. Though, in most mined systems, the major conduits are tube-like roadways that are better represented as pipes rather than planar fractures. Therefore, models like the VSS-NET, a purpose-written code in which a 3-D pipe network formulation (based on the Darcy-Weisbach formula and the Gradient Algorithm network solver) is routed through a 3-D, column-oriented (as opposed to layer-oriented), block-centred finite difference grid that is configured to solve for saturated-unsaturated flows (Younger 2002).

## **2.4 Reactive Transport Modelling**

This section presents concepts and solution approaches for modelling reactive transport. Specially, it starts with a definition of reactive transport, followed by a discussion of an equilibrium versus a kinetic formulation in reactive transport models. Since coupling techniques of models can significantly influence efficiency and accuracy of simulation results, a subsection on that topic appeared essential when existing models are combined like it was the case for RUMT3D. It concludes with a subsection to briefly discuss numerical techniques and other techniques to further improve computational efficiency.

### **2.4.1 Definition of Reactive Transport**

Reactive (geochemical) transport can be referred to as a collective understanding of mass transfer (or more general to the transformation of chemical constituents) from one phase to another and the transport of

constituents within the coexisting aqueous and solid phases (Narasimhan & Apps 1990; Cheng & Yeh 1998). As such, when water flows through a porous medium, the carried dissolved constituents or components can react with the ones present in the water body and possibly with the minerals in the transport matrix (Gao et al. 2001). Consequently, new aqueous complexes may be formed as well as minerals may be dissolved and or precipitated. Therefore, the reactive transport involves hydro-physical and chemical processes (Yeh & Tripathi 1991). The most important hydro-physical processes are solute advection and dispersion (see also Chapter 2.2.2) while the main geochemical processes are aqueous complexation, ion exchange, oxidation-reduction (redox), precipitation-dissolution and acid-base reactions (Gao et al. 2001). In addition to advective and dispersive transport, molecular diffusion can also be an important transport mechanism (Narasimhan et al. 1986) depending upon the problems. These hydro-physical and chemical processes have naturally occurred during the evolution of the earth, such as part of the weathering of the rocks (Bäverman et al. 1999).

While transport processes will tend to offset the equilibrium-state of a particular solid-aqueous phase system (e.g., through injection or infiltration of water that has a different chemical composition from the already existing groundwater), geochemical reactions will tend to re-establish an equilibrium condition. Basically, transport processes are the driving force for geochemical reactions to occur and force the groundwater system towards a new and often-different equilibrium state. Reactive transport models may be utilised to track such involved compositional changes within the water and solid phases (Mayer 1999).

#### **2.4.2 Equilibrium Vs. Kinetic Formulation in Reactive Transport Models**

During a reactive transport simulation, the temporal scales of the various transport and reaction processes control which formulation, should be used to best describe the chemical rate expressions (Mayer 1999). An equilibrium instead of a kinetic formulation for a reaction may be used as long as the local equilibrium assumption (LEA) is valid. LEA requires that the reaction time scale is sufficiently fast enough relative to the transport time scale, to establish a local equilibrium throughout a model domain (Yeh & Tripathi 1989; Novak & Sevougian 1992; Walter et al. 1994; Viswanathan 1996; Gao et al. 2001). An equilibrium formulation, however, describes only the final composition of a geochemical system while a kinetically controlled description formulates the transient chemical evolution towards an equilibrium state. Therefore, the kinetic formulation is more general, and enables essentially both equilibrium and kinetic reactions to be modelled with the same general formulation (Steeffel & Lasaga, 1994; Viswanathan 1999) as well as allows reactions to occur on any time scale (Novak & Sevougian 1992). Though, due to being dependent on the reaction path (Lasaga 1981), kinetically-controlled rate reactions are inherently more difficult to describe than an equilibrium one in reactive transport models. As a result, a kinetic formulation is computationally more intensive (Zysett et al. 1994) and causes generally more numerical difficulties to find a solution than equilibrium formulations. Mathematically expressed, for an equilibrium formulation by applying LEA to all reaction source/sink terms in the reactive

transport equation set, a set of mixed partial differential/algebraic (Zysett et al. 1994) is obtained instead of a set of a mixed partial/ordinary differential equation for a kinetic formulation (Viswanathan 1996). The resulting set of nonlinear algebraic and partial differential equations describing equilibrium concentrations and transport, respectively, can then be solved separately. By minimising the total Gibbs free energy of the chemical system (Novak & Sevougian 1992), solutions for each master or primary species or component can be found for the set of nonlinear algebraic equations. As equilibrium relationships are uniquely defined by the law of mass action (Novak & Sevougian 1992), once concentrations of the different components are known, concentrations of each complexed specie in (local) equilibrium with each component/master species can easily be computed from the concentrations of their components and their respective thermodynamic constants (K) (Viswanathan 1996). The concentration of the complexed species, calcium carbonate ( $[\text{CaCO}_3]$ ), for instance, is calculated from the concentrations of its components  $[\text{Ca}^{2+}]$  and  $[\text{CO}_3^{2-}]$  and from the K value of  $10^{-3.224}$ . Moreover, by replacing the kinetic by the equilibrium relationships, the number of unknowns describing a reaction network can greatly be reduced. This is because for each equilibrium relationship that replaces a kinetic relationship, one primary unknown can be eliminated. Numerically, the number of primary unknown ( $N_p$ ) per spatial discretisation point can be decreased to the number of components ( $N_c$ ) instead of  $N_c + N_x + N_g + N_s + N_m$  ( $N_x$  = number of aqueous complexes,  $N_g$  = number of gaseous phases,  $N_s$  = number of sorbed species to the mineral surfaces,  $N_m$  = number of mineral phases), or even less, if mineral phases are at equilibrium with the solution (Mayer 1999). With regards to the convergence, the replacement of kinetic controlled rate expressions by equilibrium relationships decreases the stiffness of the set of equations associated with an improvement of its convergence properties. Thus, an equilibrium description may also provide a solution algorithm that converges better than a kinetic description.

Despite of being computationally more intensive and having more numerical problems, kinetic formulations are often demanded to describe mineral rock interactions such as precipitation/dissolution, which often display kinetic limitations in many groundwater systems (Steefel & Lasaga 1994). For such problems, the local equilibrium assumption might not be applicable (Viswanathan 1996). The LEA assumption may also not be applicable to some very slow reactions such as the acid buffering reactions with non-carbonate minerals and redox reactions without acceleration, e.g.,  $\text{Fe}^{2+}/\text{Fe}^{3+}$  transfer without bacterial acceleration (Gao et al. 2001). In fractured system, since solid phase reactions can potentially plug pores or open fractures reducing matrix diffusion and promoting rapid flow through fractures (Yeh et al. 2001), a kinetic formulation may be required to describe such effects more appropriately. Further, amorphous phases that are commonly encountered in ashes and slags are limited by a finite dissolution rate or non-existence of equilibrium and need therefore a kinetic formulation (Bäverman et al. 1999). Nevertheless, an equilibrium formulation, although a kinetic one is required, can still be helpful in finding quicker solutions, where a chemical system will proceed with the given boundary conditions, such as those of redox systems.

Another criterion to decide whether an equilibrium formulation may be used is to

rely upon the differentiation between homogeneous and heterogeneous reactions. Geochemical processes of interest in groundwater systems can be divided into homogeneous and heterogeneous reactions. Homogeneous (or also intra-aqueous, Novak & Sevougian 1992) reactions take place in a single phase (e.g., aqueous complexation between dissolved constituents) while heterogeneous reactions involve mass exchange between two or more phases such as dissolution and precipitation of minerals (Mayer 1999). As a rule of thumb, homogeneous reactions may be described by equilibrium formulations whereas heterogeneous reactions may need kinetic formulations (Novak & Sevougian 1992).

Due to computational limitations and numerical problems as well as the virtually nonexistent database of kinetically controlled rates (Pfingsten & Carnahan 1995), the earlier simulation codes that coupled chemistry with transport typically assumed that all geochemical components present in a system were in local equilibrium (Cederberg et al. 1985; Engesgaard & Kipp, 1992; Rubin, 1983; Yeh & Tripathi 1989). In present days also, equilibrium approaches in reactive transport models are popular due to the accessibility of large geochemical databases and sophisticated software packages (Viswanathan 1999). However, to allow kinetic controlled rate expressions for certain types of reactions, the current trend in reactive transport simulation is to develop combined kinetic and equilibrium transport, mixed equilibrium/kinetic models (Viswanathan 1999) or partial equilibrium transport models (Mayer 1999). This type of approach is not as computationally intense as that of fully kinetic models. Several options are available to add a mixed kinetic/equilibrium reaction capability to reactive transport models. A common technique adopted by mixed equilibrium-kinetic reactive transport codes is the reduction of the number of independent variables by using the idea of chemical components. A set of chemical components or master or primary species is defined as the minimum number of species that uniquely describe a chemical system (Mangold & Tsang 1991). By transporting components rather than species, the number of coupled partial differential equations (PDEs) is reduced. Due to the reduction of mixed partial and ordinary differential equations, the mixed formulation solves for fewer coupled PDEs and will therefore also be computationally more efficient than a fully kinetic formulation (Viswanathan 1996). An alternative to a mixed equilibrium/kinetic approach is to make use of so-called pseudo-kinetic rate expressions like the CHEMFRONTS model developed by Bäverman et al. (1999) does. This also allows relaxing the stringent conditions of local equilibrium.

In sum, consideration of not only equilibrium but also kinetic chemistry, along with the hydrologic transport and the interaction between fluid flow and reactive transport is necessary to be able to reflect the complexity of many real systems (Yeh et al. 2001). Due to the current existence of a considerable body of knowledge of mineral kinetic rate constants, the increase in relatively inexpensive computational resources as well as developments in formulating chemical rate expressions, in recent years, a number of kinetic controlled reactions are possible to include in a simulation along with equilibrium reactions while achieving results in a reasonable time.

### 2.4.3 Coupling Techniques

As different reactive transport processes are coupled, there is always the question of the most efficient coupling technique. The accuracy and efficiency of different coupling techniques or strategies of reactive transport models have internationally been investigated for years now (Herzer & Kinzelbach 1989; Yeh & Tripathi 1989; Steefel & MacQuarrie 1996; Xu et al. 1999; Robinson et al. 2000; Saaltink et al. 2001; Barry et al. 1996, 1997, 2002).

One-step method. Conceptually, the simplest coupling technique is the one-step method, global implicit method, fully coupled method (FCA, Viswanathan 1996) or the direct method (Ghogomu & Therrien 2000). This method solves transport and reaction equations simultaneously in one time step. According to Yeh & Tripathi (1989), there are two approaches to obtain a solution for the one-step method, which are, the mixed Differential-Algebraic Equation (DAE) approach and the Direct Substitution Approach (DSA). These two approaches determine the number of primary unknowns or dependent variables of the resulting equation set in the reactive code. For the DAE approach, all chemical species or components retain as primary unknowns since the chemical reaction expressions are not substituted into the transport equations, but are nevertheless solved simultaneously with the transport equations. For the DSA, since equilibrium expressions can be substituted directly into the transport equations (compare Chapter 2.4.2), the number of primary unknowns can greatly be reduced (Mayer 1999). Another advantage of the one-step method is that, there is no stability criterion for the time step size required, provided that it is used in conjunction with an implicit temporal discretisation. However, there are two major limitations associated with the usage of this method. Although the one-step method is less computationally intensive with the DSA than with the DAE approach, for some problems, it may still be quite an effort to solve the fully coupled non-linear set of equations for each time step. Additionally, especially for problems with a large number of nodes and or chemical species/components, an extremely high CPU memory may be required (Suarez & Simunek 1996; Ghogomu & Therrien 2000). For such problems, the two-step or operation-split-methods may be the only feasible methods to use (Ghogomu & Therrien 2000).

Two-step methods. Two-step methods solve the advection and dispersion terms separately from the reaction term in the reactive transport equation. As such, the two-step methods divide the solution into physical transport and chemical steps (Walter et al. 1994). Significant savings in CPU memory can be achieved by separating calculation of the transport from the reaction terms. Other big advantages of the two-step methods are that those methods supports usage of individual routines, existing transport and geochemical models including geochemical databases as well as ease of parallelisation of the overall algorithm (Steefel & Lasaga 1994; Walter et al. 1994; Mayer 1999). Therefore, problem and or process specific algorithm can be utilised to account for the varied temporal and or spatial scales of reactive transport processes and other mathematical properties (Ghogomu & Therrien 2000; Barry et al. 2002). Better additional computational efficiency as well as convergence can thereby be achieved. A reactive transport model such as PHT3D (Prommer 2002; Prommer et al. 2003, see also Chapter 2.5.1) takes advantage of the controlled time step

refinement according to the stability or accuracy criteria of the different sub models for advective/dispersive transport and for reactions. Specially, within PHT3D, the standard transport model MT3DMS (Zheng & Wang 1999) solves the advective/dispersive transport and the PHREEQC-2 model (Parkhurst & Appelo 1999) solves for the reactions during a reactive transport simulation. Two-step methods, however, assume that there is no spatial connection for the chemical reactions and that *“the chemical reactions depend only on local conditions at each time step and at each point in the system”* (Ghogomu & Therrien 2000).

In the classical two-step method SNIA (Sequential Non-Iterative Approach), a reactive time step follows a transport time step. To make SNIA more computationally efficient, especially for problems that require small transport or reaction time step sizes, more than one transport time steps before each reaction step or vice versa are performed. Such a modified SNIA, for instance, is utilised in PHT3D. However, depending upon the temporal discretisation (for more detailed discussion, see subsection criteria for coupling techniques), a significant error (splitting error) compared to the exact solution of the reactive transport equation can be generated in SNIA. The approximation or splitting error of SNIA can be minimized or eliminated by a so-called Sequential Iterative Approach (SIA), which allows iterations between the transport and reaction steps within one time step. To make the SIA method more efficient, it is not necessary to perform a complete reaction step but only to refine the reactive terms in the iterative equation (Steefel & MacQuarie 1996). Other more sophisticated ways for enhancing the computational efficiency of SIA are to divide the full set of equations for the transport and chemical system into numerous equation sets by using certain criteria. Therefore, cycling through the full equation set is not required anymore but only through small subsets. The two sequential iteration approaches, namely the Sequential Species Iteration Approach (SSIA) and the sequential nodes iteration approach developed by Viswanathan (1996), for example, achieve small subsets of the full set of reactive transport equations by neglecting calculation of specific Jacobian cross derivative terms. With SSIA, a subset for each chemical species is obtained. The sequential nodes iteration approach computes only the derivatives with respect to the node  $p$  in the calculation. The derivatives from the neighbouring nodes,  $p-1$  and  $p+1$  are thereby neglected in the calculations. As a consequence of neglecting calculation of certain terms, SSIA and the sequential nodes iteration approach may not converge under all conditions. Another disadvantage of this method when compared to the one-step method is, outer iterations are required for these algorithms to ensure that the entire equation set is solved accurately. As a result, these algorithms may require numerous outer iterations for convergence. Viswanathan (1996) also investigated hybrid versions of SSIA, the sequential nodes iteration approach and of the one-step method. He found that the hybrid version of:

- SSIA and the sequential nodes iteration approach was less efficient than SSIA or the sequential nodes iteration approach
- SSIA and the one-step method was a flexible algorithm since it can simulate mixed kinetic-equilibrium problems.

Criteria for coupling techniques. The application as well as performance of different coupling techniques can in general be estimated by means of criteria such as Péclet, Courant and Damköhler number. The Péclet number can be used as the criterion for spatial discretisation of the transport, the Courant number for the respective temporal discretisation and the Damköhler number for temporal discretisation of the reaction. Whether the Péclet number needs to be obeyed mainly depends upon the used weighting method for spatial discretisation of the advective term in the transport equation. The spatial, central weighting method, for instance requires a Péclet number smaller than 2 to prevent numerical oscillations. Whereas forward-weighting methods or flux controlled schemes require no limitation of the Péclet number. An advective Courant number smaller than 1 is necessary for every two-step method when the time is weighted after Crank-Nicolson. A necessary requirement of SNIA is to keep the advective and diffusive Courant numbers (= Courant number for purely diffusive transport) smaller than 1. When these criteria are not kept, the aqueous or gaseous species can be transported beyond a cell within one time step without considering that through the reaction processes, transported species can be produced or consumed. SNIA can generate significant errors in this case (Mayer 1999). Viswanathan (1996) found in his study that the sequential nodes iteration approach was very sensitive to the grid Péclet and the Courant number. The Damköhler number ( $Da$ ) can be used to examine validation of the local equilibrium assumption (LEA). If  $Da \gg 1$ , the time scale for the geochemical reactions is much shorter than the one for the physical transport. Therefore, in this case, the geochemical reactions can be simulated as equilibrium reactions. In contrast, if  $Da \ll 1$ , the transport processes are much faster than the geochemical reactions. The kinetical formulations of the reactions are then necessary.  $Da$  can be divided into two numbers ( $Da_1$  and  $Da_2$ ), where  $Da_1$  and  $Da_2$  can be used to determine the slowest reaction and the fastest transport processes, respectively (Mayer 1999).

Models with more than one operator. To accelerate model developments and or to use existing models such as for biological reactions, it is necessary or possible to split the reaction operation in more than one operator. As with one operator, time step sizes more suitable for a problem, the processes and or reaction types can be chosen. In certain circumstances, it is also necessary to split the transport operator in more than one, like it was unavoidable for RUMT3D developed in this thesis. Specially, one operator was required for transport in the continuum and one in the conduits (compare Chapter 3.2).

#### 2.4.4 Numerical Techniques and Computational Time

For the simulation of multi-dimensional and multi-component reactive transport problems, the use of efficient numerical techniques is more important than for conservative transport problems due to having several unknowns at each node in the form of chemical species or components (Ghogomu & Therrien 2000). By solving transport and reactions separately within reactive transport codes, for instance, greater efficiency of a simulation can be achieved by selection of numerical methods, which better suits the nature of the different governing equations. As such, the physical and chemical heterogeneities of a particular

system that are often associated with varied spatial and temporal scales, can individually be treated (compare Chapter 2.4.3). Further, the nonlinearities of the chemical systems can be more appropriate to be accounted for (e.g., Steefel & MacQuarrie 1996). The governing equations of the physical and chemical systems can thereby not only be solved more efficiently but also numerical oscillations and dispersion can be reduced. Under certain conditions, numerical methods can be prone to numerical oscillations and dispersion in space and or time. Oscillations are caused by inappropriate choice of time step sizes. Selection of too large time step sizes produces unstable time oscillations while selection of too small time step sizes generates unstable space oscillations. Time oscillations grow larger with time, which may eventually cause a failure of a simulation. Unlike time oscillations, space oscillations do not increase with time (Fabritz 1995). Finite element methods are popular to better account for irregularly shaped boundaries in groundwater systems (Yeh & Cheng 1999).

For the determination of more appropriate time step sizes, so-called adaptive time stepping and update modification schemes can be utilised. Mayer (1999), for instance, made use of the adaptive time stepping scheme reported by Forsyth & Sammon (1986) and the modified underrelaxation scheme by Cooley (1983) similar to Therrien & Sudicky (1996) in their flow model FRAC3DVS. Mayer (1999) developed the multi-component reactive transport model MIN3P for saturated and unsaturated porous media (see Chapter 2.5.1). Those schemes in MIN3P recognise and consider processes which cause, e.g., high geochemical gradients by migration of contamination fronts, production of redox zone, the existence and non-existence of different mineral phases as well as fast kinetically controlled reactions and rapid transport. Fast kinetically controlled reactions and fast transport processes support development of stiff equations. Stiffness, a phenomenon of dynamical systems occurs when stability constraints demand a time step size that is far smaller than required for the accuracy of the results (Steefel & MacQuarrie 1996). In the employed schemes by Mayer (1999), the relative change in aqueous concentrations and the number of Newton-Iterations from previous time step control the next time step size.

Moreover, accuracy and stability of results may be improved by sub cycling certain processes in particular slow ones until time criteria of the faster processes are satisfied. As such, long time intervals are split in shorter ones. Fast processes are calculated according to the short time interval until a longer one is reached. In the next step, a slower process corresponding to the longer respective time scale is computed (Oran & Boris 2001).

Additionally to save computer time, zones or cells in the model domain in which the concentration of the aqueous or other phases over extended periods of time do not or hardly change, can temporally be excluded from the calculations of geochemical reactions. Zones of negligible activities can occur, for example, by having a point source contamination in the otherwise equilibrated aquifer. Prommer et al. (2003), for example, introduced two criteria in PHT3D (see also Chapter 7.5) to recognise and control such inactive zones. These criteria determine in which cells and to which time, the geochemical calculations are not required. They are based upon tolerance limits or acceptable errors for the relative concentration changes of the aqueous species and of the pH in a cell. As

long as one criterion is not satisfied, the reaction step is activated.

## 2.5 Reactive Transport Models

In the last couple of years, in particular such facts as:

- increase in relatively inexpensive computational power (Steeffel & Lasaga 1994),
- computational ability of supercomputers (Liu & Narasimhan 1989),
- advancements in theoretical geochemistry (Liu & Narasimhan 1989),
- the necessity to demonstrate that models can represent the *true* behaviour of a natural system (Steeffel & van Cappellen 1998)

have encouraged development and usage of multi-dimensional and multi-component reactive transport models. To simulate the contaminants that are migrating from a landfill into a groundwater aquifer, for instance, requires at least a two-dimensional model to account for vertical infiltration and horizontal groundwater movement. With regards to representation of *true* behaviour of a natural system, the limitations of predictive modelling stem from the logical impossibility of demonstrating that a model for a natural system is true (see also Chapter 4.1.1) or can capture the essential features of a system. Carrying out numerous simulations might not help capturing these features if the models fail to take into account the fundamental processes for these (Steeffel & van Cappellen 1998). Therefore, the challenge in reactive transport modelling nowadays is and should be to show that the models used can represent behaviour of existing systems at the detail looked at. The inclusion to consider various factors such as more problematic chemical processes like kinetical reactions enable more representative descriptions of, e.g., radionuclide transport than the simple decay and linear retardation models before while maintaining reasonable computational efficiency with the currently available computational resources (Viswanathan 1996). Another process very essential for some problems is redox reactions. The formation of many ore deposits of metals (two well-known cases are uranium roll front deposits and supergene sulphide enrichment of copper), for example, is mainly controlled by redox reactions. This is because of the multivalent behaviour of most natural elements existing in the natural environment (Liu & Narasimhan 1989). In the following two subsections, examples of reactive transport models are given for continuum and hybrid systems.

### 2.5.1 Continuum Systems

Due to the need as well as sort of encouragement mentioned in Chapters 2.1 and 2.5, quite a few reactive transport models for continuum systems have been developed in the past two decades. In this subsection, some of those developed models are discussed which are:

- AREAT/TEN3D (Mocker et al. 2002),
- CHEMFRONTS (Bäverman et al. 1999),

- DYNAMIX (Narasimhan et al. 1986, Liu & Narasimhan 1989),
- FEHM (Zyvoloski 1994; Viswanathan 1996; Zyvoloski et al. 1997; Viswanathan et al. 1998; Robinson et al. 2000),
- HYDROGEOCHEM (Yeh & Tripathi 1990; Yeh & Tripathi 1991), 2DHYDROGEOCHEM, 3DHYDROGEOCHEM (Cheng 1995; Yeh & Cheng 1999),
- LEHGC2.0 (Yeh et al. 2001),
- MIN3P (Mayer 1999),
- MINTRAN (Walter et al. 1994),
- PHREEQC-2 (Parkhurst & Appelo 1999),
- PHT3D (Prommer 2002; Prommer et al. 2003),
- REACTRAN2D (Gao et al. 2001),
- RT3D (Clement et al. 1998),
- TOUGHREACT (Xu et al. 2003).

These models can be roughly characterised by (Table 1):

- continuum concept for transport (i.e., single, double or multiple interacting continua concept),
- chemical formulation (i.e., equilibrium, kinetic or mixed),
- coupling technique,
- numerical techniques (e.g., finite elements, finite difference methods),
- considered chemical reactions (aqueous complexation, precipitation-dissolution, adsorption-desorption, oxidation-reduction, ion exchange, redox reactions and acid-base reactions, sorption).

DYNAMIX. DYNAMIX (acronym for DYNAMIC MIXing) is a reactive based single continuum transport model. It consists of a modified version of the transport model TRUMP to handle multiple species and the PHREEQE model (Parkhurst et al. 1980). Instantaneous mixing in a cell is assumed in the DYNAMIX model. It was first developed to simulate the neutralization process between a high-acidic mill-tailings water mixing with neutral groundwater. The model at the stage of development considered only acid-base reactions and precipitation/dissolution of minerals. Later, the model was extended to include algorithm to calculate redox reactions and aqueous complexation. In addition, a mixed (or partial) equilibrium / kinetic formulation was incorporated into the model which allowed to account for both thermodynamic equilibrium and kinetic chemical interaction between aqueous and solid phases. The transport from the chemical reaction equations are sequentially solved with a two-step approach (specially SIA, Suarez & Simunek 1996) in DYNAMIX, i.e., at each time step, the transport equation is first solved by the explicit difference or rather the integral finite difference method, then the geochemical module is called to compute the distribution of chemical species under mixed equilibrium/kinetic conditions (Liu & Narasimhan 1989).

Table 1a: Main characteristics of reactive transport models.

Model	Author(s)	Continuum concept	Model modules	Chemical formulation	Coupling technique	Numerical techniques	Chemical reactions
AREAT/TEN3D	Mocker et al. (2002)	Single		Mixed equilibrium / kinetic	Two-step method (SNIA)	Implicit method	
CHEMFRONTS	Bäverman et al. (1999)	Single		Simplified pseudo-kinetic rate expressions		Finite elements	
DYNAMIX (acronym for DYNAMIC MIXing)	Liu & Narasimhan (1989)	Single	Modified version of the transport model TRUMP and PHREEQE model	Mixed equilibrium / kinetic	Two-step method (i.e., SIA sequential iteration approach)	Integral finite difference method	Acid-base reactions, precipitation/dissolution, redox reactions and aqueous complexation
FEHM (finite element heat and mass transfer)	Zyvoloski (1994); Viswanathan (1996); Zyvoloski et al. (1997); Viswanathan et al. (1998); Robinson et al. (2000)	Single (equivalent continuum model) and dual permeability model (DKM)		Kinetic; mixed equilibrium / kinetic	One-step; two-step method (SIA, selective coupling method)	Finite elements; usage of incomplete factorisation with variable fill-in level as a pre-conditioner and a generalised minimum residual (GMRES) acceleration technique for the iterative solution; Newton-Raphson method	

Table 1b: Main characteristics of reactive transport models.

Model	Author(s)	Continuum concept	Model modules	Chemical formulation	Coupling technique	Numerical techniques	Chemical reactions
HYDROGEOCHEM; 2DHYDROGEOCHEM; 3DHYDROGEOCHEM (3D HYDROlogic transport, GEOCHMical equilibria, subsurface flow, and heat transfer in reactive multi- component/multi- species systems)	Yeh & Tripathi (1990); Yeh & Tripathi (1991); Cheng (1995); Yeh & Cheng (1999)	Single	Equilibrium model EQMOD and flow and transport models FEMWASTE / 2DFEMFAT / 3DFEMFAT	Equilibrium	One-step and two- step method (SNIA)	Flow: Galerkin finite element method; transport: conventional Eulerian and hybrid Lagrangian-Eulerian finite element method); EQMOD: hybrid Newton- Raphson and modified bisection methods	Aqueous complexation, precipitation- dissolution, adsorption (triple layer model) - desorption, oxidation- reduction, ion exchange, redox reactions and acid- base reactions
LEHGC2.0	Yeh et al. (2001)	Single		Mixed equilibrium / kinetic	One-step and two- step method (SNIA, SIA)	Flow: Galerkin finite element method; transport: conventional and hybrid Lagrangian-Eulerian finite element method); geochemistry: Newton-Raphson	
KAFKA (= Kompartimentmodell für die Ausbreitung und die Fluiddynamik in einer konvergierenden Untertageanlage für Abfälle)	Colenco (2001); Wilhelm et al. (2002)	Structural elements					

Table 1c: Main characteristics of reactive transport models.

Model	Author(s)	Continuum concept	Model modules	Chemical formulation	Coupling technique	Numerical techniques	Chemical reactions
MIN3P	Mayer (1999)	Single		Mixed equilibrium / kinetic	One-step method	Finite volume method; spatial weighting schemes for advective transport in the aqueous phase, adaptive time stepping and update modification algorithm	
MINTRAN	Walter et al. (1994)	Single	Transport model PLUME2D and the MINTEQA2	Equilibrium	Two-step method (SNIA, SIA)	Standard Galerkin finite element technique with mass lumping, combined with the Leismann time-weighting scheme	Acid-base, oxidation-reduction, ion exchange, adsorption and precipitation and dissolution reactions
No Name	Ghogomu & Therrien (2000)	Discrete-continuum		Mixed equilibrium / kinetic	Two-step method (i.e., SIA)	Standard Galerkin finite element method; Newton-Raphson technique	
No Name	Viswanathan & Sauter (2001)	Discrete-continuum (no transport in the conduits)	Transport model MT3DMS	Equilibrium	Two-step method (i.e., SNIA)	TVD, characteristic methods (MOC, MMOC, HMOC), standard finite difference methods, Newton-Raphson method	
No Name	Eckart (pers. comm., 2002)	Discrete-continuum		Mixed equilibrium / kinetic			

Table 1d: Main characteristics of reactive transport models.

Model	Author(s)	Continuum concept	Model modules	Chemical formulation	Coupling technique	Numerical techniques	Chemical reactions
PHREEQC-2	Parkhurst & Appelo (1999)	Single	PHREEQE	Mixed equilibrium / kinetic	Two-step method (SNIA)	Explicit finite difference algorithm, forward in time, central in space for dispersion and upwind for advective transport; Newton-Raphson method	Surface-complexation (two layer, diffuse layer and a non-electrostatic model), ion-exchange, reversible and irreversible reactions,
PHT3D	Prommer (2002); Prommer et al. (2003)	Single	Transport model MT3DMS and PHREEQC-2	Mixed equilibrium / kinetic	Two-step method (i.e., SNIA)	TVD, characteristic methods (MOC, MMOC, HMOC), standard finite difference methods, Newton-Raphson method	Aqueous complexation, mineral dissolution/precipitation, and ion exchange
REACTRAN2D	Gao et al. (2001)	Single	Flow and transport model SUTRA and MINTEQA2	Equilibrium	Two-step method (SIA)	Finite elements	Acid-base, oxidation-reduction, ion exchange, adsorption and precipitation and dissolution reactions
RT3D	Clement et al. (1998)		MT3D	Kinetic			Simulate various types of chemical reactions, including microbial metabolisms and microbial transport kinetics
TOUGHREACT	Xu et al. (2003)	Multiple interacting continua concept	Transport model TOUGH2	Mixed equilibrium / kinetic	Two-step method (i.e., sequential iteration approach)	Integral finite differences; implicit time-weighting scheme; Newton-Raphson method; automatic time stepping scheme	Dissolution-precipitation, sorption processes, including cation exchange and surface complexation (by double layer model)

HYDROGEOCHEM, 2DHYDROGEOCHEM, 3DHYDROGEOCHEM. HYDROGEOCHEM (Yeh & Tripathi 1990; Yeh & Tripathi 1991), 2DHYDROGEOCHEM and 3DHYDROGEOCHEM (Cheng 1995; Yeh & Cheng 1999) models are single continuum based finite element reactive multi-species transport models. They consist of the equilibrium model EQMOD and the flow and transport models FEMWASTE, 2DFEMFAT and 3DFEMFAT for saturated and unsaturated conditions. The HYDROGEOCHEM models have a matrix solver, which finds an equilibrium solution for the desired equations and components added by the user. Generalised relations are presented by Yeh & Tripathi (1991) for use in describing kinetic processes, but were not included in the models (see also Suarez & Simunek 1996). EQMOD and the HYDROGEOCHEM models can handle, aqueous complexation, precipitation-dissolution, adsorption-desorption, oxidation-reduction, ion exchange, redox reactions and acid-base reactions, all considering chemical equilibria. The Davies equation is used to compute the activity coefficients. The thermodynamic constants need to be adjusted in numbers for the particular temperature and pressure of the simulation to be run by the user. Acid-base reactions and determination of pH is based upon computation of the proton balance. By defining electron activity as a master variable whereby making it to an aqueous component subject to transport, oxidation-reduction reactions can be handled by these models. The HYDROGEOCHEM models can also let adsorption be handled by the triple layer model after Davis et al. 1978; Davis & Lecki 1978, 1980 (Yeh & Cheng 1999; Suarez & Simunek 1996).

MINTRAN and REACTRAN2D. Another finite element and single based continuum model is the MINTRAN model by Walter et al. (1994). It consists of the finite element transport model PLUME2D and the speciation model MINTEQA2. In MINTRAN, the two two-step methods SNIA and SIA can be used to solve the transport and chemical equations. MINTRAN was primarily designed to model groundwater contamination due to acidic mine tailings effluents. The reactive transport model REACTRAN2D is also based on MINTEQA2 but coupled with the flow and transport model SUTRA (Voss 1984) via SIA. SUTRA is a 2D finite-element model for saturated and unsaturated, fluid density-dependent groundwater flow with energy transport. REACTRAN2D can be used to simulate reactive transport in large groundwater systems where the single continuum concept is applicable. Since a large amount of thermodynamic database is contained in MINTEQA2, both the MINTRAN and REACTRAN2D can simulate pollutant transport involving acid-base, oxidation-reduction, ion exchange, adsorption and precipitation and dissolution reactions (Gao et al. 2001) and both these models use an equilibrium formulation.

FEHM. The finite element heat and mass transfer model FEHM is a versatile code. It utilises the one-step method but also sophisticated two-step (SIA) methods (see Chapter 2.4.3). FEHM employs a fully kinetic formulation and a mixed equilibrium/kinetic formulation. It combines coupled thermal and stress capacities with multiphase flow and transport (Zyvoloski 1994; Viswanathan 1996; Zyvoloski et al. 1997; Viswanathan et al. 1998; Robinson et al. 2000). FEHM was specially designed to model neptunium migration from the potential repository at Yucca Mountain. Along with a single or equivalent continuum concept in FEHM, a dual permeability model can also be utilised (Viswanathan et

al. 1998).

PHREEQC-2. PHREEQC is based upon the PHREEQE model developed by Parkhurst et al. (1980). PHREEQC-2 is the second version of the PHREEQC model that has dispersion in the transport module as an additional module. Compared to all other reactive transport models in this subsection, this model can perform only one-dimensional transport and batch simulations. A modified version of the SNIA is utilised in the PHREEQC-2 model. With this SNIA, for each time step, first advective transport is computed, then all equilibrium and kinetically controlled chemical reactions, then dispersive transport, followed by another computation of all equilibrium and kinetical reactions. According to Parkhurst & Appelo (1999), calculation of kinetic and equilibrium chemical reactions directly after the advection step and directly after the dispersion step reduces numerical dispersion and the need of iterating between chemistry and transport. Transport in PHREEQC-2 is solved with an explicit finite difference scheme that is forward in time, central in space for dispersion, and upwind for advective transport. To simulate surface-complexation reactions, the generalized two-layer model of Dzombak & Morel (1990), a model with an explicitly calculated diffuse layer (Borkovec & Westall 1983) and a non-electrostatic model (Davis & Kent 1990) is implemented in PHREEQC-2. Kinetically controlled reactions can be considered in PHREEQC-2 by incorporating BASIC routines in the database (Parkhurst & Appelo 1999).

MIN3P. Mayer (1999) developed a general multi-component reactive transport model (MIN3P) for variably-saturated porous media. It is a mixed equilibrium / kinetic formulation model which allows consideration of parallel and sequential reactions, as well as irreversible and reversible reactions. Mineral dissolution-precipitation reactions can be expressed as surface- or diffusion-controlled processes (see Chapter 7.4). Efficiency and robustness of MIN3P were increased by implementation of an adaptive time stepping and update modification algorithm (see also Chapter 2.4.4) as well as numerous spatial weighting schemes for advective transport. It uses the one-step method to solve the transport and geochemical processes simultaneously.

AERAT/TEN3D. Another mixed equilibrium / kinetic formulation model is the coupled multi-component reactive two-phase transport model AREAT/TEN3D developed by Mocker et al. (2002). AERAT computes the spatial pressure and saturation curves while TEN3D computes the concentration values in porous media. Aqueous and gaseous components can be transported by convection and diffusion. TEN3D was designed for the simulation of long time release of contaminants in tailings (specially in Ronneburg and Schlema-Alberoda, Germany).

RT3D. RT3D (Clement et al. 1998) is a reactive transport model, which only considers kinetic reactions. It couples the three-dimensional transport model MT3D (Zheng 1990) with a kinetic formulation. The groundwater flow heads required by MT3D are computed with the USGS groundwater flow model MODFLOW (Harbaugh & McDonald 1996). RT3D may be used to simulate various types of chemical reactions, including microbial metabolisms and microbial transport kinetics (Gao et al. 2001).

PHT3D. The reactive multi-component transport model PHT3D (Prommer 2002; Prommer et al. 2003) is a mixed equilibrium / kinetic reactive transport model. It consists of the transport model MT3DMS (Zheng & Wang 1999) and the PHREEQC-2 model (Parhurst & Appelo 1999). Kinetic rate expressions can be considered in PHT3D by implementing these in form of BASIC subroutines into the PHREEQC-2 database. By means of such subroutines in the database, data from the laboratory can directly go into a simulation. A modified version of the SNIA is employed in PHT3D (see also Chapter 3.3). The transport equation is not solved for every individual chemical species, but only for master species or total aqueous component concentrations (Yeh & Tripathi 1989; Engesgaard & Kipp 1992). The single as well as the double continuum concept can be employed in PHT3D.

LEHGC2.0. Yeh et al. (2001) developed a mechanistically based numerical model (LEHGC2.0) for the simulation of coupled fluid flow and reactive chemical transport, including both fast and slow reactions in variably saturated media, i.e., a full suite of kinetic and equilibrium geochemical processes simultaneously.

CHEMFRONTS. A model, which uses a region concept, is the CHEMFRONTS model by Bäverman et al. (1999). Models that require the domain to be divided into a fixed number of cells (or so-called compartments or boxes), have disadvantages such as the accuracy in the prediction of front position is dependent on the cell size. In the CHEMFRONTS model, the domain is grouped into regions of same set of minerals. The position of region boundaries is thereby moved during the simulation as the fronts (boundaries) move. The number of regions is constantly updated by adding or moving old regions as new minerals are formed or old minerals are exhausted. Therefore, number and sizes of the regions can vary and there exists no minimum size of the regions. CHEMFRONTS is based on the quasi-stationary state approximation (Lichtner 1988) that describes the evolution of geochemical processes as occurring in a sequence of stationary states. Such an approach is allowed when the mass of the minerals present in the system is large compared to the mass of dissolved species. Thus, a large quantity of water is required to dissolve a substantial amount of minerals in the system. The advantage of the quasi-stationary state approximation is that problems that would require an extremely large computational effort (e.g., when large masses of solid must react and the reactant concentration is low) are possible to solve with conventional models. CHEMFRONTS was specially designed to handle sharp reaction fronts, such as redox, pH or dissolution fronts. Such fronts can be found in various environments such as where water enriched with oxygen infiltrates reducing porous media. Certain species can build up at the generated redox and pH fronts as observed, such as in the uranium mine in Pocos de Caldas in Brazil, where the uranium ore is located at the redox front (Cross et al. 1991). In the CHEMFRONTS model, simplified pseudo-kinetic rate expressions for both precipitation and dissolution are used to describe the mineral phase reactions (compare Chapter 2.4.2 and Bäverman et al. 1999).

TOUGHREACT. One (if not the only one) of the reactive transport models that utilises the multiple interacting continua concept is the TOUGHREACT model by Xu et al. (2003). Advective and molecular diffusive transport in liquid as well as

gaseous phase are computed in TOUGHREACT by using the transport model TOUGH2 (Pruess 1991; Pruess et al. 1999). Flow, transport, and fluid-rock interaction in, e.g., multi-region heterogeneous and fractured rock systems are solved by the integral finite differences (IFD; Narasimhan & Witherspoon, 1976). This method allows a flexible discretisation using irregular grids to account for geologic features such as fractures, faults, and lithologic discontinuities. Reference to a global system of coordinates is not thereby required. An implicit time-weighting scheme is used for individual components of flow, transport, and geochemical reaction. The reaction equations are solved on a grid block basis using Newton-Raphson iteration. The quasi-stationary approximation (Lichtner 1988) and an automatic time stepping scheme are implemented in TOUGHREACT (Xu et al. 2003). TOUGHREACT utilises SIA and using TOUGHREACT, dissolution and precipitation of minerals can be calculated under local equilibrium or kinetic conditions. Changes in porosity and permeability due to mineral dissolution and precipitation can also be handled by TOUGHREACT. Heterogeneous surface reactions, including cation exchange and surface complexation (by double layer model) are also included in this reactive transport model (see also Chapter 7.3). The formulation for cation exchange is similar to Appelo & Postma (1993) and for surface complexation is taken from Dzombak & Morel (1990) (Xu & Pruess 2001).

### 2.5.2 Hybrid Systems

Especially in a hybrid system like an underground mine where in situ acid leaching of the ore underground was employed to extract metals (e.g., uranium),

- large numbers of aqueous and chemical species,
- species concentration ranging over several orders of magnitudes,
- multiple sharp fronts separating zones of distinct geochemistry (Steeffel & Lichtner 1998a; Ghogomu & Therrien 2000)

presumably predominate. Such conditions prevail, e.g., in the uranium mine of Königstein, Saxony, Germany (Bain et al. 2001, see also Chapter 6.2). Therefore, the main geochemical reactions (such as redox, complexation, and dissolution/precipitation) should be considered in contaminant transport models used for such domains.

Lots of research has been accomplished in understanding the physics and transport in hybrid systems, especially in discrete fractured systems. Though, reactive transport has not been investigated in such a great deal as the physics and transport in that sort of systems and as in continuum systems yet (Steeffel & Lichtner 1998a,b; Dijk & Berkowitz 1998). Reasons for that can partly be found in, e.g., the highly complex interaction between the mass transport mechanisms and the changing properties of a fractured porous medium (Dijk & Berkowitz 1998). Earlier studies considered only adsorption-desorption or precipitation-dissolution mechanisms on solute transport - all within a fracture, along the fracture walls and or within the adjacent porous host rock (Berkowitz 2002). These first studies are more or less exemplary for a simple geometry to gain understanding of the principal processes in such systems. Freeze & Cheery

(1979) developed a simple model that accounts for chemical adsorption along a planar fracture wall. This model was generalised by Wels & Smith (1994) to analyse transport of reactive solutes in a fracture network. Berkowitz & Zhou (1996) analysed transport of sorbing chemical species in a parallel wall fracture, emphasising interphase mass transfer between the fluid and the fracture walls. The surface reaction models they considered included irreversible first-order kinetics, instantaneous reversible reactions and reversible first-order kinetics (Berkowitz 2002).

First research works regarding dissolution/precipitation reactions in hybrid systems were undertaken by Steefel & Lichtner (1994); Novak (1996) and Steefel & Lichtner (1998a,b). Their motivation was to understand the control on reactive contaminant transport near waste repositories and determine mineral distribution in fractured systems (see also Ghogomu & Therrien 2000). The reactive processes occur thereby in the attached matrix where the exchange between the conduit and matrix takes place through diffusion. Transport in the matrix was simulated with diffusion only. This is at the time of development a fair assumption since flow in the attached matrix is considerably slower than in the conduits. As such, matrix diffusion may play a more important role for the case where chemical reactions occur, than in the case where no chemical reactions occur. For one, the change in water composition is largely controlled by the magnitude of diffusion into the matrix, since minerals in the simulation reside in the matrix and not in fractures (provided that minerals can only be found on fracture walls). The length of the fracture itself may not be so important (Steefel & Lichtner 1998a). Specifically, Steefel & Lichtner (1998a), e.g., demonstrated how the geochemical behaviour of reactive species in discrete fractured rock could differ substantially from that expected in homogeneous porous media. The physical and reactive models by Steefel & Lichtner (1994) and Steefel & Lichtner (1998a) were of one and two-dimensional nature, respectively. Steefel & Lichtner (1998a) in addition derived dimensionless parameters to relate the relative position of reactive fronts in the fracture and the matrix, for a simple case (see also Ghogomu & Therrien 2000). Novak & Sevougian (1992) and Novak (1996) studied the retardation of solutes in the fracture on the basis of a local equilibrium analysis. They showed how the retardation of solutes in the fracture could significantly be affected by the precipitation/dissolution reactions in rock matrix coupled via matrix diffusion to solute transport in the adjacent fracture (Steefel & Lichtner 1998a). Emrén (1998) developed the model CRACKER with which reactive transport in single conduits with heterogeneous mineral compositions in the matrix could be simulated. Dijk & Berkowitz (1998) investigated precipitation-dissolution and the thereby changing fracture opening. They assumed laminar flow in saturated conduits. They used an irreversible first-order kinetic surface reaction for one component. By means of the Damköhler and Péclet numbers, they analysed the contaminant transport, precipitation-dissolution and the evolution of fracture half-aperture. A profound effect on the reaction processes also had the initial fracture geometry and the solute saturation content of the inflowing fluid.

It is worthwhile to point out that compared to the first reactive transport processes considered in hybrid transport models, sorption mechanisms has also first been implemented in colloid-facilitated contaminant transport models for

hybrid systems. Through an interconnected network of fractures, highly mobile colloids can propagate quickly and therefore increase considerably the rate of contaminant migration (Berkowitz 2002). Equilibrium as well as kinetically controlled reactions of the contaminants occurring upon onto colloids from the water phase and or solid phase have also been simulated.

Only recently, reactive hybrid transport models have been developed specifically for hybrid systems that consider apart from dissolution/precipitation reactions, reactions such as complexation and redox reactions. Ghogomu & Therrien (2000) developed one of such model for reactive multispecies transport in saturated discretely-fractured porous media. In this model, they use the physical transport model for porous matrix and a set of discrete fractures from Therrien & Sudicky (1996). They superposed nodes forming the fractures onto matrix cells that ensured fluid and mass continuity. The porous matrix is thereby discretised with three-dimensional elements, while the discrete fractures are represented by two-dimensional planar elements. The flow and solute transport equations in the porous matrix and in the discrete fracture are solved by the standard Galerkin finite element method. Either upstream or central weighting is used to numerically treat the advective term in space and time, fully implicit schemes can be chosen, in that model. A preconditioned iterative solver by VanderKwaak et al. (1995) is used to solve the overall matrix equations. The method by Schäfer et al. (1998) is employed to handle the chemical reactions. The chemical species in both the fractures and the porous matrix can undergo either chemical equilibrium or kinetic reactions. The nonlinear algebraic system of equation resulting from the chemical system is solved with the Newton-Raphson technique. The SIA couples the physical and chemical transport equations. To eliminate direct calculation of the matrix/fracture exchange terms, Ghogomu & Therrien (2000) assume similar hydraulic conductivity and concentration values at the conduit nodes and in the matrix cells. Therefore, this limits the model to systems where exchange between the continuum and conduit systems is not controlled by a local parameter like the concentration. Viswanathan & Sauter (2001) developed a hybrid model, coupling a discrete pipe-flow model to a continuum model for the simulation of the long-term release of dissolved uranium under equilibrium. This hybrid model assumes instantaneous mixing in the conduit system. For modelling short-term concentration variations following recharge events, however, instantaneous mixing assumption may not be appropriate any more. Transport in the conduit system is then a prerequisite. On behalf of the German remediation company WISMUT GmbH, Eckart (pers. comm., 2002) designed a conceptual reactive hybrid model to simulate reactive transport in former underground mines in Thuringia and Saxony that is based upon the box concept. In this model, mass is transported 'discretely' in the different conduits, i.e., mass that enters a conduit at a certain time would leave this same conduit some time later which is controlled by the magnitude of the conductivity and length of the respective conduit.

A model which has more capacities compared to the above reactive hybrid transport models is the KAFKA model by Colenco (2001) and Wilhelm et al. (2002). This is a numerical compartment model developed for fluid flow and contaminant transport in converging underground waste repositories (= Kompartimentmodell für die Ausbreitung und die Fluidodynamik in einer

konvergierenden Untertageanlage für Abfälle). In this model, two-phase flow, diffusion and dispersion, sorption and limited solubility of radionuclides, radioactive decay, time-dependent gas generation due to corrosion and microbial degradation, dependency of pore volume (porosity) on convergence and creeping, dependency of flow and transport processes on varying permeability and cross-sections, dependency of pore volume on dissolution and precipitation and dependency of pressure on the chemical composition of the fluid are considered. The structure of the mine is imitated by a geometric abstraction, i.e., through discretisation of the mine in finite volumes. The complex geometry of the mines generated through excavating structures can be modelled by using four principal structural elements: (i) caverns, i.e., backfilled or open excavations with a high hydraulic conductivity, (ii) tunnels, i.e., man-made horizontal hydraulic connections with a distinct hydraulic conductivity, which may serve as hydraulic barriers, (iii) shafts, i.e., man-made vertical hydraulic connections with a distinct hydraulic conductivity, and (iv) teeters, i.e., vertical connections with a hydraulic conductivity caused by stress conditions in the rock. To each of these structural elements apart from specific hydraulic properties, specific chemical properties were designed. For example, the caverns are simulated as perfect mixing tanks while in the tunnels conventional two-phase flow is considered. Wilhelm et al. (2002) called the KAFKA model as a “skeleton model” of the underground mine structures. Main characteristics of these reactive hybrid transport models are also summarised in Table 1.

## 2.6 Summary and Implications

In predicting the evolution of the chemical composition of (acid) contaminated surface and groundwater with heavy metals, appropriate and sophisticated models are required. Such models should nowadays:

- consider at least advection, dispersion, redox reactions,
- handle more than one-, better three-dimensional transport,
- deal with complex time-dependent boundary conditions,
- manage a large number of chemical reactions under non-isothermal conditions to practically address realistic problems encountered in the field (see also Cheng & Yeh 1998),
- regard kinetically controlled reactions.

Kinetically controlled reactions can be implemented into a reactive transport code in various ways, i.e., with a fully kinetic or mixed equilibrium/kinetic formulation that control the complexity of solving the coupled equation set for the physical and chemical system. Generally, selection of the type and sophistication of a coupling technique is determined by such factors as:

- time and space discretisation parameters,
- the nature of the chemical reactions,
- the desired accuracy (see also Xu et al. 1999; Xu & Pruess 2001),
- available computational resources,

- current understanding of the processes.

Numerical techniques can also have a significant influence on the efficiency, convergence and stability of the models. Further, to save computational time and reduce time of development, each model may make different assumptions and simplifications whereby taking the risk that certain types of problems cannot be simulated. In general, model limitations do not cause any problem as long as those are not violated and are used primarily as tools to gain insight into the interactions of the various physical and chemical processes (Walter et al. 1994). In fact, according to Freedman & Ibaraki (2003), numerical models should be acknowledged as artificial systems with interactive components of mathematical and possible empirical variables and expressions (compare Chapter 4.1.1). Apart from reducing computational time by using sophisticated techniques, the following guiding principle behind reactive transport models should be kept in mind: “a ‘good’ model does not consider every possible reaction and species; instead, the user of the model must apply insight in order to identify the reactions and species that are truly significant” (Viswanathan 1996).

In systems with dense networks of highly interconnected fractures or in general conduits where the REV approach is applicable, major factors to be considered include

- time scale for global flow and transport and
- degree of interaction between the conduits and matrix.

These factors basically decide which type of continuum approach should be selected to simulate flow and transport in such systems, namely either the single-double- or multiple continua approach.

In contrast, in systems with less dense networks of poorly interconnected conduits (e.g., shafts, shifts, roadways in underground mines), purely reactive based continuum models cannot be used since the REV is macroscopically invalid for the discrete conduit system. For the simulation of transport in such systems, hybrid models have been suggested which combine aspects of discrete and continuum approaches. Different approaches of reactive models for hybrid systems that consider the main geochemical reactions, are however still scarce. One of the objectives of this thesis was to develop a basis for a reactive hybrid transport model (see Chapter 1.3).

*The burden of (this) lecture is just to emphasize the fact that it is impossible to explain honestly the beauties of the laws of nature in a way that people can feel, without their having some deep understanding of mathematics.*

*Richard Feynman, The Character of Physical Law (1967)*

## Chapter

### 3 Theoretical Developments

This chapter presents an insight into the underlying governing equations of the reactive hybrid transport model RUMT3D (three-dimensional reactive underground mine transport model) developed in this thesis to simulate reactive transport in coupled discrete-continuum or hybrid systems. Basically, RUMT3D couples the three-dimensional hybrid transport model UMT3D to the geochemical model PHREEQC-2 (Parkhurst & Appelo 1999). UMT3D is a coupled version of the three-dimensional multi-species solute transport model MT3DMS for saturated porous media (Zheng & Wang 1999) and a conduit transport model similar to that of Birk (2001). Fig. 2 demonstrates the different model components of UMT3D/RUMT3D. Since the two distinct (flow and transport) regimes can influence the transport of contaminants in hybrid systems to a great extent, it is important that the numerical method for solving transport in the discrete network system also produces accurate, numerically stable and computationally efficient results to make the model applicable to multi-component and reactive transport problems of varying complexity. Therefore, apart from the explicit finite difference (FD) method, a numerical scheme (i.e., EMCNOT, Liu et al. 2001) was implemented in UMT3D/RUMT3D to solve the transport in the conduit system time efficiently and with negligible numerical dispersion. Because a hybrid flow model is required to compute the flow field for UMT3D/RUMT3D, this chapter starts with a section on showing the governing equations of the CAVE model which is a MODFLOW (Harbaugh & McDonald 1996) based model coupled with a pipe-flow model. Fig. 2 also depicts the different model components of CAVE.

#### 3.1 Hybrid Flow Modelling Approach: CAVE

To compute the flow field in the combined conduit/matrix system, the CAVE model (Clemens et al. 1996; Liedl et al. 2003) was used, which is a hybrid model coupling flow in a discrete conduit system to a 3-D porous continuum. CAVE models flow in the discrete conduit system with a pipe-flow modelling approach (Horlacher & Lüdecke 1992), which covers laminar and turbulent flow cases. Flow in the porous continuum is simulated using the well-known MODFLOW code, a three-dimensional finite-difference formulation for solution of the partial differential equations describing laminar groundwater flow (Harbaugh & McDonald 1996). CAVE was originally developed for modelling the genesis of

discrete karst aquifers. However, the simulation of groundwater flow in underground mines, discrete fractured systems as well as aquifers with intersecting boreholes, i.e., in systems with both, a highly conductive network with poorly interconnected conduits and a considerably less permeable, porous matrix can be treated in an analogous way to karstified carbonate aquifers with a discrete conduit system.

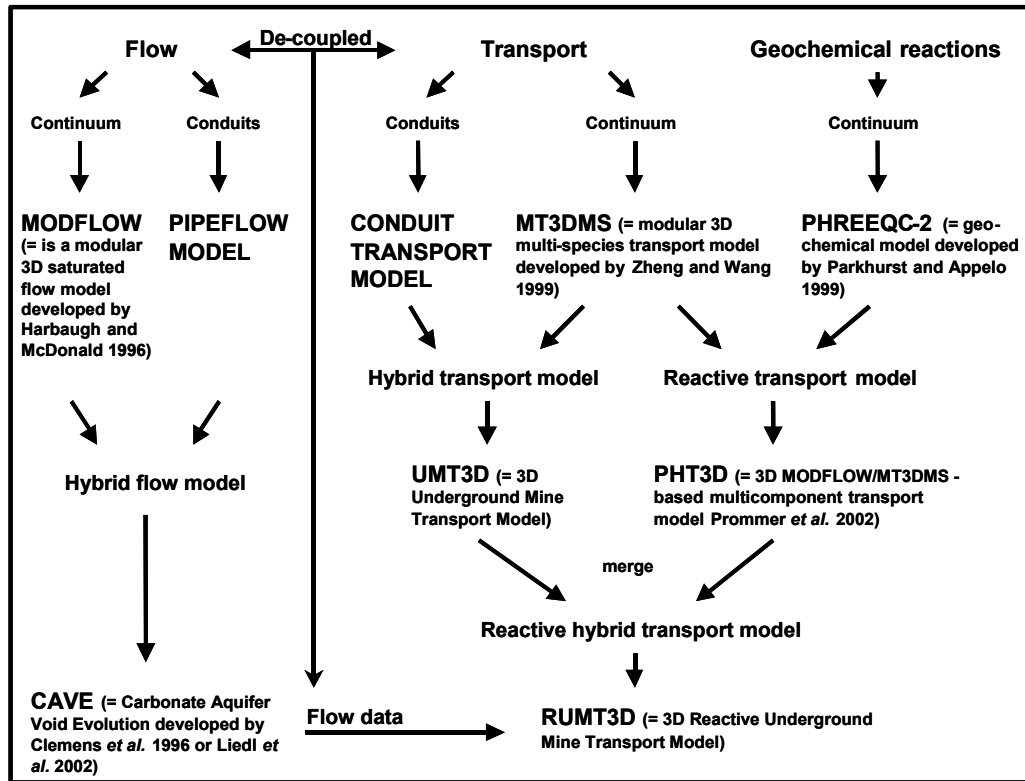


Fig. 2: Model components of CAVE, UMT3D and RUMT3D.

The three-dimensional continuum equation for flow in the porous matrix (ore material), including a further source/sink term  $\gamma$  that couples the continuum to the pipe-flow model, is described as follows:

$$\frac{\partial}{\partial x_m} \left( K_{m,xx} \frac{\partial h_m}{\partial x_m} \right) + \frac{\partial}{\partial y_m} \left( K_{m,yy} \frac{\partial h_m}{\partial y_m} \right) + \frac{\partial}{\partial z_m} \left( K_{m,zz} \frac{\partial h_m}{\partial z_m} \right) + W_m + \gamma = S \frac{\partial h_m}{\partial t_m} \quad \text{Equation 1}$$

$x_m, y_m, z_m$  (L): distance along the respective Cartesian co-ordinate axis in the porous matrix

$t_m$  (T): time

$h_m$  (L): hydraulic head in the porous matrix

$K_{m,xx}, K_{m,yy}, K_{m,zz}$  (L T<sup>-1</sup>): hydraulic conductivity along the co-ordinate axes in the porous matrix

$S$  (L<sup>-1</sup>): specific storage coefficient

$W_m$  (T<sup>-1</sup>): volumetric flux term per unit volume from a sink/source into the porous matrix, e.g., groundwater recharge

$\gamma$  (T<sup>-1</sup>): volumetric rate of fluid transfer between the porous matrix and the conduit system per unit volume.

A conduit system is defined in the model as a pipe network consisting of cylindrical tubes. Conduit nodes are introduced between the connecting tubes to allow for exchange of flow between the different tubes from different faces of a cell and between a conduit node and the continuum (porous matrix) at different locations in the model domain. Only one conduit node can be placed in a porous matrix cell. There are 6 potential faces of a cell interfacing with a tube network node, i.e., top, bottom, front, back, left and right. A conduit tube may extend over one or more porous matrix cells depending on the respective geometry of the mineshafts, adits, boreholes or karst/fractured conduits and the locations of the sinks and sources, e.g., direct recharge and fixed heads. Conduit orientations can be freely designed, i.e., they do not necessarily need to be vertical or horizontal along the same continuum layer, so that the model can easily match the actual spatial co-ordinates of real mine networks, boreholes or karst/fractured conduits. It is assumed that the conduit system is fully saturated, an assumption that will hold for most flooded underground mines and saturated karst/fracture aquifers. Flow between the porous matrix and the conduit nodes is described by a linear relationship between the two systems (Barenblatt et al. 1960):

$$\Gamma_i = \alpha_i (h_i - h_{i,m}) \quad \text{Equation 2}$$

$\Gamma_i$  (L<sup>3</sup> T<sup>-1</sup>): exchange flow rate between conduit node  $i$  and the porous matrix cell

$\alpha_i$  (L<sup>2</sup> T<sup>-1</sup>): exchange coefficient between node  $i$  and the porous matrix

$h_i$  (L): hydraulic head at conduit node  $i$

$h_{i,m}$  (L): hydraulic head in the porous matrix cell where conduit node  $i$  is located.

The magnitude of the exchange coefficient  $\alpha_i$  depends on the hydraulic conductivity of the porous matrix and geometrical factors, determined by the discretisation of the adjacent continuum cell.

Flow in each tube, i.e., flow from one to another conduit node can be determined by using Darcy-Weisbach equation:

$$\Delta h_j = -\lambda_{i,j}^f \frac{l_j}{d_j} \frac{u_{i,j}^f |u_{i,j}^f|}{2g} \quad \text{Equation 3}$$

$\Delta h_j$  (L): head difference between the two ends of tube  $j$

$\lambda_{i,j}^f$  (-): friction factor of tube  $j$  connected to face  $f$  of conduit node  $i$ .

$l_j$  (L): length of tube  $j$

$d_j$  (L): diameter of tube  $j$

$g$  (L T<sup>-2</sup>): earth's gravitational acceleration

$u_{i,j}^f$  (L T<sup>-1</sup>): average velocity of tube  $j$  connected to face  $f$  of conduit node  $i$ . It is computed by

$$u_{i,j}^f = \frac{4Q_{i,j}^f}{\pi d_j^2} \quad \text{Equation 4}$$

$Q_{i,j}^f$  (L<sup>3</sup> T<sup>-1</sup>): discharge of tube  $j$  connected to face  $f$  of conduit node  $i$  into the respective node  $i$ .

Substituting Hagen-Poiseuille equation which is valid for laminar flow

$$\lambda_{i,j}^f = \frac{64\nu}{d_j u_{i,j}^f} \quad \text{Equation 5}$$

$\nu$  (L<sup>2</sup> T<sup>-1</sup>): kinematic viscosity of water.

and equation 4 into equation 3, an expression for  $Q_{i,j}^f$  describing laminar flow can be obtained:

$$Q_{i,j}^f = -\frac{\pi d_j^4 \Delta h_j g}{128 l_j \nu} \quad \text{Equation 6}$$

For turbulent flow, the implicit Colebrook-White law is used:

$$\frac{1}{\sqrt{\lambda_{i,j}^f}} = -2 \log \left( \frac{2.51}{Re \sqrt{\lambda_{i,j}^f}} + \frac{k}{3.71 d_j} \right) \quad \text{Equation 7}$$

$Re$  (-): Reynolds number ( $= \frac{u_{i,j}^f d_j}{\nu}$ ), for turbulent flow  $Re \geq 2300$

$k$  (L): roughness of tube  $j$

By substituting the above equation and equation 4 into equation 3, an expression for  $Q_{i,j}^f$  describing turbulent flow can be obtained (Horlacher & Lüdecke 1992):

$$Q_{i,j}^f = -\sqrt{\frac{|\Delta h_j| g d_j^5 \pi^2}{2l_j}} \log \left( \frac{2.51\nu}{\sqrt{\frac{2|\Delta h_j| g d_j^3}{l_j}} + \frac{k_j}{3.71d_j}} \right) \frac{\Delta h_j}{|\Delta h_j|} \quad \text{Equation 8}$$

Conservation of volume at any conduit node  $i$  can be determined by using Kirchhoff's law that should evaluate to zero by summing up all in- and outflow terms at the respective node  $i$ :

$$\sum_f Q_{i,j}^f + \Gamma_i + \sum_s Q_{i,s} = 0 \quad \text{Equation 9}$$

$Q_{i,s}$  ( $L^3 T^{-1}$ ): volumetric flow rate of a sink/source term at conduit node  $i$ . In addition to flow from the continuum and from the different connecting tubes to a conduit node, other sink/source terms can be applied such as direct recharge and a fixed head to the conduit node.

The sum of in- and outflow at any conduit node  $i$  can be computed by using conservation of volume at any node according to the Kirchhoff's law but splitting up the flow terms after in and out, respectively, i.e.,

$$Q_i^{in} = \sum_f Q_{i,j}^{f+} + \Gamma_i^+ + \sum_s Q_{i,s}^+ \quad \text{Equation 10}$$

and

$$Q_i^{out} = \sum_f Q_{i,j}^{f-} + \Gamma_i^- + \sum_s Q_{i,s}^- \quad \text{Equation 11}$$

$Q_i^{in}$  ( $L^3 T^{-1}$ ): sum of inflow at conduit node  $i$

$Q_i^{out}$  ( $L^3 T^{-1}$ ): sum of outflow at conduit node  $i$

The superscripts + and - differentiate in- and outflow terms from each other at conduit node  $i$ , respectively. Note that conservation of the volume can easily be

checked by separately summing up  $Q_i^{in}$  and  $Q_i^{out}$  while the flow calculations and then see whether they equate.  $\gamma$  at conduit node  $i$  in equation 1 can then be quantified as

$$\gamma_i^+ = \sum_f \frac{Q_{i,j}^{f+}}{A_j^{f+} l_j^{f+}} + \frac{\Gamma_i^+}{V_{i,m}} + \frac{\sum_s Q_{i,s}^+}{\sum_f A_j^{f-} l_j^{f-}} \quad \text{Equation 12}$$

or

$$\gamma_i^- = \sum_f \frac{Q_{i,j}^{f-}}{A_j^{f-} l_j^{f-}} + \frac{\Gamma_i^-}{V_{i,m}} + \frac{\sum_s Q_{i,s}^-}{\sum_f A_j^{f+} l_j^{f+}} \quad \text{Equation 13}$$

dependent upon whether conduit node  $i$  is a source or a sink term to the conduit system.

$V_{i,m}$  (L<sup>3</sup>): volume of the matrix cell where conduit node  $i$  is located (=  $x_{i,m} \cdot y_{i,m} \cdot z_{i,m}$ ).

Clemens et al. (1996) or Liedl et al. (2003) provides a more detailed description of the pipe-flow model.

### 3.2 Hybrid Transport Modelling Approach: UMT3D

Transport of mass within the porous matrix is also simulated with a continuum approach, i.e., with the standardised three-dimensional multi-species transport model MT3DMS (Zheng & Wang 1999). MT3DMS was selected due to its compatibility to the MODFLOW model. In contrast, mass transport within the network of tubes is modelled discretely with a one-dimensional advective transport model similar to that presented by Birk (2001) in CAVE. Coupling between the continuum transport model and the transport in the conduits is achieved using the two-step method SNIA (Sequential Non-Iterative Approach, compare Chapter 2.4.3 and Walter et al. 1994; Steefel & MacQuarrie 1996). The transport of solutes in the continuum is solved first, followed by a second step during which the solute concentrations in the conduit system are updated and the solute mass is transported. The resulting coupled hybrid transport model was named UMT3D (three-dimensional Underground Mine Transport model). For the clarity of the difference between the UMT3D and CAVE model, CAVE, primarily as the hybrid flow model for the conduits and continuum, can also calculate mass transport in the conduits but not in the continuum. However, the option of conduit transport calculation in CAVE is not utilised when flow data are calculated for the UMT3D model.

The general transport equation (Zheng & Wang 1999) was extended to include a further sink/source term, i.e.,  $\xi$  to couple MT3DMS to the conduit transport model in UMT3D. Thus, the three-dimensional transport equation in the continuum is:

$$\frac{\partial(\theta_m C_m^k)}{\partial t_m} = \frac{\partial}{\partial x_{m,i}} \left( \theta_m D_{m,ij} \frac{\partial C_m^k}{\partial x_{m,j}} \right) - \frac{\partial}{\partial x_{m,i}} (\theta_m v_{m,i} C_m^k) + q_{m,s} C_{m,s}^k + \xi^k + \sum_{k=1}^N RXN_{m,k} \quad \text{Equation 14}$$

$C_m^k$  (M L<sup>-3</sup>): aqueous concentration of component  $k$  in the porous matrix

$D_{m,ij}$  (L<sup>2</sup> T<sup>-1</sup>): hydrodynamic dispersion coefficient tensor in the porous matrix

$v_{m,i}$  (L T<sup>-1</sup>): linear pore water velocity in the porous matrix

$q_{m,s}$  (T<sup>-1</sup>): volumetric flux of water per unit volume of porous matrix representing sources (positive) and sinks (negative)

$\theta_m$  (-): porosity of the porous matrix

$C_{m,s}^k$  (M L<sup>-3</sup>): concentration of component  $k$  of the sources or sinks to the porous matrix

$\xi^k$  (M L<sup>-3</sup> T<sup>-1</sup>): volumetric mass flux rate of solute transfer between the porous matrix and the conduit system per unit volume of component  $k$

$RXN_{m,k}$  (M L<sup>-3</sup> T<sup>-1</sup>): chemical reaction term of the porous matrix with respect to component  $k$ .

For the calculation of solute transport from the continuum cell to a conduit node  $i$ , the mass transfer rate is determined by multiplying the cell concentration of the pore water in the porous matrix of component  $k$ ,  $C_{m,i}^k$ , at node  $i$ , with the respective exchange flow rate  $\Gamma_i$  and dividing the mass flux by the volume of the respective cell,  $V_{m,i}$ , i.e.,

$$\frac{\Gamma_i C_{m,i}^k}{V_{m,i}} \quad \text{Equation 15}$$

Alternatively, if solute mass is transported from conduit node  $i$  into the matrix cell, then  $C_{i,m}^k$  is replaced by the nodal concentration,  $C_i^k$ . Fig. 3 illustrates this exchange for both cases. Such mass transfer rates are then treated as mass sink/source terms in MT3DMS since conduit nodes act similarly to other sinks/sources (e.g., wells) in MT3DMS. The difference between wells as implemented in MT3DMS and conduit nodes is that the mass removed by means of a well is not returned to the porous matrix, while the mass removed with an entry conduit node may be returned completely through the exit conduit nodes. Amount, location and required time for these returns mainly depend on (i) the transport velocity in the different conduits, (ii) the magnitude of the exchange coefficients between the exit conduit nodes and the porous matrix, (iii) the magnitude of conduit sink terms, and (iv) the length of the different conduit tubes.

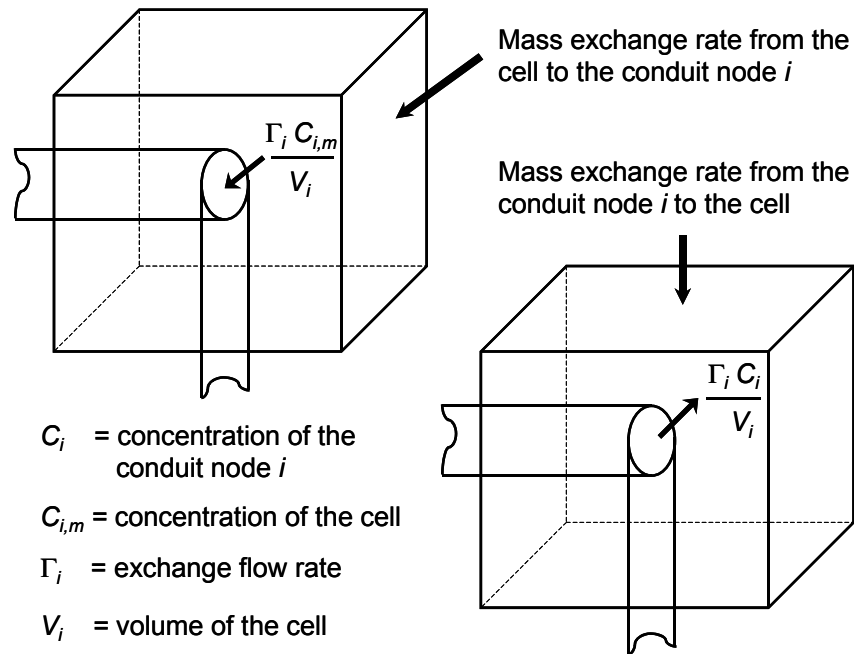


Fig. 3: Illustration of porous material cell-conduit exchange.

A one-dimensional transport equation that solely considers advection is applied to each tube, i.e.,

$$\frac{\partial C_j^k}{\partial t} = -q_j \frac{\partial C_j^k}{\partial z_j} \quad \text{Equation 16}$$

$C_j^k$  ( $\text{M L}^{-3}$ ): aqueous concentration of component  $k$  in conduit tube  $j$

$q_j$  ( $\text{L T}^{-1}$ ): flux of water in tube  $j$

$t$  (T): time

$z_j$  (L): distance along a respective Cartesian coordinate axis in the respective tube  $j$ .

Note there are no sink/source terms in this transport equation. The mass exchange rates from the porous matrix, from the six potentially connecting tubes and from conduit sink/source terms such as direct recharge, fixed head and fixed concentration as applied to the different conduit nodes are considered in terms of initial or boundary concentration values to the transport equation 16. The resulting concentration values are obtained by a weighted arithmetic mean of the single flow and transport components for each transport time step. Such an approach is common in mixing cell models (Bajracharya & Barry 1993).

Mathematically, a weighted arithmetic mean of the concentration value of component  $k$  at conduit node  $i$  can be expressed as follows:

$$C_i^k = \frac{\sum_f^6 Q_{i,j}^{f+} C_{i,j,l}^{k,f} + \Gamma_i^+ C_{i,m}^k + \sum_s Q_{i,s}^+ C_{i,s}^k}{\sum_f^6 Q_{i,j}^{f+} + \Gamma_i^+ + \sum_s Q_{i,s}^+} \quad \text{Equation 17}$$

subscript  $l$ : first or the maximum number of tube subsections or segments in the different tubes depending on the flow direction.

The tubes or conduits can further be divided into a (user-defined) number of subsections or segments as necessary to minimise numerical dispersion / improve numerical stability. Tubes within a network can be considerably longer than cell widths, lengths or thickness.

### 3.2.1 Transport Solvers for the Conduit System

Two numerical methods were implemented in UMT3D to solve equation 16 which are (i) the explicit finite difference (FD) method and (ii) a mass-conservative semi-Lagrangian scheme referred to as EMCNOT. The explicit finite difference (FD) method was already incorporated in the transport module for the conduit system in CAVE (Birk 2001). The EMCNOT scheme was developed by Liu et al. (2001) for modelling advection-dominated contaminant transport problems and is an explicit mass conservative scheme without a time step limit. By means of 1-D and 2-D benchmark problems, Liu et al. (2001) demonstrated that by using EMCNOT as the solver for the transport equations, there is no stringent stability constraint on the transport time step. Moreover, it was shown that this scheme was essentially free of spurious oscillation and numerical dispersion. The EMCNOT was implemented in UMT3D with the intention to reduce numerical dispersion and increase computational efficiency of transport calculations (see Chapter 5.3).

### 3.2.2 Time Criterion for the Transport Solvers for the Conduit System

The time criterion, i.e., the transport time step size for the FD method is the minimum residence time value within a tube segment of the conduit system multiplied by a user defined Courant number,  $Cr$ . With the EMCNOT method, a transport time step size of up to the minimum residence time value of a respective pipe,  $(tr_j)_{min}$  in the conduit system multiplied by a user defined Courant number,  $Cr$  can theoretically be used for both models. The residence time of groundwater,  $tr$  in a specific pipe transported by advection under steady state flow conditions is determined by dividing the length of a pipe,  $L_j$  by the flow velocity in a respective pipe. In mathematical form, the maximum transport time step size,  $\Delta t_{max}$  can be expressed as:

$$\Delta t_{\max} = Cr (tr_j)_{\min} = Cr \left( \frac{L_j}{q_j} \right)_{\min} \quad \text{Equation 18}$$

Such a time criterion may vary with each flow time step since the flow rate in each tube may change with each flow time step. In Chapter 5.3 is demonstrated how time efficient the EMCNOT scheme can be to solve advective transport in the conduit system over the standard finite difference (FD) method. On top of this efficiency, the numerical dispersion can significantly be reduced with the EMCNOT method.

### 3.2.3 Mass Balance in the Conduit System

Mass balance in the conduit system is determined in a similar way as in the matrix. To check performance of both transport models, mass balance calculations are also carried out independently for the different conduit nodes in MT3DMS as sink/source terms. In contrast to the conduit transport model by Birk (2001) the above-described model uses a global approach to calculate mass balance and thus improves computational efficiency. Moreover, the global variable arrays and subroutines in the modified conduit transport model are fully compatible with those used in MT3DMS. All solution options in the original MT3DMS code are retained with the conduit transport model implemented as a new package named "CON".

### 3.3 Reactive Hybrid Transport Modelling Approach: RUMT3D

The comprehensive geochemical model PHREEQC-2 (Parkhurst & Appelo 1999) was coupled with the UMT3D model as a solver for the reaction term within equation 14, i.e.,  $RXN_{m,k}$  to RUMT3D using a modified SNIA (Walter et al. 1994; Steefel & MacQuarrie 1996). PHREEQC-2 was selected as a coupled version of this model with MT3DMS, i.e., PHT3D, already existed (compare Prommer 2002; Prommer et al. 2003 or Chapter 2.5.1). Reaction time step sizes can be larger than the transport time step sizes within RUMT3D depending upon the problem considered. In contrast to the transport time step sizes, reaction time step sizes are user defined. The transport equation 14 does not have to be solved for every individual chemical species, but only for total aqueous component concentrations (Westall et al. 1976; Yeh & Tripathi 1989; Engesgaard & Kipp 1992), defined as:

$$C_u = c_u + \sum_{k=1, n_s} Y_k^s s_k \quad \text{Equation 19}$$

$C_u$  (mol L<sup>-1</sup>): total aqueous component concentration of the  $u^{th}$  component

$c_u$  (mol L<sup>-1</sup>): molar concentration of the  $u^{th}$  (uncomplexed) aqueous component

$n_s$  (-): number of dissolved species that form complexes with the  $u^{\text{th}}$  aqueous component

$Y_k^s$  (-): stoichiometric coefficient of the aqueous component in the  $k^{\text{th}}$  complexed species

$s_k$  (mol L<sup>-1</sup>): molar concentration of the  $k^{\text{th}}$  complexed species.

The (local) redox-state,  $pe$ , is at present modelled by transporting chemicals/components/master species in different redox states separately, while the pH is controlled by the equivalents of aqueous cations and anions in solution within one grid cell (i.e., by the local charge balance). The transport model UMT3D needs to solve transport for  $n_{\text{tot}}$  entities, with

$$n_{\text{tot}} = n_{e,\text{nre}} + \sum_{k=1, n_{e,\text{re}}} n_{rs,k} \quad \text{Equation 20}$$

$n_{e,\text{nre}}$  (-): number of (mobile) chemical elements occurring in only one redox state

$n_{e,\text{re}}$  (-): number of elements occurring in multiple redox states

$n_{rs,k}$  (-): appropriate number of different possible redox states of the  $k^{\text{th}}$  element.

The resulting model (RUMT3D) can handle a wide range of chemically reactive processes including aqueous complexation, mineral dissolution/precipitation, ion exchange and redox reactions. Reactions might be assumed to occur as equilibrium reactions and or kinetically controlled. As PHT3D, RUMT3D is a mixed equilibrium/kinetic reactive model. More details on the incorporation of PHREEQC-2 and MT3DMS to the PHT3D model can be found in Prommer (2002) and Prommer et al. (2003). Chemical reactions in the conduit system are at present assumed to have a negligible effect on the composition of the groundwater because of the typical short residence times of the solutes in the conduit system.

*When you have satisfied yourself that the theorem is true you start proving it.*

*G. Polya, mathematician (1954)*

## Chapter

### 4 Evaluation of Reactive Transport Models

The evaluation of newly developed models or of added modules/packages to existing models is necessary to ensure “trustworthiness” of models (Freedman & Ibaraki 2003). Two major types of tests based on the accuracy and stability of the numerical results are usually undertaken to evaluate performance of models. These are verification and validation. For these types of tests, benchmark problems are required. There are two other evaluation instruments, i.e., illustration and plausibility for which benchmark problems are not necessarily needed. Fig. 4 demonstrates these options of evaluating a newly developed model. More details about these options as well as a definition and a discussion about categorisation of benchmark problems are given in the first section of this chapter. To support understanding of the selected evaluation procedure for the (reactive) hybrid transport models UMT3D/RUMT3D developed in this thesis, the second section provides a general description of methods of evaluation. Further, it presents examples of categorised benchmark problems for reactive transport in the subsection for verification, which are then used to demonstrate the common practice of evaluating ‘state of the art’ reactive transport models. The third section summarises this chapter and provides implications for reactive transport models in general and for RUMT3D in particular.

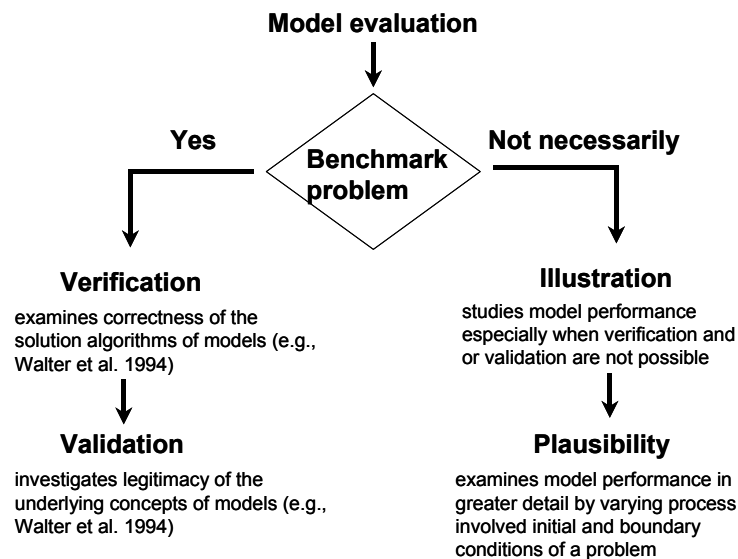


Fig. 4: Evaluation instruments for models.

## 4.1 Term Definitions and Discussions

### 4.1.1 Evaluation, Verification and Validation

Generally, verification refers to a comparison of analytical and or numerical results by using independently developed or established codes while validation is a comparison of numerical results with data from existing systems such as laboratory column and field studies. For the verification process, the same assumptions, such as initial and boundary conditions must be made at the start of the simulation for both types of models (i.e., numerical and analytical models, Fabritz 1995).

With regard to the evaluation of reactive transport models, according to Freedman & Ibaraki (2003), verification refers to “*a check that the model is accurately solving the set of chemical and transport equations*”. On the other hand, validation is a demonstration that a model can properly represent real hydrogeochemical systems. Consequently, Freedman & Ibaraki (2003) stated, “*verification can be viewed as a first step in model development that needs to be followed up with a protocol for assuring that the model accurately represents the hydrogeochemical systems it simulates.*”

Correct usage of the terms verification and validation of models are occasionally disputed. Since groundwater problems are often full of uncertainties, Konikow & Bredehoeft (1992), for instance, concluded that models “*cannot be validated but only proven not to be invalid*” (Walter et al. 1994). Freedman & Ibaraki (2003) supported this statement in the sense that validity of model results depended on the quality of its input. Verification has also been questioned when the numerical results are or can only be compared to results from other established numerical codes. Results of problems considering more complex processes (e.g., processes which require the incorporation of kinetic rate expressions, Fabritz 1995) and or considering more than one dimension can only be compared to results from other numerical models since no exact analytical or closed-form solutions are available. Numerical results are approximations of exact analytical solutions. Thus, the results can be more or less accurate depending on the numerical method. Therefore, strictly, model verifications are “*usually possible only in a limited sense where analytical or other proven solutions are available*” (Walter et al. 1994). In the dispute about correct usage of the terms verification and validation, it should also be considered that numerical models are artificial systems, although designed for the simulation of ‘portions of existing systems’. These artificial systems are limited to the current understanding of the full range of possible processes that interact in real-world systems and by computational power. Therefore, they are not able to perfectly replicate nature with all its controlled and uncontrolled interference’s. They should rather be viewed as tools to better understand the interactions of the various (physical and chemical) processes (Walter et al. 1994, compare also Chapter 2.6). In this thesis, the term evaluation is used as an overall term for verification, validation, illustration and plausibility (compare Fig. 4).

### 4.1.2 Illustration and Plausibility

Capacities or processes considered within models, for which no benchmark problem is available, can only be illustrated. However, the influence of new capacities of models can more easily be illustrated by building upon existing benchmark problems. This form of model evaluation basically examines whether the simulation results are reasonable or plausible. By varying process involved initial and boundary conditions, the consistency, stability and also accuracy of the results can be investigated in greater detail. These kind of tests of varying process involved conditions are often referred to plausibility tests, wherein the plausibility of the results is systemically evaluated.

### 4.1.3 Benchmark Problems

Benchmark problems are problems on which models can be evaluated on stability and accuracy. For verification tests, benchmark problems can be hypothetical but nevertheless should include principal processes to be simulated with the newly developed model. For instance, if a model is designed to simulate redox fronts, at least one benchmark problem should be selected which requires handling of redox reactions. While for validation tests, the benchmark problems should be derived from existing systems.

Although most recent reactive transport models have three-dimensional (3D) capacity, many benchmark problems are still of one-dimensional (1D) nature (see also Chapter 4.2.1) since, e.g.,

- analytical solutions are usually only available for 1D problems,
- data from experimental tests on 1D columns are readily obtainable and
- the processes involved in existing systems can more easily be understood or comprehended on the basis of 1D problems.

Models can be evaluated on different levels of benchmark problems. With regard to reactive transport models, the different levels of benchmark problems can be categorised by, e.g., the number of (chemical) processes and species considered. As such, the first level could consider only a single process or reaction type and their associated species. The next levels could then add more processes (or reactions) and or species until a degree of problems is reached to be simulated and or which successfully illustrates the new capacities of a newly developed model. In general, the selection of the levels of benchmark problems depends on criteria such as:

- degree of sophistication and the kind of model module to be tested,
- need of demonstrating intermediate steps to show that sub-problems can be handled satisfactorily before simulating more complex problems and
- the availability of (established) benchmark problems.

## 4.2 General Description of Methods of Evaluation and Examples

On the basis of four examples of categorised benchmark problems for reactive

transport, the common practice of evaluating 'state of the art' reactive transport models is demonstrated in this section. By the selection of the categorised benchmark problems, particular attention was paid towards the inclusion of two specific benchmark problems used for the evaluation of PHT3D (Prommer 2002; Prommer et al. 2003) to show that this model is already well-tested. The reactive multi-component and three dimensional transport model PHT3D is part of RUMT3D (compare Chapter 3.3). All the "demonstrating" models in this section have three-dimensional and multi-component capacities. Although this thesis focuses on the development and evaluation of a numerical model, it is worthwhile to note that "benchmarking" models already starts with the evaluation of models, especially when plausibility tests are undertaken. Therefore, the last subsection gives a brief discussion about benchmarking models including examples.

#### 4.2.1 Verification

Similarly to the criteria for the level selection of benchmark problems (see Chapter 4.1.3), the

- degree of sophistication and evaluation of the involved model modules,
- availability of other analytical and or numerical codes and
- accessibility of published verified simulation results

determine, which other (independent) codes should be used for verification.

In this subsection, four established levels of benchmark problems for verifying 'state of the art' reactive transport models will be discussed focusing on the Acid Mine Drainage (AMD) phenomena (also known as Acid Rock Drainage, ARD phenomena). AMD is a common environmental problem (Singer & Stumm 1970; van Berk 1987; Morrison et al. 1990; Blowes et al. 1991; Hedin et al. 1994; Walter et al. 1994; Wisotzky 1994; Wisotzky & Obermann 1995; Wisotzky 1996; [www.dep.state.pa.us/dep/deputate/minres/bamr/amd/science\\_of\\_amd.htm](http://www.dep.state.pa.us/dep/deputate/minres/bamr/amd/science_of_amd.htm)). As demonstrated in Chapter 6, RUMT3D is evaluated on the basis of two benchmark problems which require simulation of the AMD phenomena:

- level 1: dissolution/precipitation processes of a single mineral,
- level 2: dissolution/precipitation processes of multiple minerals,
- level 3: dissolution/precipitation, complexation and redox reactions of multiple mineral and aqueous species,
- level 4: simulation of the acid mine drainage phenomena.

A benchmark problem of level 1 was studied by Walsh et al. (1984) using the PHASEQL/FLOW model to simulate a hypothetical four-component dissolution/precipitation problem. Engesgaard & Kipp (1992) developed a benchmark problem of level 2 that investigates multiple calcite and dolomite precipitation/dissolution fronts. A benchmark problem of level 3 is proposed by Carnahan (1986) who studied a uranium redox reaction problem using the THCC model. It also considers diffusive transport. A benchmark problem which requires the simulation of the AMD phenomena in chemical equilibrium was developed by

Morin & Cherry (1988) and Walter et al. (1994). This problem basically includes all features of the other three levels, i.e., advective-dispersive transport of heavy metals and non-metals, precipitation-dissolution and redox reactions, but also the propagation of sharp dissolution fronts. All of the benchmark problems mentioned above are of one-dimensional nature.

Liu & Narasimhan (1989b) verified their multiple-species reactive transport model DYNAMIX on the basis of the two 1D-benchmark problems developed by Walsh et al. (1984) and Carnahan (1986). Since Walsh et al. (1984) and Carnahan (1986) provided results with the PHASEQL/FLOW and the THCC models, Liu & Narasimhan (1989) were able to compare the performance of their DYNAMIX model to these two models. Also, Ghogomu & Therrien (2000) used the first level benchmark problem studied by Walsh et al. (1984) for the verification of their reactive hybrid transport model. Engesgaard & Kipp (1992) utilised benchmark problem of level 2 to evaluate their model MST1D against the CHEMTRNS model by Noorishad et al. (1987) (see also Prommer 2002). On the basis of the AMD problem (benchmark problem of level 4), Walter et al. (1994) evaluated their reactive transport model MINTRAN against the PHREEQM model (Appelo & Willemssen 1987). Apart from the AMD problem and other eight problems, Prommer (2002) and Prommer et al. (2003) also verified PHT3D with the benchmark problems of level 2 by Engesgaard & Kipp (1992).

#### **4.2.2 Illustration**

For the illustration of the hybrid property of the multicomponent reactive transport model in discretely-fractured porous media, Ghogomu & Therrien (2000) used the chemistry of the benchmark problem of level 2 by Engesgaard & Kipp (1992). They extended this problem to a 2D physical system and introduced two simple fracture geometries. In order to illustrate the multi-dimensional capability of the reactive transport model DYNAMIX and its applicability to field problems, Liu & Narasimhan (1989) solved a hypothetical, large-scale, two-dimensional reactive transport problem.

#### **4.2.3 Validation**

The evaluation of models does not only require verification but also needs examination whether the underlying concepts agree with reality (compare Chapter 4.1.1 and Fig. 4) or not. Validation is less commonly reported than verification. This may be partly due the fact that validation can be time-consuming and tedious. Furthermore, data quality can be crucial for validation. Imprecise data can easily mislead the validation (compare Chapter 4.1.1). The AMD benchmark problem by Walter et al. (1994) may also be counted towards a benchmark problem for validation since this fourth level problem was derived from an existing system. The geochemical conditions used in this problem resemble those at the uranium mine tailings impoundment at the Nordic site near Elliot Lake in northern Ontario (Morin & Cherry 1988).

#### 4.2.4 “Benchmarking” Models

“Benchmarking” models refers to exposing computer codes to critical types of problems and parameters, which cause difficulties in solving the numerical equations in the models. Codes can be benchmarked on an appropriate selection of, e.g.,

- master or basis species,
- simulation (CPU) time,
- boundary conditions,
- grid spacing,
- coupling technique and
- numerical technique.

An example of benchmarking models on coupling and numerical techniques is given by Pfingsten & Carnahan (1995). Pfingsten & Carnahan (1995) compared the performance of the two different reactive numerical codes MCOTAC and THCC on the basis of hypothetically generated redox systems. MCOTAC solves the transport from the equilibrium chemistry sequentially while THCC couples the equilibrium chemistry directly to a finite-difference representation of the physical transport with the so-called one-step or implicit method (compare Chapter 2.4.3). MCOTAC uses the random-walk simulation to solve advection and dispersion. By exposing these codes to the redox systems, specific areas of disagreement arose from numerical difficulties in these coupled codes.

Codes can also be benchmarked towards the prevention of numerical problems by investigating how large the physical dispersion needs to be. It is known that numerical oscillations may, e.g., decrease with higher physical dispersion. In other words, numerical oscillations smears out at higher dispersivity for sharp front problems (Pfingsten & Carnahan 1995).

In conclusion, benchmarking codes are not only important for providing more confidence in the overall performance of codes but also for assessing the codes to use in specific defined ways and for particular levels of simulation problems. Therefore, by benchmarking computer codes, user-guides can be generated. It is apparent that benchmarking codes can also give indications for further improvements of codes.

### 4.3 Summary and Implications

The first step in evaluating a newly developed reactive transport model is to verify the code. The next step taken is very often to illustrate the new capacities or processes considered within the model, for which no benchmark problem is available. Plausibility tests can additionally be undertaken to support investigation of model performance in greater extent. Validation of reactive transport models is far less observed than verification.

In the case of using sophisticated model modules, which have been evaluated

---

over a wide range of problems, model evaluation basically only requires examination whether the different modules within the new code provide reasonable results in coupled form. For this sort of evaluation, benchmark problems of “advanced” level can be utilised. This applies to the reactive hybrid transport model RUMT3D developed in this thesis. Consequently, as shown in Chapter 6, RUMT3D is evaluated with an advanced level of benchmark problems similar to AMD phenomena in chemical equilibrium as PHT3D was already evaluated to this benchmark level.

Complete and unambiguous evaluation of sophisticated (reactive transport) models is not possible, e.g., due to the unavoidable non-uniqueness of simulation results (Walter et al. 1994). The challenge is to demonstrate that newly developed models appear to work properly for a wide variety of problems (Viswanathan 1996). Efforts should thereby be made towards picking benchmark problems, which allow the model to be tested under different conditions or which allow plausibility tests to be undertaken.

*It is, of course, nonsense to assert the value-freedom of natural science. Scientific practice is governed by norms and values generated from an understanding of the goals of scientific inquiry.*

*Helen E. Longino, Science as Social Knowledge (1990)*

## Chapter

### 5 Verification of UMT3D by Performance Comparison of the Transport Solvers for the Conduit System

#### 5.1 Introduction

In this chapter, performance of the two transport models MT3DMS and the conduit transport model in coupled form is investigated. For that, a method of verification is selected which does not require immediate examination of the performance of MT3DMS since this model is a standardised and sophisticated transport model (Zheng & Wang 1999). Especially, the overall performance of the two transport models is examined by testing the proper implementation of the transport solver EMCNOT (Liu et al. 2001, see Chapter 3.2.1) for advection in the conduit system within UMT3D/RUMT3D. The focus is thereby to investigate:

- the transport in the conduit system,
- the interaction with the continuum and
- the initial and boundary conditions of the conduit system.

A benchmark problem that uses a similar pipe network setup as described by Birk (2001) was chosen since for this network with imposed initial and boundary conditions, a “quasi” analytical solution could be determined. Apart from the “quasi” analytical solution, the performance of the EMCNOT solver within UMT3D/RUMT3D is also compared to the standard finite difference solution of the benchmark problem. This problem setup requires only a description of the features of the conduit system. It is worthwhile to point out that by examining performance of the EMCNOT scheme using different criteria, UMT3D/RUMT3D is benchmarked towards accuracy, numerical stability and computational efficiency.

#### 5.2 Description of the Conduit System

The conduit system used for verification purpose in this chapter is basically a 3-way pipe network with 3 conduit tubes and 4 conduit nodes ( Fig. 5). Conduit tubes 1 through 3 have diameters,  $d_i$  of 0.1, 0.05 and 0.025 m, respectively. All three tubes have a length of 500 m each. Conduit nodes 3 and 4 are supplied with a constant recharge rate,  $R$  of  $3.15 \times 10^{-4} \text{ m}^3 \text{ s}^{-1}$  each. Only, conduit node 1 allows exchange to the porous matrix. There, mass is permitted to exit the

conduit system with an exchange coefficient of  $1.0 \times 10^{-4} \text{ m}^2 \text{ s}^{-1}$ . Initially, it is assumed that the concentration in the conduit system is  $1 \text{ mg L}^{-1}$ . No mass is added to the conduit system, i.e., the concentration of the recharge flux is zero. Using the recharge rates and pipe diameters, the following pipe flow rates can be calculated for pipes 1 through 3, 0.08, 0.16 and  $0.642 \text{ m s}^{-1}$ , respectively, which yield residence times of 6233, 3117 and 779 seconds, respectively. The through the “quasi” analytical solution computed time-dependent concentration values at each conduit node could be determined by using the residence times of the different pipes and initial and inflow concentration values to the respective nodes. One difference between the here described pipe network and the one by Birk (2001) is that, Birk (2001) kept the heads fixed at the outflow conduit node 1 and in the cell where this node was located.

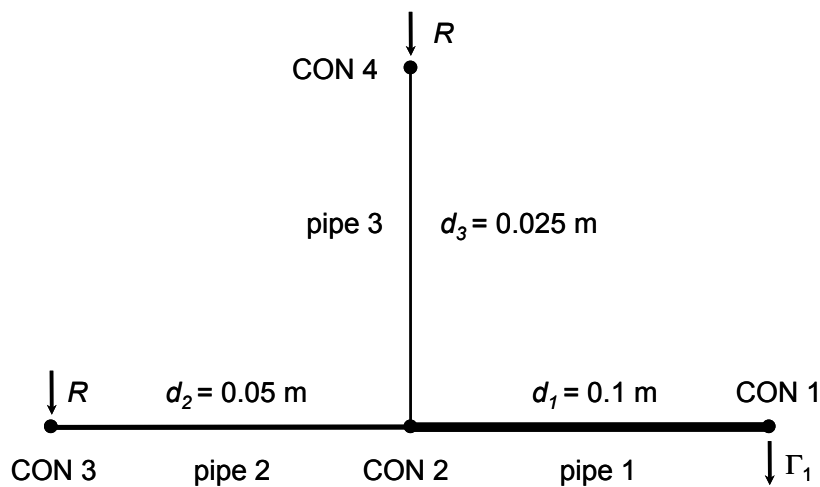


Fig. 5: Configuration of the 3 way pipe network system of the test problem.

### 5.3 Performance of UMT3D

Breakthrough curves at the conduit node 1 (CON 1, Fig. 5) are used to compare simulation results for the above-described conduit system at the outlet of the pipe network. Fig. 6 shows a comparison between the breakthrough curves at CON 1 using the FD method with two different pipe discretisation intervals of 0.1 and 1 m. The simulation results are also compared with the “quasi” analytical solution in Fig. 6. From Fig. 6, it is obvious that the finer the discretisation of the different pipes, the better the simulation results at CON 1. A pipe discretisation spacing of 0.1 m is rather small compared to a pipe length of 500 m and also results in a rather small transport time step size since a time criterion for the FD method is determined by the minimum of pipe discretisation spacing divided by the flow velocity within a respective pipe multiplied by the Courant number (see Chapter 3.2.2). Such small transport time step sizes can slow down transport calculations considerably in both models. When the concentration values at the conduit nodes are modified, concentration values in the connecting porous matrix cells need to be updated. In other words, in both models the same transport time step

size should be used. Especially for reactive transport problems where many components need to be transported, transport calculations with small transport time step sizes can be very time consuming. Therefore, it was advisable to implement a numerical method that solves advection in the conduit system with little time constraints, while at the same time numerical dispersion is reduced as shown in Fig. 6, particularly with the large pipe discretisation of 1 m. The EMCNOT method is intended to overcome these limitations.

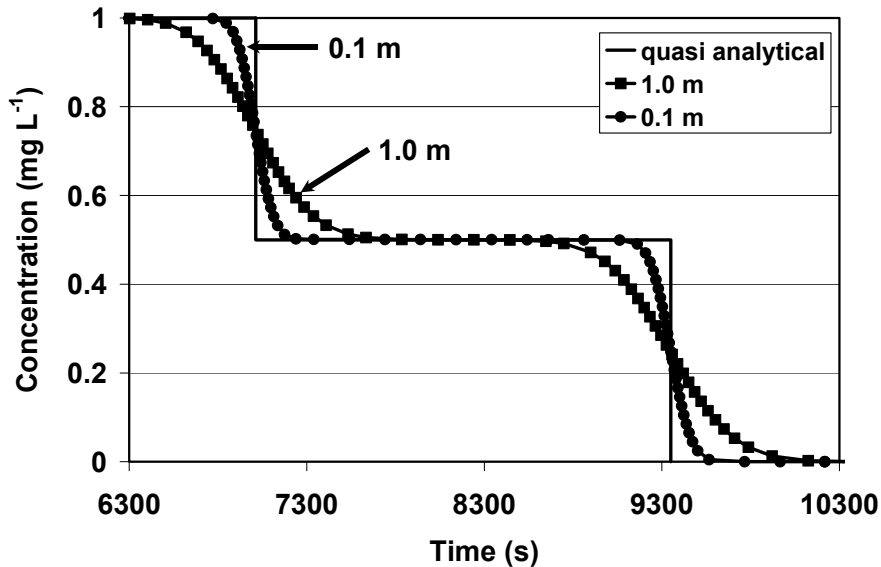


Fig. 6: Comparison of the simulation results using the FD method with pipe discretisations of 1 and 0.1 m.

Fig. 7 shows a comparison of the simulation results at CON 1 using the EMCNOT method with a pipe discretisation of 1 m and different transport time step sizes. The simulation results are also compared with the “quasi” analytical solution in Fig. 7 and with simulation results using the FD method with pipe discretisation of 1 and 0.1 m. Fig. 7 demonstrates that with transport time step sizes of 50% and 10% of the minimum residence in the pipe network ( $0.5 t_r$  and  $0.1 t_r$ , respectively) and a pipe discretisation of 1 m, comparable approximations of the transport solutions to the FD method using a tube discretisation of 1.0 and 0.1, respectively can be obtained. This implies that the EMCNOT scheme achieves time step size improvements by factors of 250 and 500 above the FD method, respectively. Further refinement of the pipe discretisation from 1 to 0.1 m for the different time criteria showed only minor improvements.

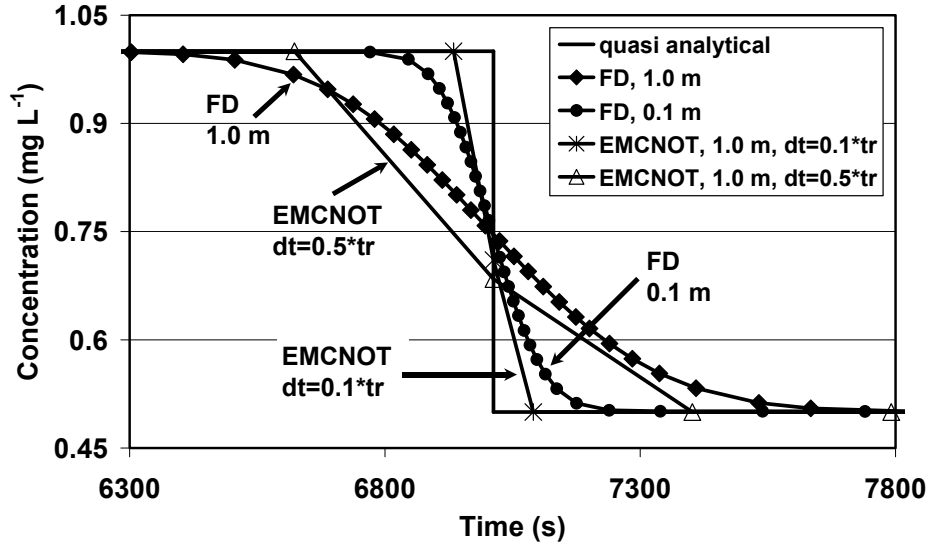


Fig. 7: Comparison of the simulation results using the EMCNOT and the FD method.

#### 5.4 Summary

In this chapter, the coupling of the transport models for the continuum and conduit system within UMT3D/RUMT3D was verified by comparison with a semi-analytical solution. Since a standard transport model was used for transport in the porous matrix, only the performance of the conduit transport model needed to be investigated. This was accomplished by testing the proper implementation of the transport solvers for the conduit system. Simulation results obtained with the explicit finite difference (FD) method to solve advection in the conduit system showed large numerical dispersion, which could be improved by using smaller pipe discretisations. However, smaller pipe discretisations are also associated with smaller transport time step sizes for both models. The numerical scheme EMCNOT developed by Liu et al. (2001) showed great improvements in the simulation results allowing much larger transport time step sizes and pipe discretisation. Therefore, the EMCNOT is especially recommended for simulation problems with complex pipe geometries and for simulations with multiple components transported and geochemical reactions. However, further testing of the EMCNOT method with more complex pipe geometries is recommended before it is used for real-world transport problems.

*Prediction is very hard, especially when it's about the future.*

*Yogi Berra, cited in Michio Kaku, Visions: How Science Will Revolutionize the 21<sup>st</sup> Century (1997)*

## Chapter

### 6 Verification of the Reactive Package within RUMT3D and Plausibility Tests

This chapter examines the coupling of the reaction model PHREEQC-2 with the transport simulator (UMT3D) and discusses the simulation results of RUMT3D on the basis of two reactive transport benchmark problems. For both simulated benchmark problems, appropriate background information and a detailed description of the modelling problem are provided. Moreover, for the first problem the consistency, stability and accuracy of the reactive simulation results are investigated with respect to the characteristics of the hybrid system by means of plausibility tests. Scenarios with and without a discrete conduit network are thereby compared and the influences of the conduit discretisation and of the magnitude of the conduit-matrix exchange are investigated.

#### 6.1 Acid Mine Drainage (AMD)

The first benchmark problem selected for evaluating the performance of the RUMT3D simulator for reactive transport has been defined by McNab (2001). Employing the local equilibrium assumption, the problem incorporates the principal processes occurring within an aquifer affected by Acid Mine Drainage (AMD). In contrast to the previously mentioned AMD simulation problem by Walter et al. (1994, see Chapter 4.2.1), it contains two different types of water chemistries and mineral phases within the model domain, i.e., a model region representing the mine tailing and one representing the adjacent aquifer. As a result, three distinct geochemical zones evolve with time when simultaneously (i) recharge solution is flushing the tailing region and (ii) buffering minerals contained in the aquifer matrix become exhausted sequentially. The buffering capacity of the aquifer material largely determines the pH of the plume. This in turn affects the leaching of metals into the aqueous phase.

McNab (2001) simulated this problem with PHREEQC-2 using its 1D transport capability. Similarly, the PHREEQC-2 model was selected for the present study to provide benchmark results for the comparison with RUMT3D as this model is (i) well-tested and (ii) because it is also used by RUMT3D for its reaction calculations (compare Chapter 3.3). With the focus of the present work being on the incorporation and simulation of conduit-matrix effects, the usage of the same reaction model had the benefit that it allowed for a quicker identification of peculiar phenomena resulting from the newly incorporated processes.

Another advantage of using the McNab problem as a benchmark problem is that

the number of components and mineral phases as well as the number of processes are relatively small and thus more easily comprehensible than more complex descriptions of the AMD phenomena. This permits a quicker differentiation of phenomena that might occur either due to (i) the true physical or chemical processes, (ii) numerical problems, or (iii) the selected model coupling procedure.

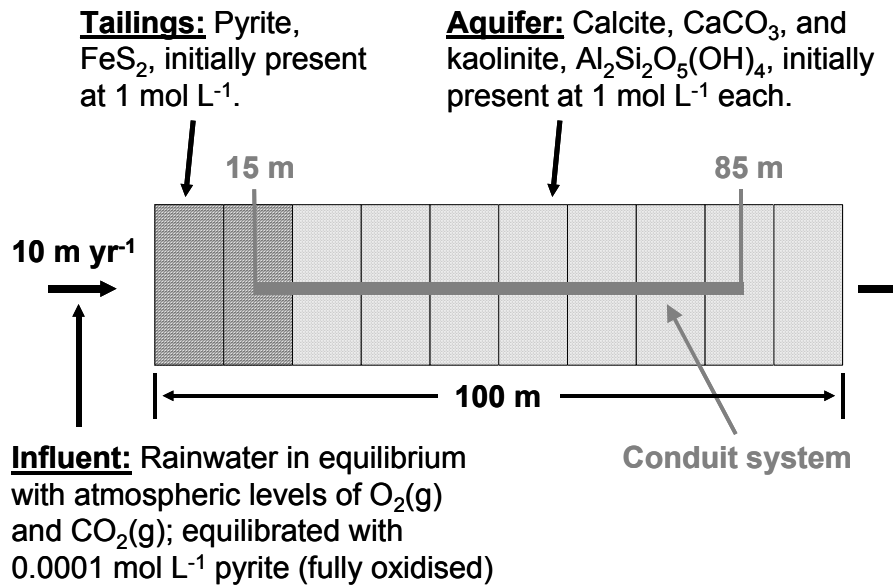


Fig. 8: 1D McNab model for simulation of simple acid mine drainage phenomena (McNab 2001).

### 6.1.1 Description of the Benchmark Problem

McNab (2001) utilised a one-dimensional model with a length of 100 m, which was discretised into 10 cells of 10 m length (Fig. 8). In this scenario-type modelling study, the oxidation of pyrite by oxidising recharge solution and the propagation of an acidic front in water-saturated mine tailings was simulated and the subsequent mineral buffering effect in an adjacent aquifer is demonstrated (see also next subsection on Geochemical Processes during Transport). In the first 2 cells, representing the tailings region, only pyrite is present (at an excess concentration of  $1 \text{ mol L}^{-1}$ ). In this thesis, mineral concentrations are expressed in  $\text{mol L}^{-1}$  that refers to moles of a respective mineral per litre water. If mineral concentrations need to be known in moles per litre groundwater, the respective concentration in  $\text{mol L}^{-1}$  needs to be divided by the porosity. Cells 3 - 10 represent the adjacent aquifer containing calcite ( $\text{CaCO}_3$ ) and kaolinite ( $\text{Al}_2\text{Si}_2\text{O}_5(\text{OH})_4$ ) to equal proportions of  $1 \text{ mol L}^{-1}$ . The initial solution composition in the tailings region consists of anaerobic de-ionised water that was equilibrated with pyrite, whereas for the remainder of the model domain, de-ionised water was equilibrated with calcite and kaolinite. After equilibration, the solution within the tailing area has a neutral pH and contains minor amounts of sulphate and

dissolved iron. In contrast, the solution representing the ambient solution in the adjacent aquifer region is alkaline. Further, it contains traces of aluminium and silicon, resulting from kaolinite dissolution during equilibration (Table 2). Concentration of a master species listed in Table 2 refers to the sum of a respective dissolved species in the aqueous phase, e.g., Fe(III) represents the sum of all dissolved ferric iron-bearing species. Gypsum ( $\text{CaSO}_4 \cdot 2\text{H}_2\text{O}$ ) and goethite ( $\text{FeOOH}$ ) are allowed to precipitate in the aquifer but not in the tailing, i.e., not in the first 2 cells. Pyrite dissolution/precipitation is only allowed to occur in the tailing region but not in the adjacent aquifer. Table 3 lists the reaction equations of the mineral phases in the McNab model, along with their thermodynamic constants (pK). The problem was simulated with the WATEQ database as provided by the PHREEQC-2 model.

The tailing is recharged at a rate of  $10 \text{ m yr}^{-1}$ , yielding a percolation rate of  $10 \text{ m yr}^{-1}$ , given the cross-sectional area (perpendicular to the flow direction) of  $1 \text{ m}^2$ , an effective porosity of 1 and a uniform hydraulic conductivity of  $100 \text{ m yr}^{-1}$ . This yields a hydraulic gradient of 9.9 m between the first cell in the tailing and the last cell in the aquifer. For simplicity, steady state flow conditions and a dispersivity of 1 m throughout the model are assumed. The simulation time is 20 years. The recharge solution is aerobic, acidic and has elevated concentrations of carbonate, Fe(III) and sulphate as a result of the equilibration with atmospheric carbon dioxide ( $\text{CO}_2(\text{g})$ ), atmospheric oxygen ( $\text{O}_2(\text{g})$ ) and pyrite (at a concentration of  $0.0001 \text{ mol L}^{-1}$ , Table 2).

Table 2: Initial chemical composition of the recharge, tailing and aquifer solution of the McNab model.

Master species / mineral	Symbol	Recharge solution (total concentration in $\text{mol L}^{-1}$ )	Tailing solution (total concentration in $\text{mol L}^{-1}$ )	Aquifer solution (total concentration in $\text{mol L}^{-1}$ )
pH		2.197 <sup>a</sup>	7.007 <sup>a</sup>	9.742 <sup>a</sup>
pe		18.408 <sup>a</sup>	-3.743 <sup>a</sup>	-5.731 <sup>a</sup>
Aluminium	Al(III)	-	-	$3.420 \times 10^{-6}$
Carbonate	C(IV)	$3.383 \times 10^{-6}$	-	$1.415 \times 10^{-5}$
Calcium	Ca(II)	-	-	$1.415 \times 10^{-5}$
Ferrous iron	Fe(II)	$1.700 \times 10^{-10}$	$5.066 \times 10^{-10}$	-
Ferric iron	Fe(III)	$1.000 \times 10^{-3}$	$4.451 \times 10^{-18}$	-
$\text{O}_2(\text{aq})$	O(0)	$4.347 \times 10^{-5}$	-	-
Sulphite	S(-II)	-	$8.838 \times 10^{-10}$	-
Sulphate	S(VI)	$2.000 \times 10^{-3}$	$1.293 \times 10^{-10}$	-
Silicon	Si(IV)	-	-	$3.420 \times 10^{-6}$
Calcite		-	-	1.0
Kaolinite		-	-	1.0
Pyrite		-	1.0	-

<sup>a</sup> Dimensionless.

Table 3: Chemical reaction equations of the considered mineral phases in the McNab model, along with their thermodynamic constants (pK, mainly taken from the WATEQ database).

Mineral	Reaction equation	pK
Pyrite	$\text{FeS}_2 + 3.5 \text{O}_2 + \text{H}_2\text{O} \Leftrightarrow \text{Fe}^{2+} + 2 \text{SO}_4^{2-} + 2 \text{H}^+$ <sup>a</sup>	-96.78 <sup>b</sup>
	$\text{FeS}_2 + 14 \text{Fe}^{3+} + 8 \text{H}_2\text{O} \Leftrightarrow 15 \text{Fe}^{2+} + 2 \text{SO}_4^{2-} + 16 \text{H}^+$ <sup>a</sup>	
Calcite	$\text{CaCO}_3 \Leftrightarrow \text{Ca}^{2+} + \text{CO}_3^{2-}$	8.48
Kaolinite	$\text{Al}_2\text{Si}_2\text{O}_5(\text{OH})_4 + 6 \text{H}^+ \Leftrightarrow 2 \text{Al}^{3+} + 2 \text{H}_4\text{SiO}_4 + \text{H}_2\text{O}$	-7.435
Goethite	$\text{FeOOH} + 3 \text{H}^+ \Leftrightarrow \text{Fe}^{3+} + 2 \text{H}_2\text{O}$	1.0
Gypsum	$\text{CaSO}_4 \cdot 2\text{H}_2\text{O} \Leftrightarrow \text{Ca}^{2+} + \text{SO}_4^{2-} + 2 \text{H}_2\text{O}$	4.58

<sup>a</sup> Singer & Stumm (1970)

<sup>b</sup> Bain et al. (2001)

### 6.1.2 Geochemical Processes during Transport

During transport, dissolved oxygen and ferric iron entering the tailings region through the model boundary with the recharge solution oxidises pyrite, leading to a release of protons, Fe(II) and sulphate ions within the aqueous phase and decreases the pH in that region. According to Singer & Stumm (1970), pyrite oxidation is initiated by oxygen but propagated by Fe<sup>3+</sup>. Under certain conditions, the major oxidising agent of pyrite is ferric iron. A more acidic environment promotes the presence of Fe(III) in solution. Table 3 lists the overall reactions to oxidise pyrite with oxygen and ferric iron.

When solution is transported from the tailings region to the adjacent aquifer, it triggers a sequence of reactions: calcite dissolves and the free available protons complex to HCO<sub>3</sub><sup>-</sup> until the calcite solubility is reached, leading to a significant pH increase in the aquifer. Simultaneously, Fe<sup>2+</sup> is oxidised to Fe<sup>3+</sup> by sulphate reduction. The product of this oxidation is the generation of sulphite. However, most of the dissolved Fe<sup>3+</sup> precipitates as goethite (pK = -1.0). Sulphate is also required for the competitive precipitation reaction of gypsum but the reaction is less favourable (pK = -4.58) and thus more goethite precipitates than gypsum. Besides calcite, kaolinite is a second acid buffering mineral phase. Though, its buffering capacity is much smaller compared to calcite dissolution. The reaction for kaolinite is strongly pH-dependent whereas the one for calcite is not (see Table 3). Thus, kaolinite dissolves only in noticeable amounts at a low pH once calcite is fully depleted. Under condition of calcite depletion, goethite dissolution and subsequent Fe(III) reduction are promoted. As a result, elevated Fe(II) and sulphate concentrations are observed. Fig. 9 schematically depicts the interrelations of the different geochemical reactions in the aquifer. Interaction between the different phases is assumed to occur in equilibrium.

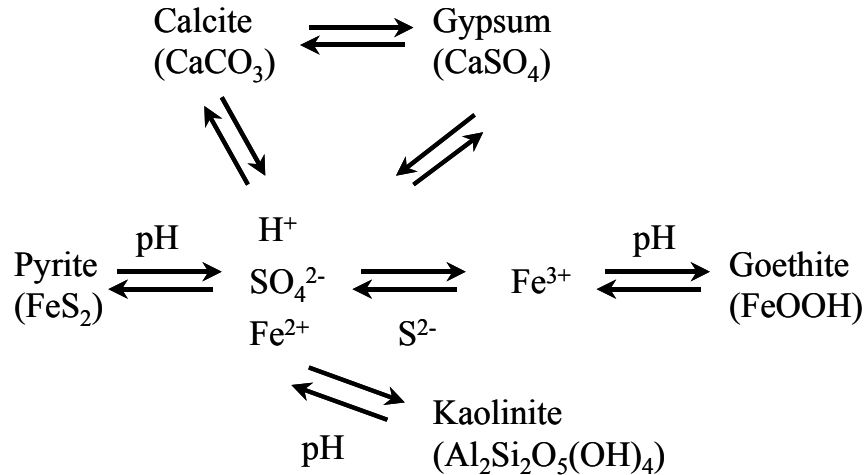


Fig. 9: Simplified dissolution/precipitation processes of the aqueous and solid phases in the aquifer in the McNab model.

### 6.1.3 Setup of the Benchmark Problem and Model Comparison

To achieve accurate and numerically stable reactive simulation results using RUMT3D, this subsection examines appropriate spatial and temporal discretisations required for the present benchmark problem. Simulation results of RUMT3D are thereby compared with the PHREEQC-2 model. At the end of this subsection, once appropriate discretisations are found, minor differences in results between these two models and a non-physical effect occurring with both models are discussed.

**Spatial scale.** Initial tests for numerical stability, such as simulating a tracer breakthrough (chloride) revealed that a discretisation of 10 m per cell causes significant numerical dispersion when using RUMT3D/MT3DMS's numerical solver TVD (third-order total-variation-diminishing scheme) for the simulation of advective transport. To ensure that TVD would not only handle the discretisation chosen but also different concentrations of the recharge, tailing and aquifer water, the following initial tracer concentrations were assumed: 0.01, 0.005, 0.001 mol L<sup>-1</sup> in the recharge, tailing and aquifer solution, respectively. Fig. 10 illustrates the simulated tracer concentrations after one year for both, the RUMT3D and the PHREEQC-2 model in comparison for different spatial discretisations of 10, 2 and 1 m per cell, respectively. As the different solutions have different initial concentrations, two moving fronts can be seen in Fig. 10: the first front starts at the beginning of the tailing with the concentration of the recharge solution (0.01 mol L<sup>-1</sup>) and stops at the end of tailing (at 20 m) with the concentration of the tailing solution (0.005 mol L<sup>-1</sup>); the second front begins at the end of the tailing/beginning of the aquifer with the concentration of the tailing solution (0.005 mol L<sup>-1</sup>) and stops 20 m further downgradient in the aquifer with the concentration of the aquifer solution (0.001 mol L<sup>-1</sup>). Fig. 10 demonstrates that for conservative transport of chloride, the PHREEQC-2 model shows less numerical dispersion in comparison with RUMT3D for the simulations that use the coarse discretisation of 10 m per cell. However, significant numerical

dispersion (flatter curve) becomes also apparent for PHREEQC-2 in the reactive case, especially for the early parts of the simulation when the most significant geochemical changes occur (Fig. 11). Fig. 11 shows the simulated calcium (a-d Figs.) and pH (e-h Figs.) profiles after 0, 1, 2 and 5 years for different discretisations of 10 and 1 m per cell, respectively. Though, as for the non-reactive case, the magnitude of numerical dispersion of PHREEQC-2 for the reactive case compared to the one of RUMT3D is not as large. When recharge solution reaches the right hand boundary of the aquifer after approximately 10 years, numerical dispersion becomes negligible.

For a discretisation of 1 m per cell, the simulation results of RUMT3D and PHREEQC-2 are in good agreement. Fig. 10 indicates that a discretisation of 2 m per cell would also be sufficient to generate satisfactory results. Nonetheless, since subsequently a conduit system (which might trigger numerical instability) is introduced into the original McNab problem, a discretisation of 1 m per cell was selected for the following investigations.

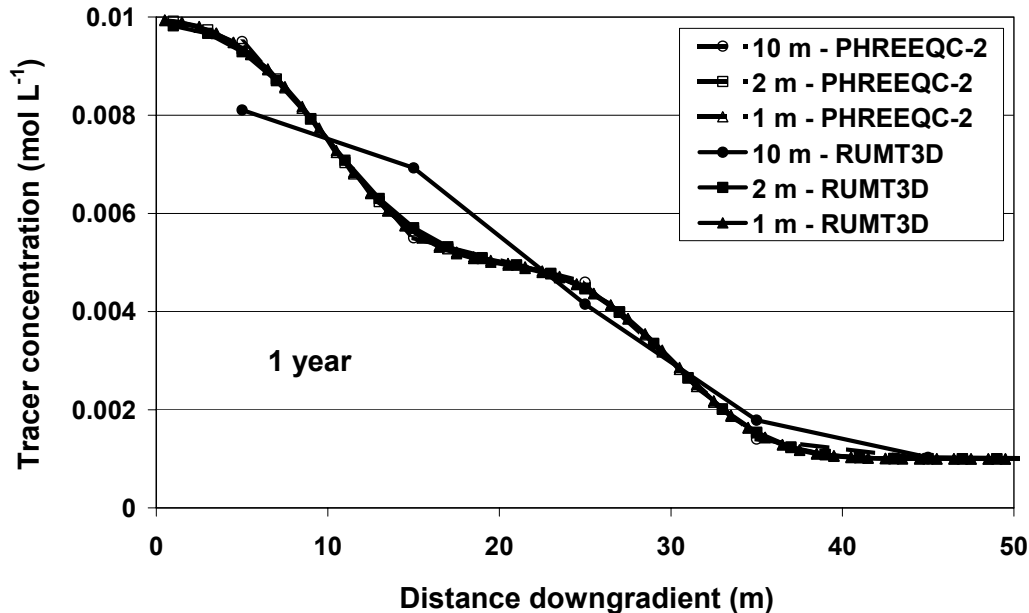
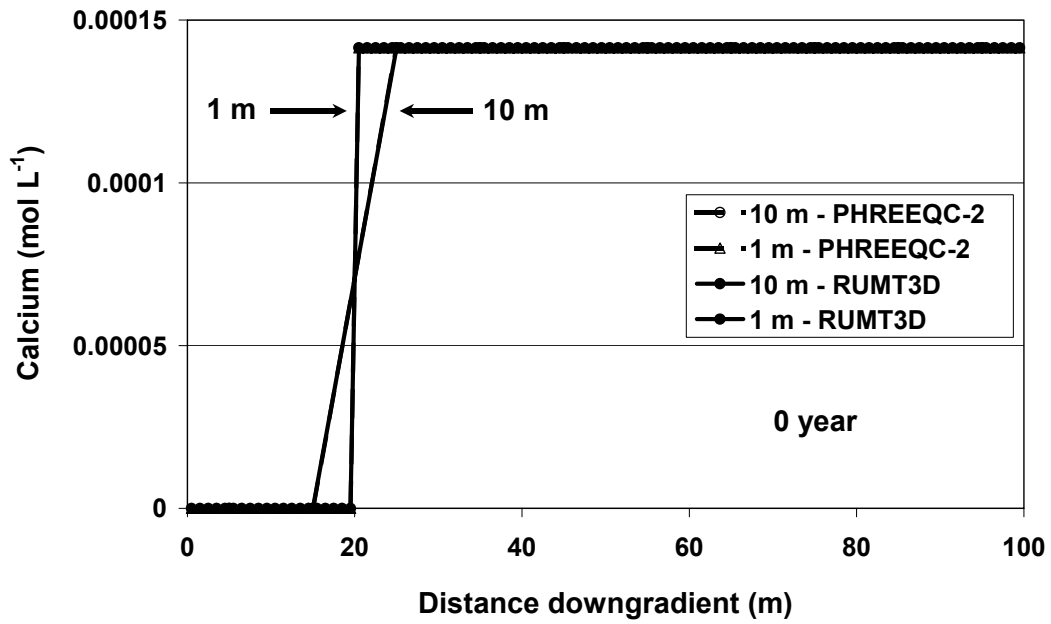
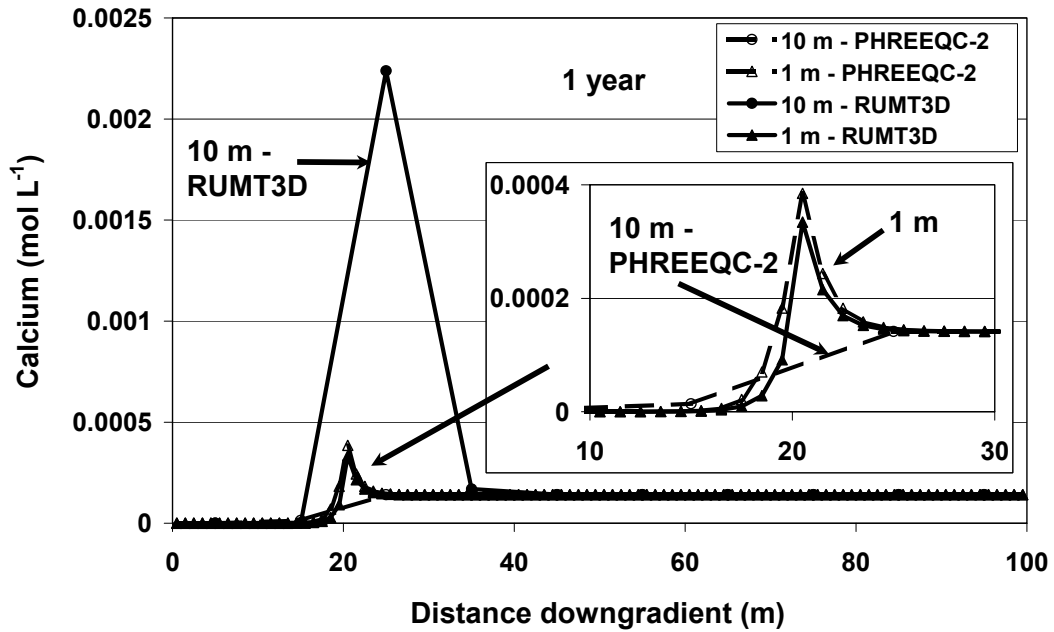


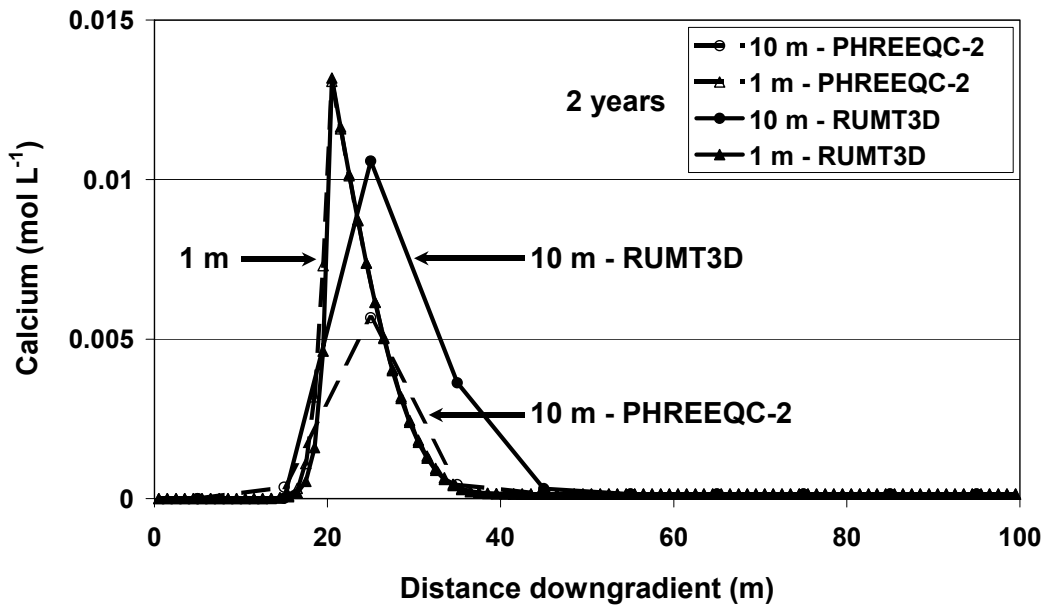
Fig. 10: Comparison of simulated tracer profiles of the McNab problem with the RUMT3D and PHREEQC-2 models using different spatial discretisations of 10, 2 and 1 m per cell after 1 year. The recharge, tailing and aquifer solution had initial concentrations of 0.01, 0.005, 0.001 mol L<sup>-1</sup>, respectively.



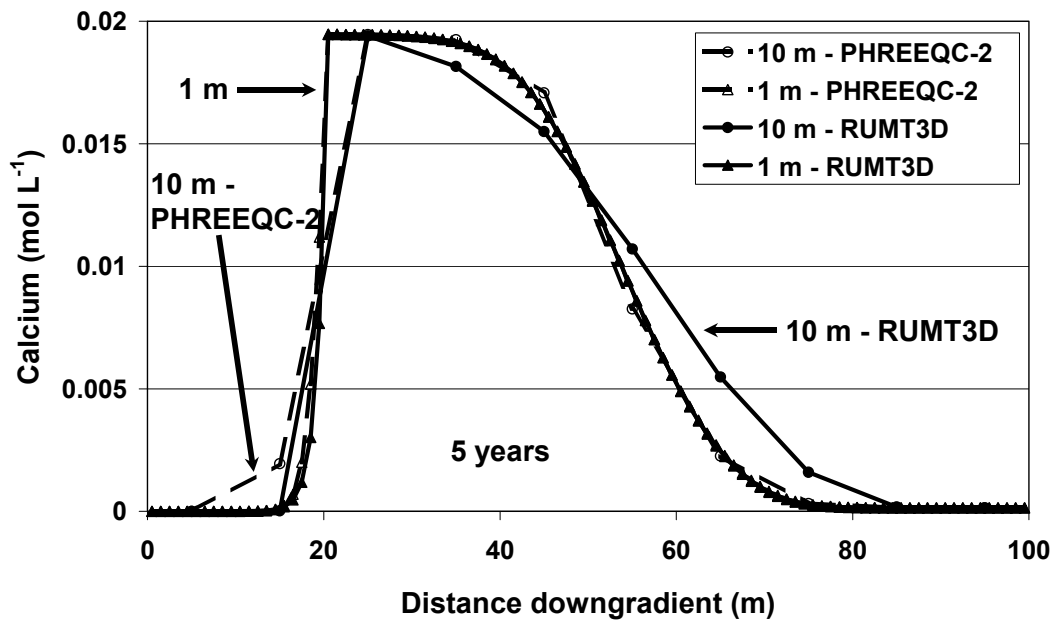
a) Calcium profile at the beginning of the simulation.



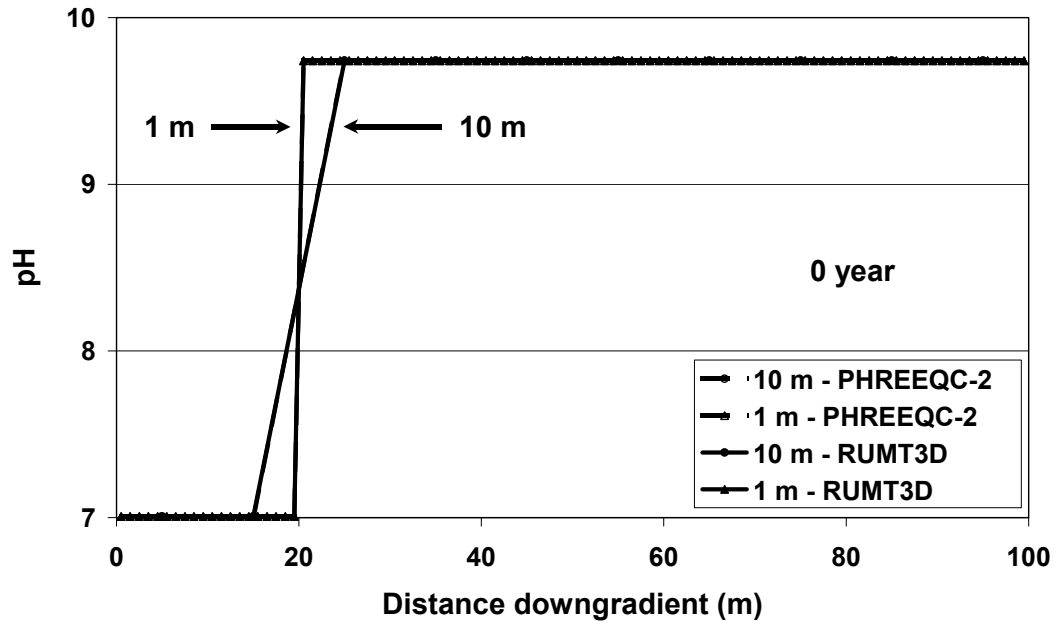
b) Simulated calcium profile after 1 year.



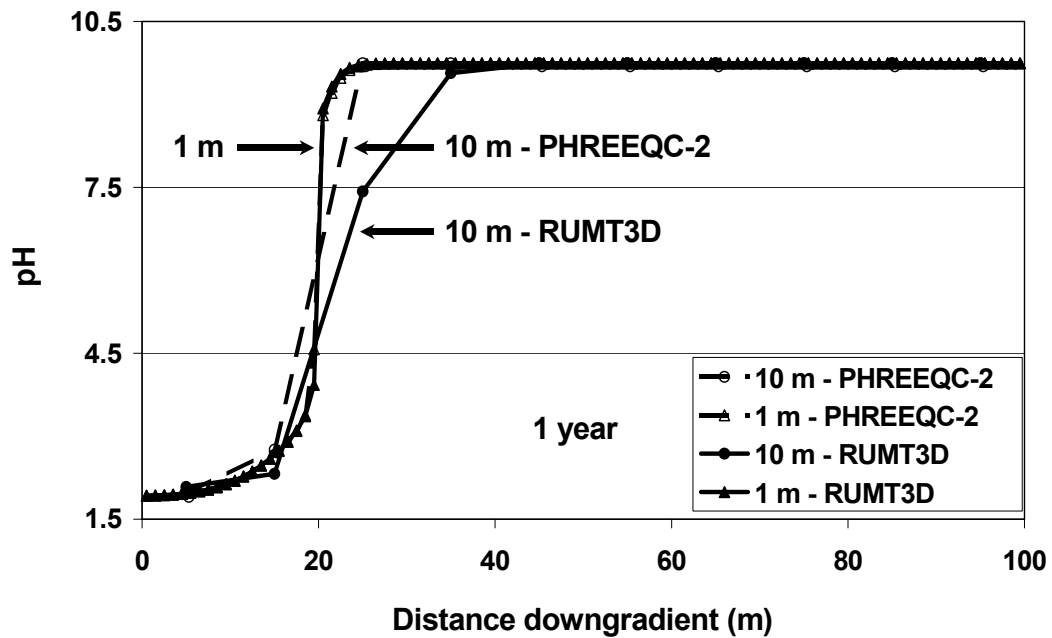
c) Simulated calcium profile after 2 years.



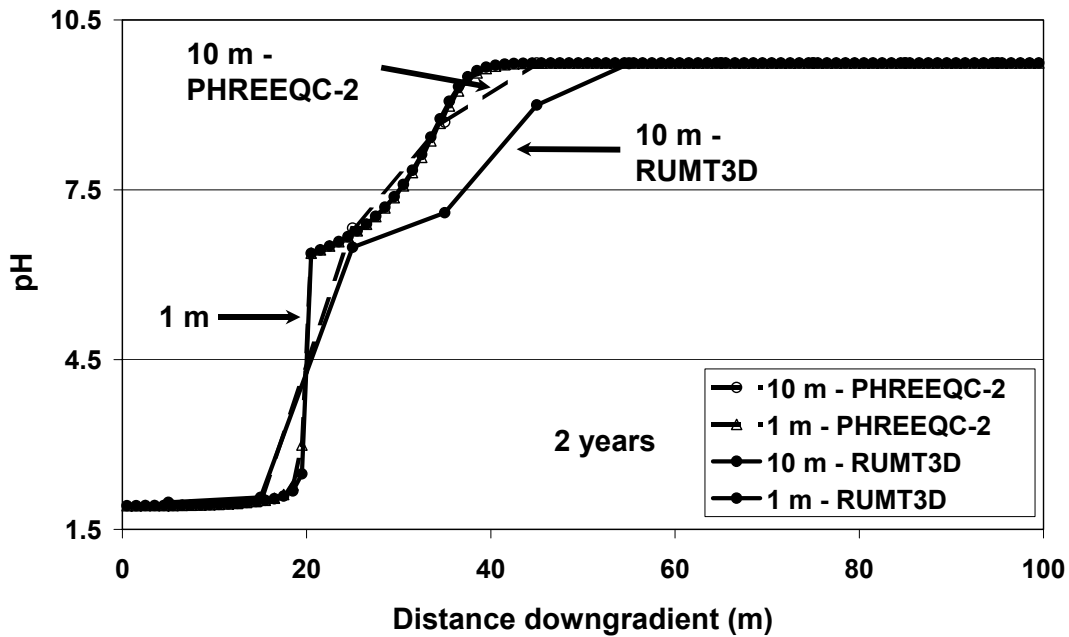
d) Simulated calcium profile after 5 years.



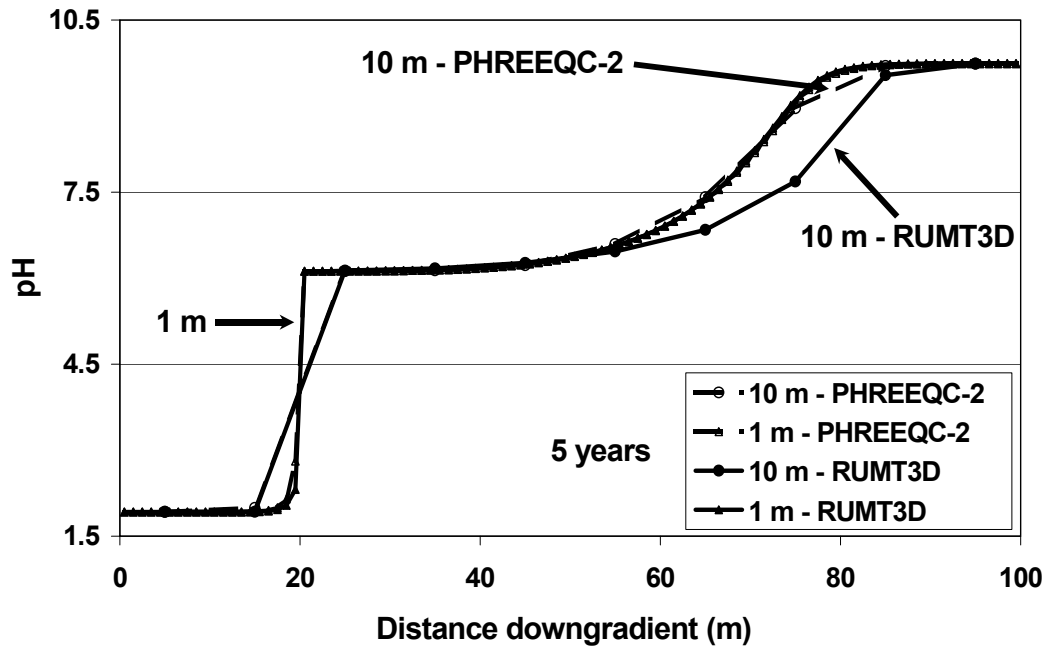
e) pH profile at the beginning of the simulation.



f) Simulated pH profile after 1 year.



g) Simulated pH profile after 2 years.



h) Simulated pH profile after 5 years.

Fig. 11: Comparison of simulated calcium (a, c, e, g) and pH (b, d, f, h) profiles after 0, 1, 2 and 5 years, respectively, for the McNab problem using different discretisations of 10, 2 and 1 m per cell. Results are compared to the PHREEQC-2 model.

Reaction time step frequency. In RUMT3D, the number of transport but not the number of reaction time steps (see Chapters 2.5.1 and 3.3) is automatically controlled such that the appropriate stability criteria for physical transport are satisfied (Zheng & Wang 1999; Prommer et al. 2003). Therefore, the influence of the selected reaction time step length in RUMT3D was further investigated for the present simulation problem. For cases like the McNab problem, where all reactions are assumed to be in equilibrium, any error that occurs as a result of the (user-)selected reaction time-step length is based on temporal operator splitting errors (usual OS error, Walter et al. 1994; Steefel & MacQuarrie 1996), whereas in the case of kinetic reactions the solution accuracy might also depend, e.g., on the integration method used for the kinetic reactions (Parkhurst & Appelo 1999). It should be noted that within an investigated range of reaction step frequencies, an increase in the number of reaction time steps does not necessarily improve the accuracy of results once an inappropriate spatial discretisation is selected (Fig. 12). Fig. 12 displays the simulated calcium concentration profiles for RUMT3D after 1 year using a discretisation of 10 m per cell and reaction time step sizes of 100 and 1000 per year. Results obtained with the PHREEQC-2 model are shown in comparison.

When comparing simulated concentration profiles (after 1, 2, 5, 10, 15 and 20 years, respectively), a good agreement of results can be observed for both, the PHREEQC-2 and the RUMT3D solutions for all investigated cases with the following selection of reaction time steps per year: 100, 150 and 200 if a spatial discretisation of 1 m per cell is selected. Fig. 13a-d show the comparison of results for pH, sulphate, Fe(II) and goethite profiles after 20 years using either 10, 100 or 200 reaction time steps per year. Results from the PHREEQC-2 model are also shown in comparison. Based upon the good agreements of the RUMT3D model using 100, 150 and 200 reaction time steps per year with the PHREEQC-2 model, for all simulations in this section, 100 reaction time steps per year were used.

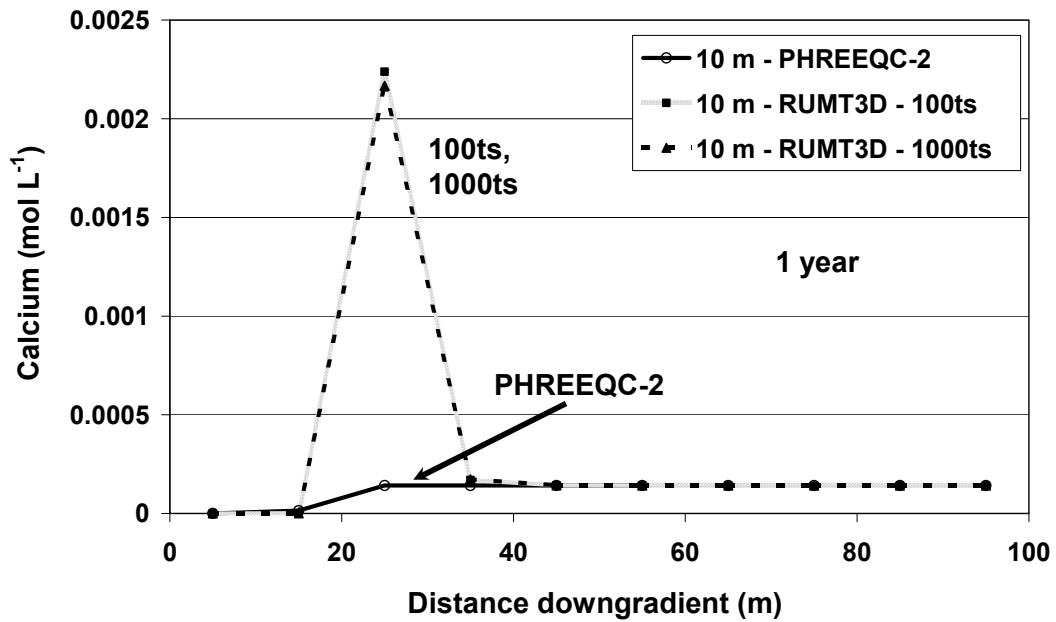
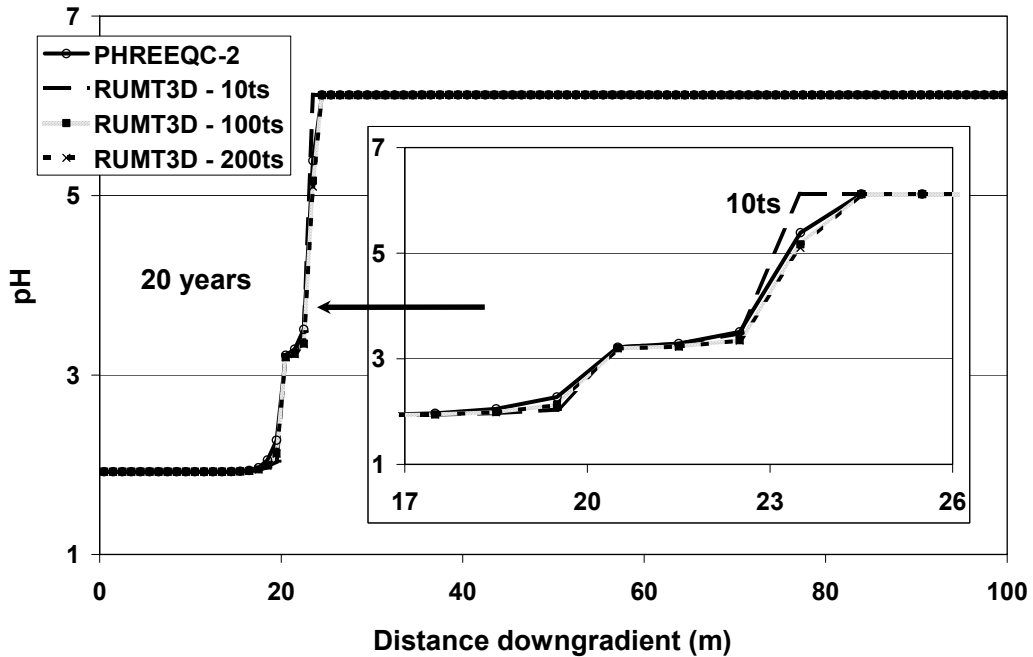
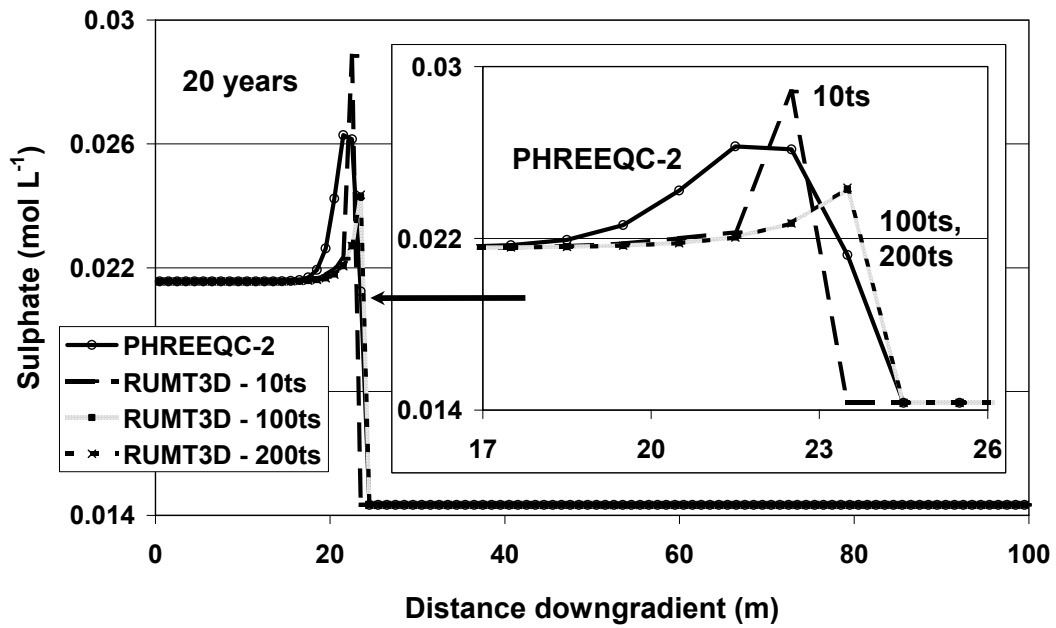


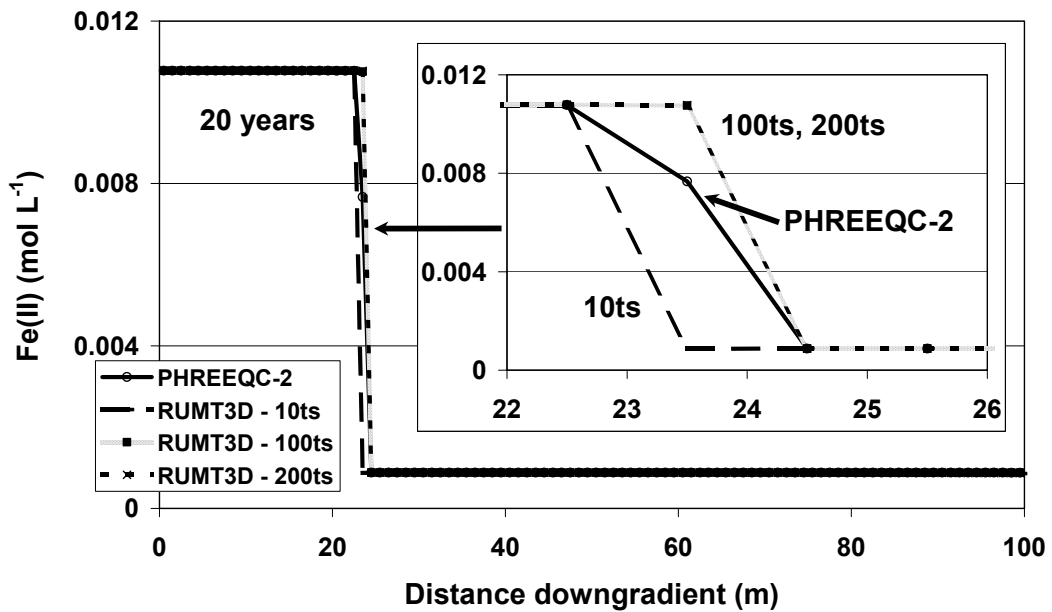
Fig. 12: Comparison of simulated calcium profiles with the PHREEQC and RUMT3D models after 1 year, for the McNab problem using discretisation of 10 m per cell. Two different reaction time step (ts) sizes were used for the RUMT3D model per year (100 and 1000).



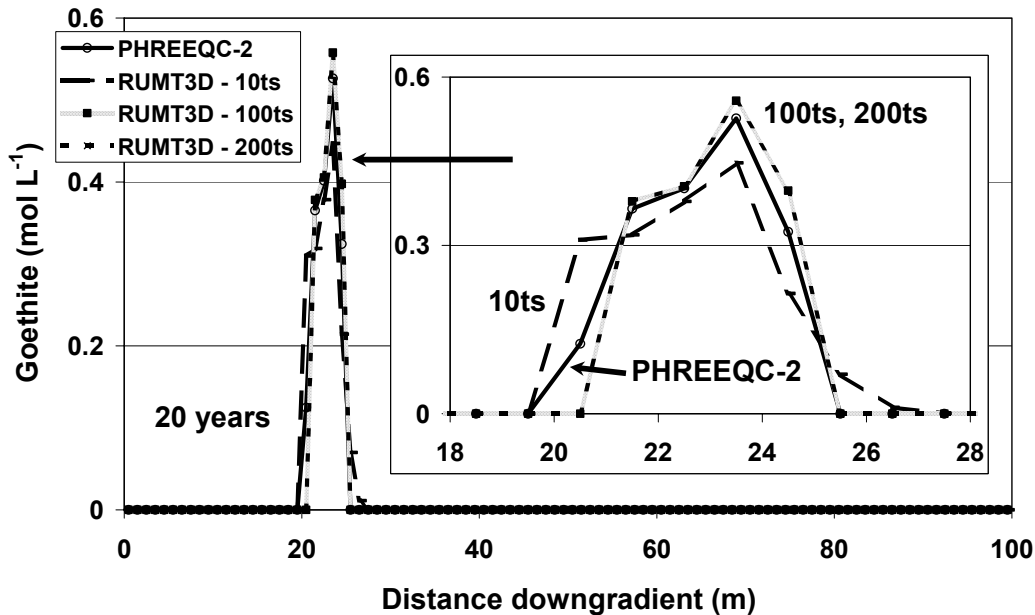
a) Simulated pH profile.



b) Simulated sulphate profile.



c) Simulated Fe(II) profile.

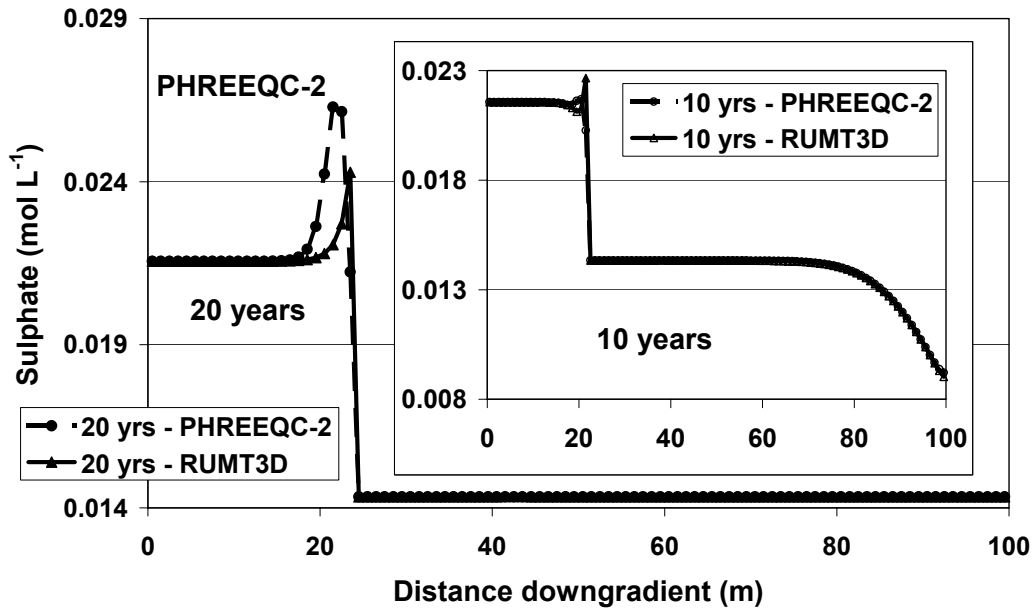


d) Simulated goethite profile.

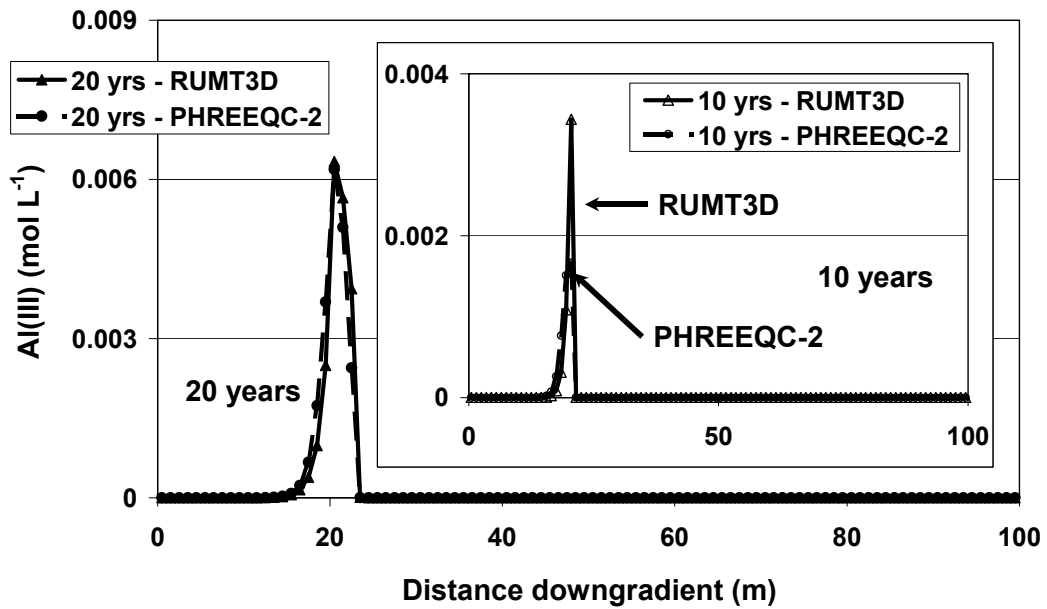
Fig. 13: Comparison of simulated pH, sulphate, Fe(II) and goethite profiles after 20 years, for the McNab problem using 10, 100 and 200 reaction time steps (ts) per year in RUMT3D. Results are compared to the PHREEQC-2 model.

Differences between the RUMT3D and PHREEQC-2 model. With a spatial discretisation of 1 m per cell and a reaction time step size of 100 per year, some minor deviations can be noticed in aquifer cells where calcite was depleted after 10 years. These are particularly reflected by the peak concentrations of aluminium, silicon, Fe(II), sulphate and goethite. These differences appear to decrease with time, while the ones of sulphate seem to increase. These deviations may be related to the selection of the reaction time step size where equilibrium is calculated and or how dispersion is calculated in the RUMT3D and PHREEQC-2 model. Fig. 14 shows the simulated sulphate, Al(III) and goethite profiles after 10 and 20 years, respectively using both models.

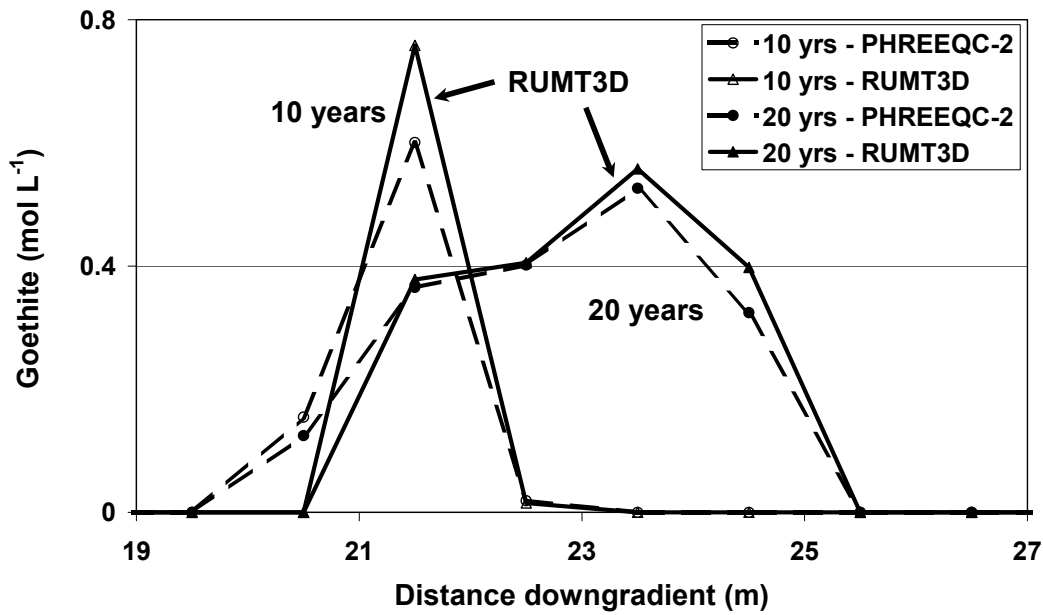
Non-physical effect. Pyrite precipitates in the last cell of the tailing before intersecting the aquifer (about 14 mols, fraction of about 9 % of the dissolved amount in the first cell of the tailing, Fig. 15). This is probably because sulphite migrates gradient upwards from the first aquifer cell into the tailing, which is of course a non-physical, artificial effect, caused by the calculation of the dispersion through the finite difference method by taking average of the concentrations over two cell interfaces. The influence of calculation of dispersion upon results can however be best demonstrated by the aluminium and silicon concentrations in the tailing region. These start to increase to noticeable concentration values from cell 16 onwards (out of 20 cells representing the tailings region) despite the absence of kaolinite within this section. Both models, i.e., the RUMT3D and PHREEQC-2 model show this behaviour.



a) Simulated sulphate profile.



b) Simulated Al(III) profile.



c) Simulated goethite profile.

Fig. 14: Simulated sulphate, Al(III) and goethite profiles after 10 and 20 years, for the McNab problem using the PHREEQC-2 and RUMT3D models.

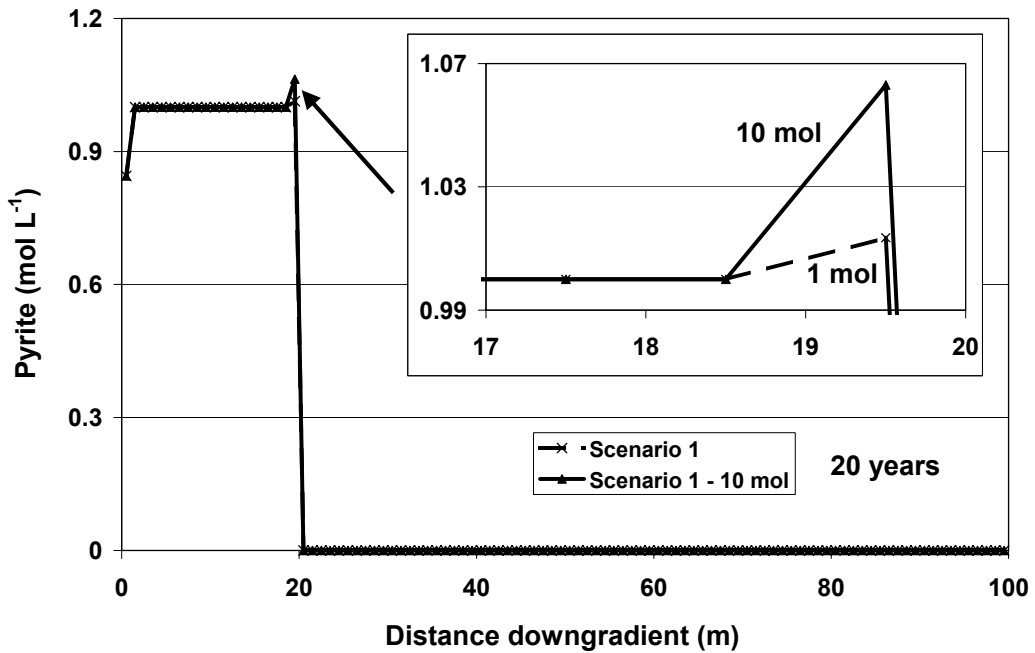


Fig. 15: Simulated pyrite profiles after 20 years, for the McNab problem with the PHREEQC-2 and RUMT3D models, using initial calcite concentrations of 1 and 10 mol L<sup>-1</sup> in the aquifer.

### 6.1.4 Description of the Hybrid System

The McNab problem described in Chapter 6.1.1 can easily be expanded to a hybrid system. This is achieved by adding a conduit system into the model domain that represents the standard porous media flow and transport system (pure continuum system). The selected conduit system (see Fig. 8) starts in the tailing area (centre of cell 15 at 14.5 m) and ends in the aquifer (centre of cell 65 at 84.5 m). The total length of the conduit system is 70 m. Different cases of a hybrid system are investigated by varying discretisation of the conduit system and magnitudes of exchange coefficients. Basically, a coarse and a fine discretisation of the conduit system are investigated, both for a range of different exchange coefficients, as listed in Table 4.

Table 4: Characteristics of the investigated cases for the introduced conduit system in the McNab problem.

Name	Type of discretisation	Number of conduits within the conduit system	Number of connecting nodes to the continuum	Length of the conduits within the conduit system (m)	Magnitude of the used exchange coefficients (ex) ( $\text{m}^2 \text{s}^{-1}$ )	Approximate initial diversion fraction into the conduit system (%)
1con	coarse	1	2	70	$1 \times 10^{-7}$	52.5
					$6 \times 10^{-7}$	98.5
70con	fine	70	71	1	$1 \times 10^{-8}$	5.3
					$5 \times 10^{-8}$	11.8
					$1 \times 10^{-7}$	16.3
					$5 \times 10^{-7}$	32.6

### 6.1.5 Setup of the Hybrid System

To also achieve accurate and numerically stable reactive simulation results for the hybrid system using RUMT3D, this subsection examines the appropriate spatial and temporal scales for the conduit system as well as the necessary reaction time step size for the hybrid system. Spatial scale of the hybrid system does not need to be investigated as this was already done for the pure continuum system (see Chapter 6.1.3).

*Spatial and temporal discretisation of the conduit system.* In RUMT3D, the conduits can be further divided into tube subsections. Generally, this will increase numerical accuracy since conduits can have considerable lengths (see Chapter 3.2). The coarse discretisation case (1con) consisting of a single conduit of 70 m length was investigated with different number of tube subsections (i.e., 50, 500 and 750) within this single conduit. For all subsections, a transport time step size criterion for the EMCNOT solver of 20 % of the minimum residence time within the conduit was used. At the entry and exit node of the single conduit, an exchange coefficient of  $6 \times 10^{-6} \text{ m s}^{-1}$  was applied. In Fig. 16, tracer

concentration profiles for these different subdivisions are compared. The plot demonstrates that the chosen transport time step size criterion for the EMCNOT solver in combination with a spatial discretisation of 50 subsections for the conduit are sufficient. In hindsight to the plausibility tests (see Chapter 6.1.7), a sufficiently fine discretisation was required to account for potential numerical instabilities. Thus, a subdivision into 500 subsections was selected for all conduit simulations with a single conduit. For the conduit system with 70 conduits (70con), a subdivision into 10 subsections per 1-m conduit was chosen for the corresponding case fulfilling the same time step size criterion as in the single conduit case.

**Reaction time step frequency.** The influence of the reaction step frequency was repeated for the hybrid system case. In the presence of the conduit system, similar solutions were obtained for all investigated cases (100, 150 and 200 reaction time steps per year). Both discretisations of the conduit system (1con and 70con) were studied using the exchange coefficients of  $1 \times 10^{-7}$  and  $6 \times 10^{-6}$   $\text{m s}^{-2}$  for 1con and  $1 \times 10^{-7}$   $\text{m s}^{-2}$  for the 70con case. From the results of those simulations, it was concluded that a reaction step frequency of 100 reaction time steps per year was appropriate for the following investigations of the hybrid system.

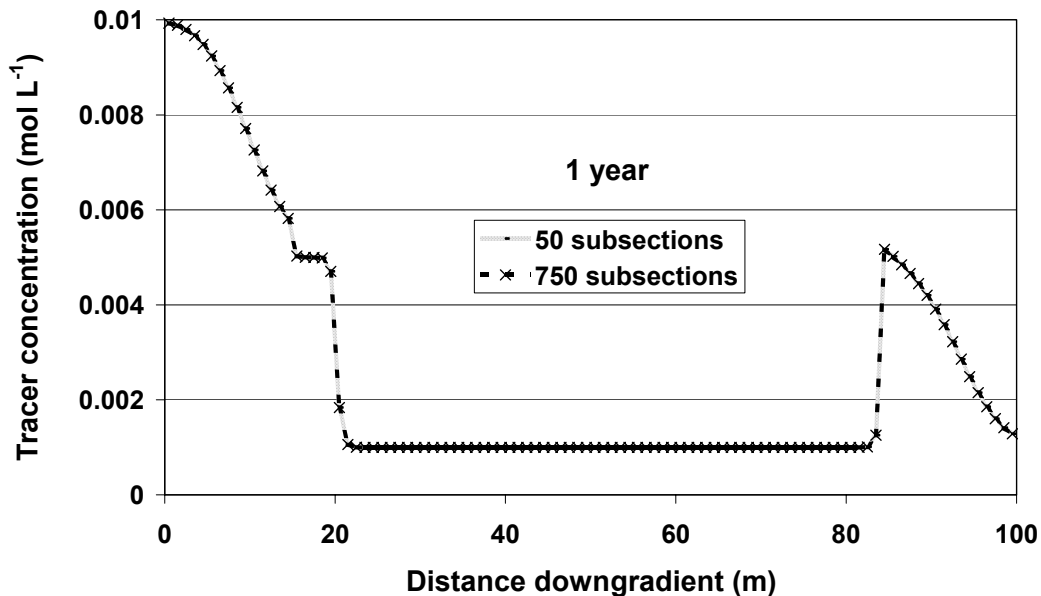


Fig. 16: Comparison of simulated tracer profiles for a hybrid system consisting of a single conduit after 1 year using 50 and 750 subsections within the single conduit.

### 6.1.6 Flow Field of the Hybrid System

It is demonstrated in this subsection, how the different cases of a conduit system

introduced in the present benchmark problem can influence head distribution and flow rates along the tailing and aquifer. Fig. 17 and Fig. 18 illustrate their impact upon head distribution and flow rates in the continuum, respectively. The head distributions and flow rates in Fig. 17 and Fig. 18 are shown for both discretisations of the conduit system using the exchange coefficients ( $ex$ )  $1 \times 10^{-8}$ ,  $5 \times 10^{-8}$ ,  $1 \times 10^{-7}$ ,  $5 \times 10^{-7}$  and  $6 \times 10^{-7} \text{ m}^2 \text{ s}^{-1}$ . As for the simulation of the reactive case, a length of 1 m per cell (see Chapters 6.1.3 and 6.1.5) was utilised for the generation of the head distributions and flow rates in these two figures using the hybrid flow model CAVE. The results in Fig. 17 and Fig. 18 are compared to the ones without a conduit system (case 'no con').

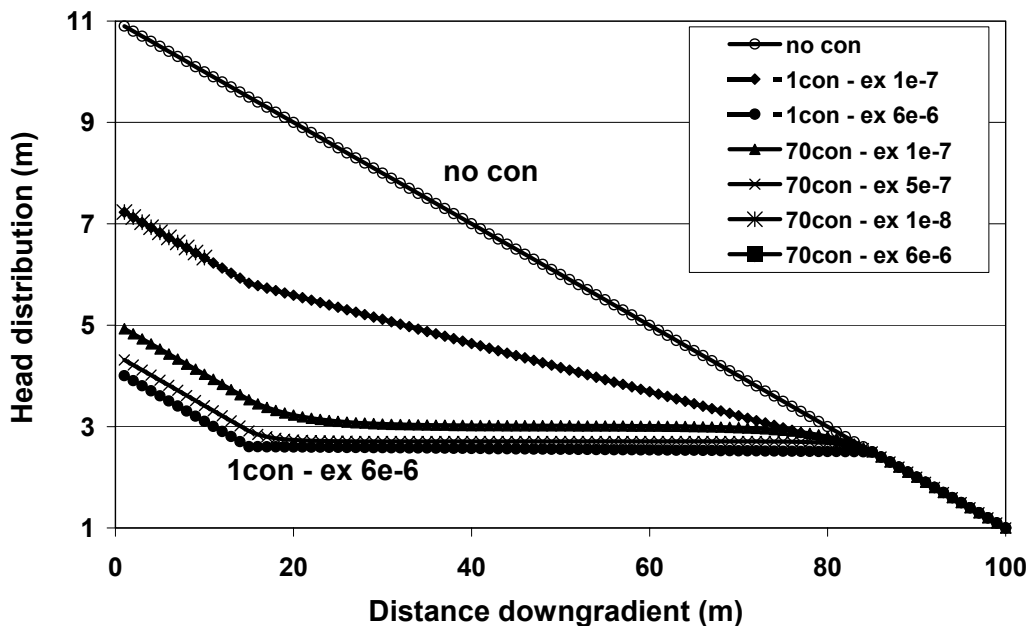


Fig. 17: Effect of the conduit system in the McNab problem upon head distribution along the tailing and aquifer.

Head distribution in the continuum. In the absence of the conduit system, piezometric heads decrease linearly with distance from the upstream boundary, as expected for a homogeneous, one-dimensional problem. In the presence of a conduit system, the overall flow resistance is smaller and the piezometric heads at the upstream model boundary are lower compared to the pure continuum system case. The total head difference within the model domain depends of course also upon the exchange coefficient between the continuum and the conduit system.

Flow rates in the continuum. In the absence of a conduit system, the flow rate remains constant throughout the tailing and aquifer. In the presence of a conduit system, the flow rates within the continuum decrease where the conduit system diverts water into the conduit system and increase where the conduit system drains water back into the continuum. The degree of decrease/increase depends upon the exchange coefficient and the prevailing head differences between the

two systems. In the case of an exchange coefficient of  $6 \times 10^{-6} \text{ m}^2 \text{ s}^{-1}$ , little resistance exists for the exchange flow and most of the total flux is essentially diverted into the conduit system (approximately 98.5 %, see Table 4). With a larger number of connecting nodes, the exchange flux decreases or increases smoother along locations in the tailing and aquifer where the conduit system is situated.

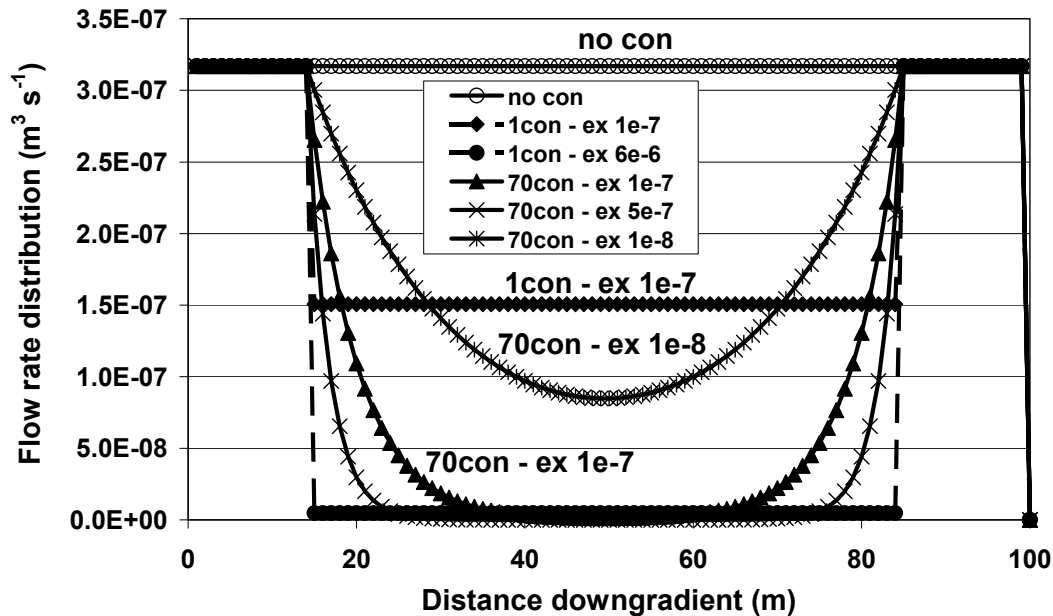


Fig. 18: Effect of the conduit systems in the McNab problem upon flow rates in the continuum.

### 6.1.7 Plausibility Tests

Plausibility tests support the interpretation of simulation results with respect to their consistency, stability and accuracy. Such tests can be helpful for evaluating model components for which no benchmark problem and or simulator is available (compare Chapter 4.1.2), as is the case for evaluating the reactive transport (simulation) results when the conduit transport model within RUMT3D is activated. Since plausibility tests require varying initial and boundary conditions for individual processes, three different scenarios of the McNab problem were set up in addition to the base case. Table 5 lists those three additional scenarios (scenarios 2-4). Scenario 1 presents the base case, as described earlier (see Chapter 6.1.1). Scenario 2 reflects a scenario, which is perhaps more realistic than the scenario 1 as all mineral phases can precipitate/dissolve within the tailings region as well as within the aquifer. Scenarios 3-4 are further variations of scenario 2. Scenario 3 investigates the system behaviour without the presence of the kaolinite phase whereas scenario 4 studies the system behaviour with less extensive pyrite oxidation in the tailing. While the tailing in scenarios 1-3 is recharged with an acidic solution containing two oxidising agents, i.e., oxygen

and ferric iron, the tailing in scenario 4 is recharged with rainwater that is equilibrated with atmospheric carbon dioxide ( $\text{CO}_2(\text{g})$ ) and atmospheric oxygen ( $\text{O}_2(\text{g})$ ). As a result, the recharge solution in scenario 4 does not contain the major oxidising agent ferric iron.

Scenarios 1-4 have very similar initial chemical compositions. Exceptions are the compositions of the aquifer of scenario 3 and of the recharge solution of scenario 4. Due to the lower concentrations of calcium and carbonate (by  $1.88 \times 10^{-6}$ ) in the aquifer caused through the absence of kaolinite, scenario 3 has an increased pH (by 0.168) and a reduced pe (by 0.167) compared to scenarios 1, 2 and 4. Moreover, it contains no traces of aluminium and silicon. The recharge solution of scenario 4 has a much higher pH (by 3.2) and a more reduced pe (by 3.2) mainly resulting from the absence of dissolved iron and sulphate. There are also small differences in the concentrations of oxygen and carbonate (Table 6).

Table 5: Description of the scenarios for the plausibility tests.

Scenario	Description
1	Base case - original setup, i.e., as given by McNab (2001)
2	All minerals in the base case can dissolve and or precipitate in the tailing and aquifer regions (i.e., calcite, goethite, gypsum, kaolinite, pyrite)
3	As in 2) but without kaolinite
4	As in 2) but with less extensive pyrite oxidation in the tailing. That implies that there is only dissolved $\text{CO}_2$ and $\text{O}_2$ in the recharge solution.

Table 6: Initial chemical composition of the recharge solution for scenario 4 and of the aquifer solution for scenarios 3.

Component / master species / mineral	Recharge solution (scenario 4) ( $\text{mol L}^{-1}$ )	Aquifer solution (scenario 3) ( $\text{mol L}^{-1}$ )
pH	5.410 <sup>a</sup>	9.910 <sup>a</sup>
pe	15.195 <sup>a</sup>	-5.898 <sup>a</sup>
Carbonate	$3.794 \times 10^{-6}$	$1.227 \times 10^{-5}$
Calcium	-	$1.227 \times 10^{-5}$
$\text{O}_2(\text{aq})$	$4.376 \times 10^{-5}$	-
Calcite	-	1.0

<sup>a</sup> Dimensionless.

The plausibility of the RUMT3D results is examined in two steps. In a first step, the geochemical processes occurring in the pure continuum system, i.e., in the McNab problem under the different scenarios are discussed in detail. It is expected that scenarios 1-3 would show similar behaviour with respect to pH and pe as a result of the rather minor variations in the initial and boundary conditions. Deviations between these scenarios would especially occur at locations where calcite is depleted. Scenario 3 would display a lower pH in the calcite-depleted zone due to the absence of kaolinite. Differences in the pe's would especially result in the scenario with and without oppression of pyrite precipitation due to the precipitation of sulphite. Finally, in comparison to scenarios 1-3, scenario 4, having less extensive pyrite oxidation due to the absence of the major oxidising

agent ferric iron in the recharge solution, would show

- a higher pH,
- a lower pe and
- reduced amount of mobilised pyrite, dissolved calcite and kaolinite as well as less precipitation of goethite and gypsum

If results of scenarios 1-4 do not reflect these expectations, there is presumably a coupling error, i.e., in the way PHREEQC-2 was incorporated into the RUMT3D model.

The examination of plausibility in a continuum system follows one in a hybrid system by addressing same expectations. Depending upon the number of conduit nodes and the magnitude of the exchange coefficients, deviations would occur in location and amount of dissolved calcite and kaolinite as well as precipitated goethite and gypsum.

### 6.1.8 Plausibility of the Reactive Transport Results in the Pure Continuum System

In this subsection, plausibility of the reactive transport results for the different scenarios in the pure continuum system is demonstrated.

Effect of pyrite oxidation on pH. The comparison of the modelling results for scenarios 1-3 show that the simulated pH-profiles are very similar in both time and space. This is illustrated in Fig. 19 for a simulation time of 20 years. The same applies to the mass of pyrite that is oxidised in the first tailing cell (~ 155 mols for all three scenarios, Table 7). Table 7 lists the locations and quantities of mass turnover by mineral dissolution/precipitation for all scenarios after 20 years. In contrast, scenario 4 draws a different picture, which is explained by the absence of the major oxidising agent ferric iron in the recharge solution (compare Chapter 6.1.7 and Table 7). Here as little as 12 mols of pyrite are mobilised from the first cell (tailing) after 20 years. Consequently, the pH values in both the tailing and aquifer in this scenario do not drop as low as in the other scenarios with time. In the tailing, the pH drops from 7 to 1.9 for scenarios 1-3 while for scenario 4, it decreases only to 3.9. In the aquifer, the pH decreases from about 9.7 to 6.1 for scenarios 1-3 and for scenario 4, it decreases to only 8.9. Those differences in temporal pH development are illustrated in Fig. 20 and Fig. 21 for scenarios 1 and 4, respectively. Fig. 20 shows that after 1 year, the pH established in scenario 1 at around 10 m in the tailing and that the front progressed to the end of the tailing. This is due to that the tailing was flushed with a velocity of 10 m yr<sup>-1</sup>. After 2 years, the pH nearly established at the beginning of the aquifer (at around 20 m) while the front moved already 20 m further downgradient. After 5 years, the effect of dispersivity (of 1 m) can more extensively be seen in Fig. 20 since the pH front already progressed 80 m downgradient. After the aquifer is flushed with one pore volume, i.e., after 10 years, the pH remains constant at the downstream end of the aquifer for all scenarios. This is depicted in Fig. 20 and Fig. 21 for scenarios 1 and 4, respectively.

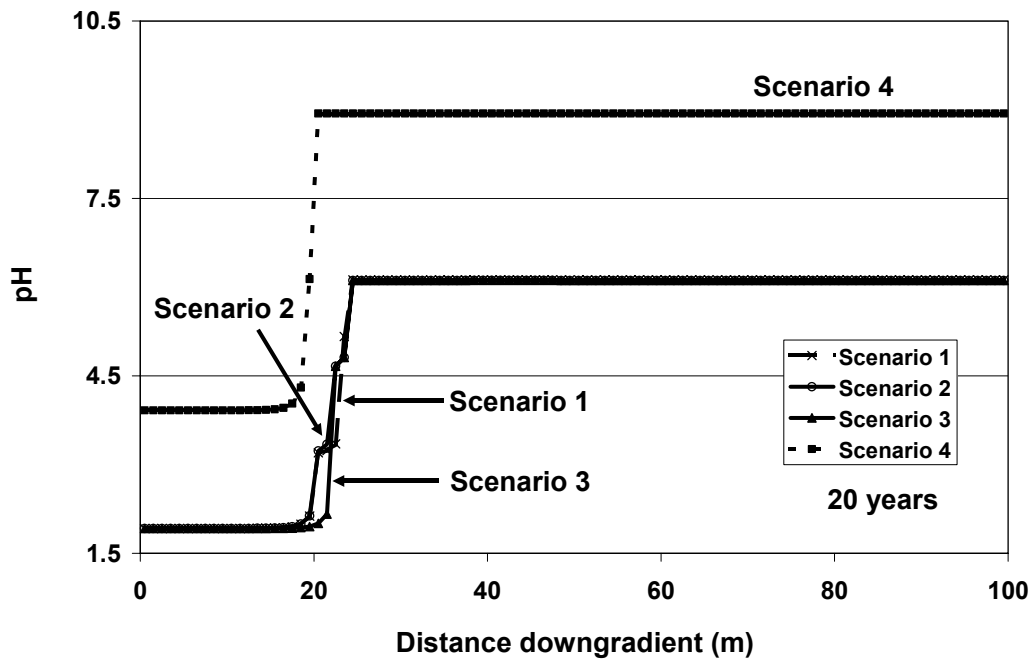


Fig. 19: Simulated pH profiles of scenarios 1-4 for a continuum system after 20 years.

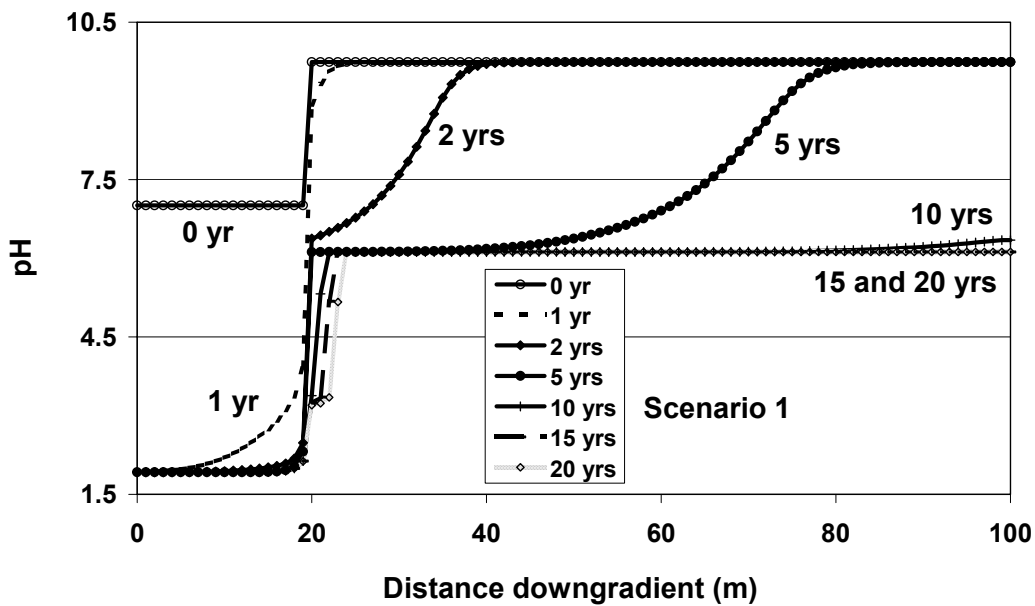


Fig. 20: Simulated temporal pH profiles of scenario 1 for a continuum system.

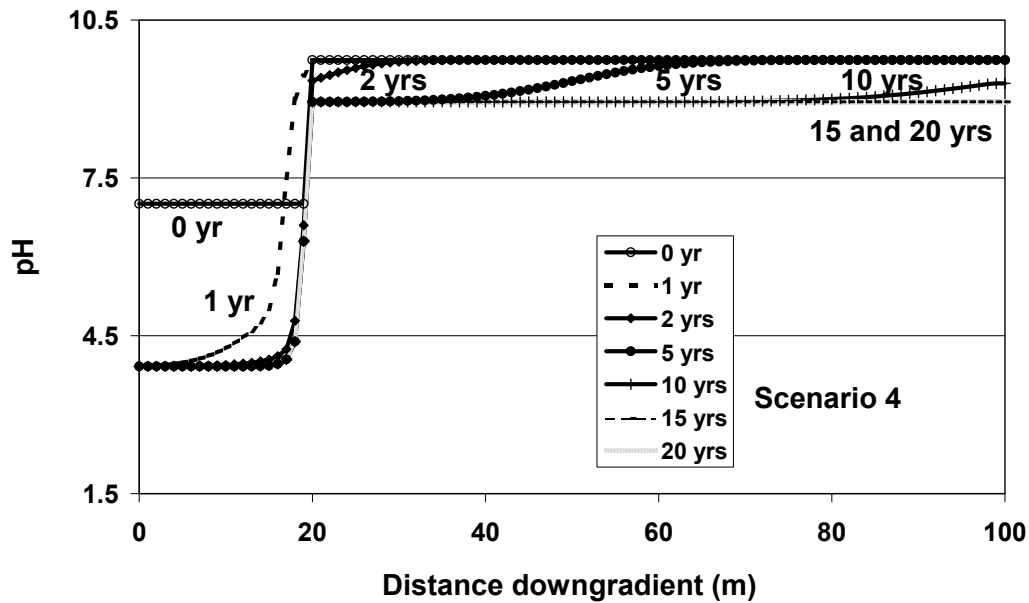


Fig. 21: Simulated temporal pH profiles of scenario 4 for a continuum system.

*Dissolution of calcite and kaolinite.* After a simulation time of 20 years, scenarios 1-3 show a dissolution of calcite of approximately 4500 mols from the first 5 aquifer cells (Table 7), which corresponds to a complete depletion of calcite in the first 4 cells. As soon as a cell is completely depleted in calcite, kaolinite starts to dissolve. In scenarios 1-2, approximately 400 mols of kaolinite are dissolved after 20 years in the first aquifer cell. This leads to some concentration peaks of aluminium and silicon within this first aquifer cell. Scenarios 1-2 show aluminium and silicon concentrations of  $6.34 \times 10^{-3}$  and  $5.71 \times 10^{-3}$  mol L<sup>-1</sup>, respectively (Fig. 14b). Note that the increased concentrations of aluminium and silicon in the adjacent calcite-depleted cells rather result from physical transport (from the first cell of the aquifer where kaolinite dissolves) and not through the dissolution of kaolinite within these cells. This is due to reaching saturation of the aquifer solution with aluminium and silicon by receiving these components from previous cells.

In contrast to scenarios 1-3, in the scenario with less extensive pyrite oxidation (scenario 4) significant less calcite (~ 59 mols) is consumed and after 20 years, dissolution has not progressed past the first aquifer cell. Under the pH-conditions of this scenario, only about 2 mols of kaolinite are dissolved from the first aquifer cell (Table 7). After one pore volume, the pH remains almost constant across the aquifer cells in this scenario, which also results in constant aluminium and silicon concentrations of  $1.07 \times 10^{-5}$  mol L<sup>-1</sup> throughout the aquifer and with time.

Table 7: Dissolved and precipitated amounts and fractions of the different mineral phases of scenarios 1-4 for a continuum system after 20 years.

Scenario		1			2			3			4		
		cell	amount (mols)	fraction (%)	cell	amount (mols)	fraction (%)	cell	amount (mols)	fraction (%)	cell	amount (mols)	fraction (%)
Pyrite	dissolv.	t 1	155.2		t 1	155.2		t 1	155.2		t 1	12.4	
	precip.	t 20	13.5		aq 3-5	124.8	100.0	aq 3-5	124.8	100.0	aq 1	0.5	
	pre/dis			8.7	aq 1,2,6-80	$1.5 \times 10^{-2}$	$1.2 \times 10^{-2}$	aq 1,2,6-80	$1.6 \times 10^{-2}$	$1.3 \times 10^{-2}$			
					aq all	124.8	100.0	aq all	124.8	100.0			4.3
Calcite	dissolv.	aq 1-5	4514.9	99.5	aq 1-5	4546.9	99.5	aq 1-5	4546.9	99.5	aq 1	58.9	
		aq 6-80	22.3	0.5	aq 6-80	21.1	0.5	aq 6-80	21.4	0.5			
		aq all	4537.2	100.0	aq all	4568.0	100.0	aq all	4568.3	100.0			
Kaolinite	dissolv.	aq 1	396.7		aq 1	405.9					aq 1	1.9	
	precip.	aq 2-5	386.1		aq 2-5	398.6							
	prec/dis			97.3			98.2						
Goethite	precip.	aq 2-5	1739.2	99.9	aq 3-5	1747.7	100.0	aq 3-5	1747.6	100.0	aq 1-2	10.6	100.0
		aq 19-80	1.6	0.1	aq 12-80	0.2	0.0	aq 12-80	0.2	$1.1 \times 10^{-2}$	aq 3-80	$6.8 \times 10^{-6}$	$6.4 \times 10^{-5}$
		aq all	1740.8	100.0	aq all	1747.9	100.0	aq all	1747.8	100.0	aq all	10.6	100.0
Gypsum	precip.	aq 4-5	996.2	100.0	aq 4-5	1004.2	100.0	aq 4-5	1004.5	100.0			
		aq 6-7	$9.4 \times 10^{-3}$	$9.4 \times 10^{-4}$	aq 6-9	$2.2 \times 10^{-3}$	$2.2 \times 10^{-4}$	aq 6-9	$2.2 \times 10^{-3}$	$2.2 \times 10^{-4}$			
		aq all	996.3	100.0	aq all	1004.2	100.0	aq all	1004.5	100.0			

Where t=tailing, aq=aquifer and all=all cells.

Precipitation of kaolinite. Like its dissolution, the precipitation of kaolinite depends strongly on the pH. Therefore, the increased aluminium and silicon concentrations from calcite-depleted cells will precipitate readily in form of kaolinite in cells where a non-acidic environment is predominant. For scenarios 1-2, this implies that, as soon as the dissolved kaolinite from a calcite-depleted cell enters a calcite buffered environment, it will precipitate. The difference between scenario 1 and 2 is that in scenario 2, all minerals in the base case can dissolve in the tailing and aquifer regions (compare Table 5). Table 7 shows that in these two scenarios, up to 98 % of the dissolved kaolinite from the first aquifer cell precipitates in the adjacent 2-3 cells of the aquifer (see also Fig. 22). Consequently, the aqueous concentrations of aluminium and silicon in these cells decrease to a concentration of  $8.56 \times 10^{-7} \text{ mol L}^{-1}$ , which represents the solubility of kaolinite at this pH.

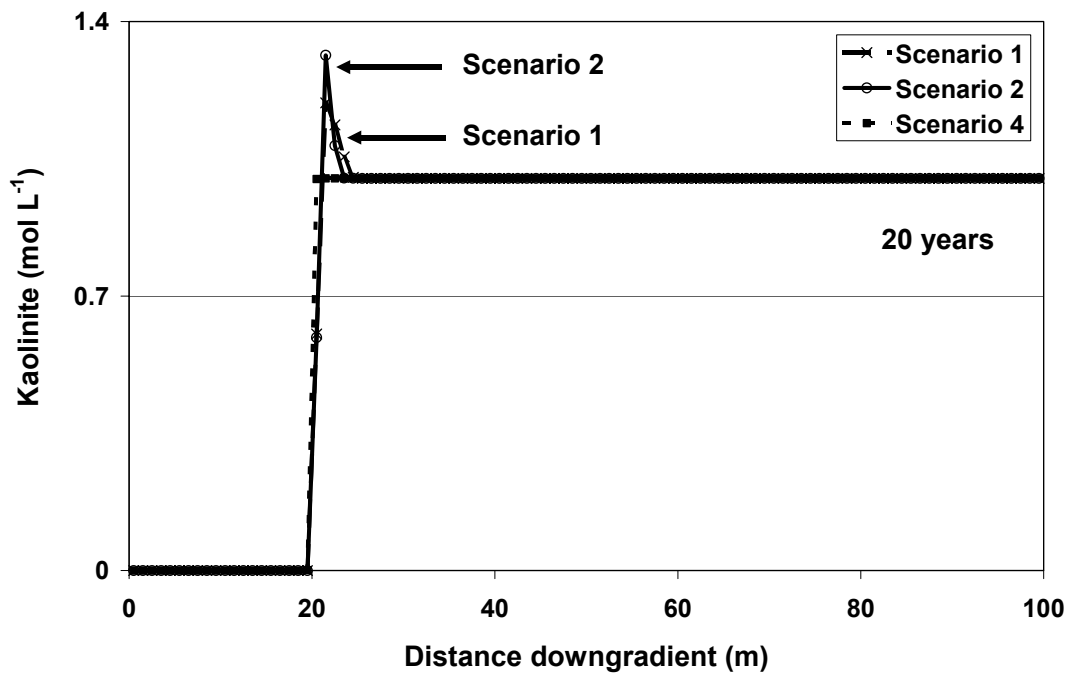


Fig. 22: Simulated kaolinite profiles of scenarios 1, 2 and 3 for a continuum system after 20 years.

Goethite and gypsum precipitation. Fig. 23 depicts that in a scenario with more extensive pyrite oxidation (1-3), goethite mainly precipitates in the first 2-5 aquifer cells after 20 years (up to 1748 mols, Table 7). For scenarios 1-3, gypsum shows very little variation with respect to the location and the amount of precipitation (up to 1005 mols). Most of the precipitated amount occurs only over 2 cells in the first portion of the aquifer (Fig. 24 and Table 7).

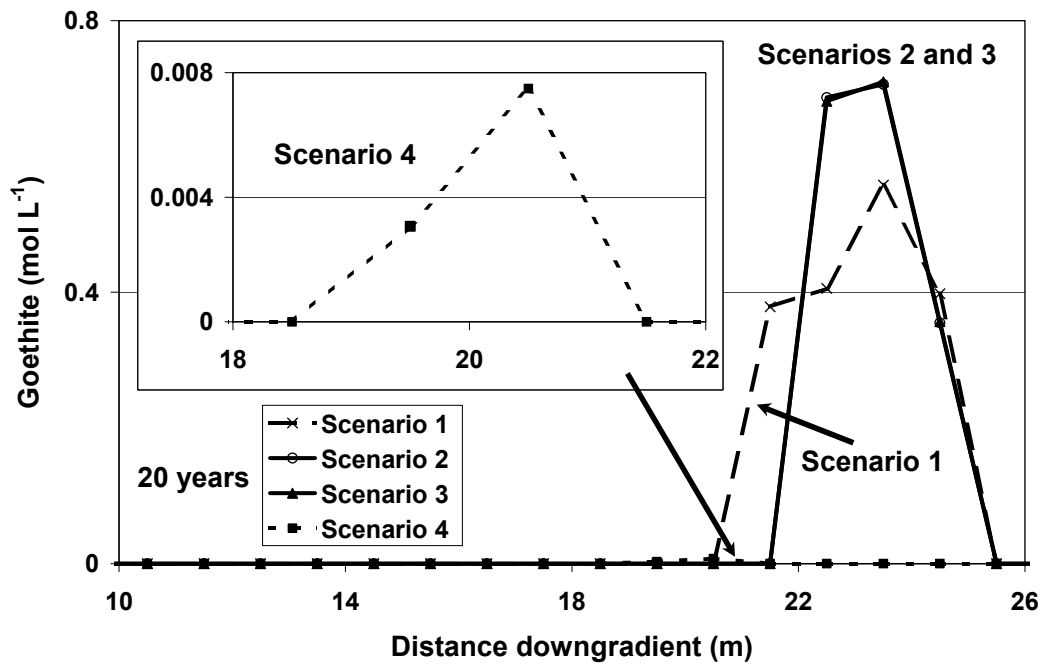


Fig. 23: Simulated goethite profiles of scenarios 1-4 for a continuum system after 20 years.

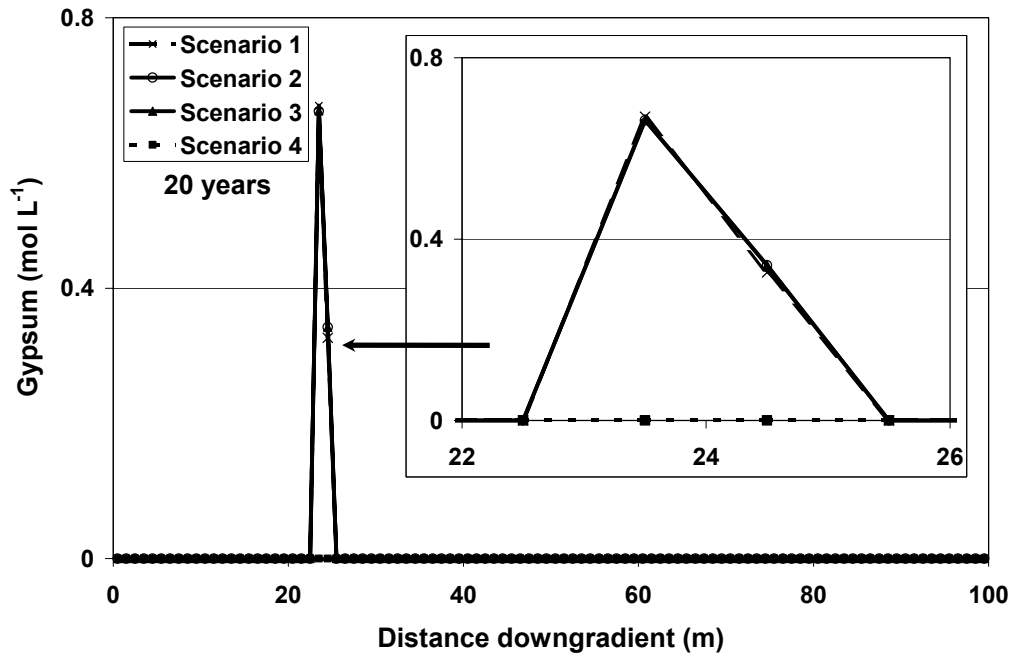


Fig. 24: Simulated gypsum profiles of scenarios 1-4 for a continuum system after 20 years.

At high pH-values and respective low iron concentrations in scenario 4, very little goethite precipitates (~11 mols). Gypsum does not precipitate at all in this scenario, since only little calcite is required to buffer the acidic solution. Therefore, the solubility of gypsum is not exceeded.

***Influence of pyrite precipitation in the aquifer.*** In all scenarios where pyrite is promoted to precipitate in the aquifer (scenarios 2-4) but especially in those with more extensive pyrite oxidation (scenarios 2 and 3), sulphite is precipitated as pyrite. In scenarios 2 and 3, the largest fractions of pyrite precipitation (about 80.4 % of the amount dissolved further upstream) occur in the aquifer cells 3-5 (Table 7 and Fig. 25). In scenario 4, where pyrite oxidation is less extensive, only about 4 % of the dissolved amount of pyrite in the first cells precipitate subsequently in the first aquifer cell after a simulation time of 20 years.

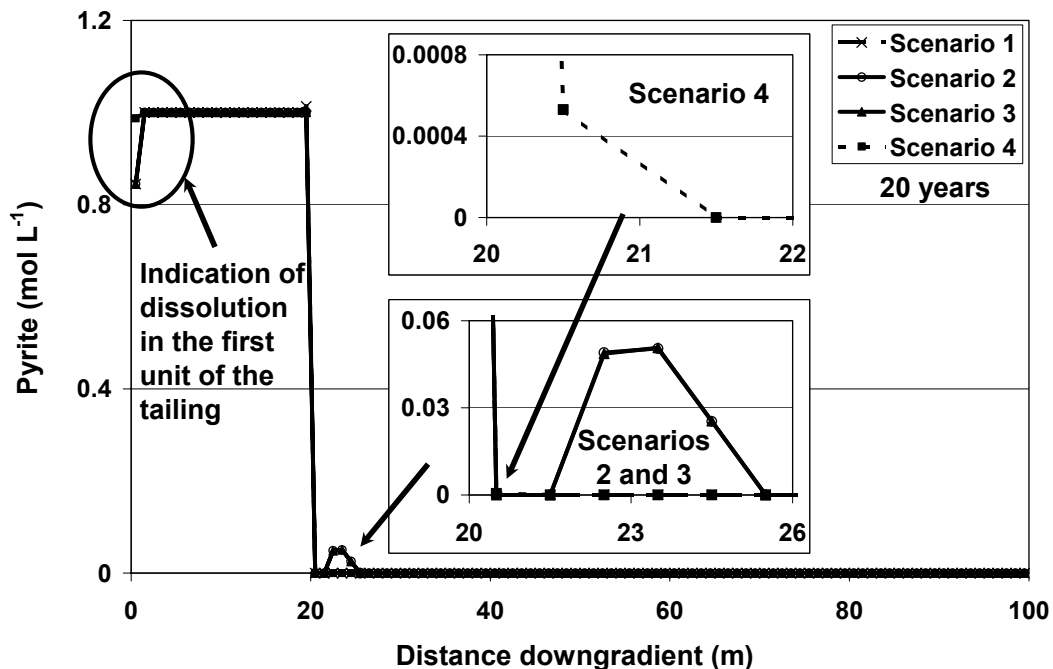


Fig. 25: Simulated pyrite profiles of scenarios 1-4 for a continuum system after 20 years.

In the scenario where pyrite precipitation is oppressed in the aquifer (scenario 1), sulphite remains in solution. As sulphite inhibits the oxidation of  $\text{Fe}^{2+}$  to  $\text{Fe}^{3+}$  by means of sulphate ions required for goethite precipitation, the concentrations of Fe(II) and sulphate in cells with calcite are higher for scenario 1 in comparison with scenarios 2 and 3. The equilibrated Fe(II) concentration in the aquifer of scenario 1 is about  $8.16 \times 10^{-4} \text{ mol L}^{-1}$  higher than in scenarios 2 and 3 (Fig. 26). The same applies to the equilibrated sulphate concentration, the difference is  $2 \times 10^{-4} \text{ mol L}^{-1}$  (Fig. 27) in that case. As a result of these elevated dissolved Fe(II) and sulphate, the redox potential within the aquifer is lower in scenario 1 compared to scenarios 2 and 3 (~ 0.9, see Fig. 28).

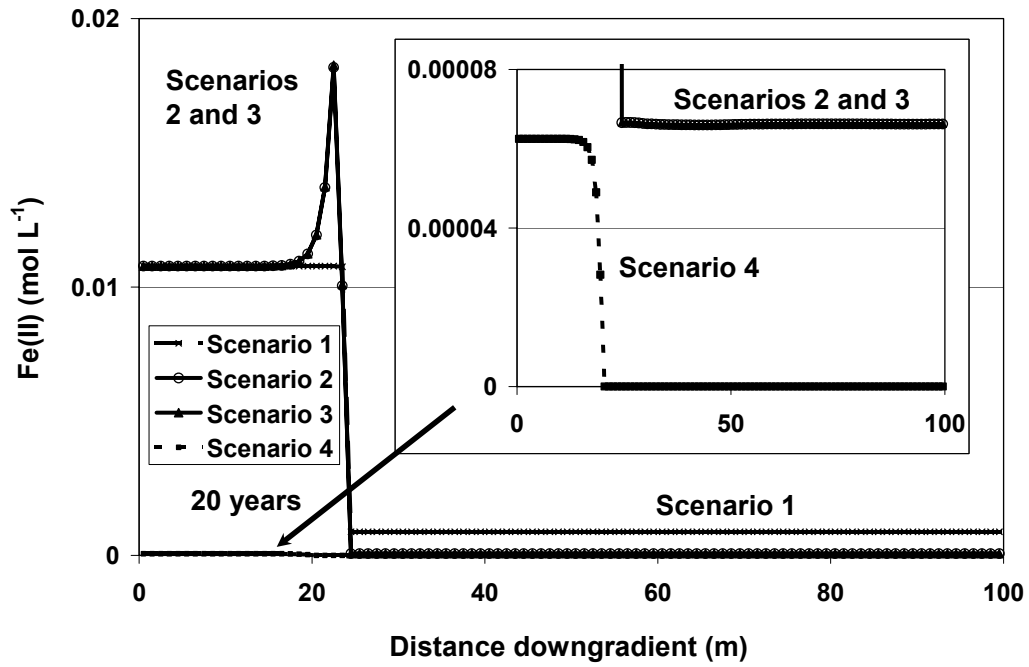


Fig. 26: Simulated Fe(II) profiles of scenarios 1-4 for a continuum system after 20 years.

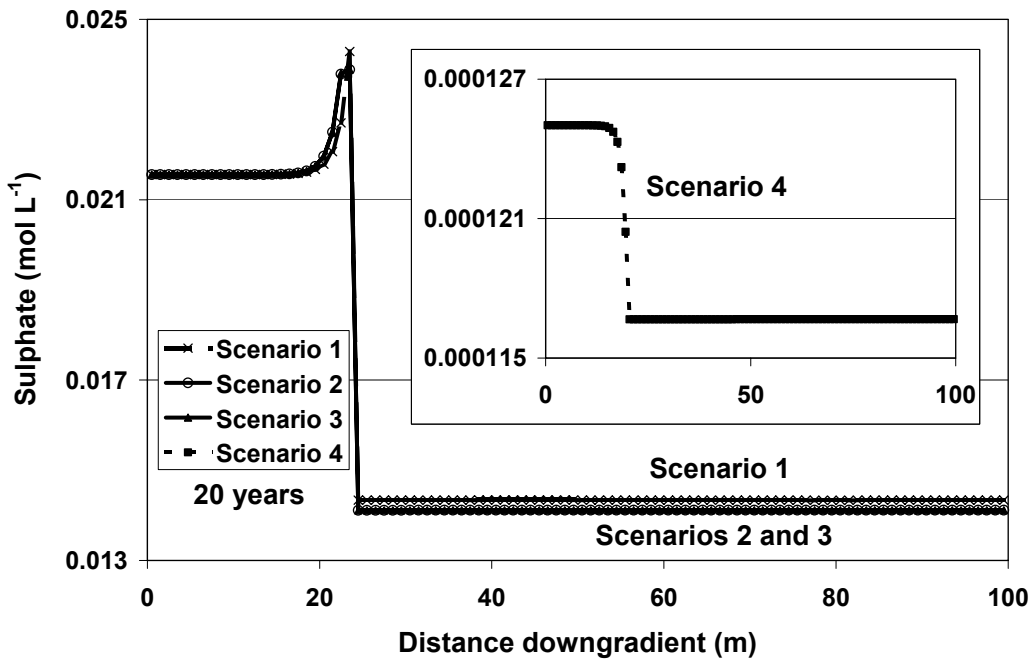


Fig. 27: Simulated sulphate profiles of scenarios 1-4 for a continuum system after 20 years.

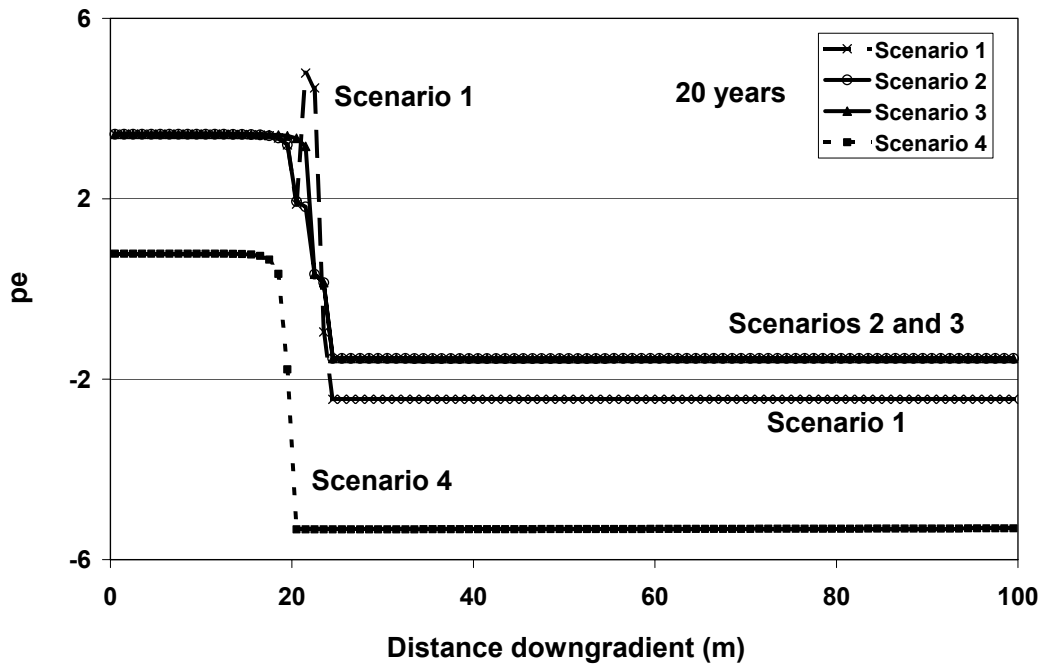


Fig. 28: Simulated pe profiles of scenarios 1-4 along the column for a continuum system after 20 years.

***Effect of calcite absence.*** When calcite is absent, even more elevated Fe(II) and sulphate concentrations are observed (Fig. 26 and Fig. 27). This applies to the first 4 aquifer cells of scenarios 1-3 after 20 years. While in the scenario with oppression of pyrite (scenario 1), the resulting Fe(III) from goethite dissolution in calcite depleted cells oxidise sulphite to sulphate, the ones in scenarios 2 and 3 cause oxidation of the accumulated pyrite, releasing Fe(II) and sulphate ions. To illustrate this increase of dissolved Fe(II) concentrations at the first portion of the aquifer, (e.g., after 20 years simulation time in scenario 1), the unaltered and an altered Fe(II) concentration profile are compared in Fig. 29. The altered Fe(II) concentration profile is with a large excess calcite concentration (uniform concentration of 10 instead of 1 mol L<sup>-1</sup> in the aquifer). While the Fe(II) concentrations in Fig. 29 already start to decrease in cell 14 with an initial calcite concentration of 10 mol L<sup>-1</sup> (Fe(II) concentration of 6.28 x 10<sup>-4</sup> mol L<sup>-1</sup>), the ones with an initial calcite concentration of 1 mol L<sup>-1</sup>, only start to decrease past cell 24 (Fe(II) concentration of 8.78 x 10<sup>-4</sup> mol L<sup>-1</sup>). The decrease of Fe(II) before cell 20 is related to pyrite precipitation in the last cell of the tailing (Fig. 15). This was already observed for scenario 1 with an initial calcite concentration of 1 mol L<sup>-1</sup> due to upgradient migration of sulphite from the first aquifer cell into the tailing (see Chapter 6.1.3). For the case with an initial calcite concentration of 10 mol L<sup>-1</sup>, this non-physical, artificial effect is even more pronounced.

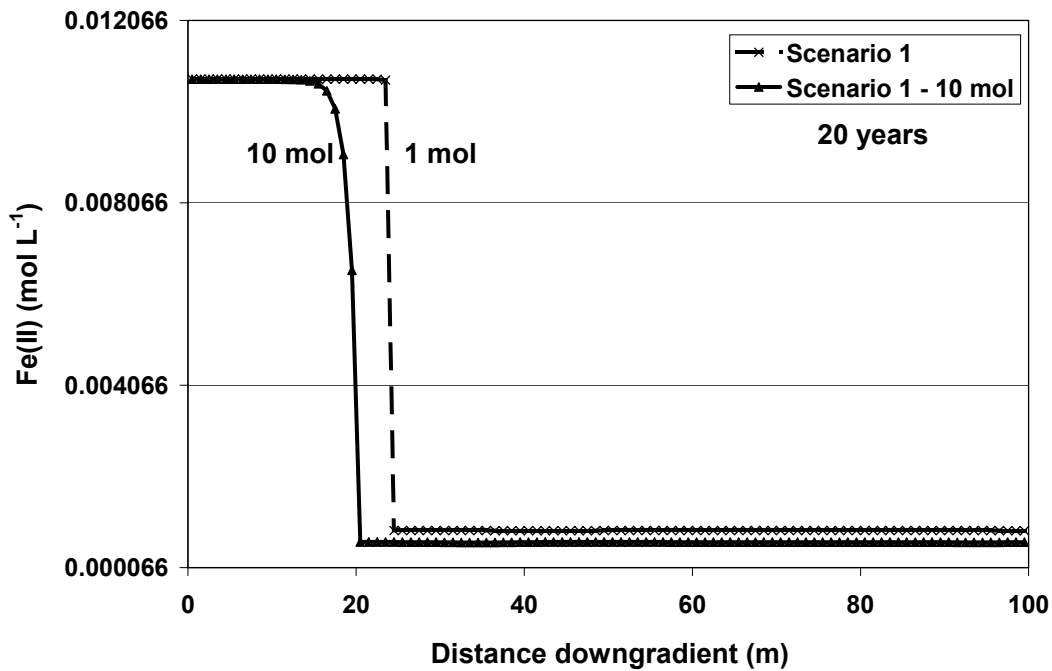


Fig. 29: Simulated Fe(II) profiles of scenario 1 for a continuum system after 20 years, using initial calcite concentrations of 1 and 10 mol L<sup>-1</sup> in the aquifer.

Depending upon the free available protons, Fe(II) and sulphate ions in the calcite-depleted cells after equilibration of scenarios 1-3, the pH's and pe's vary for these scenarios in the respective cells. Fig. 19 and Fig. 28 show these variations in the pH and in the pe profiles at the tailing/aquifer front for these scenarios after 20 years, respectively. The scenarios with kaolinite (scenarios 1 and 2) expose higher pH values in the first 4 aquifer cells than the corresponding scenario without it (scenario 3) once calcite is depleted. This results from the proton consumption during kaolinite dissolution. Fig. 30 and Fig. 31 demonstrate that under condition of calcite excess, such variations in the pH and pe profiles at the tailing/aquifer front in scenarios 1-3 do not occur. In these figures, the pH and pe profiles with an initial calcite concentration of 10 mol L<sup>-1</sup> throughout the aquifer after 20 years are plotted against the ones with an initial calcite concentration of 1 mol L<sup>-1</sup>.

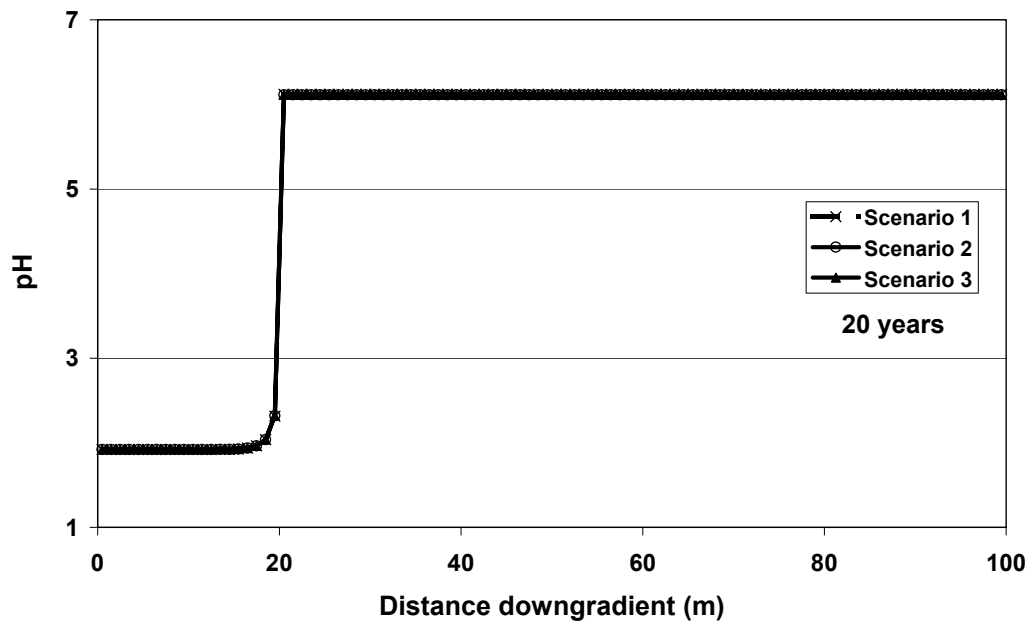


Fig. 30: Simulated pH profiles of scenarios 1-3 for a continuum system after 20 years, using an initial calcite concentration of  $10 \text{ mol L}^{-1}$  in the aquifer.

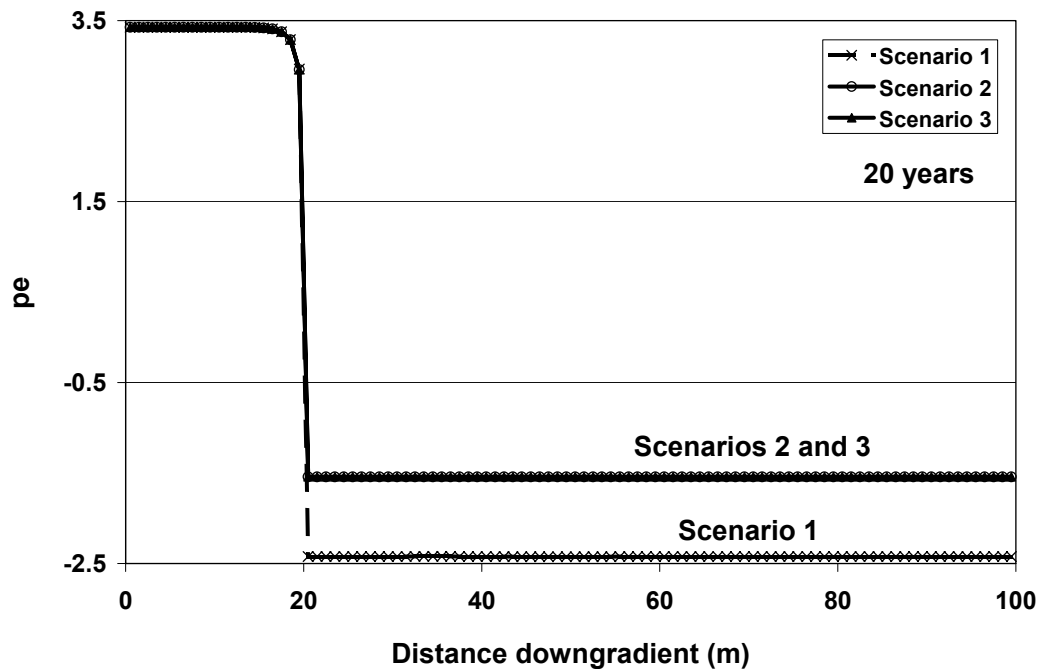


Fig. 31: Simulated pe profiles of scenarios 1-3 for a continuum system after 20 years, using an initial calcite concentration of  $10 \text{ mol L}^{-1}$  in the aquifer.

### 6.1.9 Plausibility of the Reactive Transport Results in a Hybrid System

In a second step of examining the plausibility of RUMT3D simulations, results from a hybrid system are discussed in comparison with simulation results from a corresponding pure continuum system (Chapter 6.1.8). Initially, the simulations for the coarse discretisation of the conduit system (2 nodes, i.e., one entry, one exit node) and two different exchange coefficients ( $6 \times 10^{-6} \text{ m}^2 \text{ s}^{-1}$ , subsection a and  $1 \times 10^{-7} \text{ m}^2 \text{ s}^{-1}$ , subsection b) are considered. In subsection c, the behaviour of the finer discretised conduit system (70 tubes, 71 nodes) is investigated for 4 different exchange coefficients ( $1 \times 10^{-8}$ ,  $5 \times 10^{-8}$ ,  $1 \times 10^{-7}$  and  $5 \times 10^{-7} \text{ m}^2 \text{ s}^{-1}$ ). Since the aquifer has uniform initial concentrations, it has the same buffering capacity at a location of 84.5 m as it has in the first aquifer cell.

#### a) Coarse discretisation of the conduit system using an exchange coefficient of $6 \times 10^{-6} \text{ m}^2 \text{ s}^{-1}$

Effect of pyrite oxidation on pH. Due to the same initial and boundary conditions in the hybrid and the pure continuum system, comparable amounts of pyrite are mobilised. In scenarios 1-3, about 155 mols are dissolved after 20 years while in scenario 4 only about 12 mols of pyrite are dissolved in the first cell of the tailing (Table 8). This results in similar pH values as well as Fe(II) and sulphate concentrations upstream of the beginning of the conduit system (i.e., before cell 15). This is shown for the pH and for Fe(II) concentrations after 20 years in Fig. 32 and Fig. 33, respectively. For a comparison with the corresponding pure continuum system see Fig. 19 and Fig. 26.

Since an exchange coefficient of  $6 \times 10^{-6} \text{ m}^2 \text{ s}^{-1}$  deviates nearly the complete water flux (i.e., the acidic solution) from cell 15 (tailing) into the conduit system (about 98.5 %), the pH-values in aquifer cells with very little acidic inflow (aquifer (aq) cells 1-64) remain fairly constant over the whole simulation period. Where the conduit system discharges the acidic solution back into the aquifer, i.e., at 84.5 m (Fig. 34), the pH values decrease to the one observed immediately downgradient of the tailings region in the pure continuum system. Fig. 34 demonstrates the spatial and temporal development of pH for this hybrid system (scenario 1). A similar behaviour is observed for all other scenarios (Fig. 32). Like in the case of a pure continuum system, the pH does not drop as low in scenario 4 as it does in a scenario with more extensive pyrite oxidation (scenarios 1-3). A final pH value of about 8.9 instead of 6.1 is observed.

This hybrid system (conduit system of 70 m, 2 nodes, exchange coefficient of  $6 \times 10^{-6} \text{ m}^2 \text{ s}^{-1}$ ) yields a velocity of approximately  $1254 \text{ m yr}^{-1}$  in the conduit system. With that velocity, a constant pH can already be observed after about 5 years at the end of the aquifer (see, e.g., Fig. 34 for scenario 1) while in the corresponding continuum system case (see Chapter 6.1.8 and or Fig. 20), this takes twice as long.

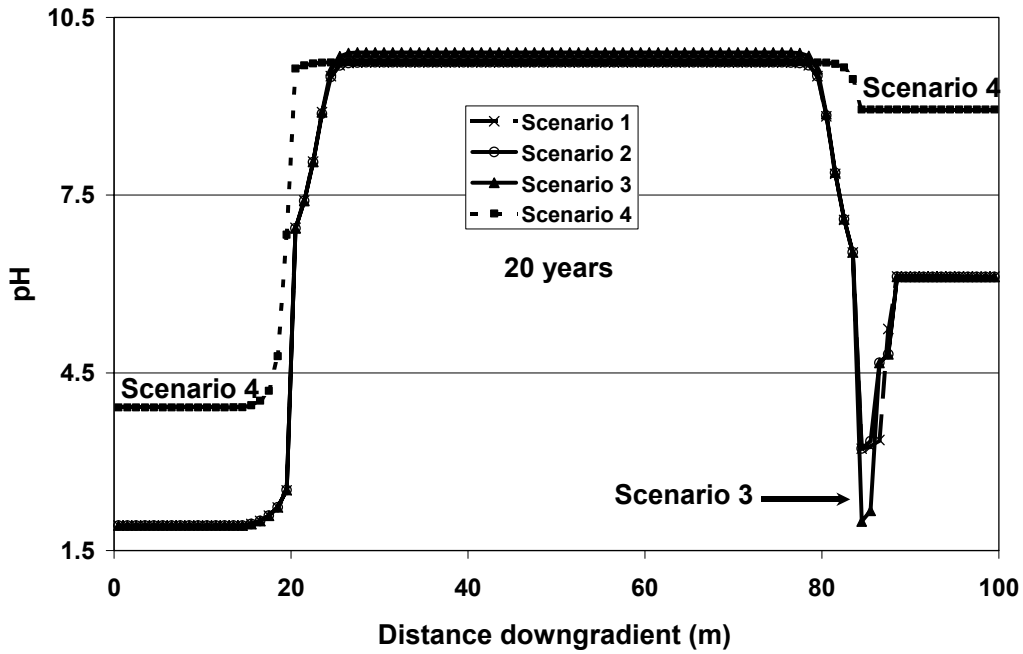


Fig. 32: Simulated pH profiles of scenarios 1-4 for a hybrid system consisting of 1 conduit with 2 nodes, using an exchange coefficient of  $6 \times 10^{-6} \text{ m}^2 \text{ s}^{-1}$  after 20 years.

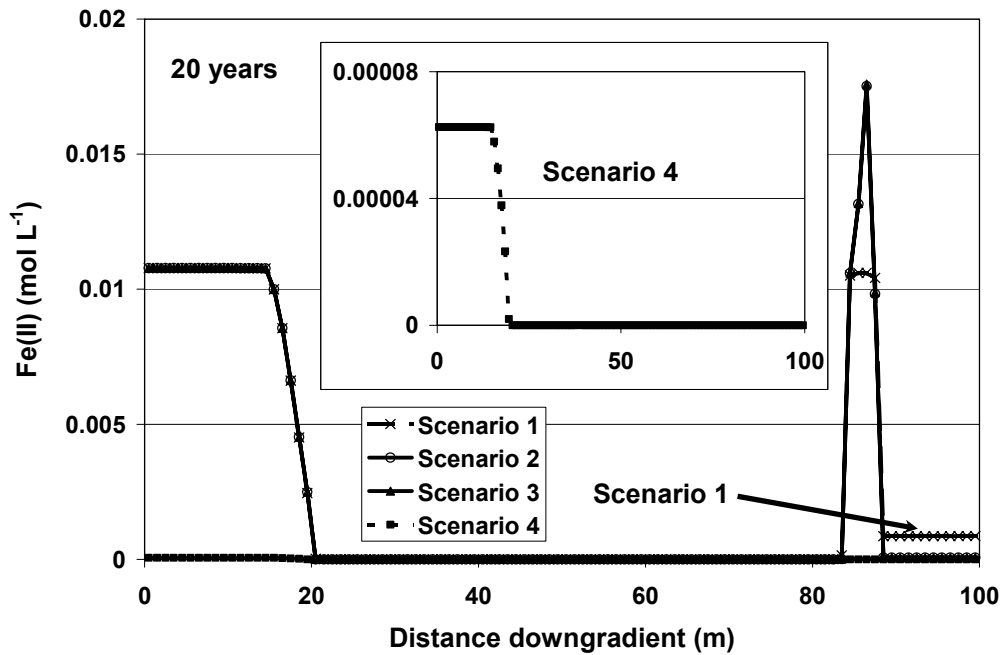


Fig. 33: Simulated Fe(II) profiles of scenarios 1-4 for a hybrid system consisting of 1 conduit with 2 nodes, using an exchange coefficient of  $6 \times 10^{-6} \text{ m}^2 \text{ s}^{-1}$  after 20 years.

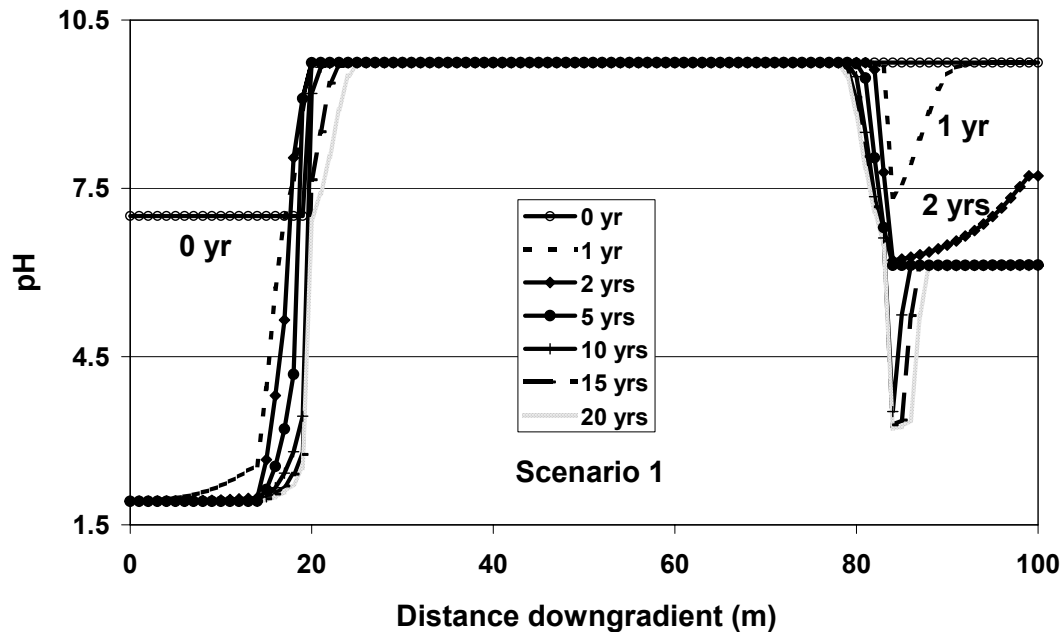


Fig. 34: Simulated pH profiles of scenario 1 for a hybrid system consisting of 1 conduit with 2 nodes, using an exchange coefficient of  $6 \times 10^{-6} \text{ m}^2 \text{ s}^{-1}$ .

Dissolution of calcite and kaolinite. Most of the calcite and kaolinite required for the buffering reactions dissolves at the discharge location of the conduit system. Table 8 shows that in scenarios 1-3 about 99 % of the calcite dissolution within the first 20 years is confined to cells 65-69. Similar to a pure continuum system, the total amount of calcite dissolution is approximately 4600 mols.

Up to 330 mols of kaolinite dissolve in the first calcite-depleted cell (65) in the aquifer. As in a pure continuum system, a peak concentration of aluminium and silicon occurs in the first cell where calcite is fully depleted. The concentration of these components after 20 years is about  $5.8 \times 10^{-3} \text{ mol L}^{-1}$  for scenarios 1-2. This peak concentration is very close to the corresponding case of a pure continuum system ( $5.7 \times 10^{-3} \text{ mol L}^{-1}$ ).

Precipitation of kaolinite. The strong pH-dependency of its dissolution causes most of the kaolinite from cell 65 to precipitate in the adjacent 2-3, where calcite is present. There, up to 97.2 % of the previously dissolved kaolinite precipitates in scenarios 2-3 (Table 8).

Table 8: Dissolved and precipitated amounts and fractions of the different mineral phases of scenarios 1-4 for a hybrid system with a conduit system consisting of 2 nodes, using an exchange coefficient of  $6 \times 10^{-6} \text{ m}^2 \text{ s}^{-1}$  after 20 years.

Scenario		1			2			3			4		
		cell	amount (mols)	fraction (%)	cell	amount (mols)	fraction (%)	cell	amount (mols)	fraction (%)	cell	amount (mols)	fraction (%)
Pyrite	dissolv. precip.	t 1	155.1		t 1	155.1		t 1	155.1		t 1	12.4	
		aq 67-69	124.9	99.0	aq 67-69	124.9	99.0	aq 67-69	124.9	99.0	aq 65	0.8	99.9
	pre/dis	aq 1-3,62-66,70-80	1.2	1.0	aq 1-3,62-66,70-80	1.2	1.0	aq 1-4,62-64,66,70-80	1.2	1.0	aq 66	$8.4 \times 10^{-4}$	0.1
		aq all	126.2	100.0	aq all	126.2	100.0	aq all	126.2	100.0	aq all	0.8	100.0
Calcite	dissolv.	aq 1	10.3	0.2	aq 1	10.6	0.2	aq 1	10.6	0.2	aq 1	0.6	1.0
		aq 64	33.4	0.7	aq 64	33.3	0.7	aq 64	33.3	0.7	aq 65	58.3	99.0
		aq 65-69	4524.8	98.9	aq 65-69	4554.2	98.9	aq 65-69	4554.2	98.9	aq rest	$5.4 \times 10^{-3}$	$9.2 \times 10^{-3}$
		aq rest	7.0	0.2	aq rest	6.3	0.1	aq rest	6.5	0.1	aq all	58.8	100.0
		aq all	4575.4	100.0	aq all	4604.4	100.0	aq all	4603.1	100.0			
Kaolinite	dissolv. precip. pre/dis	aq 65	285.2		aq 65	329.5					aq 65	1.2	
		aq 66-68	272.7	95.6	aq 66-67	320.2	97.2						
Goethite	precip.	aq 66-69	1742.2	99.0	aq 67-69	1748.9	99.0	aq 67-69	1748.8	99.0	aq 65	10.6	99.9
		aq 1-5, 60-64, 70-80	18.2	1.0	aq 1-5, 8, 60-64, 70-80	17.5	1.0	aq 1-3, 5, 9, 60-64, 70-80	17.5	1.0	aq 1-2,5-6,62,64,66-80	$1.1 \times 10^{-2}$	0.1
		aq all	1760.4	100.0	aq all	1766.4	100.0	aq all	1766.3	100.0	aq all	10.6	100.0
Gypsum	precip.	aq 68-69	958.0	99.9	aq 68-69	963.6	100.0	aq 68-69	963.8	100.0			
		aq 70-77,80	0.6	0.1	aq 70-80	0.3	$2.8 \times 10^{-2}$	aq 70-80	0.3	$2.8 \times 10^{-2}$			

Where t=tailing, aq=aquifer and all=all cells.

Goethite and gypsum precipitation. Table 8 shows that similar amounts of goethite precipitate in the hybrid and the pure continuum system, although the precipitation occurs at different locations. However, less gypsum precipitates (about 40 mols), probably because calcite dissolution extends over a larger portion of the aquifer. As a small portion of the acidic solution reaches the aquifer (about 1.5 %), calcite is additionally dissolved in the first aquifer cell. Apart from this first aquifer cell, by upgradient migration of some acidic solution from the discharge location of the conduit system (caused by the calculation of dispersion), calcite contained in an upgradient cell (aquifer cell 64) contributes moreover to buffer the acidity.

Effect of calcite depletion. Similar to the pure continuum system case, the effect of a complete calcite depletion at particular aquifer cells are (i) decreasing pH values and (ii) increasing pe. This, however, occurs in the hybrid system simulations (scenarios 1-3) at locations where acidic solution is discharged from the conduit system and is due to: (i) the absence of calcite and (ii) elevated Fe(II) and sulphate concentrations, respectively. Fig. 33 and Fig. 32 illustrate the elevated concentrations of dissolved Fe(II) and the decrease in pH at around 84.5 m, respectively. Due to the missing buffer capacity of kaolinite, the largest drop in pH occurs in scenario 3. In a scenario with more extensive pyrite oxidation, four cells are depleted of calcite (cells 65-69), like in the corresponding pure continuum case. To confirm that the decrease in pH and the increases in dissolved Fe(II) and sulphate concentrations in scenarios 1-3 are indeed resulting from the absence of calcite and subsequent goethite dissolution, additional simulations were performed. In those additional simulations, the same initial and boundary conditions were used with exception of the initial calcite concentration, which was set to 10 instead of 1 mol L<sup>-1</sup> outside the model region representing the tailings.

Influence of pyrite precipitation in the aquifer. From Table 8 follows that about 125 mols of pyrite (fraction of about 80.5 % of the dissolved amount) precipitate in cells 67-69 in the aquifer in a scenario with more extensive pyrite oxidation (2-3). This amount is comparable to the continuum case for the corresponding scenarios. The only major difference is, again, the location of the precipitation. In the scenario with less extensive pyrite oxidation (scenario 4), only about 6 % of the dissolved pyrite re-precipitates in cell 65.

In the scenario with oppression of pyrite precipitation (scenario 1), elevated Fe(II), sulphite and sulphate concentrations also occur beyond the end of the conduit system in cells with calcite, as it is the case for the pure continuum system. As a result of these elevated concentrations, a lower pe (of about 0.9) compared to scenarios 2 and 3, is also observed for this hybrid system.

### b) Coarse discretisation of the conduit system using an exchange coefficient of $1 \times 10^{-7} \text{ m}^2 \text{ s}^{-1}$

In simulations with an exchange coefficient of  $1 \times 10^{-7} \text{ m}^2 \text{ s}^{-1}$ , about 52.5 % of the flux is deviated to the conduit system (tailings region, Table 4), resulting in a flow velocity of approximately  $668 \text{ m yr}^{-1}$  within the conduit system. In analogy to Chapter 6.1.8 and Chapter 6.1.9(a), the geochemical processes are generally the same, apart from the location where dissolution/precipitation of calcite, goethite and gypsum take place. This implies for this particular hybrid system, that about half of the mass turnover due to dissolution/precipitation occurs at the first section of the aquifer (cells 1-3) whereas the other half occurs near the outlet of the conduit system (cells 64-67). Specifically, two cells near the upstream fringe of the aquifer are depleted with respect to calcite after 20 years and two more cells are depleted near the end of the conduit system. This can be attributed to the fact that the same amount of pyrite is mobilised in the corresponding pure continuum and hybrid system cases. However, up to 153 mols of calcite dissolve additionally in this hybrid system case compared to the pure continuum system case. Again, calcite dissolution extends over a greater aquifer distance. Therefore, significantly less kaolinite dissolves (< 9%) and significantly less gypsum precipitates (< 53 %). Table 9 lists the locations and quantities of mass turnover by mineral dissolution/precipitation for the different scenarios for this hybrid system. The pH decreases along the aquifer to the one simulated by a pure continuum system case because about half of the acidic solution reaches the first part of the aquifer (Fig. 35). This occurs similarly for all scenarios.

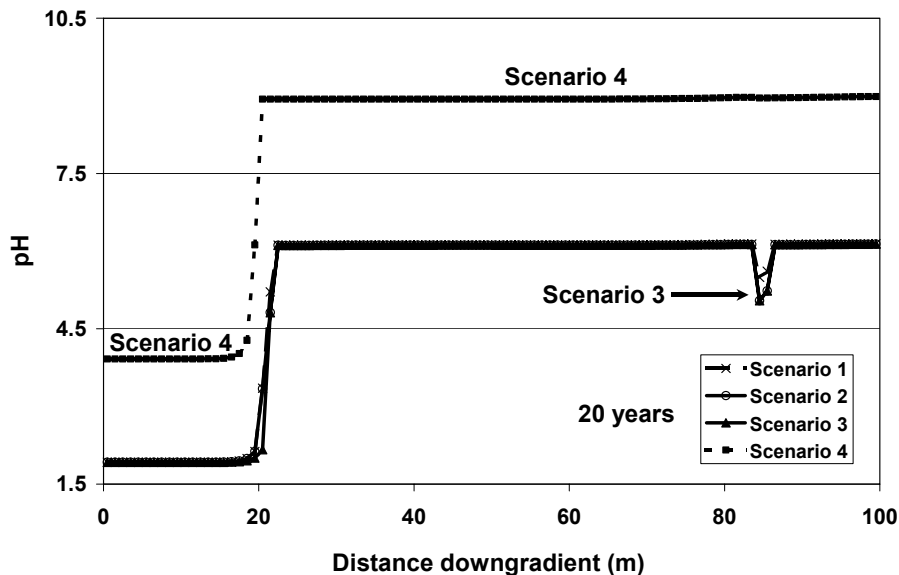


Fig. 35: Simulated pH profiles of scenarios 1-4 for a hybrid system consisting of 1 conduit with 2 nodes, using an exchange coefficient of  $1 \times 10^{-7} \text{ m}^2 \text{ s}^{-1}$  after 20 years.

Table 9: Dissolved and precipitated amounts and locations of the different mineral phases of scenarios 1-4 for a hybrid system with a conduit system consisting of 2 nodes, using an exchange coefficient of  $1 \times 10^{-7} \text{ m}^2 \text{ s}^{-1}$  after 20 years.

Scenario		1			2			3			4		
		cell	amount (mols)	fraction (%)	cell	amount (mols)	fraction (%)	cell	amount (mols)	fraction (%)	cell	amount (mols)	fraction (%)
Pyrite	dissolv.	t 1	155.2		t 1	155.2		t 1	155.2		t 1	12.4	
		aq 20	13.7		aq 2-3,64-67	126.5	100.0	aq 2-3,64-67	126.5	100.0	aq 2,65	0.7	100.0
					aq 4-63,68-80	$2.1 \times 10^{-2}$	$1.7 \times 10^{-2}$	aq 4-63,68-80	$2.2 \times 10^{-2}$	$1.7 \times 10^{-2}$	aq 66	$1.4 \times 10^{-8}$	$2.1 \times 10^{-6}$
	pre/dis			aq all	126.6	100.0	aq all	126.6	100.0	aq all	0.7	100.0	
Calcite	dissolv.	aq 1-3	2099.9	44.8	aq 1-3	2115.9	44.9	aq 1-3	2115.8	44.9	aq 1	27.8	48.7
		aq 64-67	2539.7	54.1	aq 64-67	2551.5	54.1	aq 64-67	2551.7	54.1	aq 65	29.2	51.3
		aq rest	50.5	1.1	aq rest	46.0	1.0	aq rest	46.9	1.0	aq all	57.0	100.0
		aq all	4690.1	100.0	aq all	4713.4	100.0	aq all	4714.5	100.0			
Kaolinite	dissolv.	aq 1	35.4		aq 1	25.0					aq 1,65	1.4	
	precip.	aq 2	32.1	99.8	aq 2	21.6	99.3				t 20	0.3	
		aq 63-64	0.1	0.2	aq 3,63-64	0.2	0.7						
	pre/dis	aq all	32.1	100.0	aq all	21.8	100.0						
Goethite	precip.	aq 2	740.1	41.9	aq 2	747.0	42.2	aq 2	746.6	42.1	aq 1,65	9.3	100.0
		aq 64-66	863.8	49.0	aq 64-66	897.3	50.6	aq 64-66	897.0	50.6	aq 2-64,66-80	$8.7 \times 10^{-6}$	$9.4 \times 10^{-5}$
		aq 3,12-63,67,75-80	160.4	9.1	aq 1,3,8-63,67,76-80	127.5	7.2	aq 3,8-63,67,76-80	128.1	7.2	t 20	1.2	
		aq all	1764.3	100.0	aq all	1771.8	100.0	aq all	1771.8	100.0	aq all	9.3	100.0
Gypsum	precip.	aq 2	381.9	72.5	aq 2	377.8	70.9	aq 2	377.9	70.9			
		aq 3-5	66.8	12.7	aq 3-5	75.9	14.3	aq 3-6	75.9	14.2			
		aq 64,67	78.3	14.8	aq 64,67	79.0	14.8	aq 64,67	79.0	14.8			
		aq 68-73	0.1	$1.1 \times 10^{-2}$	aq 68-73	$6.8 \times 10^{-3}$	$1.3 \times 10^{-3}$	aq 68-73	$6.8 \times 10^{-3}$	$1.3 \times 10^{-3}$			
		aq all	527.0	100.0	aq all	532.8	100.0	aq all	532.8	100.0			

Where t=tailing, aq=aquifer and all=all cells.

### c) Fine discretisation of the conduit system

As would be expected, the situation becomes more complex if the conduit system is subdivided into a larger number of nodes such that exchange of solution occurs in a more distributed manner. Now, the conduit system might also draw “background” aquifer solution, having a neutral pH, from the continuum, which is then mixed with the more acidic solution within the conduit system. A consequent increase in pH of the conduit solution compared to the one entered at the first node can be observed. As a result, less calcite is required for the buffering of the acidic conduit solution in the aquifer section downgradient. Depending upon the magnitude of the exchange flow rate, the pH either remains rather constant at the first part of the aquifer or decreases to the one for a pure continuum system (Fig. 36). Fig. 36 shows the spatial distribution of the pH in the continuum system in scenario 1 after 20 years. The simulations of a hybrid system containing 70 conduits are compared for four different exchange coefficients with the corresponding pure continuum system cases. A similar behaviour is observed for all other scenarios. In the scenario with less extensive pyrite oxidation (scenario 4), the pH is not decreased as much as in a scenario with more extensive pyrite oxidation. As an example for a conduit system with 70 conduits, the locations and quantities of mass turnover by mineral dissolution/precipitation using an exchange coefficient of  $5 \times 10^{-8} \text{ m}^2 \text{ s}^{-1}$  are listed in Table 10. Similar to the previously simulated conduit systems due to calcite dissolution over a greater aquifer distance, less kaolinite dissolves (fraction between 12 to 16%) and less gypsum precipitates (fraction of up to 62 %) in this hybrid system.

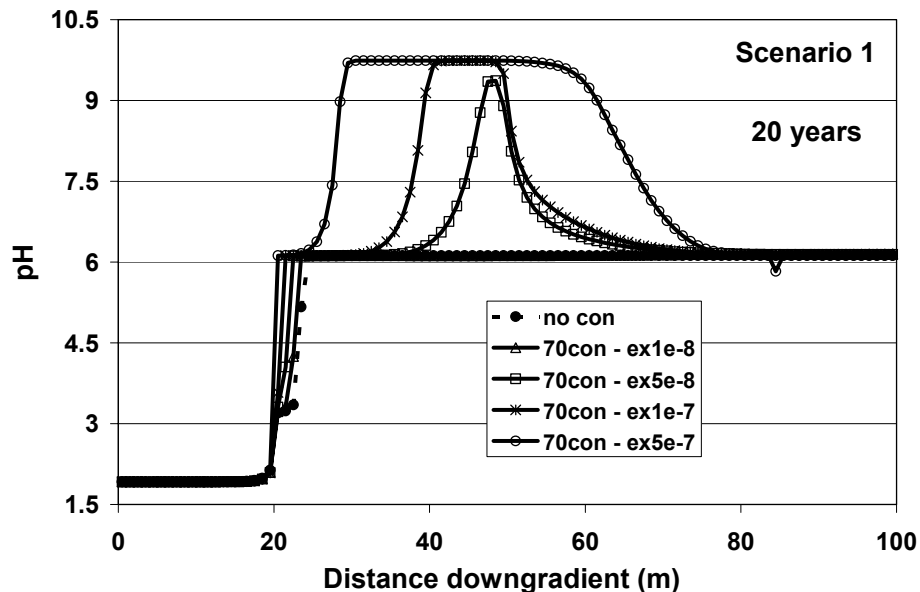


Fig. 36: Simulated pH profiles of scenario 1 after 20 years for a hybrid system consisting of 70 conduits (70con) using 4 different exchange coefficients (ex) versus only a continuum system.

Table 10: Dissolved and precipitated amounts and locations of the different mineral phases of scenarios 1-4 for a hybrid system with a conduit system consisting of 70 nodes, using an exchange coefficient of  $5 \times 10^{-8} \text{ m}^2 \text{ s}^{-1}$  after 20 years.

Scenario		1			2			3			4		
		cell	amount (mols)	fraction (%)	cell	amount (mols)	fraction (%)	cell	amount (mols)	fraction (%)	cell	amount (mols)	fraction (%)
Pyrite	dissolv.	t 1-3	155.2		t 1-3	155.2		t 1-3	155.2		t 1-2	12.5	
	precip.	t 20	10.2		aq 2-26,31-80	126.7		aq 2-3	55.3	41.8	aq 1-3,35-67	0.7	
	pre/dis			6.5			81.7	aq 1,4-26,31-80	77.0	58.2			
								aq all	132.3	100.0			5.9
Calcite	dissolv.	aq 1-3	2097.7	45.0	aq 1-3	2108.9	44.9	aq 1-3	2108.9	44.9	aq 1	28.8	51.5
		aq 38-66	2503.7	53.7	aq 38-66	2523.1	53.8	aq 38-66	2523.7	53.8	aq rest	27.1	48.5
		aq rest	61.3	1.3	aq rest	60.6	1.3	aq rest	61.1	1.3	aq all	55.9	100.0
		aq all	4662.7	100.0	aq all	4692.7	100.0	aq all	4693.7	100.0			
Kaolinite	dissolv.	aq 1	63.1		aq 1	50.4					aq 1	0.8	
		aq 2-3	53.5	94.9	aq 2-3	42.2	92.0				t 20	0.3	
		aq 54-65	2.9	5.1	aq 54-65	3.7	8.0						
		aq all	56.4	100.0	aq all	45.8	100.0						30.8
	pre/dis			89.4		90.9							
Goethite	precip.	aq 1-2	715.3	40.5	aq 2	695.8	39.2	aq 2	695.3	39.2	aq 1	5.1	48.8
		aq 3-63	823.5	46.6	aq 1,3-63	848.0	47.8	aq 3-63	848.4	47.8	aq 2-22, 26-28, 30-80	5.4	51.2
		aq 64-65	215.8	12.2	aq 64-65	218.8	12.3	aq 64-65	218.8	12.3	aq all	10.5	100.0
		aq 66, 67,72-80	11.0	0.6	aq 66-68,74-80	11.0	0.6	aq 66-68,74-80	11.0	0.6			
		aq all	1765.6	100.0	aq all	1773.7	100.0	aq all	1773.6	100.0			
Gypsum	precip.	aq 2	365.1	59.0	aq 2	360.0	57.6	aq 2	360.2	57.6			
		aq 3-5	62.5	10.1	aq 3-5	69.4	11.1	aq 3-5	69.3	11.1			
		aq 54-67	191.0	30.9	aq 54-67	196.1	31.4	aq 54-67	196.1	31.4			
		aq 68-77	0.1	0.0	aq 75-80	0.0	0.0	aq 75-80	0.0	0.0			
		aq all	618.7	100.0	aq all	625.5	100.0	aq all	625.6	100.0			

Where t=tailing, aq=aquifer and all=all cells.

### 6.1.10 Summary

In this section, RUMT3D was verified with a benchmark problem defined by McNab (2001). This problem required simulation of the principle processes of the Acid Mine Drainage (AMD) phenomena in chemical equilibrium. Simulation results of RUMT3D were thereby compared to the original PHREEQC-2 simulator as this simulator was used by McNab (2001). Satisfactory results were generally achieved for the comparison of simulation results obtained by both simulators.

To investigate whether RUMT3D would generate plausible results when the McNab problem was expanded to a hybrid system, four different scenarios including the original McNab problem (i.e., pure continuum system case) were investigated. Basically, in these scenarios, inclusion of the kaolinite phase, the oppression of precipitating pyrite in the aquifer and extent of pyrite oxidation were varied. The influences of the spatial discretisation of the conduit system and magnitude of the exchange flow rate were thereby also investigated.

In all scenarios, with and without a conduit system, in response to calcite depletion, lowering of pH occurred and elevated dissolved Fe(II) and sulphate concentrations were observed due to goethite dissolution and subsequent processes. These elevated dissolved Fe(II) and sulphate concentrations caused a higher redox potential at respective aquifer locations without calcite. In the scenarios where kaolinite was present as the “secondary” buffer mineral, increased aluminium and silicon concentrations occurred near locations where calcite was absent. Due to the buffering capacity of kaolinite, the pH in calcite-depleted cells was higher than in the scenario where kaolinite was not included. These increased aluminium and silicon concentrations were declining as soon as they were transported to a calcite buffered environment. In the scenario that oppressed pyrite precipitation within the aquifer, sulphite remained in the solution, associated with increased Fe(II) and sulphate concentrations as well as a lower  $p_e$ . In the other investigated scenarios, sulphite precipitated as pyrite within the aquifer region, especially near locations where acidic inflow from upgradient occurs. In the scenario with less extensive pyrite oxidation, significantly smaller amounts of calcite and kaolinite were required to buffer the pH. Consequently, significantly less goethite precipitated. No gypsum precipitated as concentrations of calcium and sulphate remained below its solubility product. Also, the pH was not lowered as much as in a corresponding scenario with more extensive pyrite oxidation, which implies that the recharge solution supplied to a region should possibly contain no oxidising agents or if present only in low concentrations to prevent or minimise pyrite oxidation. Based upon results in this section, plausibility could be demonstrated for both system cases: the pure continuum and hybrid system cases using two different discretisations of the conduit system and four different exchange coefficients.

Simulation results of RUMT3D in all scenarios indicate that in general, a conduit system can significantly affect the spatial variation of buffering processes in an aquifer due to its case dependent extreme impact on the flow dynamics. The higher the exchange flow rate between the continuum and the conduit system,

the more rapidly acidic solution is transported via the (faster) conduit system, where the buffering capacity provided by calcite is also successively consumed. A reduced magnitude of exchange flow between continuum and conduit system and the simultaneous distribution of acidic solution over a wider aquifer section resulted in less kaolinite dissolution and less gypsum precipitation.

## 6.2 Effect of acidic process water upon an aquifer from a uranium mine site

Acidic process waters remaining in the pore space of abandoned mines often contain high concentrations of metals (e.g., iron and aluminium) as well as heavy metals (e.g., copper and zinc), resulting from the dissolution of silicate, oxide and carbonate minerals (e.g., White et al. 1984; Bain et al. 2001; McNab 2001). As discussed in Chapter 6.1 for the AMD problem developed by McNab (2001), the pH is clearly the prime variable controlling the concentration of the contaminants. In addition, when exposed to oxygen or oxidising conditions, sulphide minerals contained in the ore body or adjacent aquifer may be oxidised, causing further acidification of the pore water. An even more severe threat to groundwater resources is the potential mobilisation of radionuclides (Bain et al. 2001) under specific geochemical conditions that allow their release from, for example, uranium-bearing ore bodies.

One such site is the Königstein uranium mine site (Fig. 37), located in the Saxony region of Eastern Germany (near the Elbe River, about 20 km south of the city of Dresden). There, low-pH pore water in the mine workings resulted from the extraction of uranium (i.e., uraninite,  $\text{UO}_2$ ) by *in situ* acid-leaching. The leaching process, applied over more than four decades from 1946 until the end of 1990 involved the application of a highly oxidising sulphuric acid solution. Extensive dewatering of the mine workings was required to facilitate the drainage of the acids and the recovery of dissolved uranium.

WISMUT GmbH, the company responsible for the remediation of mine sites in Germany, has investigated the option of flooding the groundwater in the mining area to its natural level to rehabilitate and remediate the Königstein mine. If realised, flooding would occur in several stages distributed over a number of years. It is thought that flooding would allow to re-establish more reducing conditions and prevent further oxidation of sulphide minerals, in particular of pyrite oxidation (compare Chapter 1.1). To support the estimation of the relevant timescales and to predict appropriate flooding levels, WISMUT contracted the University of Waterloo, Canada to conduct a theoretical reactive modelling study. The objective of this study was to predict the movement of dissolved metals, radionuclides, sulphate and low pH pore water that is thought to result from flooding the Königstein uranium mine. The primary concern of reflooding the mine is that dissolved metals contained in the highly acidic pore water and in aquifer minerals could contaminate the aquifer. It was determined that under various geochemical settings, contaminants could eventually discharge into the Elbe River. Bain et al. (2001) used the general-purpose multicomponent reactive transport model MIN3P (Mayer, 1999, compare Chapter 2.5.1) for the modelling study. The model setup and the boundary conditions of one of the scenarios as

described by Bain et al. (2001) was selected as a second benchmark problem for reactive transport for RUMT3D. It was chosen because it considers the complex interactions between a large number of species and mineral phases, including uranium-containing species and minerals. The results from the MIN3P simulations provided an independently developed set of results against which the performance of RUMT3D could be verified.

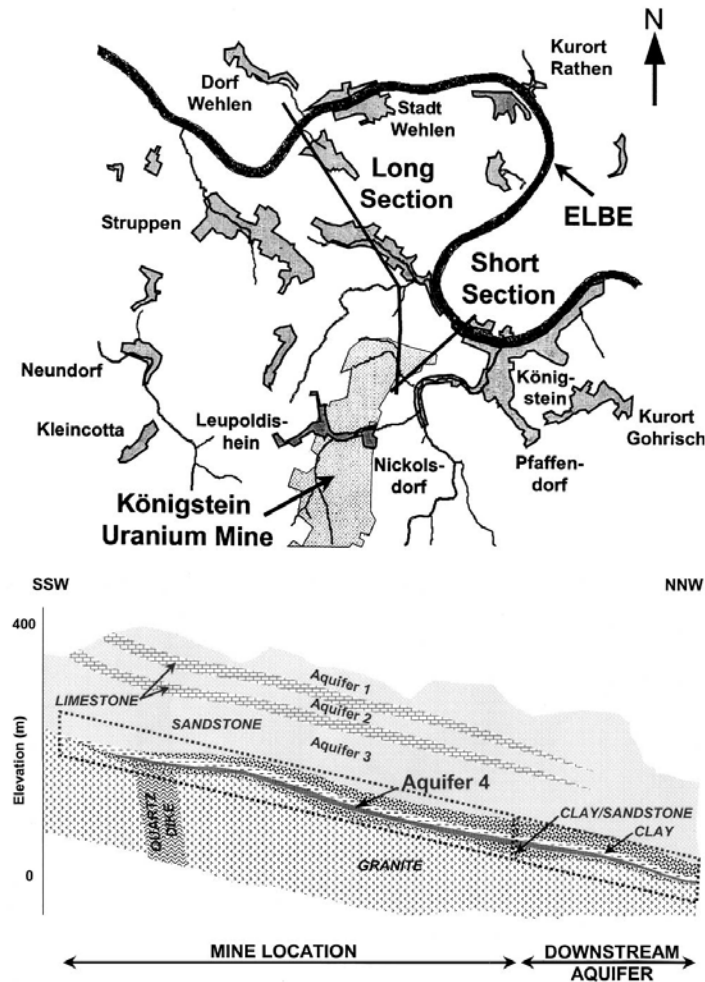


Fig. 37: Geographical and hydrogeological setting of the Königstein mine as provided by Bain et al. (2001).

### 6.2.1 Description of the Benchmark Problem

The ore body of the mine is situated in a lower sandstone layer, locally known as the 4<sup>th</sup> aquifer ('Quadersandstein', Fig. 37). A clay aquitard separates the overlying 3<sup>rd</sup> aquifer (an unconfined sandstone cell) from the 4<sup>th</sup> aquifer. Flow through this aquitard is low according to the results of a groundwater flow modelling study conducted by WASY (1995) using the 3D-flow and transport model FEFLOW (Diersch, 1997). Based on the results from this study, two

distinct and representative flow paths within the 4<sup>th</sup> aquifer from the mine workings toward the Elbe River could be identified:

- a long flow path extending approximately 5000 m north (“*Long Section*” in Fig. 37) and
- a short flow path extending approximately 1000 m east north (“*Short Section*” in Fig. 37).

1D simulations along those selected flow paths rather than 3D simulations were conducted to save computing resources. This was an advisable simplification given the large number of reactive simulations that needed to be performed. It could be assumed that the flow in the 4<sup>th</sup> aquifer was uniform due to a relatively consistent thickness along its length, indicating that the simplification to a 1D system was well justified. Further, for simplicity, it was assumed that the geochemical processes within the 4<sup>th</sup> aquifer would essentially be independent of the conditions in the neighbouring confining cells. A number of simulations were conducted by Bain et al. (2001) in support of their use of a 1D conceptual model for addressing reactive mass transport in the 4<sup>th</sup> aquifer. In their simulations, the effects of the confining layers on mass transport within the aquifer and of retardation within the confining layers were also investigated. Both main flow directions downgradient of the mine, the north-easterly (*Short*) and the northerly (*Long*) directions were simulated in 1D whereby the northern end of the mine workings was the inflow source boundary of the generic model. Results indicated that these effects are negligible and therefore that the 1D simulations would be sufficient for the task at hand.

Of all simulations, most were conducted for the *Short Section* since this section represents a worst-case scenario with respect to the potential environmental impact on the Elbe River. This is due to the *Short Section* having a significantly higher flow velocity (7 times) compared to the *Long Section* as result of a higher hydraulic gradient. Given the velocity estimates for the flow path, a time frame of 100 years was considered to be an appropriate length for the investigation and comparison of a range of different discharge periods (stages) of contaminants into the Elbe River (see Chapter 6.2.4).

Since the available mineralogical data for the 4<sup>th</sup> aquifer were sparse and of limited detail, the modelling study was undertaken as a sensitivity study in which the potential movement of metals, radionuclides and sulphate was predicted for a conceptual hydrogeochemical model, with an emphasis on variations in the mineralogy. Bain et al. (2001) considered different combinations of minerals known to commonly control the pH and pe of the groundwater within aquifer systems. Specifically, the mass and mineralogy of the carbonate minerals, the presence of oxidised (ferrihydrite) and reduced phases (sulphide minerals) and the initial mass of uraninite within the aquifer were varied. Table 11 lists the different scenarios for the sensitivity studies as provided by Bain et al. (2001), including the one for conservative transport. One of those scenarios, i.e., the calcite scenario was selected to serve as a benchmark problem for RUMT3D within the present study. The conservative scenario is additionally used to examine the proper setup of the problem, and, for example, to test whether the simulations were potentially affected by numerical dispersion.

Table 11: Reactive transport sensitivity studies as given by Bain et al. (2001).

Simulation	Composition	Quantity (wt. %)
"Conservative"	Non-reactive	n/a
"Calcite"	Carbonate present	0.2 wt.% calcite
"Ferrihydrite"	Me-oxides present	1 wt.% ferrihydrite
"Calcite + ferrihydrite"	Carbonates and Me-oxides present	0.2 wt.% calcite 1 wt.% ferrihydrite
"Calcite + pyrite"	Carbonates and Me-sulphides present	0.2 wt.% calcite 1 wt.% sulphides and trace sulphides

## 6.2.2 Model Parameters

The model parameters and input used by Bain et al. (2001), such as

- groundwater flow velocities,
- aquifer porosity,
- ambient water composition in the aquifer and in the pore water of the mine workings and
- estimation of the bulk composition and mineralogy of the aquifer

were based upon previous investigations conducted by WISMUT. Table 12 lists the physical parameters of the *Short Section* and Table 13 summarises the source and background water composition of the aquifer. Similarly to Chapter 6.1.1, concentration of a master species listed in Table 13 represent the sum of a respective dissolved species in the aqueous phase and concentration of a mineral is expressed in mol L<sup>-1</sup> which stands for moles of a respective mineral per litre water.

The data for the source water were obtained from a limited flooding experiment at the mine site undertaken by WISMUT, sampled 190 days after the experiment began. The pH of the drainage water from this experiment was very low (2.3) and conditions were oxidising. From the Fe(II)/Fe(III) ratio, a pe of approximately 13.5 was estimated. The low pH and high pe are favourable conditions for high concentrations of dissolved metals, in particular Fe(III), Al(III), Cd(II), Cr(III) and Zn(II).

Table 12: Hydrogeological parameters of the 4<sup>th</sup> aquifer (*Short Section*, WASY, 1995, Bain et al. 2001).

Parameter	<i>Short Section</i> (high velocity)
Domain length	1000 m
Domain width	1-D, 1 m cell width
Hydraulic conductivity	1x10 <sup>-5</sup> m s <sup>-1</sup>
Hydraulic gradient	0.117
Particle velocity	194 m yr <sup>-1</sup>
Porosity	0.19
Simulation time	100 yrs

Table 13: Source and background water composition (Bain et al. 2001).

Master species / mineral	Symbol	Equilibrated source water <sup>a</sup> (mol L <sup>-1</sup> )	Equilibrated HG 7013 water for the conservative scenario (mol L <sup>-1</sup> )	Equilibrated HG 7013 water for the calcite scenario <sup>b</sup> (mol L <sup>-1</sup> )
Aluminium	Al(III)	$6.574 \times 10^{-3}$	$3.707 \times 10^{-8}$	$3.477 \times 10^{-8}$
Barium	Ba(II)	$3.542 \times 10^{-8}$	$9.319 \times 10^{-7}$	$1.931 \times 10^{-6}$
Calcium	Ca(II)	$1.174 \times 10^{-2}$	$1.847 \times 10^{-4}$	$6.854 \times 10^{-3}$
Cadmium	Cd(II)	$8.850 \times 10^{-6}$	$6.510 \times 10^{-6}$	$1.910 \times 10^{-6}$
Chloride	Cl(-I)	$1.311 \times 10^{-2}$	$9.254 \times 10^{-4}$	$9.254 \times 10^{-4}$
Carbonate	C(IV)	$1.008 \times 10^{-8}$	$1.662 \times 10^{-3}$	$8.047 \times 10^{-3}$
Chromium	Cr(III)	$1.640 \times 10^{-5}$	$1.163 \times 10^{-9}$	$1.163 \times 10^{-9}$
Copper	Cu(II)	$1.000 \times 10^{-10}$	$1.000 \times 10^{-10}$	$1.000 \times 10^{-10}$
Fluoride	F(-I)	$5.305 \times 10^{-7}$	$3.949 \times 10^{-5}$	$3.949 \times 10^{-5}$
Ferrous iron	Fe(II)	$1.363 \times 10^{-4}$	$2.813 \times 10^{-4}$	$3.047 \times 10^{-6}$
Ferric iron	Fe(III)	$1.061 \times 10^{-2}$	$2.563 \times 10^{-8}$	$7.270 \times 10^{-11}$
Silicon	Si(IV)	$9.336 \times 10^{-4}$	$9.586 \times 10^{-4}$	$9.535 \times 10^{-4}$
Potassium	K(I)	$5.787 \times 10^{-7}$	$2.093 \times 10^{-3}$	$2.093 \times 10^{-3}$
Magnesium	Mg(II)	$2.031 \times 10^{-3}$	$1.687 \times 10^{-4}$	$1.687 \times 10^{-4}$
Sodium	Na(I)	$2.402 \times 10^{-2}$	$1.784 \times 10^{-3}$	$1.784 \times 10^{-3}$
Nickel	Ni(II)	$1.133 \times 10^{-4}$	$1.704 \times 10^{-9}$	$1.704 \times 10^{-9}$
Lead	Pb(II)	$4.864 \times 10^{-7}$	$4.828 \times 10^{-10}$	$4.828 \times 10^{-10}$
Phosphorus	P(V)	$8.383 \times 10^{-5}$	$6.320 \times 10^{-7}$	$6.320 \times 10^{-7}$
Radium	Ra(II)	$3.121 \times 10^{-4}$	$9.413 \times 10^{-9}$	$1.951 \times 10^{-8}$
Sulphate	S(VI)	$5.299 \times 10^{-2}$	$2.717 \times 10^{-4}$	$2.727 \times 10^{-4}$
Uranium	U(IV)	$4.490 \times 10^{-26}$	$5.095 \times 10^{-12}$	$5.152 \times 10^{-12}$
	U(VI)	$1.777 \times 10^{-4}$	$1.570 \times 10^{-7}$	$1.693 \times 10^{-7}$
Zinc	Zn(II)	$1.542 \times 10^{-3}$	$1.683 \times 10^{-7}$	$1.683 \times 10^{-7}$
pH <sup>c</sup>		2.300	$6.600 \times 10^0$	$6.614 \times 10^0$
pe <sup>c</sup>		$1.335 \times 10^1$	$1.407 \times 10^0$	$9.937 \times 10^{-1}$
Calcite				$7.328 \times 10^{-2}$
Cr(OH) <sub>3</sub> (am)				0
Ferrihydrite (Fe(OH) <sub>3</sub> (am))				0
Gibbsite				$1.617 \times 10^{-9}$
Gypsum				0
Jarosite-K				0
Otavite				$9.811 \times 10^{-6}$
Ra-barite				$1.12 \times 10^{-4}$
Siderite				0
Amphorous silica				$4.410 \times 10^0$
Smithsonite				0
Uraninite				$1.862 \times 10^{-4}$

<sup>a</sup> Based on the observed source water composition from a limited flooding experiment, sampled 190 days after the begin of the experiment and equilibrated with respect to K-jarosite and silica, pH and pe were held constant.

<sup>b</sup> The representative background water is determined by PHREEQC-2 by equilibrating water present at well HG 7013 in the 4<sup>th</sup> aquifer with primary minerals phases assumed to be present in the scenario calcite (see Table 14).

<sup>c</sup> Dimensionless.

Water from a particular well (HG 7013), located mid-way between the mine workings and the Elbe River was assumed to be representative for the water quality of the 4<sup>th</sup> aquifer. The water contains moderate to high concentrations of dissolved iron, uranium, heavy metal and sulphate. Downgradient to the mine, the 4<sup>th</sup> aquifer consists primarily of quartz, with trace amounts of metal oxides (gibbsite (Al(OH)<sub>3</sub>), amorphous ferric hydroxide (ferrihydrite (Fe(OH)<sub>3</sub>)), metal sulphides (e.g., pyrite (FeS<sub>2</sub>), galena (PbS)), clays and carbonate minerals according to the limited drilling information and mine records. Also, traces of Cd(II), Cr(III) and Zn(II) are contained in the aquifer in form of otavite (CdCO<sub>3</sub>), Cr(OH)<sub>3</sub> and smithsonite (ZnCO<sub>3</sub>). Table 14 shows the quantities, volume fractions, densities, molecular weights and concentrations of the different minerals initially considered in the calcite scenario. The densities and molecular weights are required to convert the volume fractions into concentration values (= volume fraction \* density / molecular weight \* 1000). Fig. 38 depicts the conceptual model for the *Short Section*, calcite scenario.

Table 14: Initial aquifer mineralogy for the calcite scenario.

Mineral	Molecular weight (g mol <sup>-1</sup> )	Density (g cm <sup>-3</sup> )	Quantity	Volume fraction	Concentration (mol L <sup>-1</sup> )
Calcite	100.089	2.710	0.2 wt. %	$2.709 \times 10^{-3}$	$7.334 \times 10^{-2}$
Otavite	172.419	4.884	0.5 ppm	$3.468 \times 10^{-7}$	$9.823 \times 10^{-6}$
Ra-barite	234.279	4.480		$5.850 \times 10^{-6}$	$1.118 \times 10^{-4}$
Amorphous silica	60.085	2.650		$1.000 \times 10^{-1}$	$4.410 \times 10^0$
Uraninite	270.028	10.964	20 ppm	$4.586 \times 10^{-6}$	$1.862 \times 10^{-4}$

**Aqueous composition:**

Equilibrated water at well HG 7013 in the 4<sup>th</sup> aquifer, see Table 13.

**Assumed minerals initially present for the**

**calcite scenario:** Calcite (CaCO<sub>3</sub>), Otavite (CdCO<sub>3</sub>), Ra-barite, SiO<sub>2</sub>(am), uraninite (UO<sub>2</sub>), gibbsite (Al(OH)<sub>3</sub>).

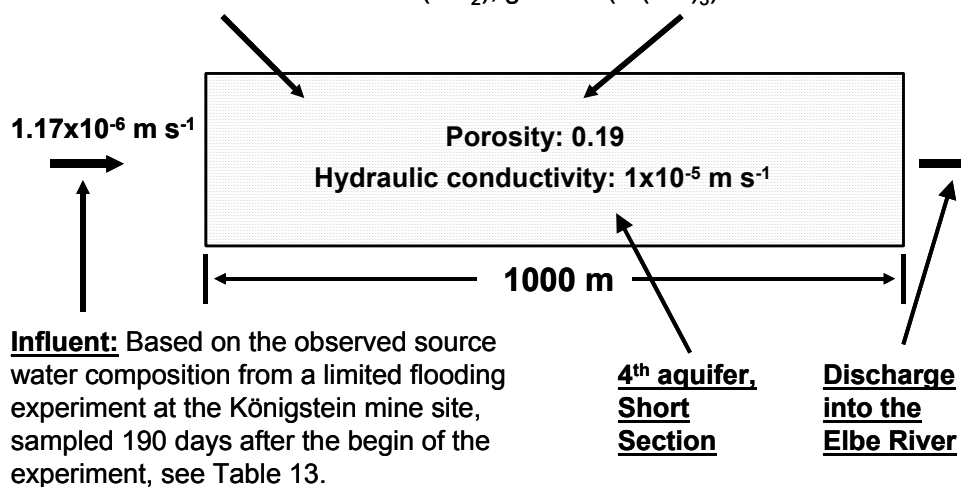


Fig. 38: Conceptual model for the *Short Section*, calcite scenario.

Due to their consistency and widespread availability, the thermodynamic equations and equilibrium constants from the WATEQ4F and MINTEQA2 databases were used in the simulations of Bain et al. (2001) and therefore also in this study. Table 15 shows the reaction equations of the mineral phases for the calcite scenario, along with their thermodynamic solubility (pK). Reactions involving dissolved uranium are given by Bain et al. (2001).

Table 15: Chemical reaction equations of the considered mineral phases for the *Short Section*, calcite scenario (Bain et al. 2001).

Mineral	Reaction equation	pK
Calcite	$\text{CaCO}_3 \Leftrightarrow \text{Ca}^{2+} + \text{CO}_3^{2-}$	8.475
Cr(OH) <sub>3</sub> (am)	$\text{Cr(OH)}_3 + \text{H}^+ \Leftrightarrow \text{Cr(OH)}_2^+ + \text{H}_2\text{O}$	0.75
Ferrihydrite (Fe(OH) <sub>3</sub> (am))	$\text{Fe(OH)}_3 + 3 \text{H}^+ \Leftrightarrow \text{Fe}^{3+} + 3 \text{H}_2\text{O}$	-4.891
Gibbsite	$\text{Al(OH)}_3 + 3 \text{H}^+ \Leftrightarrow \text{Al}^{3+} + 3 \text{H}_2\text{O}$	-8.11
Gypsum	$\text{CaSO}_4 \cdot 2\text{H}_2\text{O} \Leftrightarrow \text{Ca}^{2+} + \text{SO}_4^{2-} + 2 \text{H}_2\text{O}$	4.58
Jarosite-K	$\text{KFe}_3(\text{SO}_4)_2(\text{OH})_6 + 6 \text{H}^+ \Leftrightarrow \text{K}^+ + 3 \text{Fe}^{3+} + 2 \text{SO}_4^{2-} + 6 \text{H}_2\text{O}$	9.21
Otavite	$\text{CdCO}_3 \Leftrightarrow \text{Cd}^{2+} + \text{CO}_3^{2-}$	12.1
Ra-barite	$0.01\text{Ra} \cdot 0.99\text{Ba} \cdot \text{SO}_4 \Leftrightarrow 0.99 \text{Ba}^{2+} + 0.01 \text{Ra}^{2+} + \text{SO}_4^{2-}$	9.976
Siderite	$\text{FeCO}_3 \Leftrightarrow \text{Fe}^{2+} + \text{CO}_3^{2-}$	10.45
Amorphous silica (SiO <sub>2</sub> (am))	$\text{SiO}_2 + 2 \text{H}_2\text{O} \Leftrightarrow \text{H}_4\text{SiO}_4$	3.018
Smithsonite	$\text{ZnCO}_3 \Leftrightarrow \text{Zn}^{2+} + \text{CO}_3^{2-}$	10.0
Uraninite	$\text{UO}_2 + 4 \text{H}^+ \Leftrightarrow \text{U}^{4+} + 2 \text{H}_2\text{O}$	4.85

### 6.2.3 Problem Setup

A good agreement between the two different models (i.e., RUMT3D and MIN3P) was achieved. However, not astonishingly the accuracy of the results depended on the spatial and temporal discretisation being used as well as on iteration options in the PHREEQC-2 model. The model setup and the dependency of the simulation results will be discussed in the following. Mainly in this subsection, the occurrence (or absence) of numerical dispersion is examined by comparing simulated breakthrough curves (BTC's) of chloride in the (reactive) calcite scenario as well as the conservative scenario. Chloride is transported conservatively in these two scenarios (see also Chapter 6.2.4). A discussion of accuracy of the results for the calcite scenario is postponed to Chapter 6.2.5.

Interestingly, the simulated BTC's of chloride for the conservative and calcite scenario by MIN3P differed slightly, indicating that the simulation results were perhaps affected by numerical dispersion. It is thought that MIN3P's upstream spatial weighting and implicit time weighting with variable time stepping promoted the occurrence of numerical dispersion. A refinement of the spatial discretisation would potentially have eliminated the numerical dispersion occurring in the MIN3P model but the error was found acceptable by Bain et al. (2001) in the light of the additional computational resources that would have been required.

In comparison, RUMT3D produces only very little numerical dispersion, for example when the TVD solver for advective transport is used. This can be seen in particular in the chloride BTC without dispersivity (Fig. 39). To obtain a breakthrough curve that approximately reproduces the one obtained by MIN3P in the conservative scenario, a dispersivity of 2.5 m appeared to be most appropriate. For the calcite scenario, a dispersivity of 5 m provided a good agreement with the MIN3P results (Fig. 39 and Fig. 40).

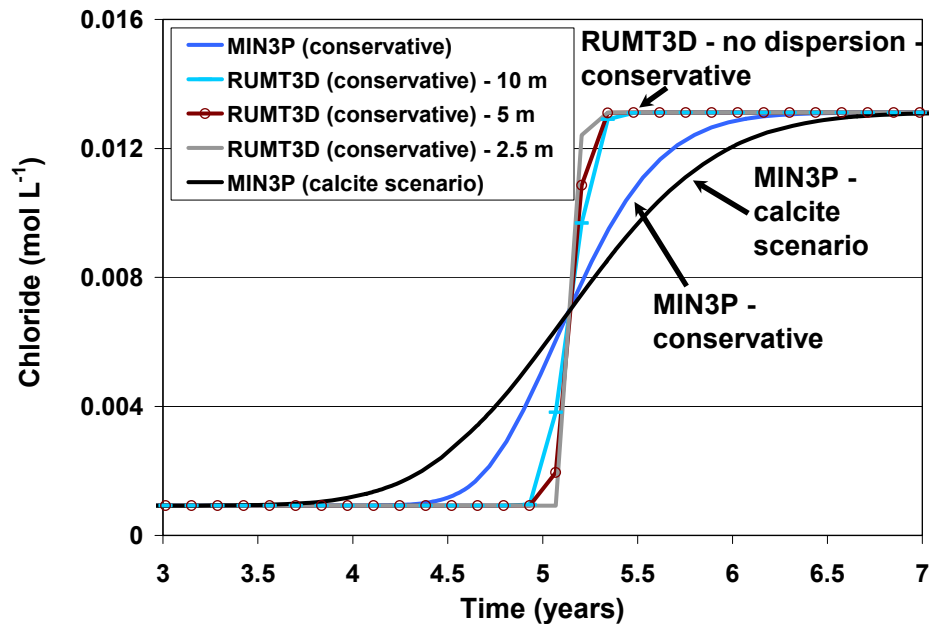


Fig. 39: Comparison of simulated chloride concentrations for the conservative scenario with the RUMT3D model using different spatial discretisations (2.5, 5 and 10 m per cell). The conservative and the calcite scenario of the MIN3P model are also shown.

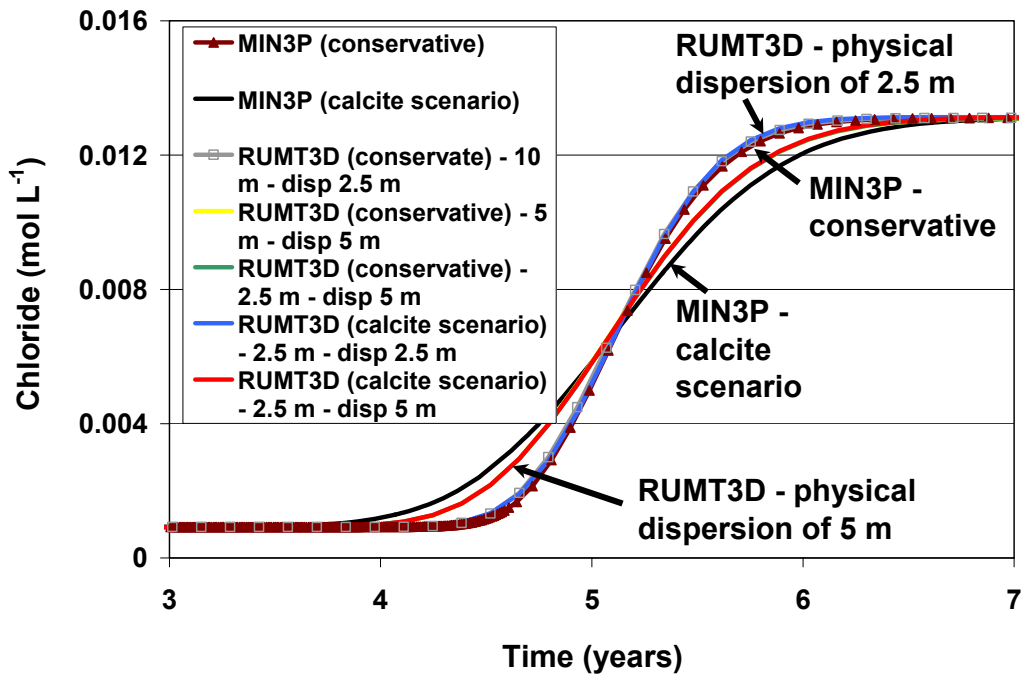


Fig. 40: Comparison of simulated chloride concentrations for the conservative and calcite scenario with the RUMT3D model using different spatial discretisations (2.5, 5 and 10 m per cell) and dispersivities (disp) of 2.5 and 5 m. The calcite scenario of the MIN3P model is also depicted.

Results shown in the next subsection and in the appendix for the calcite scenario using RUMT3D (Fig. 42 - Fig. 62) are with

- a spatial discretisation of 5 m per cell,
- a reaction step size of 5 days,
- a dispersivity of 5 m,
- the TVD solver for advective transport

and the with the following two iteration options for the PHREEQC-2 model:

- a maximum step size for the multiplicative change in the activity of an aqueous species on each iteration (step\_size) of 2 and
- a maximum step size for the activity of the electron (pe\_step\_size) of 2.

The accuracy of the results associated with varying the above parameters are discussed in more detail in Chapter 6.2.5. The deviations in the simulated curves of silicon and barium before breakthrough at the 1000 m observation (Fig. 59 and Fig. 61) are probably due to having counterbalanced the water composition of the aquifer with an  $A^-$  species in the RUMT3D model. The initial aquifer solution had a significant charge balance error of about 32 %. The negatively-charged  $A^-$  species was introduced in database of PHREEQC-2 to be considered during the simulation. A concentration of  $1.0875 \times 10^{-2} \text{ mol L}^{-1}$  was necessary to reduce the charge balance error to nearly zero. Additionally, to balance the minor charge

balance error (about 0.3 %) of the source water, a positively-charged species, i.e.,  $\text{Ain}^+$  was introduced in the database. For that, a concentration of 0.0004 was sufficient to reduce the charge balance error to nearly zero.

#### **6.2.4 Simulation Results and Geochemical Processes during Transport (Calcite Scenario)**

The site specific reaction network for the benchmark problem investigated in this section includes the aqueous master species listed in Table 13 and the mineral phases shown in Table 15. For simplicity, all reactions were assumed to be in thermodynamic equilibrium, mainly because site-specific data required to simulate kinetically-limited reaction processes were not available.

According to Bain et al. (2001), the aquifer geochemistry evolves during the simulation period for the calcite scenario as follows: Initially, when the acidic source water (pH 2.2) enters the aquifer from the mine workings, calcite is the acid-buffering mineral. For about 50 years, its dissolution maintains the pH near 6 at the discharge point into the Elbe River, i.e., after a travel distance of 1000 m. The dissolution of calcite induces the precipitation of siderite, gibbsite and ferrihydrite. As soon as calcite is depleted at a particular location, these minerals dissolve sequentially, thereby still buffering the acidity but on a lower level. The dissolution of these minerals is according to their solubility thus, siderite dissolves first, followed by gibbsite. Because its low solubility, there is no particularly pronounced siderite buffering stage (Fig. 41). The dissolution of gibbsite keeps the pH at around 4 for about 21 years at the discharge point to the Elbe River. Finally, ferrihydrite dissolves which buffers the pH at around 3. Fig. 42 depicts these different stages/periods of pH buffering as simulated for the 1000 m observation point, i.e., the discharge point into the Elbe River. Accordingly, the pH BTC's correspond to the BTC's for the minerals calcite, gibbsite and ferrihydrite (Fig. 43).

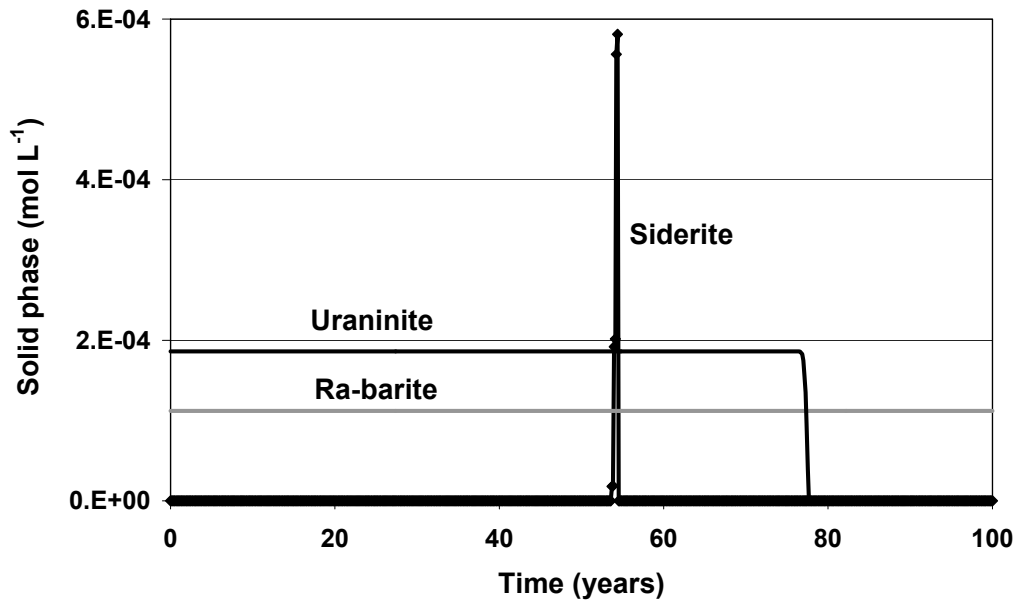


Fig. 41: Simulated concentrations of siderite, uraninite and ra-barite at the 1000 m observation point using RUMT3D (calcite scenario).

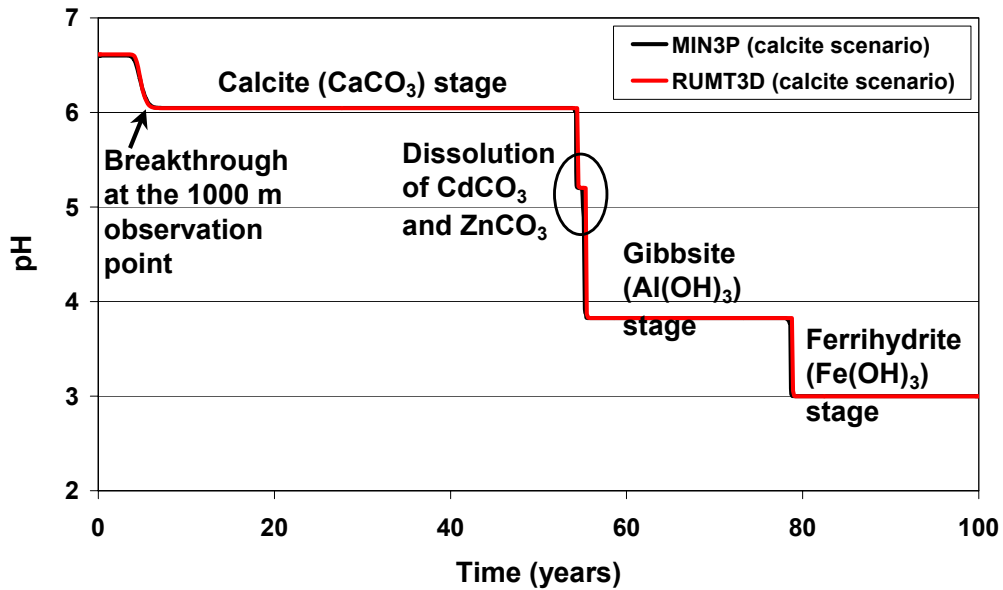


Fig. 42: pH buffering stages for the calcite scenario as simulated at the 1000 m observation point.

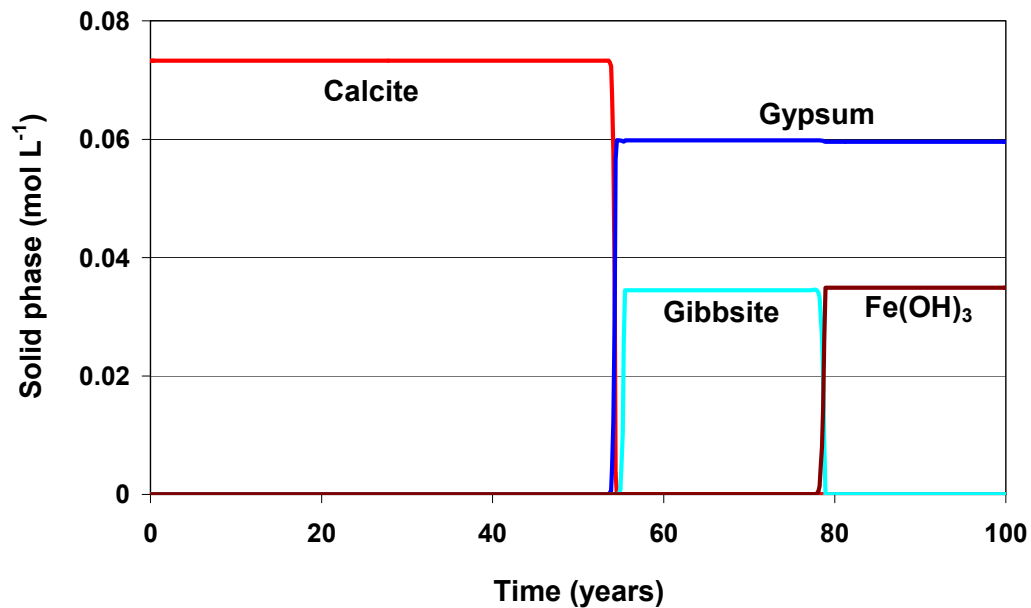
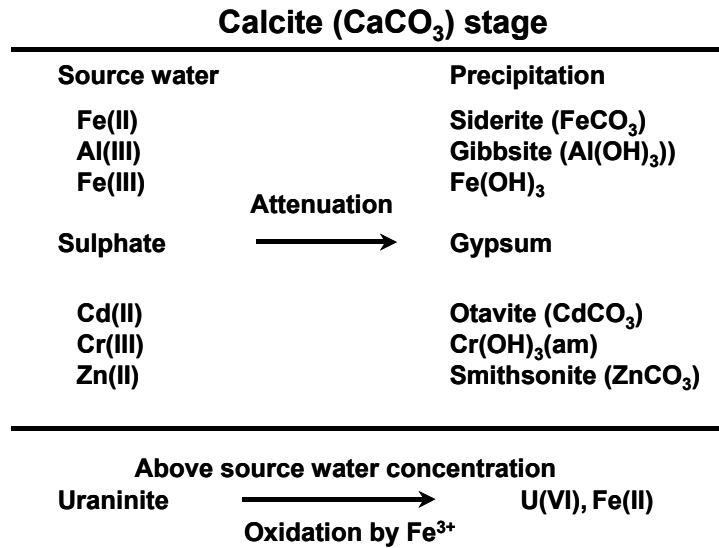


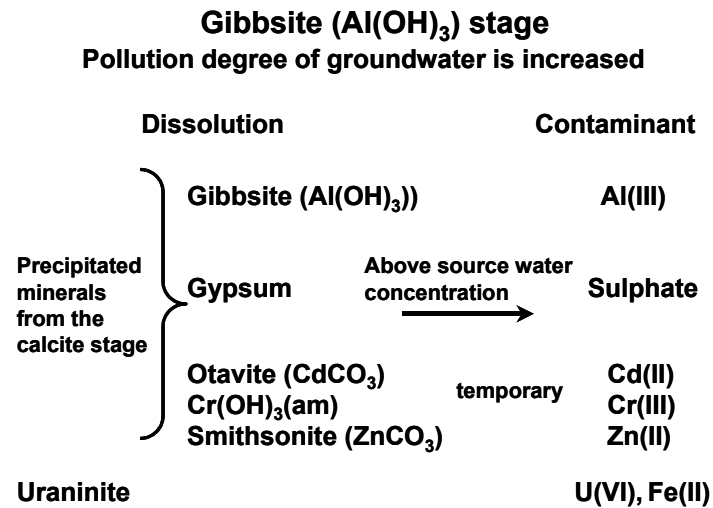
Fig. 43: Simulated concentrations of calcite, gibbsite, ferrihydrite and gypsum at the 1000 m observation point using RUMT3D (calcite scenario).

The different pH buffering stages (i.e., the calcite, gibbsite and ferrihydrite stages) have a controlling effect on the concentrations of the dissolved metals as well as sulphate. They all break through at the 1000 m observation point after about one pore volume, i.e., after about 5 years based on the hydraulic and geometric parameters in Table 12. The transport and attenuation of sulphate and metals in the calcite, gibbsite and ferrihydrite stages are illustrated in Fig. 44.

a)



b)



c)

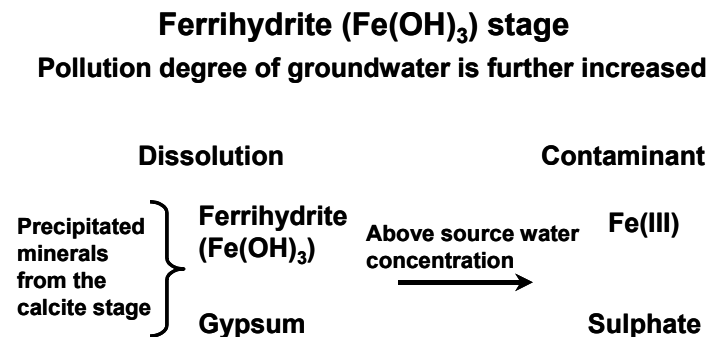
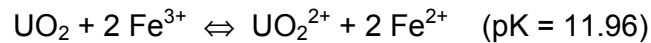


Fig. 44: Transport and attenuation of sulphate and metals in the calcite, gibbsite and ferrihydrite stages.

All dissolved metal concentrations, with the exception of dissolved ferrous iron and uranium decrease during the calcite stage. As not all of the ferric iron precipitates (as ferrihydrite, retardation factor is about 15, Fig. 43 and Fig. 45), it causes oxidative dissolution of uraninite close to the source. This occurs from an early time on and results in Fe(II) and U(VI) concentrations that are much higher than those in the source water. After about 5 years, the Fe (II) concentrations at the 1000 m observation point increase to  $2.76 \times 10^{-4} \text{ mol L}^{-1}$  compared to  $1.36 \times 10^{-4} \text{ mol L}^{-1}$  in the source water whereas U(VI) concentrations increase to  $2.5 \times 10^{-4} \text{ mol L}^{-1}$  compared to  $1.7 \times 10^{-7} \text{ mol L}^{-1}$  in the source water (Fig. 46 and Fig. 47). These increases persist until uraninite is depleted which is around 77 years. The oxidation and dissolution reaction of uraninite by ferric iron is described by Bain et al. (2001) as follows:



Fe(II) is only slightly attenuated by siderite precipitation during the calcite stage (Fig. 41) and U(IV) further decreases after calcite is depleted and completely diminishes after the depletion of uraninite (Fig. 41 and Fig. 48). The pe is mainly determined by the ratios of Fe(II)/Fe(III) and U(IV)/U(VI) (Fig. 49).

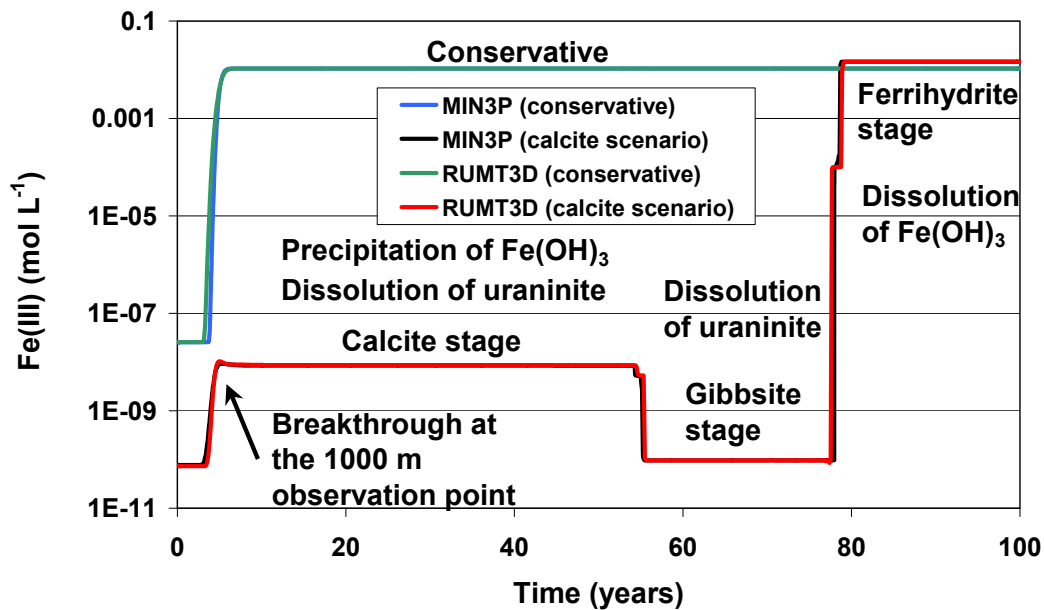


Fig. 45: Simulated Fe(III) concentrations at the 1000 m observation point for both, the MIN3P and RUMT3D models (conservative case and calcite scenario).

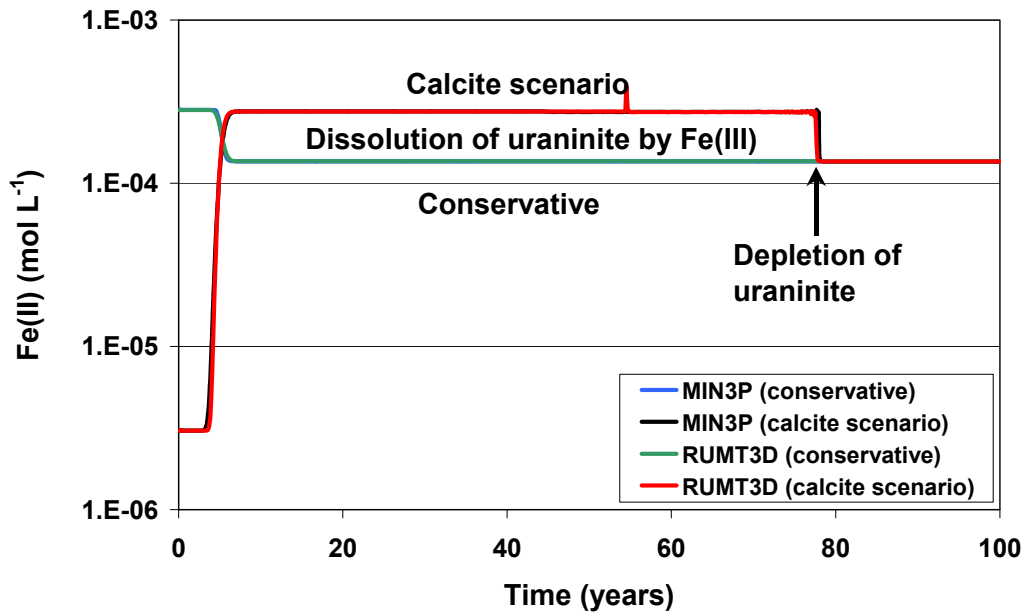


Fig. 46: Simulated Fe(II) concentrations at the 1000 m observation point for both, the MIN3P and RUMT3D models (conservative case and calcite scenario).

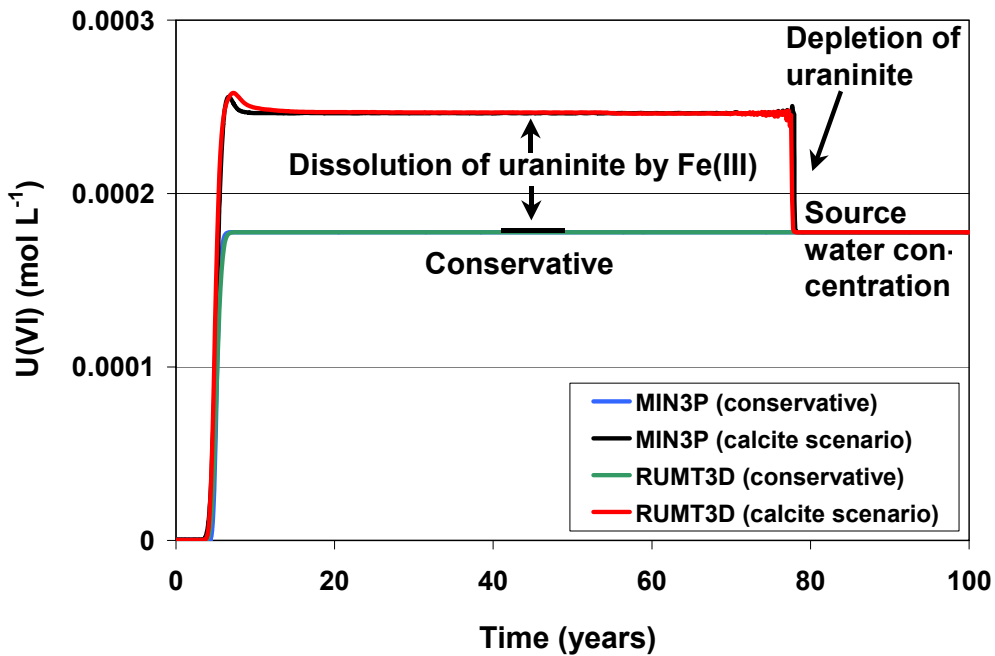


Fig. 47: Simulated U(VI) concentrations at the 1000 m observation point for both, the MIN3P and RUMT3D models (conservative case and calcite scenario).

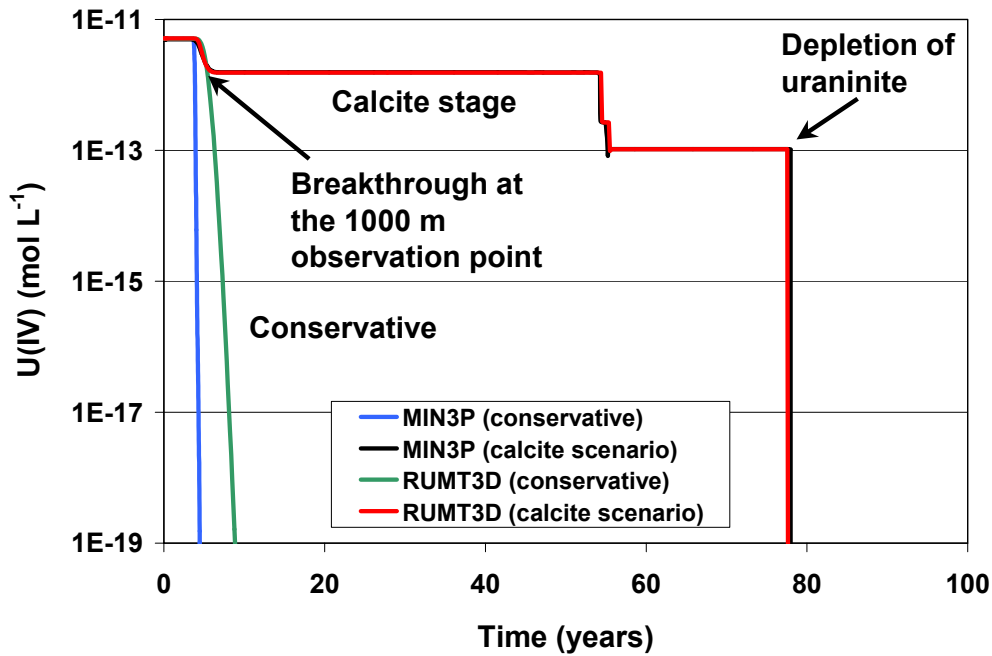


Fig. 48: Simulated U(IV) concentrations at the 1000 m observation point for both, the MIN3P and RUMT3D models (conservative case and calcite scenario).

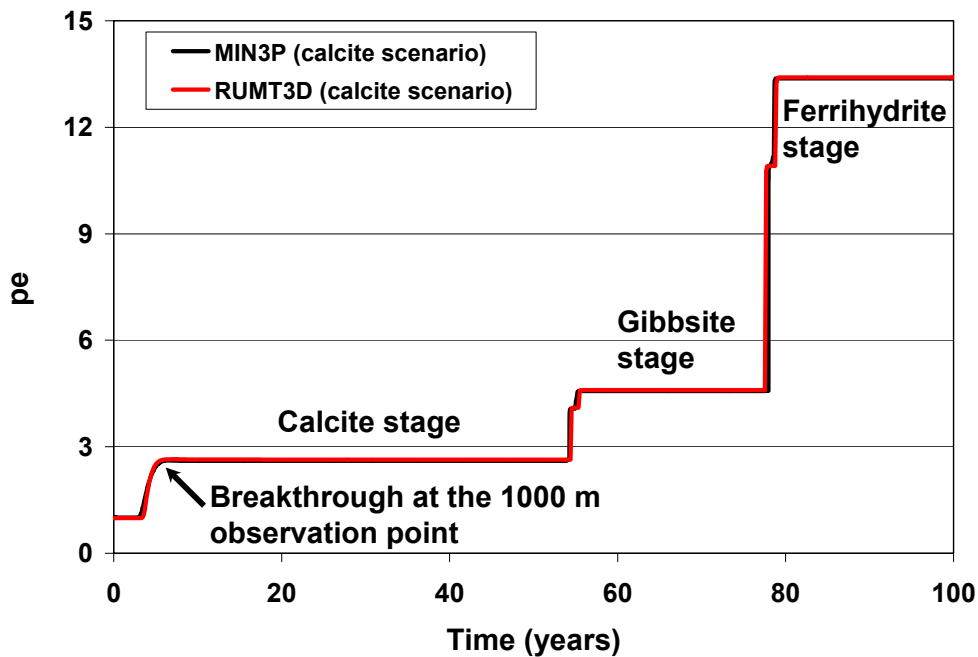


Fig. 49: Simulated pe at the 1000 m observation point for both, the MIN3P and RUMT3D models (conservative case and calcite scenario).

During the calcite stage, dissolved sulphate concentrations in the source water are decreased by gypsum ( $\text{CaSO}_4 \cdot 2\text{H}_2\text{O}$ ) precipitation. As the attenuation of sulphate is controlled by the availability of calcium (Fig. 50) and the high solubility of gypsum, sulphate is only removed from the source water by a factor of about 11. As soon as calcite is exhausted at a particular location, gypsum dissolves as a result of the lower calcium concentrations in the source water. This raises the sulphate concentration in the aquifer water to values above the source water concentration (see Fig. 51). Similar to calcium, carbonate increases during the calcite stage. After this stage, its concentration reduces to the concentration of the source water (Fig. 52).

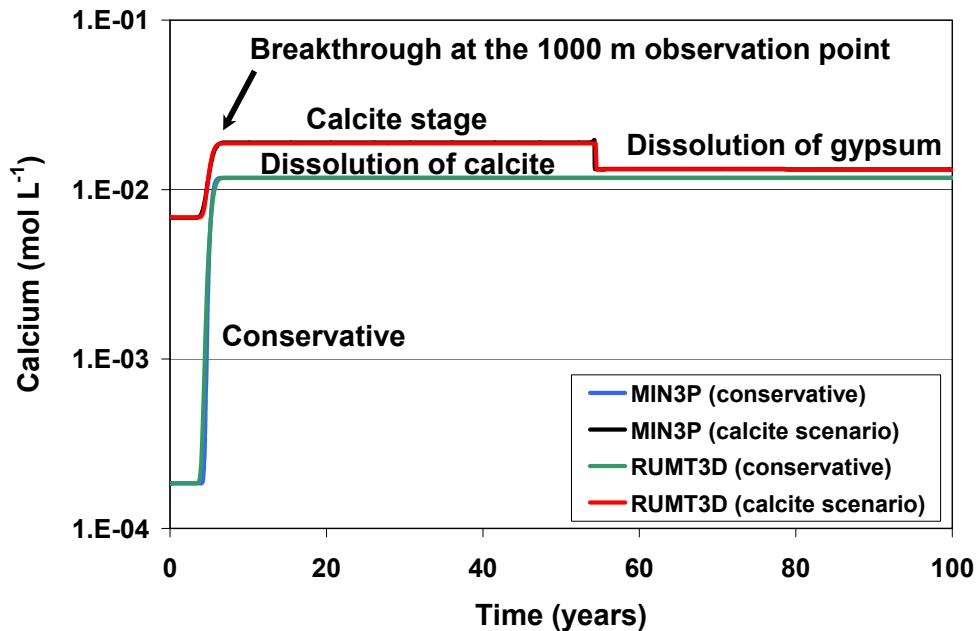


Fig. 50: Simulated calcium concentrations at the 1000 m observation point for both, the MIN3P and RUMT3D models (conservative case and calcite scenario).

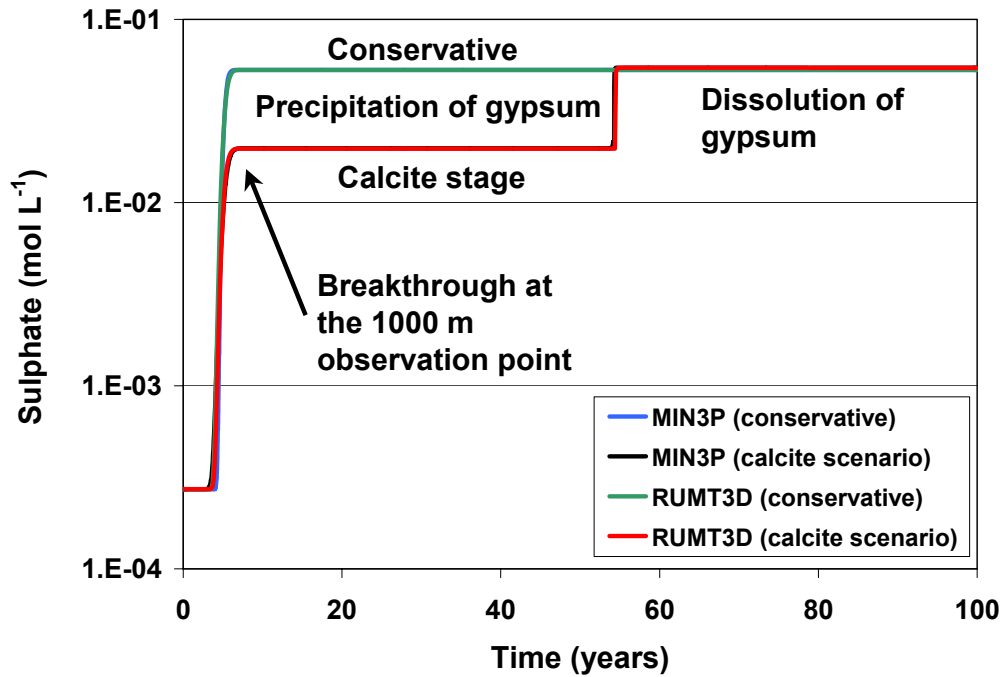


Fig. 51: Simulated sulphate at the 1000 m observation point for both, the MIN3P and RUMT3D models (conservative case and calcite scenario).

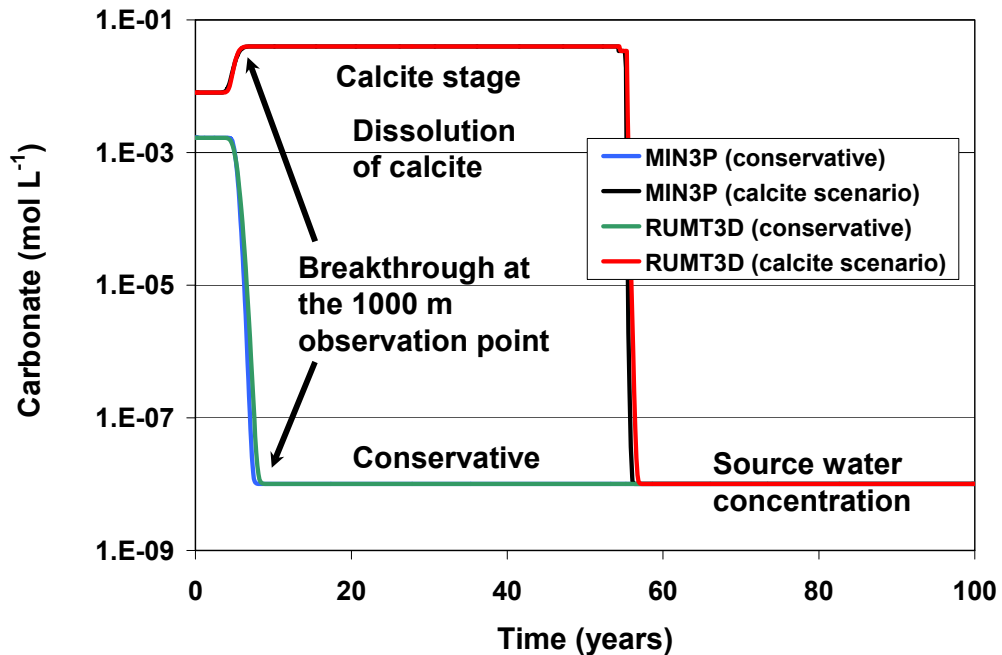


Fig. 52: Simulated carbonate concentrations at the 1000 m observation point for both, the MIN3P and RUMT3D models (conservative case and calcite scenario).

The pH also controls the mobility of heavy metals such as Cd(II), Cr(III) and Zn(II). Therefore, calcite is a key factor for the evolution of the water's hydrochemistry that discharges to the Elbe River. Generally, at pH values greater than 5, existing, for example, under calcite-buffering conditions, heavy metals are immobile and the respective minerals for example otavite,  $\text{Cr}(\text{OH})_3$  and smithsonite precipitate (Fig. 53). Those precipitates represent sinks for dissolved Cd(II), Cr(III) and Zn(II) (retardation factor is about 11). After calcite is depleted, the pH decreases, triggering the subsequent dissolution of otavite,  $\text{Cr}(\text{OH})_3$  and smithsonite. As a consequence of their dissolution, Cd(II), Cr(III) and Zn(II) are released into the pore water (Fig. 54, Fig. 55 and Fig. 56) and concentrations increase sharply, with maximum values occurring at the mineral dissolution fronts. The dissolution buffers the pH between 4 and 6, but only for a relatively short period of time (about 1 year, Fig. 42).

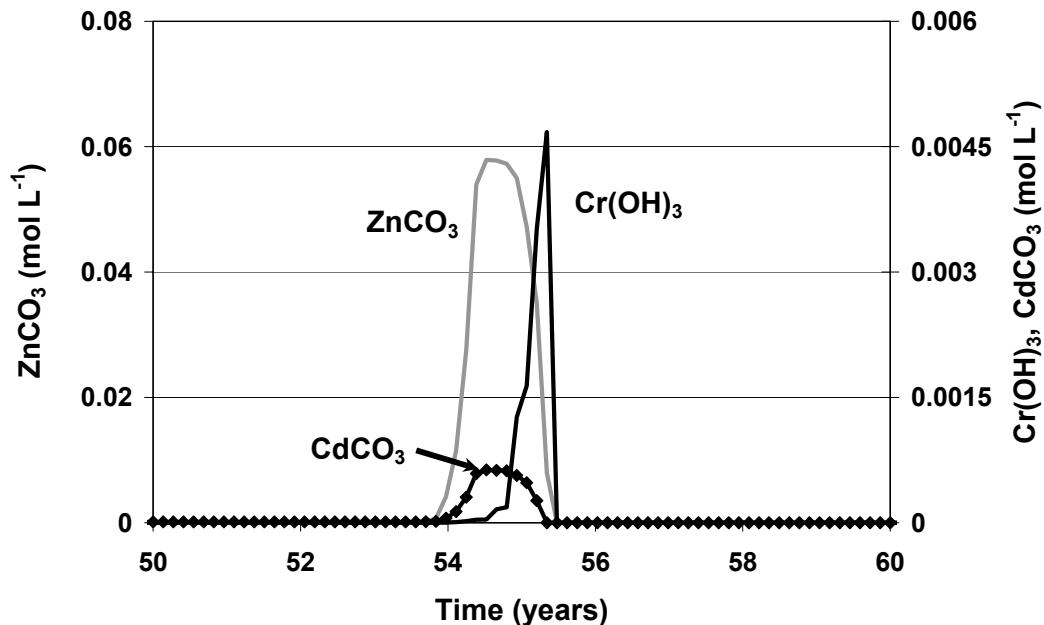


Fig. 53: Simulated otavite,  $\text{Cr}(\text{OH})_3$  and smithsonite concentrations at the 1000 m observation point for both, the MIN3P and RUMT3D models (conservative case and calcite scenario).

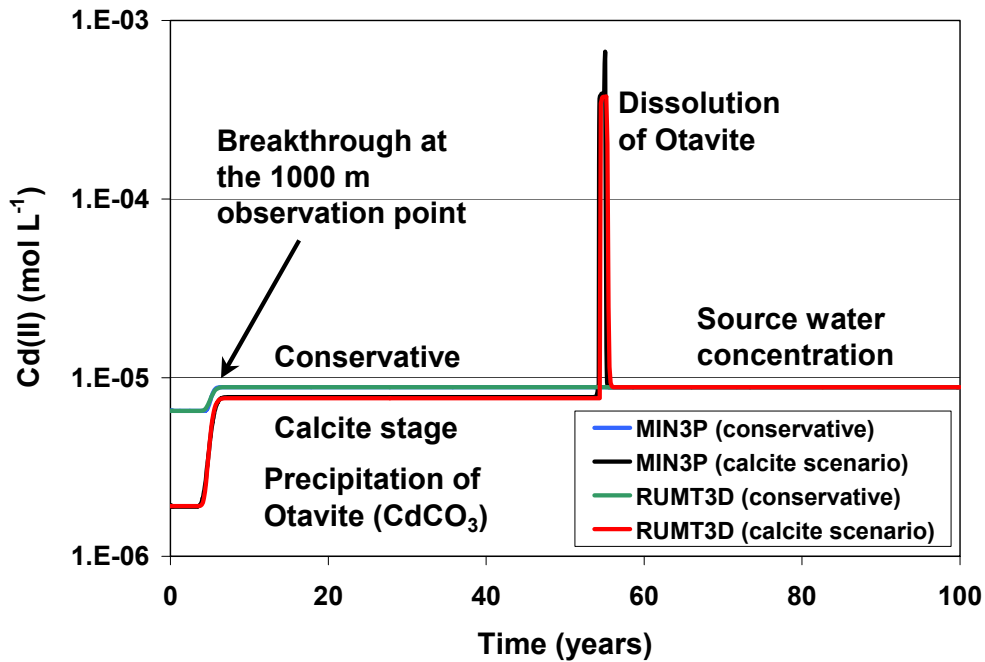


Fig. 54: Simulated Cd(II) concentrations at the 1000 m observation point for both, the MIN3P and RUMT3D models (conservative case and calcite scenario).

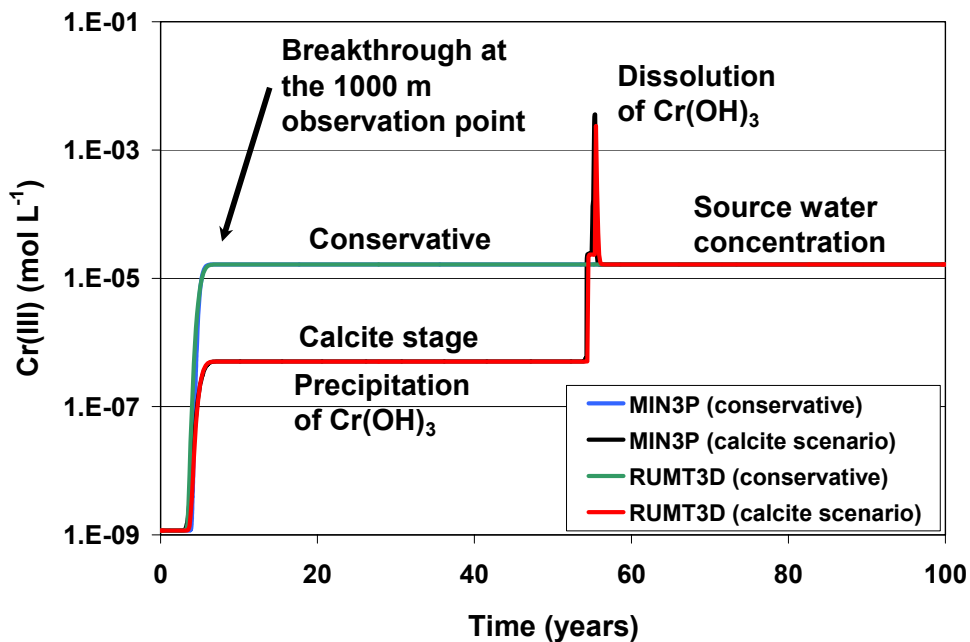


Fig. 55: Simulated Cr(III) concentrations at the 1000 m observation point for both, the MIN3P and RUMT3D models (conservative case and calcite scenario).

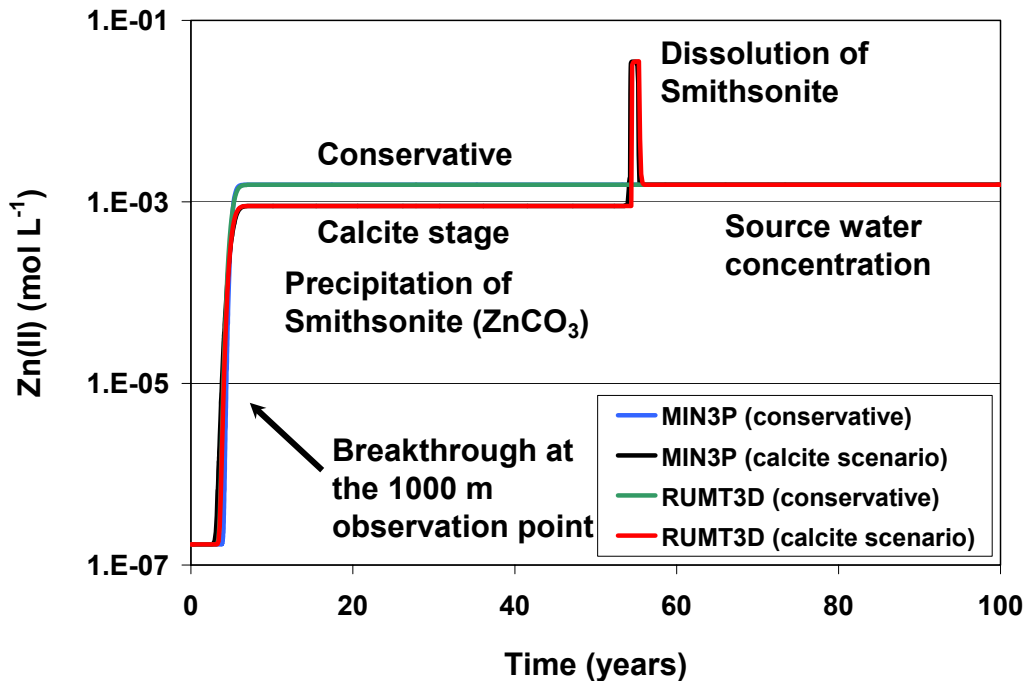


Fig. 56: Simulated Zn(II) concentrations at the 1000 m observation point for both, the MIN3P and RUMT3D models (conservative case and calcite scenario).

During the gibbsite and ferrihydrite stages, despite the fact that the dissolution of gibbsite and ferrihydrite consumes protons,  $\text{Al}^{3+}$  and  $\text{Fe}^{2+}$  are released. Thus, during the stages when these minerals are dissolving at a particular location, the aquifer is polluted with these metals at concentrations above the ones in the source water (Fig. 57 and Fig. 45).

In the model, amorphous silica ( $\text{am-SiO}_2$ ) is assumed to be present in infinite supply (Fig. 58), reflecting that the aquifer mainly consists of quartz-sandstone. This, however, has little effect upon the degree to which the groundwater becomes contaminated with metals (Fig. 59).

Chloride, fluoride, phosphorus and the metals lead, magnesium, nickel, sodium are transported conservatively (i.e., with source water concentrations) in the calcite scenario (Fig. 65 - Fig. 71 in the appendix). Since the dissolved fluoride concentration is initially higher in the pore water than in the source water, a decrease of fluoride occurs at the 1000 m observation point after the first pore flush, as can be seen in Fig. 66. Potassium precipitates almost completely (to a concentration of  $2.63 \times 10^{-11}$  mol L<sup>-1</sup>, Fig. 60) near the source location in form of jarosite-K. Cu does not undergo any reaction in the simulations because no potential Cu-bearing mineral phases were considered in the simulations.

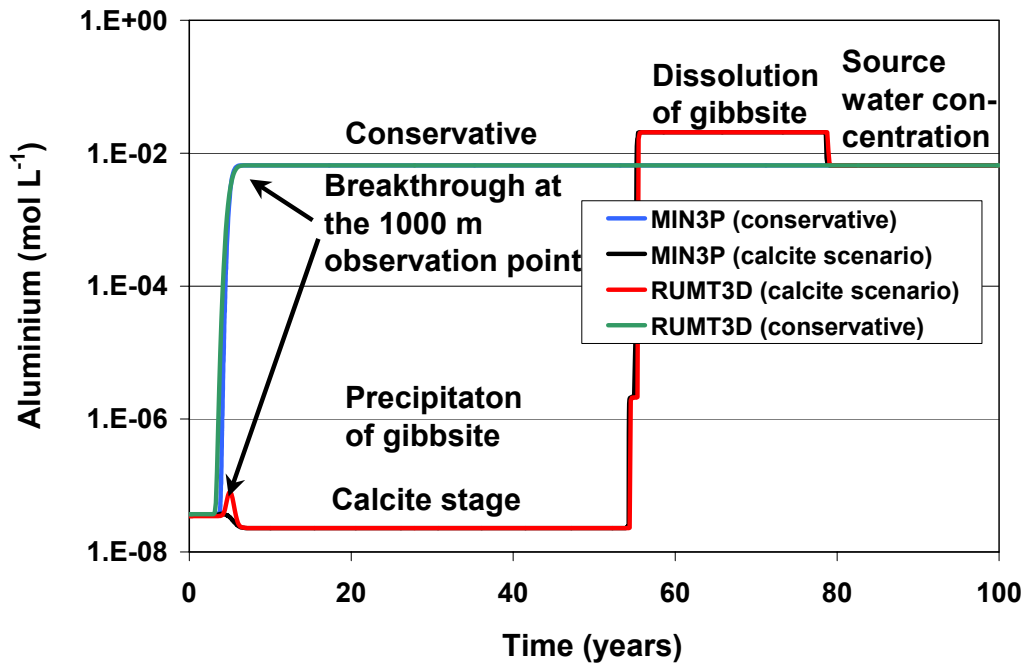


Fig. 57: Simulated aluminium concentrations at the 1000 m observation point for both, the MIN3P and RUMT3D models (conservative case and calcite scenario).

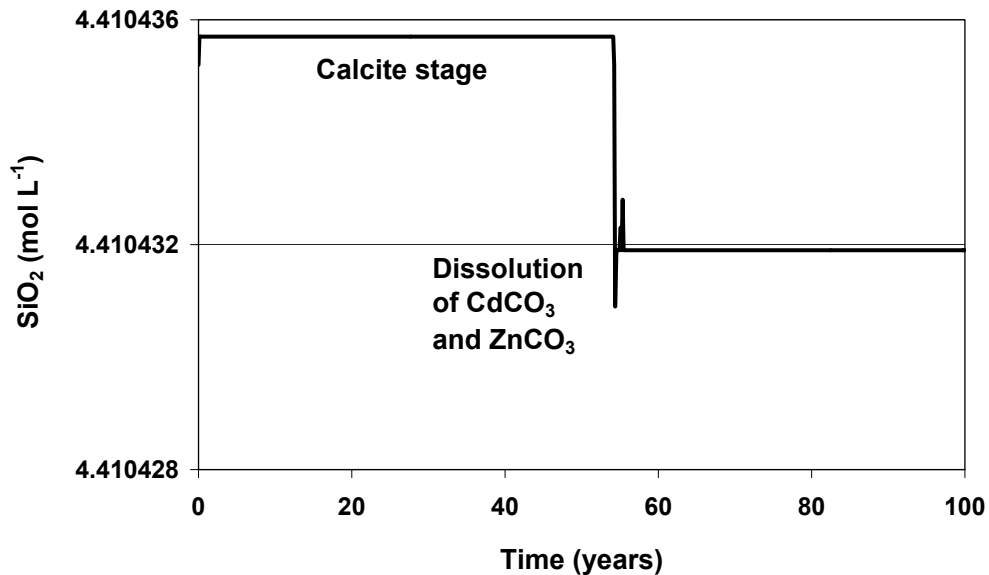


Fig. 58: Simulated SiO<sub>2</sub> concentrations at the 1000 m observation point for both, the MIN3P and RUMT3D models (conservative case and calcite scenario).

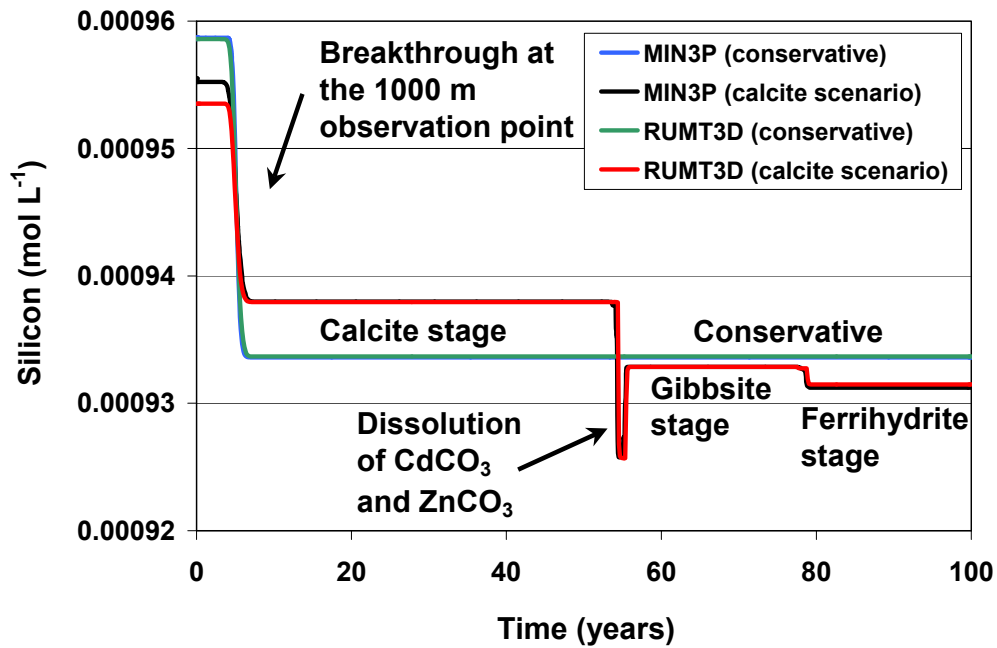


Fig. 59: Simulated silicon concentrations at the 1000 m observation point for both, the MIN3P and RUMT3D models (conservative case and calcite scenario).

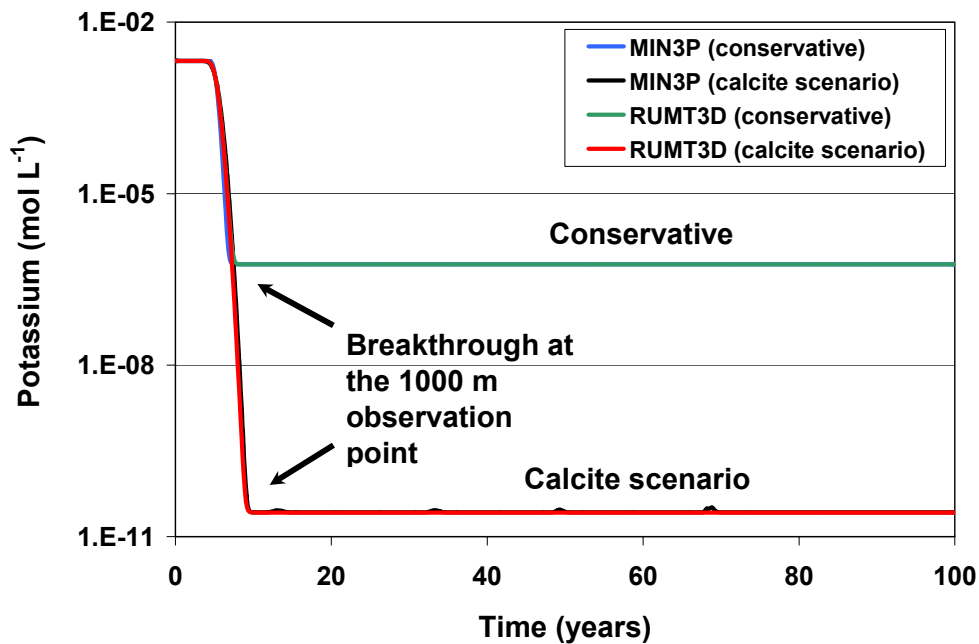


Fig. 60: Simulated potassium concentrations at the 1000 m observation point for both, the MIN3P and RUMT3D models (conservative case and calcite scenario).

WISMUT defined the Ra-barite mineral as the only potential source or sink for dissolved radium. Since the source water is supersaturated with respect to Ra-barite and because the aquifer is in equilibrium with respect to barite from the beginning of the simulation, barium and radium are nearly transported conservatively, in particular radium (compare Fig. 61 and Fig. 62). Barium remains only slightly above source concentration during the calcite stage. During the subsequent stages, it is slightly reduced to values below source concentration.

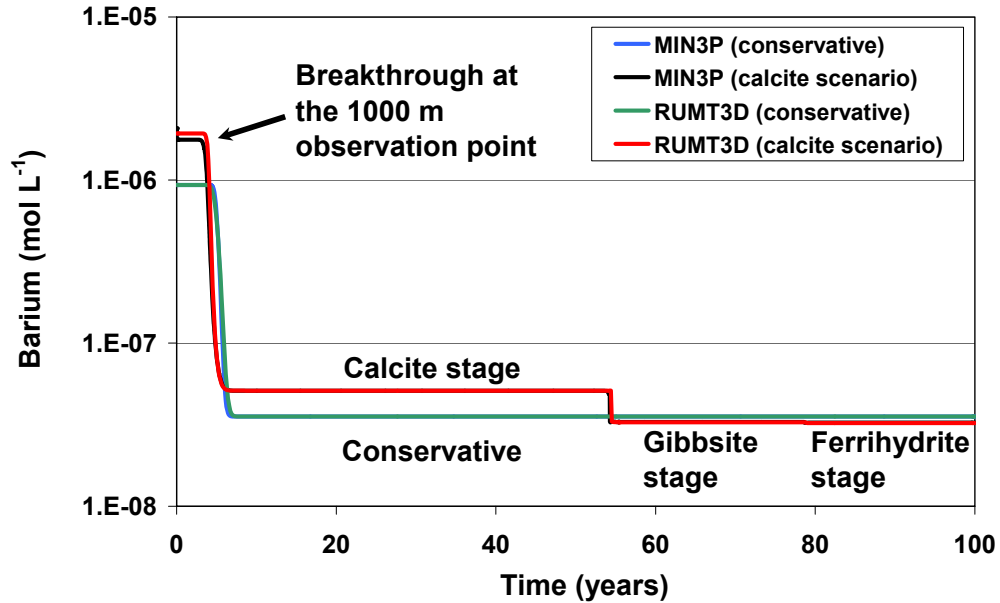


Fig. 61: Simulated barium concentrations at the 1000 m observation point for both, the MIN3P and RUMT3D models (conservative case and calcite scenario).

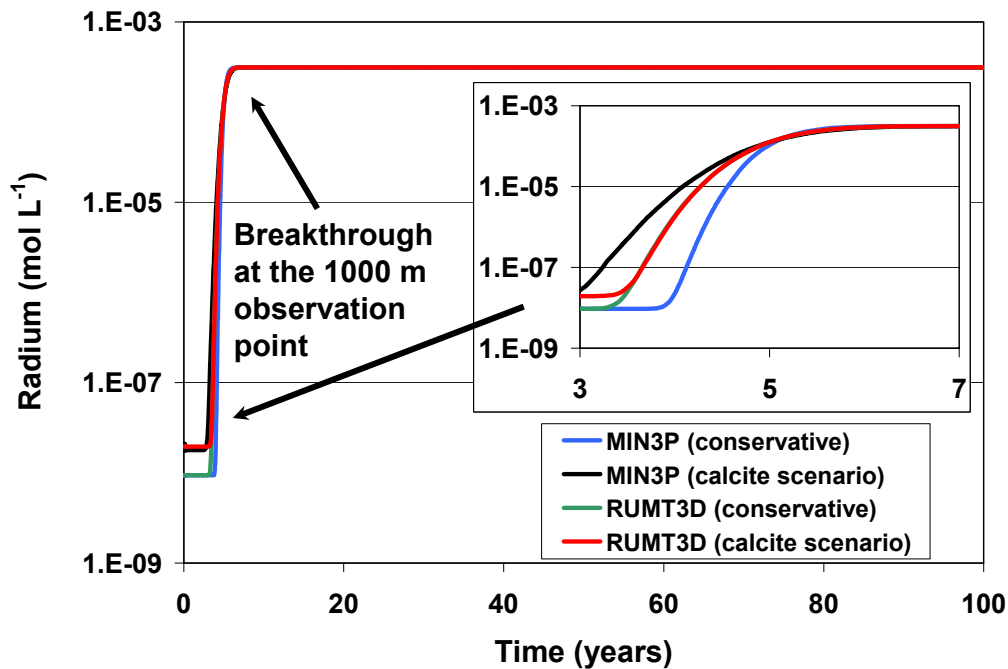


Fig. 62: Simulated radium concentrations at the 1000 m observation point for both, the MIN3P and RUMT3D models (conservative case and calcite scenario).

### 6.2.5 Accuracy of the Simulation Results

For the simulation of the calcite scenario, the most critical master species for achieving accurate results were the ones representing uranium (U(VI)) and iron (Fe(II), Fe(III)) species. Fig. 63 displays simulated U(VI) breakthrough curves (BTC's) using RUMT3D and a reaction time step size of 5 days and

1. a spatial discretisation of 5 m and a dispersivity of 5 m,
2. a spatial discretisation of 2.5 m and a dispersivity of 2.5 m,
3. a spatial discretisation of 2.5 m and a dispersivity of 5 m.

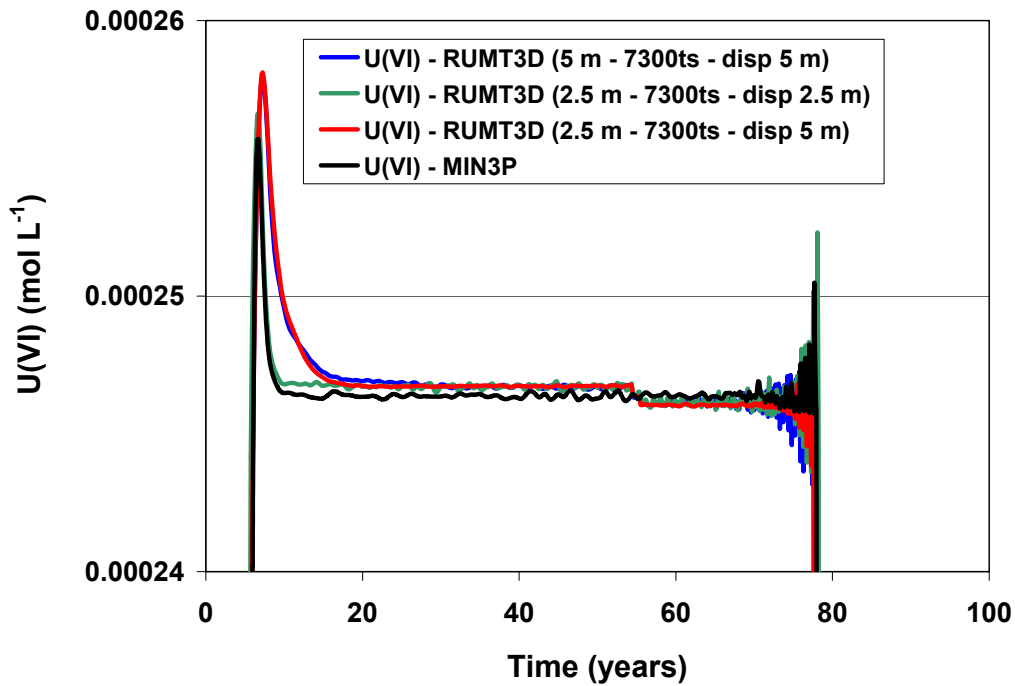


Fig. 63: Comparison of simulated U(VI) concentrations of the calcite scenario with the RUMT3D and MIN3P models. 5 m and 2.5 m represent a spatial discretisation of 5 m and 2.5 m per cell, 7300ts refers to a reaction time step size of 5 days and disp denotes dispersivity.

For each of the simulated breakthrough curves in Fig. 63, the TVD solver for advective transport and the following two iteration options for the PHREEQC-2 model were utilised:

- a maximum step size for the multiplicative change in the activity of an aqueous species on each iteration (`step_size`) of 2 and
- a maximum step size for the activity of the electron (`pe_step_size`) of 2.

As shown in Fig. 63, fewer oscillations occur when using a dispersivity of 5 m for both discretisations (2.5 m and 5 m per cell). However, the inaccuracy is somewhat higher compared to the case of a dispersivity of 5 m in combination with a spatial discretisation of 2.5 m. With a spatial discretisation of 2.5 m per cell and a dispersivity of 2.5 m, oscillations were more significant at around 77 years. The simulated U(VI) BTC's with RUMT3D in Fig. 63 are also compared to the U(VI) BTC using MIN3P. The U(VI) BTC using MIN3P shows small oscillations as well comparable to the ones with a discretisation of 2.5 m per cell and a dispersivity of 2.5 m.

Results with some numerical problems but with a significantly reduced simulation time (Fig. 64) can be achieved with

- a spatial discretisation of 10 m per cell,
- a reaction time step size of 36.5 days,

- a dispersivity of 2.5 m,
- default iteration options for the PHREEQC-2 model (e.g., `step_size` of 100 and `pe_step_size` of 10) and
- the MMOC (Modified Method of Characteristics) solver for advective transport.

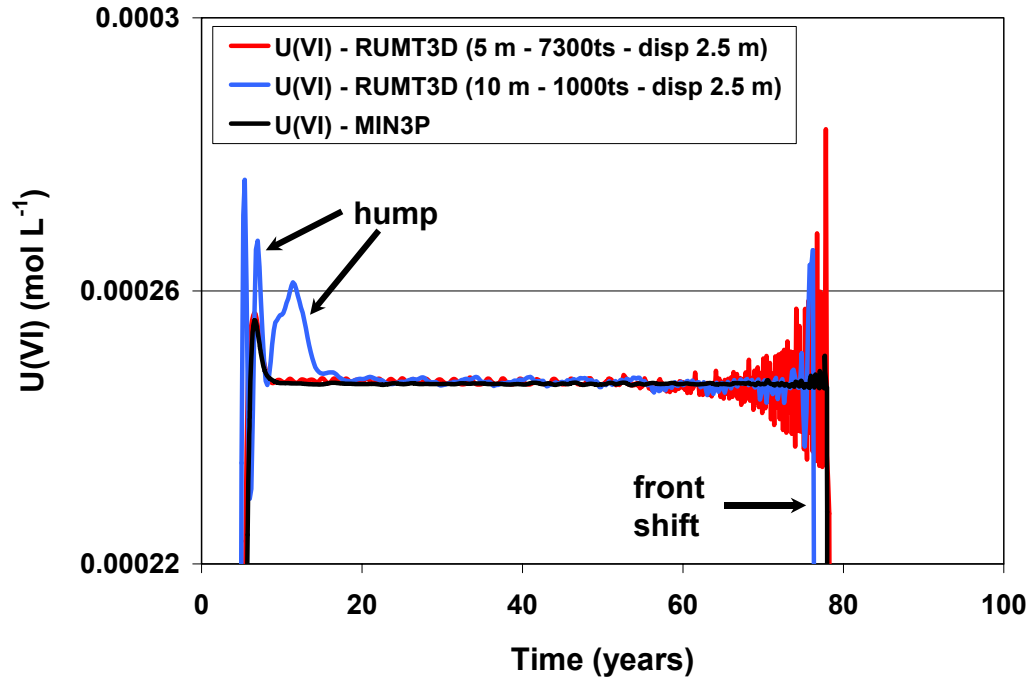


Fig. 64: Comparison of simulated U(VI) concentrations of the calcite scenario with the RUMT3D and MIN3P models. A spatial discretisation of 5 and 10 m per cell and a reaction time step size of 5 and 36.5 m are used in the RUMT3D model, respectively.

The numerical problems occur in particular in the U(VI) and Fe(III) BTC's (Fig. 64) in form of

- numerical oscillations in the gibbsite stage,
- front shift caused by earlier exhaustion of uraninite at around 77 years and
- hump after breakthrough (see Fig. 64 for U(VI)).

Also, in the Fe(II) concentration BTC are oscillations in the gibbsite stage and a front shift. For this model setup, the Courant number plays a role. Without a dispersivity, a Courant number of 0.6 and with a dispersivity of 2.5 m, a Courant number of greater than 0.64 can be used.

## 6.2.6 Summary

In this section, RUMT3D was verified with a simulation problem, i.e., the conservative and the calcite scenario as developed and discussed by Bain et al. (2001). The calcite scenario required the simulation of a large number of aqueous species, including dissolved metals and radionuclides and the quantification of how their mobility would be affected by mineral dissolution/precipitation reactions. The results of RUMT3D for both scenarios were compared with the results of Bain et al. (2001), who used the MIN3P model for their simulations.

The simulation problem clearly demonstrates that buffering minerals (e.g., carbonates, aluminium and ferric iron hydroxides) and redox buffering minerals (sulphides, certain carbonates and hydroxides) substantially influence the pH and pe of the aquifer and therefore the presence of dissolved metal contaminants (e.g., Al(III), Cd(II), Cr(III), Fe(II), Fe(III), Ni(II), Pb(II), Zn(II)), U(VI) and sulphate in the pore water. Bain et al. (2001) also concluded that for reactive transport modelling studies such as the one discussed here, it is essential to know

- which minerals are present in aquifer,
- in which quantity,
- which minerals precipitate and
- presence of oxidising master species (e.g., ferric iron) during the course of a simulation.

They as well acknowledge that an incorrect conceptual model or incorrect assumptions for the initial conditions can easily lead to erroneous results. In such cases, the predicted concentrations of dissolved constituents may differ significantly from reality. Apart from gibbsite and ferrihydrite, for instance, other Al(III)- and Fe(III)-bearing phases such as am-Al(OH)<sub>3</sub> or goethite (FeOOH) may form in the aquifer. These minerals were however not considered in the simulations. Depending upon the concentrations of Al(III) and Fe(III) and the solubility of other Al(III)- and Fe(III)-bearing phases, the mobility of Al(III) and Fe(III) might vary from the ones in this study. Further, the high velocity in the aquifer (*Short Section*) and also the relatively insoluble minerals, such as sulphides, may promote non-equilibrium.

A good agreement of results between the RUMT3D and MIN3P models was obtained for both the conservative and the calcite scenario. Minor deviations between the simulated breakthrough curves were only found to occur at the discharge point to the Elbe River. It is thought that those deviations are most likely caused by the different approaches on how charge balance errors were handled in the RUMT3D model compared to MIN3P.

It may be worthwhile to also find a more appropriate setup of the calcite scenario without a dispersivity. Further, it is suggested with regards to a hybrid system, to investigate potential rapid transport of the different master species, caused by the introduction of a conduit system. More interesting would be to extend the 1D to a 2D model and introduce a more complex conduit system.

*Religion is always right. Religion solves every problem and thereby abolishes problems from the universe. ... Science is the very opposite. Science is always wrong. It never solves a problem without raising ten more problems.*

*George Bernard Shaw, in an after dinner toast to Albert Einstein, (Oct. 27, 1930)*

## Chapter

### 7 Recommendations

To analyse and assess factors such as the impact of contamination and the efficacy of remediation techniques in existing hybrid systems, respectively it is recommended

1. to test RUMT3D for the inclusion of kinetically controlled intra-aqueous reactions,
2. to consider geochemical reactions in the conduit system,
3. to include heterogeneous surface reactions (in particular adsorption / desorption, ion exchange and surface complexation reactions),
4. to regard rate limiting dissolution-precipitation reactions,
5. to numerically optimise the code,
6. to consider colloidal transport,
7. to study more than 1D problems and
8. to examine importance of the different physical and geochemical parameters, boundary conditions and other influences in hybrid systems by systematically varying these parameters (sensitivity studies).

Parameters like hydraulic conductivity, exchange coefficients, pH, chemical components (species, complexes, mineral phases) and redox potential and conditions like recharge rate and model geometry (continuum and conduit system) can be varied. Moreover, it would be interesting to investigate for which cases, it is sufficient to only consider instantaneous mixing in the conduit system during a simulation. It is likely that transport in the conduit system is negligible for long term events. Reactive barriers could also be introduced in the conduit system to study whether they have any effect in remediation strategies. Further recommendations in respect to the simulated benchmark problems are given in the subsections on summary (Chapters 5.4 and 6.2.6). The first six recommendations are discussed in more detail in the following subsections.

#### 7.1 Kinetically Controlled Intra-Aqueous Reactions

RUMT3D retains the option to include BASIC subroutines into the PHREEQC-2 database as in the original PHREEQC-2, to consider kinetically controlled intra-aqueous reactions during a simulation. Kinetically controlled rate equations from the laboratory can thereby directly be implemented into the PHREEQC-2

database, which can be different for each simulation. This provides an advantage for the users of not having to deal with modifications of the original code of RUMT3D.

## 7.2 Geochemical Reactions in the Conduit System

The assumption of a negligible effect of geochemical reactions in the conduit system due to much shorter residence times of the components/master species in the conduit system than in the continuum may require further investigation. Under certain conditions as solution of different composition is entering the conduit system, aqueous species may be precipitated upon the walls of the conduits or dissolved from the walls into the aqueous phase. In some cases, the precipitated mineral phases attached to the walls of the conduit system, may be very unstable, i.e., they may readily dissolve. While minerals precipitate/dissolve, the pH and the pe (if redox species are included in a simulation) as well as concentrations of the associated changes in dissolved constituents. Therefore, geochemical reactions may also play an important role in the conduit system not only in adjacent continuum on the degree of contamination. It is recommended to investigate their influence by sensitivity studies once the PHREEQC-2 module can as well be used for the conduit system.

## 7.3 Heterogeneous Surface Reactions

Surface reactions on aquifer material such as adsorption/desorption, ion exchange or surface complexation can greatly influence the transport behaviour of dissolved species. Depending upon the nature of those species, surface reactions may need further consideration in reactive transport simulations. They may not only be of relevance in the continuum but also in the conduit system. Especially in attenuation studies, type and degree of surface reactions can play a significant role in attenuating contaminants. Also, certain factors such as the pH especially when the protons ( $H^+$ ) are exchanged or removed, may severely control some surface reactions.

Adsorption/desorption. Adsorption refers to a mass transfer process of contaminants by partitioning between different phases (e.g., between liquid-solid interfaces). Desorption is the reverse process of adsorption. Traditionally, adsorption has been grouped into two extremes, which are weak physi-sorption and strong chemi-sorption (i.e., specific adsorption). While physi-sorption is rapid and reversible, chemi-sorption is likely to be slow, and less readily reversible. In case of a chemi-sorption, the adsorbate is strongly bonded to the adsorbent, which often change characters of both the surface and the adsorbed contaminants (Atkins 1998; Licha 2003).

When considering transport, it is generally postulated that the aqueous-phase concentration and the adsorbed solid-phase concentration are always in equilibrium. Further, it is assumed that this type of reaction can nearly always be treated as instantaneous by being fast enough compared to the groundwater velocity. Under these conditions, the functional relationship between dissolved and adsorbed concentrations can be expressed by an adsorption isotherm

(commonly with the Henry, Freundlich, Langmuir adsorption isotherms, Zheng 1990). Each of these adsorption isotherms offers a convenient way for fitting quantitative descriptions of surface partitioning behaviour to experimental data (McNab 2001). Especially, with the usage of the Henry adsorption isotherm, direct proportionality between the adsorbed and dissolved concentration is assumed by means of a so-called distribution coefficient ( $K_d$ ). This adsorption isotherm basically assumes an unspecific distribution/adsorption between the phases. With the Freundlich and Langmuir adsorption isotherms, non-linearity in the adsorption process can be described. Due to its empirical nature, the Freundlich isotherm is solely applicable to physi-sorption and considers multi-layer coverage. The Langmuir adsorption isotherm, however, considers saturation of a finite number of adsorption sites on a mineral surface (McNab 2001) leading to a mono-layer coverage and can therefore only be used to describe chemi-sorption effects. By using a retardation factor ( $R$ ) in the transport equation, all adsorption isotherms are incorporated into transport models. Within RUMT3D, these adsorption isotherms may be used in the continuum by activating these in the transport model MT3DMS. Contaminants that may adsorb very specifically (expressed in step like isotherms) cannot be considered within RUMT3D, yet. For these processes, the incorporation of specific interactions is then necessary.

*Ion exchange and surface complexation.* Ion exchange and surface complexation may also be important processes under certain conditions. These two surface reactions cannot be described with a retardation factor in the transport equation but need to be treated in the form of a sink term. They follow very specific laws and thus are not based upon empirical relationships like the adsorption isotherms.

Ion exchange refers to the exchange of ions from the surface of the mineral lattice and from the aqueous solution (Novotny & Olem 1994). Similar to speciation and precipitation/dissolution reactions, ion exchange reactions are also described by means of mass action expressions. As such, it is postulated that there are a number of exchange sites ( $X$ ) associated with the solid phase and that the exchangeability between different ions can be characterised by an equilibrium constant (McNab 2001).

Complexation is generally defined as any combination of dissolved cations with molecules or anions containing free pairs of electrons. The complexation of dissolved cations with molecules or anions upon mineral surfaces is referred to surface complexation. Iron(III) oxides are one example, which offer, charged surfaces for complexation. Such oxides can play an important role for the mobility of many contaminants (e.g., uranium) and thus need consideration.

The PHREEQC-2 model within RUMT3D offers the option to include ion exchange as well as surface complexation reactions. Ion-exchange reactions can be simulated with the Gaines-Thomas convention theory using the equilibrium constants by Appelo & Postma (1993). Models like the generalized two-layer model by Dzombak & Morel (1990), the explicitly calculated diffuse layer by Borkovec & Westall (1983) and the non-electrostatic model by Davis & Kent (1990) may be utilised to consider surface-complexation reactions within PHREEQC-2 (compare Chapter 2.5.1). For the simulation of complexation to

charged surfaces, it would be worthwhile to activate these models as well within RUMT3D.

#### 7.4 Rate Limiting Dissolution-Precipitation Reactions

As discussed in Chapter 2.4.2, dissolution-precipitation reactions can display kinetic limitations in groundwater systems. Based on the rate limiting process of a dissolution-precipitation reaction, Berner (1978), Murphy et al. (1989), Steefel & Lasaga (1994) and Mayer (1999), for example, classified dissolution-precipitation reactions as “surface-controlled” or “diffusion-controlled” reactions. If the reaction progress is rather limited by the actual chemical reaction on the mineral surface, the dissolution-precipitation reaction can be expressed as a surface-controlled reaction. Alternatively, if the reaction progress is pretty much restricted by microscale transport processes involving reactant or product species, the dissolution-precipitation reaction can be formulated as a diffusion-controlled reaction (Mayer 1999). Eckart (1988) indicated that reactions could be simplified as surface- and diffusion-controlled reactions depending upon the required time to follow different steps of a reaction. According to Pinder et al. (1982), there are 5 different steps for a heterogeneous reaction:

- a) diffusive transport of the reactants through the pores and through the immobile phase to the mineral surface
- b) adsorption onto the mineral surface
- c) reaction
- d) desorption
- e) diffusive reversal transport of the reaction products

If steps b), c) and d) require less time than the steps a) and e) the whole reaction is called diffusion or transport controlled reaction. Alternatively, if steps a) and e) require less time than steps b), c) and d), the reaction is called surface controlled. Often, however, the slowest step of the above mentioned steps controls the type of the whole reaction (Eckart 1988).

Specially, factors such as:

- temporal scales of the various transport and reaction processes,
- chemical composition of the water and solid phase,
- effective surface area of the solid phase for interaction,
- thickness of the diffusive layer on the surface of the solid phase,
- surface coating,
- the activities or concentrations of dissolved reactant and product species

determine type of kinetic controlled reaction during the course of a reactive transport simulation.

It is worthwhile to note that at some point a surface-controlled reaction may turn to a diffusion-controlled reaction if outer layers of the minerals are removed and or if during the process, pores become partially clogged up with the reaction

products (for example with  $\text{CaSO}_4$ , Eckart 1988).

In analogy to kinetically controlled intra-aqueous reactions, a general rate expression for surface-controlled dissolution-precipitation reactions can be derived (see Mayer 1999). This one can then be implemented into the PHREEQC-2 database to be considered within a simulation using RUMT3D. Sonnefeld, pers. comm. (2003), e.g., is planning to develop an algorithm to describe the surface-controlled release of uranium. On the basis of laboratory experiments, the characteristic parameters for that process will be determined. The experiments will thereby be performed under conditions close to reality in the presence of relevant ions that cause complexation. Nonlinear regression will presumably be necessary to develop the algorithm from the obtained data. Diffusion-controlled release of contaminants from mineral phases needs special treatment, such as in form of a shrinking core approach similar to that of Levenspiel (1972). This approach was used in models by Davis & Ritchie (1986); Wunderly et al. (1996); Gerke et al. (1998) and Mayer (1999). It can be added to RUMT3D as an additional module. Alternatively, a mobile-immobile concept can be utilised to simulate surface as well as diffusion controlled dissolution/precipitation reactions. In this concept, surface controlled reaction is considered as phase transition from the solid to the mobile phase and diffusion controlled from the solid to the immobile phase. The diffusive exchange to the reaction front can be accomplished by integrating a transient diffusion term. Eckart (1988) used a similar approach in his model. Another alternative to simultaneously simulate both reaction processes is to adopt a "mixed reaction control" approach as suggested, e.g., by Stone & Morgan (1990) or Steefel & Lasaga (1994) (Mayer 1999).

## 7.5 Numerical Optimisation

Coupled reactive transport models like RUMT3D are usually computationally highly intensive and thus demand lots of computer time and memory (compare Chapters 2.4.3 and 2.4.4). The computer times are controlled by finding an iterative solution for (i) the coupled transport systems (continuum and conduit) and (ii) the reactions, in particular for small spatial discretisation and small time steps. Small spatial and also small time discretisation are especially required for systems, which exhibit significant spatial (physical) and geochemical variabilities. The spatial and geochemical variabilities are often referred to heterogeneities in geological environments. Yucca Mountain, Nevada, USA, for example, which has been selected as a possible site for the first high level radioactive waste repository in the United States, is a site that exhibits significant spatial variability. Yet, scientifically rigorous estimations of radionuclide migration for the event of a repository breach are needed (Viswanathan 1999) since it has to be proven that such a repository will isolate waste for at least 10,000 years. As a result, the probability of radionuclide release into the groundwater and also atmosphere must be estimated. In other words, the complex flow and transport of contaminants must be modelled for at least 10,000 years using presumably primarily three-dimensional models and small grid spacing due to the heterogeneities in the model domain (Viswanathan 1996). Moreover, problematic geochemical reactions often demand the transport of numerous (reacting)

chemical components, which result in a system of many coupled partial differential equations. Thus, especially when RUMT3D is considered as a model for large problems with numerous components and significant heterogeneities, it is worthwhile to numerically optimise RUMT3D.

To achieve numerical optimisation of RUMT3D, it is suggested to use different strategies such as to introduce criteria for (i) global estimation of the reaction time step sizes of the two-step method (operator-split technique), (ii) temporal elimination of the reaction time steps in cells where negligible geochemical activities occur and (iii) sub-cycling of slow processes. The basic idea behind these strategies is to minimise calls to the reaction module. Moreover, adaptive time step control strategies could be developed which consider steep geochemical gradients and stiff systems. Besides, it was observed by using the PHT3D model that an optimal coding of the kinetic reaction equations in the PHREEQC-2 database by means of BASIC subroutines could significantly reduce computer time. The first four options for numerical optimisation are discussed in more details further below.

The temporal discretisation of the two-step method in RUMT3D (modified version of SNIA, Chapter 3.3) for the reaction package is currently determined by user defined limits. The user needs to estimate a temporal discretisation prior to a simulation to produce an acceptable splitting error for the chosen problem. A negligible or acceptable splitting error is given when the simulation results are almost independent from the temporal discretisation. Since it is difficult to find a user defined "optimal", i.e., an efficient temporal discretisation, it is advisable to develop a modified two-step method in RUMT3D. This can be achieved by introducing new criteria that determine on a global scale under which condition the calculation of the geochemical reactions is less or more frequently required. It is not necessary to perform a reaction time step after each transport time step in RUMT3D. The transport time step size in RUMT3D is dependent on mainly the highest flow velocity in the conduit system and is therefore relatively small. The simulation of chemical kinetics does not usually require such short time steps. Consequently, the introduction of a SIA method would enhance the simulation time. The objective of a new or further modified SNIA method in RUMT3D is basically to find an adaptive adjustment of the two-step method step size to reach an acceptable splitting error by means of criteria in accordance to for instance the Damköhler Number and or the time step control strategies. Adaptive time step control strategies, which consider steep concentration gradients and stiff systems, can significantly reduce the simulation time. Such a technique that was applied by Mayer (1999, compare Chapter 2.4.4) to his model can be further investigated for its applicability in RUMT3D.

In selected cells, the reaction step can further temporally be de-activated. In the PHT3D model, Prommer et al. (2003) already introduced two criteria that finds cells and time when reactions should be calculated during the course of a simulation. These criteria are based upon tolerance limits or acceptable error estimations for all reactive concentration changes of the aqueous phases and of the pH in a cell (compare Chapter 2.4.4). Similar to adaptive time step control strategies, a critical point of the temporal de-activation of the reaction step in selected cells is to find a robust and efficient search algorithm that can recognize

developments of steep concentration gradients. When such steep gradients start to develop, the reaction step in respective cells should be re-activated. Once potential criteria for search algorithm are identified, sensitivity tests can be used to test these.

The number of cells in which reactive calculations are performed can additionally be minimised by dividing the different time scales into intervals. In a model domain, heterogeneous spatial concentration contributions of different constituents and mineral phases usually exist and the concentration changes with the time can be very spatially variable. Cells that demand fast temporal concentration variations require more frequent calls to the reaction package. The number of these cells is however limited. Therefore, it is recommended to find criteria that identify the cell in which the reaction time steps are more frequent necessary than in others. A similar technique to a sub-cycling technique can be used. Accuracy and stability of results as well as the simulation time can thereby be improved (Oran & Boris 2001).

## 7.6 Colloids

The mobility of dissolved metal contaminants as well as radionuclides (e.g., plutonium) in groundwater systems can significantly be influenced by attachment/adsorption to colloids as well as filtration of colloids (McCarthy & Zachara 1989; Mills et al. 1991; Puls & Powell 1992 and Ryan & Elimelech 1996). Colloids can be divided into two groups, namely the true and pseudo colloids. True colloids are formed from the contaminants themselves when their concentrations exceed their solubility in the aqueous phase. Colloids, which consist of minerals such as clay, are referred to as pseudo colloids (Ibaraki & Sudicky 1995). Due to the charge and size exclusion effects, colloids can have a much higher flow velocity than a tracer or aqueous species (Baumann et al. 2002). The pore walls and colloids are generally electrically charged. Colloids such as the ones that carry the same electric charge than small pores are not transported through these small pores. Colloids, which are larger in size than pores and openings, are also excluded from being transported through these particular pores and openings. Therefore, on one hand, the charge and size exclusion effects support filtration or the immobile status of colloids (by being filtrated, colloids can become immobile). On the other hand, they promote colloids being primarily transported in larger pores with higher flow velocities than with the average tracer velocity. Moreover, the velocity profile within the pores plays a significant role. Through the electrostatic exclusion, colloids are accumulated into the centre of pores, i.e., into zones of higher velocities (Corapcioglu & Jiang 1993; Ibaraki & Sudicky 1995).

The possibility of having colloids as the vehicle to transport contaminants was especially observed in areas where weapons were produced and tested (Buddemeier & Hunt 1988) as well as in areas where long term behaviour of radioactive waste was investigated (McCarthy & Zachara 1989). Also in mine water, colloids have been observed, especially inorganic colloids. These mostly consist of iron and aluminium which are generated by the production of oxyhydroxides and hydroxysulphates of Fe(III) and Al(III) by the oxidation of

Fe(II) and the hydrolysis of Fe(III) and Al(III) (Zänker et al. 2000, 2001, 2002, 2003). Colloid borne heavy metal transport in mine water was investigated in various mine sites such as in the uranium mine Krunkelbach at Menzenschwand, South black forest, Germany (Hofmann 1989), uranium ore mine Cigar Lake, Canada (Vilks et al. 1988), the abandoned Zn-Pb-Ag-mine Freiberg, Saxony, Germany (Zänker et al. 2000) and the abandoned uranium mine Königstein, Saxony (Zänker et al. 2001; Zänker et al. 2003). It was found that colloid formation and heavy metal adsorption were significantly controlled by the pH. By observation, mine water can be divided in two distinct different types:

1. Type 'acidic pore water'. These waters have high salt concentrations and have a pH value of 1 to 3. Thus, this water type is very acidic. Most colloids are ultrafine particles of size less than 5 nm and a colloidal concentration of more than  $1\text{ g L}^{-1}$  can be found in such type water. Hydronium jarosite and schwertmannite can be parts of these colloids and As and Pb can easily be absorbed to these colloids.
2. Type 'bulk water'. This water type refers to the water in mines, which flows freely like adit waters. It has a pH near 7. Concentrations of colloids around  $1\text{ mg L}^{-1}$  and colloid sizes of 100 to 300 nm are typically found in such waters. They consist of Fe(III) and Al(III) oxyhydroxides. Since their electrostatic stabilisation is weak, they have a larger tendency to coagulate. Contaminants such as arsenic, lead, copper, thorium, U(IV) and polonium are strongly bound onto these colloids.

Interesting colloid-chemical processes are observed during flooding of abandoned ore mines which lets type water a) transfer into type water b). Under such conditions, by supplying  $\text{O}_2$  and raising the pH, huge amounts of Fe(III) colloids with sizes of 100 to 300 nm are formed. When the pH reaches the near-neutral status, adsorption is enhanced drastically. For cases like, uranyl adsorption to Fe(III) particles is neither suppressed by high acidity nor by uranyl carbonate complexation in the pH range of 4 to 6, most of the U(VI) is colloid-borne in such waters (Zänker et al. 2002).

Depending upon the degree of contaminant (uranium) attachment (adsorption) onto the solid phase, the neglect of colloidal transport in mines is justified or not. If there is no attachment, colloids can be neglected. This case applies to U(VI) in waters with pH under 4 and in carbonate-rich waters with pH above 6. However, attachment occurs between pH 4 and 6. In this case, model results without the consideration of colloids would be too pessimistic. On the other hand, uranium in oxidation state IV commonly treated as immobile, may attach to or precipitate as colloid. In such cases, the "immobile" uranium becomes mobile. By neglecting colloidal transport mechanism, modelling results for uranium would be too optimistic (Zänker, pers. comm. 2001; Zänker et al. 2003). Few reactive transport models can be found in literature that consider colloids (e.g., HYTEC, De Windt & van der Lee 2000 and CHEMTARD, Ivanovich et al. 1994). Primarily, transport models for fractured systems have a transport capacity for colloids.

Briefly, the description of colloidal transport is dependent upon composition, size and therefore type of colloids and geochemical milieu as well as the characteristics of the groundwater system. If there are only true colloids in the groundwater system, partitions of contaminants between the different phases

can be considered by introducing a retardation factor in the transport equation (Ibaraki & Sudicky 1995). Especially, due to the relatively large sizes of pseudo colloids as results of the size exclusion effects, significant colloidal transport will presumably primarily occur in conduits but not so much in the continuum. Under certain conditions, it is necessary to model pseudo colloids as another phase besides the aqueous and solid phases. This is dependent upon the magnitude of the transport parameters such as the flow rates and dispersion. If these are very different from those of the aqueous species/complexes, it is advisable to consider colloids as another phase. Lührmann (1999), however, suggests to simulate colloids as another phase in any case with considerations of mobile and immobile parts of colloids since the behaviour of complexed ions onto or from colloids and or onto the solid phase is difficult to know. Colloids can also become immobile by deposition (caused e.g., by saturated solutions). Colloidal deposition is increased by factors such as the changes in hydro-chemical boundary conditions (e.g., ionic strength). This can occur in the surrounding of waste dumps through an increase in the total concentrations (Baumann et al. 2002). Nevertheless, in a first approach, the effect of colloidal transport can be investigated by introducing a retardation factor in the transport equations. The dynamic filtration/deposition and or sorption of colloids can be considered by incorporating a kinetic expression such as Freundlich or Langmuir isotherm into the transport equation (van der Lee et al. 1992; Ibaraki & Sudicky 1995; Lührmann 1999). Alternatively, a two-region (mobile-immobile) model based upon the idea of Baumann et al. (2002) can be utilised to describe the physical and geochemical non-equilibrium caused by the presence of the colloids. Baumann et al. (2002) used the one-dimensional analytical model CXTFIT (Toride et al. 1999) to obtain the transport parameters for the colloids. If a two region model approach is thought to be an appropriate choice for characterising colloidal transport within RUMT3D, the two region model provided by MT3DMS can be facilitated. Principally, there are three different approaches to model colloidal transport: a) the hydrodynamic-dispersive model, b) the random walk model and c) the population balance model. Hydrodynamic-dispersive models are based upon mass balance and random walk models are based on statistical theories. Population balance models consider growth of particles (Liew et al. 1994).

## 7.7 Summary

As the reactive hybrid transport model RUMT3D developed in this thesis is only at the initial stage of development, further testing, application to more than 1D and field studies as well as sensitivity studies, numerical optimisation and capacities as discussed in this chapter would allow to more generalise and apply RUMT3D to a large spectrum of (field) problems.

*The seed which ripens into vision may be a gift of the gods but the labor of cultivating it so that it may bear nourishing fruit is the indispensable function of arduous scientific technique.*

*Morris R. Cohen, Reason and Nature (1978)*

## Chapter

### 8 Conclusions

A new approach is presented to simulate reactive contaminant transport in underground mines or generally in hybrid or coupled discrete-continuum systems. Hybrid flow systems are characterised by two distinct flow regimes, (i) i.e., rapid, perhaps turbulent flow in discrete conduits and (ii) flow at comparably small velocities within the surrounding, less permeable continuum flow system. In flooded mines, for example, shafts and adits represent such conduits. They can also be predominant in fractured and karstic systems and in aquifers containing intersecting boreholes. A reactive “hybrid” transport model (RUMT3D) was developed in this thesis for more accurate and efficient simulation of contaminant transport in such systems with two different transport regimes.

By examining the performance of a new-implemented numerical solver within RUMT3D solving advection in the conduit system, the coupling of the two transport models for the continuum and conduit system was verified by comparison with a semi-analytical solution. By using this new solver, great improvements in the simulation results allowing much larger transport time step sizes and pipe discretisation could be achieved compared to the standard finite difference method.

The coupling of the reactive module within RUMT3D was verified by two benchmark problems and two different numerical codes. One of these problems simulates the principle processes of Acid Mine Drainage (AMD) phenomena. Due to the few components and mineral phases involved, this problem was also used to investigate consistency, accuracy and stability of the reactive results in a hybrid system since no benchmark problem was available. This was accomplished by means of plausibility tests. Four different scenarios with and without a conduit system were simulated and the influence of the conduit discretisation and of the magnitude of the conduit-matrix exchange were studied. The plausibility of the RUMT3D results was thereby examined in two steps. In a first step, the geochemical processes occurring in the pure continuum system, i.e., in the AMD problem under the different scenarios are discussed in detail. The examination of plausibility in a continuum system follows one in a hybrid system by addressing same geochemical processes. The second problem simulates the effect of low-pH process water upon an aquifer downgradient from a uranium mine site.

Good agreements of the reactive results using RUMT3D compared to the other numerical codes could be obtained. In addition, the plausibility tests generated

satisfactory numerical results. Simulation results indicate that conduit systems can significantly affect the spatial variability of buffering processes in an aquifer due to their impact on the flow dynamics. The higher the matrix-conduit exchange flow, the more rapid acidic water is transported via the conduit system. As a result, the downgradient water chemistry can be changed significantly. Further, the results gained in this thesis suggested that RUMT3D was a useful and powerful tool to study the presence of discrete conduit systems on reactive transport.

## Literature

- Appelo, C.A.J., Postma, D., 1993. *Geochemistry, groundwater and pollution*. Rotterdam, The Netherlands, Balkema, 536p.
- Appelo, C.A.J., Willemsen, A., 1987. Geochemical calculations and observations on saltwater intrusion, I, A combined geochemical/mixing cell model. *Journal of Hydrology*, 94: 313-330.
- Atkins, P.W., 1998. *Physical Chemistry*. Sixth edition. Oxford University Press.
- Bain, J.G., Mayer, K.U., Blowes, D.W., Frind, E.O., Molson, J.W.H., Kahnt, R., Jenk, U., 2001. Modelling the closure-related geochemical evolution of groundwater at a former uranium mine. *Journal of Contaminant Hydrology*, 52: 109-135.
- Bajracharya, K., Barry, D.A., 1993. Mixing cell models for nonlinear equilibrium single species adsorption and transport. *Journal of Contaminant Hydrology*, 12: 227-243.
- Barenblatt, G.I., Zheltov, I.P., Kochina, I.N., 1960. Basic concepts in the theory of seepage of homogeneous liquids in fissured rocks. *Journal of Applied Mathematics and Mechanics*, 24: 1286-1303.
- Barry, D.A., Bajracharya, K., Miller, C.T., 1996a. Alternative split-operator approach for solving chemical reaction/groundwater transport models. *Advances in Water Resources*, 19: 261-275.
- Barry, D.A., Miller, C.T., Culligan-Hensley, P.J., 1996b. Temporal discretisation errors in non-iterative split-operator approaches to solving chemical reaction/groundwater transport models. *Journal of Contaminant Hydrology*, 22: 1-17.
- Barry, D.A., Miller, C.T., Culligan, P.J., Bajracharya, K., 1997. Analysis of split operator methods for nonlinear and multispecies groundwater chemical transport models. *Mathematics and Computers in Simulation*, 43: 331-341.
- Barry, D.A., Prommer, H., Miller, C.T., Engesgaard, P., Brun, A., Zheng, C., 2002. Modelling the fate of oxidisable organic contaminants in groundwater. *Advances in Water Resources*, 25(8-12): 945-983.
- Baumann, T., Müller, S., Niessner, R., 2002. Migration of dissolved heavy metal compounds and PCP in the presence of colloids through a heterogeneous calcareous gravel and a homogeneous quartz sand – pilot scale experiments. *Water Research*, 36: 1213-1223.
- Bäverman, C., Strömberg, B., Moreno, L., Neretnieks, I., 1999. CHEMFRONTS: a coupled geochemical and transport simulation tool. *Journal of Contaminant Hydrology*, 36: 333-351.
- Bear, J., 1972. *Dynamics of fluids in porous media*. American Elsevier, New York.
- Berkowitz, B., Zhou, J., 1996. Reactive solute transport in a single fracture. *Water Resources Research*, 32(4): 901-913.
- Berkowitz, B., 2002. Characterizing flow and transport in fractured geological media: A review. *Advances in Water Resources*, 25: 861-884.
- Berner, R.A., 1978. Rate control of mineral dissolution under earth surface conditions. *American Journal of Science*, 278: 1235-1252.
- Birk, S., 2001. Characterisation of karst systems by simulating aquifer genesis and spring responses: model development and application to gypsum karst. *Geowissenschaftliche Arbeiten*, C60, Tübingen, Germany.
- Blomqvist, R., Ruskeeniemi, T., Kaija, J., Ahonen, L., Paananen, M., Smellie, J., Grundfelt, B., Pedersen, K., Bruno, J., Pérez del Villar, L., Cera, E., Rasilainen, K., Pikänen, P., Suksi, J., Casanova, J., Read, D., Frape, S., 2000. The Palmottu natural analogue project – Phase II: Transport of radionuclides in a natural flow system at Palmottu. Luxembourg: European Commission. 174 s. (Nuclear Science and Technology Series EUR 19611 EN).
- Blowes, D.W., Reardon, E.J., Jambor, J.L., Cherry, J.A., 1991. The formation and potential importance of cemented layers in inactive sulfide mine tailings. *Geochimica et Cosmochimica Acta*, 55: 965-978.
- Borkovec, M., Westall, J., 1983. Solution of the Poisson-Boltzmann equation for surface excesses of ions in the diffuse layer at the oxide-electrolyte interface. *Journal of Electroanalytical Chemistry*, 150: 325-337.
- Buddemeier, W.R., Hunt, J.R., 1988. Transport of colloidal contaminants in groundwater: radionuclide migration at the Nevada Test Site. *Applied Geochemistry*, 3: 535-548.
- Carnahan, C.L., 1986. Simulation of uranium transport with variable temperature and oxidation potential: The computer program THCC, Rep. 21639, Lawrence Berkeley Lab., Berkeley, Calif.
- Cederberg, G.A., Street, R.L., Leckie, J.O., 1985. A groundwater mass transport and equilibrium chemistry model for multicomponent systems. *Water Resources Research*, 21: 1095-1104.
- Cheng, H.P., 1995. Development and application of a three-dimensional finite element model of subsurface flow, heat transfer, and reactive chemical transport. Ph.D. thesis, Department of Civil Engineering, The Pennsylvania State University, University Park, PA 16802.
- Cheng, H.P., Yeh, G.-T., 1998. Development and demonstrative application of a 3-D numerical model of subsurface flow, heat transfer, and reactive chemical transport: 3DHYDROGEOCHEM. *Journal of Contaminant Hydrology*, 34: 47-83.
- Clemens, T., Hückinghaus, D., Sauter, M., Liedl, R., Teutsch, G., 1996. A combined continuum and discrete network reactive transport model for the simulation of karst development. *Proc ModelCARE 1996*, Golden, Colorado, IAHS Publ. 237, 309-318.

- Clement, T.P., Sun, Y., Hooker, B.S., Petersen, J.N., 1998. Modeling multispecies reactive transport in ground water. *Ground Water Monitoring and Remediation*, 18(2): 79-92.
- Colenco, 2001. KAFKA User's guide, internal report.
- Cooley, R.L., 1983. Some new procedures for numerical solution of variably saturated flow problems. *Water Resources Research*, 19(5): 1271-1285.
- Corapcioglu, M.Y., Jiang, S., 1993. Colloid-Facilitated Groundwater Contaminant Transport. *Water Resources Research*, 29(7): 2215-2226.
- Cross, J.E., Haworth, A., Neretnieks, I., Sharland, S.M., Tweed, C.J., 1991. Modeling of redox front and uranium movement in an uranium mine at Pocos de Caldas. *Radiochimica Acta*, 52/53, 445-451.
- Cvetkovic, V., 1997. Transport of reactive solutes. In *Subsurface flow and transport: The Stochastic approach*, Dagan, G., Neuman, S. (eds.), Cambridge University Press, 133-145.
- Davis, J.A., James, R.O., Leckie, J.O., 1978. Surface ionization and complexation at the oxide/water interface. I. Computation of electrical double layer properties in simple electrolytes. *Journal of Colloid and Interface Science*, 63: 480-499.
- Davis, J.A., Kent, D.B., 1990. Chapter 5: Surface complexation modeling in aqueous geochemistry. In: Hochella, M.F., White, A.F. (eds.), *Mineral-Water Interface Geochemistry*: Washington D.C., Mineralogical Society of America, *Reviews in Mineralogy*, 23: 177-260.
- Davis, J.A., Leckie, J.O., 1978. Surface ionization and complexation at the oxide/water interface. II. Surface properties of amorphous iron oxyhydroxide and adsorption of metal ions. *Journal of Colloid and Interface Science*, 67: 90-107.
- Davis, J.A., Leckie, J.O., 1980. Surface ionization and complexation at the oxide/water interface. III. Adsorption of anions. *Journal of Colloid and Interface Science*, 74: 32-43.
- Davis, G.B., Ritchie, A.I.M., 1986. A model of oxidation in pyritic mine wastes: Part 1: equations and approximate solution. *Applied Mathematical Modelling*, 10: 314-322.
- De Windt, L., van der Lee, J., 2000. The reactive transport code HYTEC: verification and demonstration for version 3.0. Technical report No. LHM/RD/00/23, CIG-École des Mines de Paris, Fontainebleau, France.
- Diersch, H.-J.G., 1997. Interactive, graphics-based finite element simulation system FEFLOW for modeling groundwater flow, contaminant mass and heat transport processes. FEFLOW User's Manual Version 4.7, August 1997. WASY Institute for Water Resources Planning and Systems Research, Berlin.
- Dijk, P., Berkowitz, B., 1998. Precipitation and dissolution of reactive solutes in fractures. *Water Resources Research*, 34(3): 457-470.
- Dzombak, D.A., Morel, F.M.M., 1990. *Surface complexation modeling – Hydrous ferric oxide*. New York, John Wiley Interscience, 393p.
- Eckart, M., 1988. Ein Beitrag zur Infiltrationslaugung von Uranerzen mit Unterstützung numerisch-diskreter geoströmungstechnischer Modelle. PhD thesis, Technical University Freiberg.
- Emrén, A.T., 1998. CRACKER: A program coupling inhomogeneous chemistry and transport. *Computers and Geosciences*, 24 (8): 753-763.
- Engesgaard, P., Kipp, K.L., 1992. A geochemical transport model for redox-controlled movement of mineral fronts in groundwater flow systems: A case of nitrate removal by oxidation of pyrite. *Water Resources Research*, 28: 2829-2843.
- Fabritz, J.E., 1995. A two dimensional numerical model for simulating the movement and biodegradation of contaminants in a saturated aquifer. Master of Science Thesis, University of Washington.
- Forsyth, P.A., Sammon, P.H., 1986. Practical considerations for adaptive implicit methods in reservoir simulation. *Journal of Computational Physics*, 62: 265-281.
- Freedman, V.L., Ibaraki, M., 2003. Coupled reactive mass transport and fluid flow: Issues in model verification. *Advances in Water Resources*, 26: 117-127.
- Freeze, R.A., Cherry, J.A., 1979. *Groundwater*. Englewood Cliffs, NJ: Prentice-Hall.
- Gao, H., Butler, A., Wheeler, H., Vesovic, V., 2001. Chemically reactive multicomponent transport simulation in soil and groundwater: 1. Model development and evaluation. *Environmental Geology*, 41(3-4): 274 - 279.
- Gerke, H.H., Molson, J.W., Frind, E.O., 1998. Modelling the effect of chemical heterogeneity on acidification and solute leaching in overburden mine spoils. *Journal of Hydrology*, 209: 166-185 (special issue on reactive transport modeling).
- Ghogomu, N.F., Therrien R., 2000. Reactive mass transport modelling in discretely-fractures porous media. *Computational methods in Water resources XIII*, Bentley et al. (eds.), Balkema, Rotterdam, 285-292.
- Gwo, J.P., Jardine, P.M., Wilson, G.V., Yeh, G.T., 1996. Using a multiregion model to study the effects of advective and diffusive mass transfer on local physical nonequilibrium and solute mobility in a structured soil. *Water Resources Research*, 32: 561-570.
- Gylling, B., Moreno, L., Neretnieks, I., 1999. The channel network model – a tool for transport simulations in fractured media. *Groundwater*, 37(3): 367-375.
- Harbaugh, A.W., McDonald, M.D., 1996. User's documents for MODFLOW-96, an update to the U.S. Geological Survey modular finite-difference ground-water flow model. US Geological Survey Open File Report 96-485.

- Hedin, R.S., Narin, R.W., Kleinmann, L.P., 1994. Passive treatment of coal mine drainage. United States Department of Interior, Bureau of Mines, Information Circular, 35.
- Herzer, J., Kinzelbach, W., 1989. Coupling of transport and chemical processes in numerical transport models. *Geoderma*, 44: 115-127.
- Hofmann, B., 1989. Genese, Alteration und rezentes Fließ-System der Uranlagerstätte Krunkelbach (Menzenschwand, Südschwarzwald). Nagra Technischer Bericht NTB 88-30, Baden 1989. Dissertation, Universität Bern.
- Horlacher, H.-B., Lüdecke, H.-J., 1992. Strömungsberechnung für Rohrsysteme. Expert Verlag.
- Ibaraki, M., Sudicky, E.A., 1995. Colloid-facilitated contaminant transport in discretely fractured porous media 1. Numerical formulation and sensitivity analysis. *Water Resources Research*, 31(12): 2945-2960.
- Ivanovich, M. et al., (1994): Development and testing of a coupled process model incorporating the colloidal phase: A study of thorium transport in the presence of silica colloids. UKDOE Report DOE/HMIP/RR.94.036.
- Kinze, M., 2002. Dose limits and maximum concentration limits (MCL's) for radionuclides – implication on remediation of uranium mining and milling facilities in Saxony, Germany. *Uranium in the Aquatic Environment*, B.J. Merkel, B. Planer-Friedrich, C. Wolkersdorfer (eds), Springer Berlin, 1-7.
- Konikow, L.F., Bredehoeft, J.D., 1992. Groundwater models cannot be validated. *Advances in Water Resources*, 15: 75-83.
- Lasaga, A.C., 1981. Rate laws of chemical reactions. In: *Reviews in Mineralogy, Kinetics of Geochemical Processes*, Lasaga, A.C. & R.J. Kirkpatrick eds. BookCrafters Inc., Chelsea, Michigan, 8: 1-68.
- Levenspiel, O., 1972. *Chemical Reaction Engineering*, J. Wiley and Sons, New York.
- Licha, T., 2003. Short chained alkyl phenols (SCAP) in groundwater – chemical analysis, adsorption mechanism and field cases. PhD Thesis. Friedrich-Schiller-University of Jena, Germany.
- Lichtner, P.C., 1988. The quasi-stationary state approximation to coupled mass transport and fluid-rock interaction in a porous medium. *Geochimica et Cosmochimica Acta*, 52: 143-165.
- Lichtner, P.C., 1995. Continuum model for simultaneous chemical reactions and mass transport in hydrothermal system. *Geochimica et Cosmochimica Acta*, 49: 779-800.
- Lichtner, P.C., 1996. Continuum formulation of multi-component reactive transport. In: Lichtner, P.C., C.I. Steefel & E.H. Oelkers (eds.), Chapter 1, *Reactive Transport in Porous Media*, Reviews in Mineralogy, 34, Mineralogical Society of America.
- Liedl, R., Sauter, M., Hückinghaus, D., Clemens, T., Teutsch, G., 2003. Simulation of the development of karst aquifers using a coupled continuum pipe flow model. *Water Resources Research*, 39(3): 1057.
- Liew, S.K., Haywood, G., Thomas, J.B., 1994. Review of physico-chemical processes controlling transport and the approaches by which colloid-radionuclide transport may be modelled. In: Ivanovich, M. et al. Development and testing of a coupled process model incorporating the colloidal phase: A study of thorium transport in the presence of silica colloids. UKDOE Report DOE/HMIP/RR.94.036.
- Liu, C.W., Narasimhan, T.N., 1989. Redox-controlled multiple-species reactive chemical transport: 1. Model development. *Water Resources Research*, 25(5): 869-882.
- Liu, C.W., Narasimhan, T.N., 1989. Redox controlled multiple-species reactive chemical transport: 1. verification and application. *Water Resources Research*, 25: 883-910.
- Liu, G., Wang, P., Zheng, C., 2001. An explicit and mass-conservative scheme without time-step limit for modeling advection-dominated contaminant transport, 2001 MODFLOW international conference in Golden, Colorado.
- Lührmann, L., 1999. Modellierung des kolloidgetragenen Schadstofftransports unter Berücksichtigung von Sorptions- und Filtrationsprozessen. Dissertation, Friedrich-Alexander-Universität-Erlangen-Nürnberg, Naturwissenschaftlichen Fakultäten.
- Mangold, D.C., Tsang, C.-F., 1991. A summary of subsurface hydrological and hydrochemical models. *Reviews of Geophysics*, 29(1): 51-79.
- Mayer, K.U., 1999. A numerical model for multicomponent reactive transport in variably saturated porous saturated porous media. PhD Thesis, University of Waterloo, Ontario, Canada.
- McCarthy, J.F., Zachara, J.M., 1989. Subsurface transport of contaminants; Mobile colloids in the subsurface environment may alter the transport of contaminants. *Environmental Science & Technology*, 23: 496-502.
- McNab, W.W., 2001. Computer-Mediated Distance Learning: Course on MULTISPECIES REACTIVE TRANSPORT IN GROUNDWATER, TOPIC C: INTRODUCTION TO REACTIVE TRANSPORT MODELING WITH PHREEQC: EXAMPLE APPLICATIONS Lecture 1: Acid Mine Drainage. [http://www.heath-hydrology.com/cmdl/demos/msrt-course/Lecture\\_C\\_1.html](http://www.heath-hydrology.com/cmdl/demos/msrt-course/Lecture_C_1.html).
- Merkel, B., Hurst, S., Struckmeier, W., Löhnert, E.P., 1995. Forword in *Uranium-Mining and Hydrogeology*. Proceedings of the International Conference and Workshop, Freiberg, Germany, Oct. 1995, ed. by Merkel, B., Hurst, S., Löhnert, E.P., Struckmeier, W., Köln: von Loga, GeoCongress, 1, ISBN 3-87361-256-9.
- Mills, W.B., Liu, S., Fong, F.K., 1991. Literature review and model (COMET) for colloid / metals transport in porous media. *Ground Water*, 29: 199-208.
- Mocker, D., Eckart, M., Volland, B., Heeg, W., 2002. TEN3D, Programmdokumentation. Mehrmigranten-Stofftransport – Zweiphasenströmung.

- Morin, K.A., Cherry, J.A., 1988. Migration of acidic groundwater seepage from uranium-tailings impoundments, 3. Simulation of the conceptual model with application to seepage area A. *Journal of Contaminant Hydrology*, 2 (4): 323-342.
- Morrison, J.L., Scheetz, B.E., Strickler, D.W., Williams, E.G., Rose, A.W., Davis, A., Parizk, R., 1990. Predicting the occurrence of acid mine drainage in the Alleghenian coal-bearing strata of western Pennsylvania. *Geol. Soc. Am., Sp. Pap.*, 248: 87-99.
- Murphy, W.M., Oelkers, E.H., Lichtner, P.C., 1989. Surface reaction versus diffusion control of mineral dissolution and growth rates in geochemical processes. *Chemical Geology*, 78: 357-380.
- Narasimhan, T.N., Witherspoon, P.A., 1976. An integrated finite difference method for analyzing fluid flow in porous media. *Water Resources Research*, 12: 57-64.
- Narasimhan, T.N., White, A.F., Tokunaga, T., 1986. Groundwater contamination from an inactive uranium mill tailings pile. 2. application of a dynamic mixing model. *Water Resources Research*, 22(13): 1820-1834.
- Narasimhan, T.N., Apps, J.A., 1990. Reactive chemical transport in ground-water hydrology: challenges to mathematical modeling. LBL-29492 report, Earth Science Division, Lawrence Berkeley Laboratory, Berkeley, CA.
- Noorishad, J., Carnahan, C.L., Benson, L.V., 1987. Development of the non-equilibrium reactive chemical transport code CHMTRNS. Technical report, Lawrence Berkeley Laboratory, Earth Science Division.
- Nordstrom, D.K., Alpers, C.N., 1998. Geochemistry of acid mine waters, part A – Processes, techniques and health, in *Environmental Geochemistry of Mineral Deposits*, Rev. Econ. Geol., edited by Plumlee, G., Logsdon, M., 6a, Chapter 6. Soc. Econ. Geol.
- Novak, C.F., Sevougian, S.D., 1992. Propagation of dissolution/precipitation waves in porous media. In: Petruzzelli, D., Helfferich, F.G. (Eds.), *Migration and fate of pollutants in soils and subsoils*. NATO ASI series. Series G: Ecological Sciences, 32: 275-307.
- Novak, C.F., 1996. Development of the FMT chemical transport simulator: coupling aqueous density and mineral volume fraction to phase compositions. *Journal of Contaminant Hydrology*, 21: 297-310.
- Novotny, V., Olem, H., 1994. *Water Quality, prevention, identification and management of diffuse pollution*. Van Nostrand Reinhold, 410.
- Oran, E.S., Boris, J.P., 2001. *Numerical simulation of reactive flow*. Second Edition. Cambridge University Press, ISBN 0 521 58175 3.
- Parkhurst, D.L., Thorstenson, D.C., Plummer, L.N., 1980. PHREEQE: A computer program for geochemical calculations, U.S. Geol. Surv. Water Resour. Invest., PB81-167801.
- Parkhurst, D.L., Appelo, C.A.J., 1999. User's guide to PHREEQC (version 2) – a computer program for speciation, batch-reaction, one-dimensional transport, and inverse geochemical calculations. Water-Resources Investigations Report 99-4259, U.S. Dept. of the Interior, U.S. Geological Survey.
- Pfingsten, W., Carnahan, C.L., 1995. Heterogeneous redox reactions in groundwater flow systems – investigation and application of two different coupled codes. Technical report 95-01. National Cooperative for the Disposal of Radioactive Waste (nagra).
- Pinder, G.F., Gray, W.G., Botha, J.F., 1982. A theoretical investigation on a transport of chemicals in a reactive porous media. Princeton University, NJ 08544.
- Prommer, H., 2002. A reactive multicomponent transport model for saturated porous media. User's manual version 1.0. Contaminated Land Assessment and Remediation Research Centre, The University of Edinburgh, UK.
- Prommer, H., Barry, D.A., Zheng, C., 2003. PHT3D - A MODFLOW/MT3DMS based reactive multi-component transport model. *Ground Water*, 42(2): 247-257.
- Pruess, K., 1983. GMINC: A mesh generator flow simulations in fractured reservoirs: Lawrence Berkeley Laboratory Report LBL-15227, Berkeley, California.
- Pruess, K., Narasimham, T.N., 1985. A practical method for modeling fluid and heat flow in fractured porous media: *Society of Petroleum Engineers Journal*, 25: 14-26.
- Pruess, K., Wang, J.S.Y., Tsang, Y.W., 1990. On thermohydrological conditions near high-level nuclear wastes emplaced in partially saturated fractured tuff, Part 2, Effective continuum approximation. *Water Resources Research*, 26: 1249-11261.
- Pruess, K., 1991. TOUGH2: A general numerical simulator for multiphase fluid and heat flow, Lawrence Berkeley Laboratory Report LBL-29400, Berkeley, California.
- Pruess, K., Oldenburg, C., Moridis, G., 1999. TOUGH2 user's guide, Version 2.0, Lawrence Berkeley Laboratory Report LBL-43134, Berkeley, California.
- Puls, R.W., Powell, R.M., 1992. Transport of inorganic colloids through natural aquifer material: Implications for contaminant transport. *Environmental Science & Technology*, 26(3): 614-621.
- Rasilainen, K., Suksi, J., Ruskeeniemi, T., Pitkänen, P., Poteri, A., 2003. Release of uranium from rock matrix—a record of glacial meltwater intrusions? *Journal of Contaminant Hydrology*, 61(1- 4): 235-246.
- Robinson, B.A., Viswanathan, H.S., Valocchi, A.J., 2000. Efficient numerical techniques for modeling multicomponent ground-water transport based upon simultaneous solution of strongly coupled subsets of chemical components. *Advances in Water Resources*, 23: 307-324.

- Rubin, J., 1983. Transport of reacting solutes in porous media: Relation between mathematical nature of problem formulation and chemical nature of reaction. *Water Resources Research*, 19: 1231-1252.
- Ryan, J.N., Elimelech, M., 1996. Colloid mobilization and transport in groundwater. *Colloids and Surfaces, A: Physicochemical and Engineering Aspects*, 107: 1-56.
- Saaltink, M., Carrera, J., Ayora, C., 2001. On the behavior of approaches to simulate reactive transport. *Journal of Contaminant Hydrology*, 48: 213-235.
- Schäfer, D., Schäfer, W., Kinzelbach, W., 1998. Simulation of reactive processes related to biodegradation in aquifers. 1. Structure of the three-dimensional reactive model. *Journal of Contaminant Hydrology*, 31: 167-186.
- Singer, P.C., Stumm, W., 1970. Acidic mine drainage: the rate-determining step. *Science*, 167: 1121-23.
- Steefel, C.I., Lasaga, A.C., 1994. A coupled model for transport of multiple chemical species and kinetic precipitation/dissolution reactions with application to reactive flow in single phase hydrothermal systems. *American Journal of Science*, 294: 529-592.
- Steefel, C.I., Lichtner, P.C., 1994. Diffusion and reaction in a rock matrix bordering a hyperalkaline fluid-filled fracture. *Geochimica et Cosmochimica Acta*, 58(17): 3595-3612.
- Steefel, C.I., MacQuarrie, K.T.B., 1996. Approaches to modeling of reactive transport in porous media. In: *Reactive Transport in Porous Media: General Principles and Applications to Geochemical Processes*, Lichtner, P.C., Steefel, C.I., Oelkers, E.H. (eds), *Rev. Mineralogy, Min. Soc. Of America*, 83-129.
- Steefel, C.I., Lichtner, P.C., 1998a. Multicomponent reactive transport in discrete fractures: I. Controls on reaction front geometry. *Journal of Hydrology*, 209: 186-199.
- Steefel, C.I., Lichtner, P.C., 1998b. Multicomponent reactive transport in discrete fractures II: Infiltration of hyperalkaline groundwater at Maqarin, Jordan, a natural analogue site. *Journal of Hydrology*, 209: 200-224.
- Steefel, C.I., van Cappellen, P., 1998. Preface. *Reactive transport modeling of natural systems. Journal of Hydrology*, 209: 1-7.
- Stone, A.T., Morgan, J.J., 1990. Kinetics of chemical transformations in the environment. In *Aquatic Chemical Kinetics, Reaction rates of processes in natural waters*, edited by W. Stumm, John Wiley & Sons, Inc., New York.
- Suarez, D.L., Simunek, J., 1996. Solute transport modeling under variably saturated water flow conditions. In: Lichtner, P.C., Steefel, C.I., Oelkers, E.H. (eds.), Chapter 5, *Reactive Transport in Porous Media, Reviews in Mineralogy*, 34, Mineralogical Society of America.
- Suksi, U.J., Rasilainen, K., Ruskeeniemi, T., Marcos, N., Hellmuth, K.-H., 2002. Natural U occurrences as a palaeo-hydrogeological indicator – observations from the Palmottu natural analogue site, Finland. *Uranium in the Aquatic Environment*, Merkel, B.J., Planer-Friedrich, B., Wolkersdorfer, C. (eds), Springer Berlin, 227-236.
- Therrien, R., Sudicky, E.A., 1996. Three-dimensional analysis of variably-saturated flow and transport in discretely-fractured porous media. *Journal of Contaminant Hydrology*, 23: 1-44.
- Toride, N., Leij, F.J., van Genuchten, M.T., 1999. The CXTFIT code for estimating transport parameters from laboratory or field tracer experiments, version 2.1. Research Report 137, US Salinity Laboratories, Agri Res Serv, US Department of Agri., Riverside, CA.
- van Berk, W., 1987. Hydrochemische Stoffumsetzungen in einem Grundwasserleiter beeinflusst durch eine Steinkohlenbergehalde. *Bes. Mitt. Z. Dtsch. Gewässerkd. Jb.*, 49, 175.
- van der Lee, J., Ledoux, E., de Marsily, G. 1992. Modeling of colloidal uranium transport in a fractured medium. *Journal of Hydrology*, 139: 135-158.
- VanderKwaak, J.E., Forsyth, P.A., MacQuarrie, K.T.B., Sudicky, E.A., 1995. WATSOLV sparse matrix iterative solver package version 1.01. Unpublished report, Waterloo Centre for Groundwater Research, University of Waterloo, Ontario, Canada.
- Vilks, P., Cramer, J.J., Shewchuk, T.A., Larocque, J.P.A., 1988. Colloid and Particulate Matter Studies in the Cigar Lake Natural-Analog Program. *Radiochimica Acta*, 44-45: 305-310.
- Viswanathan, H.S., 1996. Modification of the finite element heat and mass transfer code (FEHM) to model multicomponent reactive transport. Master of Science Thesis, University of Illinois at Urbana-Campaign, Illinois, Los Alamos National Laboratory Report LA-13167-T.
- Viswanathan, H.S., 1999. The development and application of reactive transport modeling techniques to study radionuclide migration at Yucca Mountain, NV. PhD Thesis, University of Illinois at Urbana-Campaign, Illinois, Los Alamos National Laboratory Report LA-13642-T.
- Viswanathan, H.S., Robinson, B.A., Valocchi, A.J., Triay, I.R., 1998. A reactive transport model of neptunium migration from the potential repository at Yucca Mountain. *Journal of Hydrology*, 209: 251-280.
- Viswanathan, H.S., Sauter, M., 2001. Contaminant migration from underground mines using a coupled continuum-pipe-flow model. In: *Water-Rock Interaction*, Cidu, R. (ed.) Proc. Tenth Int. Symp. WRI-10, held 10-15 June 2001, Villasimius, Italy, A.A. Balkema Publishers, Swets & Zeitlinger, Lisse, ISBN 90 2651 824 2., 1285-1288.
- Voss, C.I., 1984. A finite-element simulation model for saturated-unsaturated, fluid-density-dependent groundwater flow with energy transport or chemically reactive single species solute transport. USGS, National Center, Reston, Virginia.
- Walsh, M.P., Bryant, S.L., Schechter, S.R., Lake, L.W., 1984. Precipitation and dissolution of solids attending flow through porous media. *AIChE Journal*, 30(2): 317-328.

- Walter, A.L., Frind, E.O., Blowes, D.W., Ptacek, C.J., Molson, J.W., 1994. Modeling of multicomponent reactive transport in groundwater. 1. Model development and evaluation. *Water Resources Research*, 30(11): 3137-3148.
- WASY, 1995. Gesellschaft für wasserwirtschaftliche Planung und Systemforschung mbH, Berlin. Stofftransportmodellierung im grossräumigen Bereich um die Lagerstätte Königstein und in der Grube Königstein, Report prepared for WISMUT, Chemnitz.
- Wels, C., Smith, L., 1994. Retardation of sorbing solutes in fracture media. *Water Resources Research*, 30(9): 2547-63.
- Westall, J.C., Zachary, J.L., Morel, F.M.M., 1976. MINEQL: A computer program for the calculation of chemical equilibrium composition in aqueous systems, Tech. Note 18, Water Qual. Lab., Dep. of Civ. Eng., Mass. Inst. of Technol., Cambridge.
- White, A.F., Delany, J.M., Narasimhan, T.N., Smith, A., 1984. Groundwater contamination from an inactive uranium mill tailings pile. 1. Application of a chemical mixing model. *Water Resources Research*, 20(11): 1743-1752.
- Wilhelm, St., Poppei, J., Mayer, G., Schwarz, R., Klubertanz, G., Siegel, P., Förster, B., 2002. Influence of chemical reactions on the flow system and contaminant transport in a former salt mine. *Uranium in the Aquatic Environment*, B.J. Merkel, B. Planer-Friedrich, C. Wolkersdorfer (eds), Springer Berlin, 1083-92.
- Wisotzky, F., 1994. Untersuchungen zur Pyritoxidation in Sedimenten des Rheinischen Braunkohlenreviers und deren Auswirkungen auf die Chemie des Grundwassers. *Bes. Mitt. Z. Dtsch. Gewässerkl. Jb.*, 58: 153.
- Wisotzky, F., 1996. Hydrogeochemische Reaktionen im Sicker- und Grundwasserbereich von Braunkohlentagebaukippen. *Grundwasser, Zeitschrift der Fachsektion Hydrogeologie*, 3-4: 129-36.
- Wisotzky, F., Obermann, P., 1995. Hydrogeochemie der Pyritoxidation am Beispiel des Rheinischen Braunkohlenreviers. In *Nieders. Landesamt für Bodenforschung: Grundwassergüteentwicklung in den Braunkohlegebieten der neuen Länder*, 1: 167-183.
- Wunderly, M.D., Blowes, D.W., Frind, E.O., Ptacek, C.J., 1996. Sulfide mineral oxidation and subsequent reactive transport of oxidation products in mine tailings impoundments: a numerical model. *Water Resources Research*, 32(10): 3173-3187.
- Xu, T., Pruess, K., 2001. Modeling multiphase non-isothermal fluid flow and reactive geochemical transport in variably saturated fractured rocks: 1. Methodology. *American Journal of Science*, 301: 16-22.
- Xu, T., Samper, J., Ayora, C., Manzano, M., Custodio, E., 1999. Modeling of non-isothermal multicomponent reactive transport in field-scale porous media flow system: *Journal of Hydrology*, 214: 144-164.
- Xu, T., Sonnenthal, E., Spycher, N., Pruess, K., 2003. TOUGHREACT: A new code of the tough family for non-isothermal multiphase reactive geochemical transport in variably saturated geologic media. *Proceedings, TOUGH Symposium*, Lawrence Berkeley National Laboratory, Berkeley, California, May 12-14.
- Yeh, G.-T., Cheng, H.-P., 1999. 3DHYDROGEOCHEM: a three-dimensional model of density-dependent subsurface flow and thermal multispecies-multicomponent HYDROGEOCHEMical Transport. EPA report, EPA/600/R-98/159.
- Yeh, G.-T., Tripathi, V.S., 1989. A critical evaluation of recent developments in hydrogeochemical transport models of reactive multichemical components. *Water Resources Research*, 25(1): 93-108.
- Yeh, G.-T., Tripathi, V.S., 1990. HYDROGEOCHEM: A coupled model of HYDROlogical transport and GEOCHEMical equilibria in reactive multicomponent systems, ORNL-6371, Oak Ridge National Laboratory, Oak Ridge, TN 37831.
- Yeh, G.-T., Tripathi, V.S., 1991. A model for simulating transport of reactive multispecies components: model development and demonstration. *Water Resources Research*, 27(12): 3075-3094.
- Yeh, G.-T., Siegel, M.D., Li, M.-H., 2001. Numerical modeling of coupled variably saturated fluid flow and reactive transport with fast and slow chemical reactions. *Journal of Contaminant Hydrology*, 47: 379-390.
- Younger, P.L., 2002. Deep mine hydrogeology after closure: insights from the UK. *Uranium in the Aquatic Environment*, Merkel, B.J., Planer-Friedrich, B., Wolkersdorfer, C. (eds), Springer Berlin, 25-40.
- Zänker, H., Richter, W., Brendler, V., Nitsche, H., 2000. Colloid-borne uranium and other heavy metals in the water of a mine drainage gallery. *Radiochimica Acta*, 88: 619-624.
- Zänker, H., Richter, W., Schreyer, J., Jenk, U., 2001. Die Anlagerung von radiotoxischen Schwermetallen an Kolloidpartikel im Flutungswasser einer stillgelegten Urangrube. *GDCh-Jahrestagung Chemie 2001*, Würzburg, 23.-29. September 2001.
- Zänker, H., Richter, W., Brendler, V., Moll H., Huettig, G., 2002. The sorption of toxic and radiotoxic heavy metals by inorganic colloids in mine waters. *GeoPro2002 – Geochemical Processes*, March 4-7, 2002, Bremen, Germany.
- Zänker, H., Richter, W., Huettig, G. 2003. Scavenging and immobilization of trace contaminants by colloids in the waters of abandoned ore mines. *Colloids and Surfaces A: Physicochemical and Engineering Aspects*, 217: 21-31.
- Zheng, C., 1990. MT3D a modular three-dimensional transport model for simulation of advection, dispersion and chemical reactions of contaminants in groundwater systems. *Documentation and Input Instructions*. S.S. Papadopoulos & Associates, Maryland.
- Zheng, C., Wang, P.P., 1999. MT3DMS: A modular three-dimensional multispecies model for simulation of advection, dispersion and chemical reactions of contaminants in groundwater systems. *Documentation and User's Guide*, Contract Report SERDP-99-1, U.S. Army Engineer Research and Development Center, Vicksburg, MS (available at <http://hydro.geo.ua.edu>).

- Zysset, A., Stauffer, F., Dracos, T., 1994. Modeling of chemically reactive groundwater transport. *Water Resources Research*, 30(7): 2217-2229.
- Zyvoloski, G.A., 1994. Science and Technology Assessment and External Review Committee Meeting, May 16-18.
- Zyvoloski, G.A., Robinson, B.A., Dash, Z.V., Trease, L.L., 1997. Summary of models and methods for FEHM application. A Finite Element Heat and Mass Transfer Code, LA-13307-MS.

## Appendix

Simulated conservatively transported concentrations at the 1000 m observation point for both, the MIN3P and RUMT3D models (conservative case and calcite scenario).

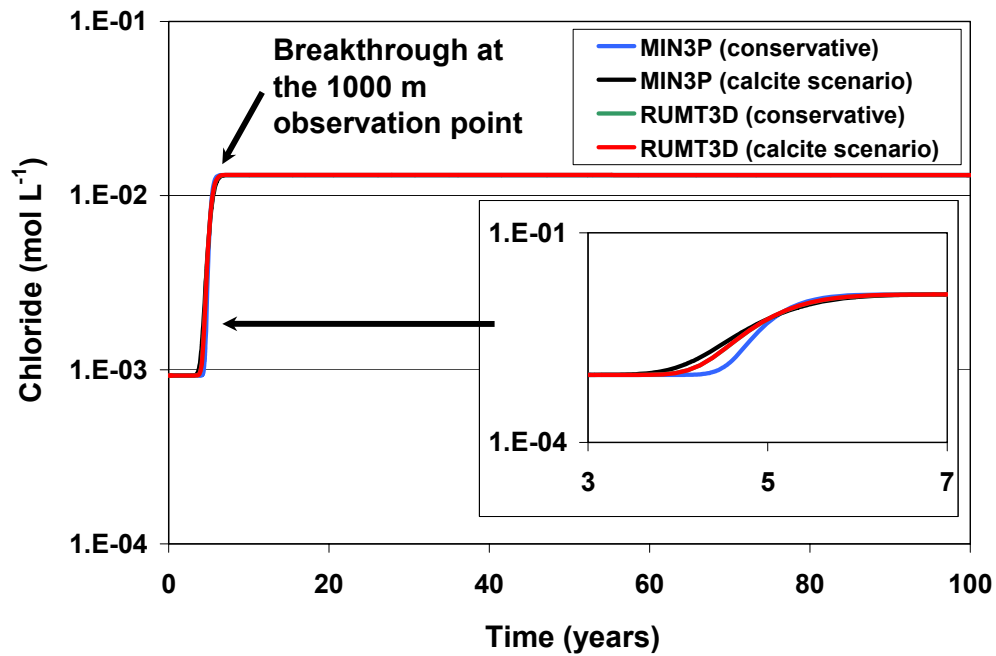


Fig. 65: Simulated chloride concentrations at the 1000 m observation point for both, the MIN3P and RUMT3D models (conservative case and calcite scenario).

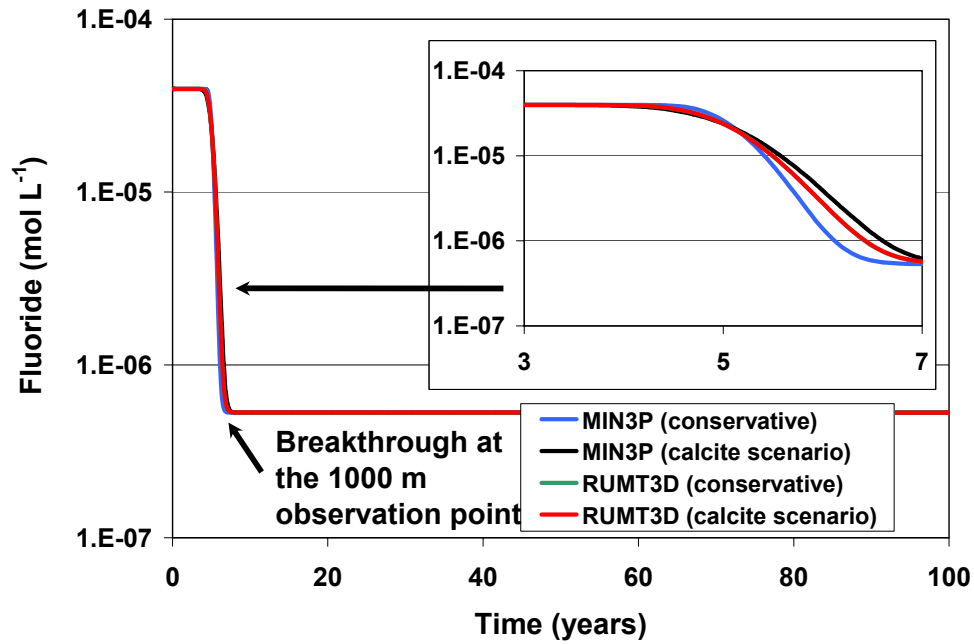


Fig. 66: Simulated fluoride concentrations at the 1000 m observation point for both, the MIN3P and RUMT3D models (conservative case and calcite scenario).

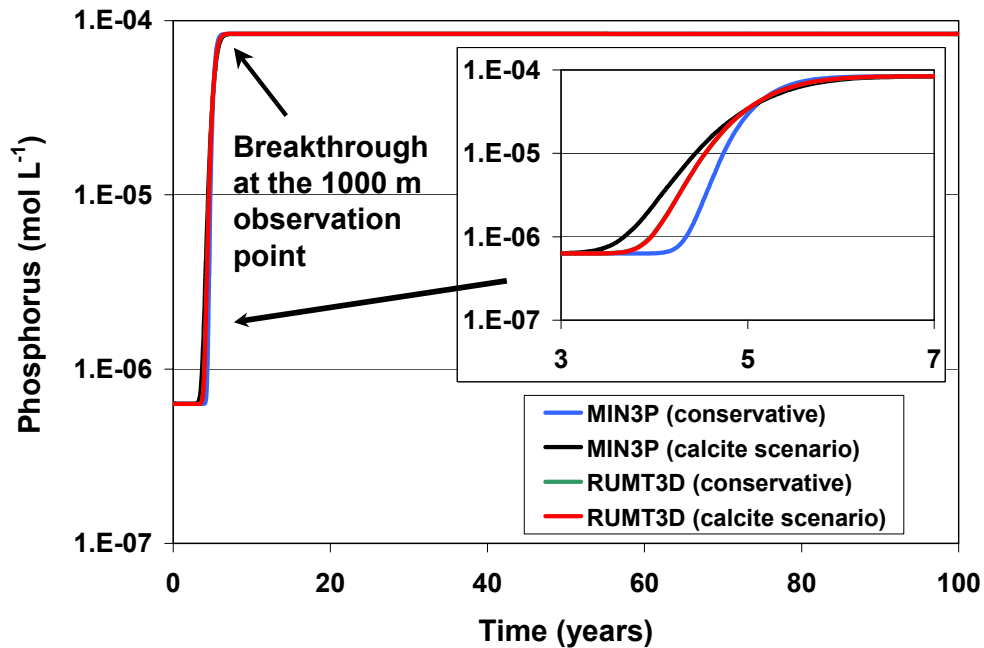


Fig. 67: Simulated phosphorus concentrations at the 1000 m observation point for both, the MIN3P and RUMT3D models (conservative case and calcite scenario).

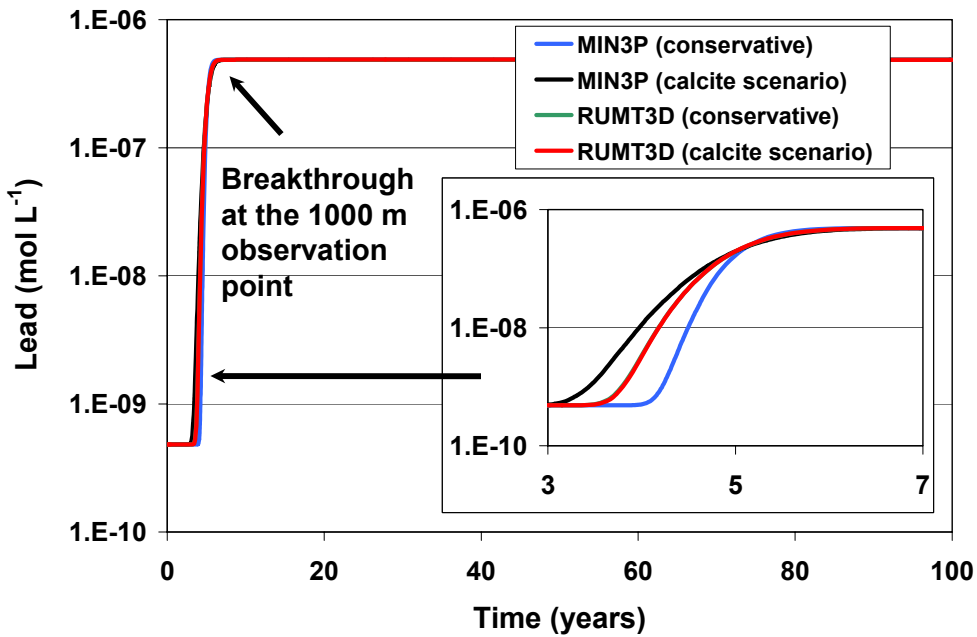


Fig. 68: Simulated lead concentrations at the 1000 m observation point for both, the MIN3P and RUMT3D models (conservative case and calcite scenario).

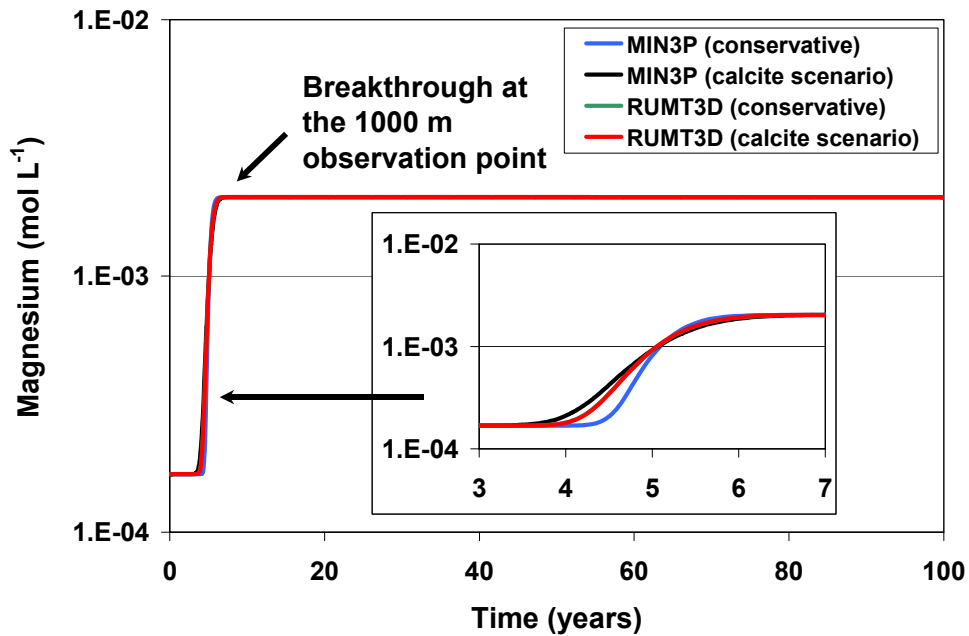


Fig. 69: Simulated magnesium concentrations at the 1000 m observation point for both, the MIN3P and RUMT3D models (conservative case and calcite scenario).

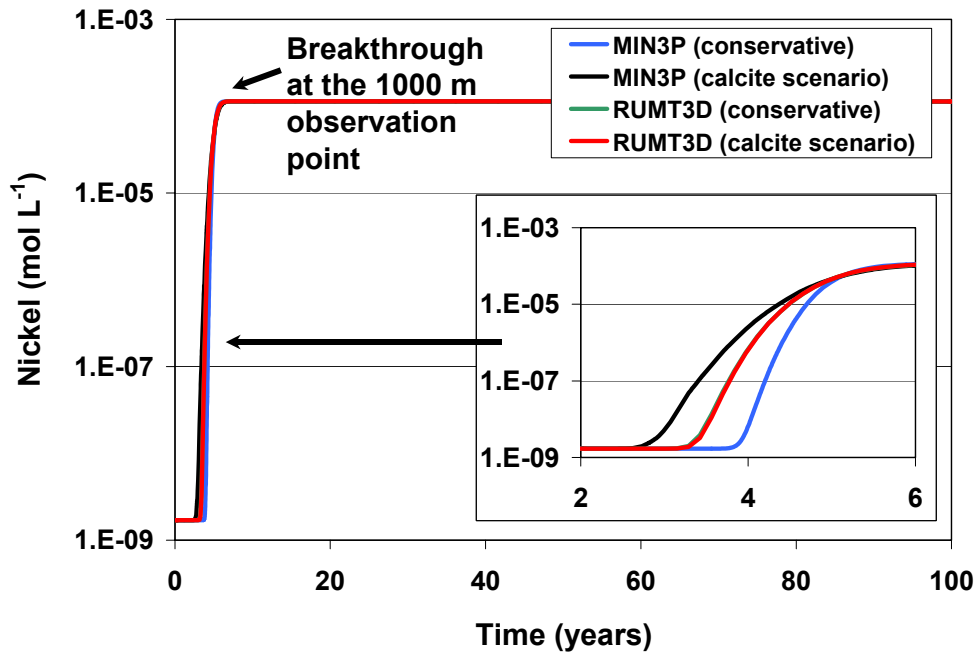
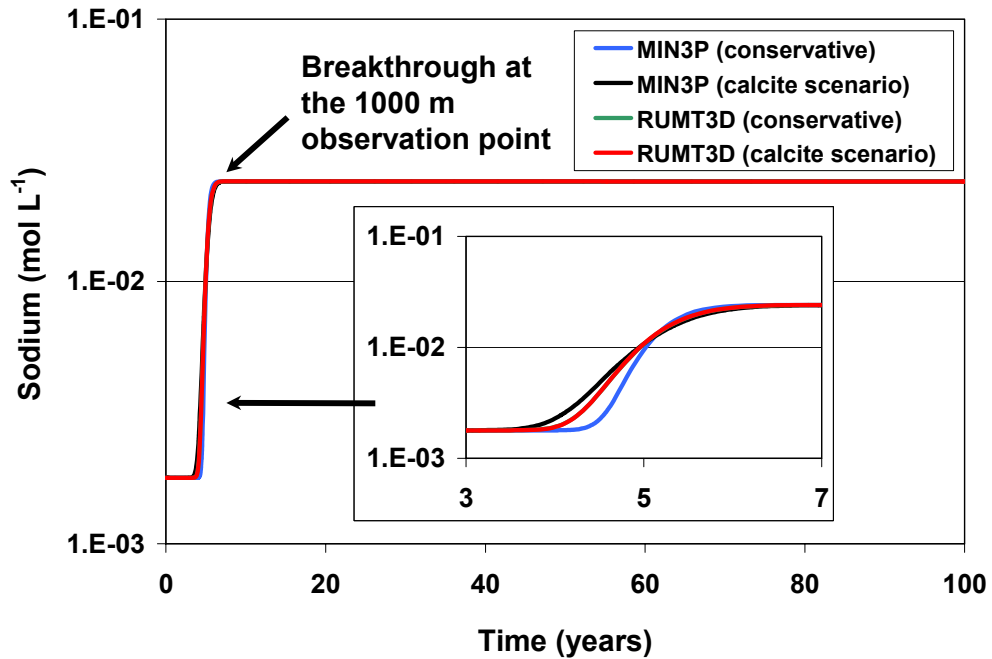


Fig. 70: Simulated nickel concentrations at the 1000 m observation point for both, the MIN3P and RUMT3D models (conservative case and calcite



scenario).

Fig. 71: Simulated sodium concentrations at the 1000 m observation point for both, the MIN3P and RUMT3D models (conservative case and calcite scenario).

## Lebenslauf

Name Sabine Maria Spießl (Spiessl)  
Geburtsdatum 23. Februar 1969  
Geburtsort Oberviechtach  
Nationalität Deutsch

### Hochschulbildung:

2000 - 2004 **Dr. rer. nat.** - Geologie, Schwerpunkt: Geowissenschaften bzw. Hydrogeologie, Georg-August-Universität Göttingen  
1994 - 1997 **"Master of Science"** - Natural Resources, Schwerpunkt: Bodenforschung/Hydrologie, "University of Connecticut", USA  
1989 - 1994 **Diplom** - Angewandter Mathematik (FH), Fachrichtung Technik, Fachhochschule Regensburg

### Beschäftungsverhältnisse:

2003 - **Wissenschaftliche Mitarbeiterin.** Georg-August-Universität Göttingen  
2000 - 2003 **Wissenschaftliche Mitarbeiterin.** Friedrich-Schiller-Universität Jena  
1999 - 2000 **Wissenschaftliche Mitarbeiterin.** Umweltforschungszentrum (UFZ) Leipzig-Halle GmbH  
1997 - 1999 **"Research assistant"**. City University, London, UK  
1994 - 1996 **"Graduate research assistant"**. University of Connecticut, USA  
1993 **Praktikum.** University of Connecticut, USA